Université de Lille

THESE DE DOCTORAT

Pour l'obtention du titre de

DOCTEUR DE L'UNIVERSITÉ DE LILLE

Aspects moléculaires et cellulaires de la biologie

Présentée par

Sarah TROUVILLIEZ

Caractérisation des interactions entre TrkA, CD44 et les molécules de leur signalisation dans les cancers du sein triple négatifs

Soutenue le 28 Septembre 2022 devant la commission d'examen :

Rapporteurs :	Dr. Sandrine BOURDOULOUS Pr. Curzio RUEGG
Examinateurs :	Pr. Réjane PAUMELLE-LESTRELIN Pr. Antoine GALMICHE Pr. Xuefen LE BOURHIS
Directeur de thèse :	Pr. Robert-Alain TOILLON

Remerciements

Les trois premières années de ce travail de thèse, on été financé sous la forme d'une allocation de recherche par le Ministère de l'enseignement supérieur et de la recherche et la région Hauts-de-France, que je remercie.

La quatrième année de ces travaux a été financé par la Ligue contre le cancer, que je remercie également.

Je remercie l'ensemble des membres de mon jury pour avoir accepter de participer à ma soutenance et l'intérêt porté à nos travaux de recherche. Je remercie en particulier mes rapporteurs pour leur relecture et leurs conseils pour mon manuscrit.

Je remercie le Pr. Xuefen Le Bourhis pour m'avoir accueillie dans son laboratoire depuis ma licence 3 et m'avoir permie de réaliser cette thèse.

Merci au Pr. Antoine Galmiche et au Pr. Fabrice Allain pour leur suivi et leurs conseils durant l'ensemble de ma thèse.

Je remercie le Pr. Robert-Alain Toillon, sans qui rien de tout cela n'aurait été possible. Merci pour vos conseils, vos corrections et surtout nos discussions durant mon parcours. Merci d'avoir fait naitre en moi la passion de la signalisation et de m'avoir initiée aux WB (même si je n'ai visiblement pas gardé votre protocole ;)). Merci pour votre soutien, surtout les nombreuses fois où j'ai douté. Je sais que cela n'a pas toujours été facile mais malgrès les épreuves nous avons continué. Je pars, mais j'espère sincèrement que je continuerai à avoir de vos nouvelles (avec un peu moins de « TrkA » peut-être ?!).

Merci au Pr. Eric Adrianssens pour m'avoir transmis un peu de son savoir-faire. Merci également au Dr. Roland Bourette pour l'aide et les conseils techniques, mais aussi et surtout les discussions scientifiques, les paroles rassurantes et les conseils pour l'après thèse. Malheureusement pour vous 2, je pense que je n'ai toujours pas le niveau pour les discussions foots.

Merci à Pamella et au Pr. Pierre Olivier Angrand pour votre aide pour mes débuts en biologie moléculaire. Merci Pamella de m'avoir donné les petits tips qui font la diffèrence.

Je remercie le Pr. Véronique Orian Rousseau pour m'avoir acceuillie dans son laboratoire et m'avoir laissée l'opportunité de découvrir un autre environnement de recherche et des personnes incroyables.

Merci à Xavier Thuru et Romain Magnez pour les MST (private joke). Bien que tu ne sois pas dans l'astophysique Romain, j'espère que certaines de ces expériences (et les autres nombreux travaux auquels vous contribuez) auront un plus grand retentissement.

Merci au Dr. Jérôme de Ruyck, Dr. Catherine Michaux et Pr. Éric Perpète pour m'avoir permis d'explorer d'autres mondes (modélisation, chimie, physique) que le mien (biologie cellulaire).

Merci à Isabelle, pour tes encouragements et ta gentillesse. Merci pour toutes ces « petites choses » que tu accomplies et qui nous font gagner un temps précieux.

Merci aux autres doctorants pour avoir tenté de me faire sortir du laboratoire. Je n'avais rien contre vous, bien au contraire, je faisais juste tout ce que je pouvais pour "changer le monde".

Antoine, merci pour toutes ces discussions que nous avons pu avoir scientifiques ou non (et tous les chocolats) lorsque j'allais chercher de la glace. Merci pour ta bienveillance.

Merci à Marie, pour ta gentillesse, tes encouragements et ta main tendue quand j'en ai eu besoin. Je te souhaite le meilleur pour ta « nouvelle vie » aux US avec Alexis.

Merci à Amina. Merci pour ta douceur, ta bienveillance et tes câlins. Merci pour le shopping, même si je crois que l'on cherche toujours … ! :') J'espère que tu passeras me voir dans ma nouvelle vie.

Karo, thank you for everything. You will be always my weird girl ! During all the last year of my PhD I had remenbered all of our discussions and these nice moments (especially with glue wine ;)). You are amazing girl !

Léo, thank you for your advices. Actually, I think that I've found the way at least (even if it was not easy). You will be always a model for me. I hope I'll meet others amazing researchers during my post-doc !

Julien, mon affreux ! Je t'ai connu lorsque tu étais un petit L3 (qui faisait des bétises) et aujourd'hui, l'élève a dépassé le maître. Te voire réussir est sans doute l'une des plus belles réussite de ma thèse. Merci de m'avoir donné cette opportunité mais aussi pour toutes les fois où tu as été là pour me rassurer et m'aider. Je n'oublierai jamais ces manips de fous que nous avions l'art d'entreprendre à 2. Tu resteras mon "Stanley Cohen" à moi ;)

Tony, merci pour les fous rires et les sueurs froides… (je crois que tout le monde se souviendra des cellules tombées dans le canister… !)

Alexandre, merci pour m'avoir fait découvrir la MD et d'avoir accepté de poursuivre le projet que j'ai initié en Allemagne. J'espère que tu trouveras ton chemin.

Eloise, merci pour ta fraicheur, ta spontanéité, ton investissement, les petites douceurs laissées sur mon bureau. Tu es incroyable, ne t'inquiete pas, tu seras une très bonne thésarde. Tu es déjà exceptionnelle, tu ne le sais juste pas encore.

Merci à Edouard, pour m'avoir "diverti" à la fin de ma thèse. Je me souviendrai longtemps de la moitié de mon café soluble par terre et de la pub pour l'aspirateur qui en a suivi ! Ne t'inquiète pas, on ne pourra plus se serrer sous la hotte mais on reste en contact depuis l'espace ! Sarah Pesquet

Loris, merci d'avoir été mon dernier "Pioupiou". Je sais que tu as peur de ne pas y arriver, mais ne t'inquiète pas cela se passera bien. Souviens toi " Si je peux le faire tout le monde peut le faire".

Merci à Martine, pour ton sourire, ta ténacité, ton soutien. Crois en toi, tu deviendras une grande chercheuse, j'en suis convaincue (enfin, pas en taille, on en est au même point pour ça !).

Camille, merci d'être ma meilleure amie. Tu m'as fait le plus beau des cadeaux en me présentant Louise. Tu me manques.

Je remercie également tous les soignants que j'ai pu rencontrer, notamment ceux du service Soins de suite de l'hopital de Saint-Amand-Les-Eaux. Je n'oublierai jamais leur investissement et leur gentillesse. Merci également aux patients qui auront su voir en moi une personne douce et battante. Je n'ai jamais abandonné grâce à vous.

A mon frère, pour m'avoir donné le bon (?) exemple de faire une thèse mais surtout m'avoir encouragé à sortir du labo. Nos moments partagés à la chorale et durant les cours de Rock resteront de très beaux souvenirs pour moi. Je ne te le dis jamais mais je t'aime et j'espère que tu trouveras le bonheur que tu mérites.

A Théo, mon cousin. Nous avons grandi à 2, fais nos bétises à 2 et nous passerons notre thèse la même année. Merci d'avoir toujours été là pour moi.

Mon coeur, merci pour ton amour, ton soutien, ta bienveillance. Je ne pourrai jamais assez te remercier d'avoir été là quand j'en avais le plus besoin. Tu es la preuve que les plus belles découvertes sont fortuites. Tu es mon CD44 à moi, celui qui interagit avec moi, change ma conformation, me renforce et fait naitre d'autres projets en moi. Je n'ai pas encore résolu la structure de cette interaction, ni décrypté l'ensemble de sa signalisation, mais je suis convaincue qu'a nous deux nous finirons par y arriver (# Stoup & Trouvilliez). Je t'aime.

Maman, merci pour ton soutien et ton amour inconditionnels. Cette thèse, c'était un combat, mais ce n'était rien à côté de celui que tu as mené. Je suis fière de toi. Tu es LA meilleure maman du monde, ne l'oublie jamais. Je t'aime très fort.

Marraine, merci d'avoir toujours été là pour moi depuis que je suis toute petite. Tu seras toujours un modèle pour moi. Quelques soient les épreuves, je ne t'ai jamais vue abandonner. Je n'ai plus de père mais j'ai eu une deuxieme wondermaman. Je t'aime.

Mamie, je suis désolée de ma longue absence. Lorsque ce n'était pas facile, je pensais à ces moments que nous avons partagés lorsque je vivais avec toi. Même si tu ne l'as jamais réalisé, tu es une femme exceptionnelle. Je t'aime.

A papi, parti trop tôt.

A Cassiopée, ma petite constellation partie pendant ma thèse

A Pauline, Beethoven et Chris.

A ma petite Nouille, mon Pepsou d'amour et Oscars qui m'ont rendus le sourire quand la vie m'a blessée.

“Dans votre vie tout ce que vous ferez sera insignifiant,
mais il est très important que vous le fassiez quand même”

Gandhi

Tu vois mamie, je n’ai jamais oublié.

Résumé

Le cancer du sein est la tumeur maligne la plus fréquente chez les femmes dans le monde (OMS). Le cancer du sein est une maladie hétérogène et le pronostic varie en fonction des caractéristiques moléculaires. En particulier, la prise en charge des cancers du sein triple négatifs (TNBC) reste un défi clinique en raison de l'absence de thérapie spécifique et efficace. Dans ce contexte, notre équipe a mis en évidence le rôle du récepteur à activité tyrosine kinase TrkA dans les TNBC. Plus précisément, les travaux du Pr. Toillon montrent que TrkA agit non seulement *via* sa phosphorylation mais aussi *via* un complexe de récepteurs membranaires. En particulier, le NGF induit une interaction de TrkA avec la glycoprotéine CD44. Le complexe TrkA/CD44 active une signalisation indépendante de la phosphorylation de TrkA impliquée dans la résistance des inhibiteurs de la phosphorylation de TrkA. Afin de cibler ce mécanisme de résistance, les interactions entre TrkA, CD44 et leurs partenaires de signalisation ont été étudiées. Tout d'abord, j'ai déterminé que le complexe TrkA/CD44 implique uniquement le variant 3 de CD44. En déterminant les motifs moléculaires impliqués, un peptide bloquant l'association TrkA/CD44v3 a été synthétisé et un mutant H112A de TrkA. J'ai ainsi confirmé l'importance des acides aminés de CD44v3 (IDDDEDFISST) et de l'acide aminé H112 de TrkA dans cette interaction. De façon intéressante, ce peptide bloquant réduit la croissance tumorale et la charge métastastatique. De plus nous avons montré que l'inhibition de CD44 n'affecte pas la liaison d'autres molécules de la signalisation de TrkA/CD44. Nous avons ensuite décrypté l'interaction TrkA/molécule de la signalisation et montré qu'un inhibiteur de cette interaction bloque la migration de cellules cancèreuses triples négatives. En conclusion, nos études ont révélé le rôle des interactions TrkA/CD44/molécules de leur signalisation dans l'agressivité des cancers du sein et la résistance aux inhibiteurs de TrkA. Ceci suggère que si les inhibiteurs de la phosphorylation de TrkA actuels ne sont pas efficaces dans le TNBC, de nouveaux inhibiteurs perturbant la signalisation TrkA/CD44 pourraient être de nouvelles stratégies thérapeutiques efficaces.

Abstract

Breast cancer is the most common malignancy in women worldwide (WHO). Breast cancer is a heterogeneous disease and prognosis varies according to molecular characteristics. In particular, the management of triple-negative breast cancer (TNBC) remains a clinical challenge due to the lack of specific and effective therapy. In this context, our team has highlighted the role of the receptor tyrosine kinase TrkA in TNBC. More precisely, the work of Prof. Toillon shows that TrkA acts not only via its phosphorylation but also via a complex of membrane receptors. In particular, NGF induces an interaction of TrkA with the glycoprotein CD44. The TrkA/CD44 complex activates TrkA phosphorylation-independent signaling involved in the resistance of TrkA phosphorylation inhibitors. To target this resistance mechanism, the interactions between TrkA, CD44 and their signaling partners were investigated. First, I determined that the TrkA/CD44 complex involves only CD44 variant 3. By determining the molecular motifs involved, a peptide blocking the TrkA/CD44v3 association was synthesized and an H112A mutant of TrkA. I thus confirmed the importance of the amino acids of CD44v3 (IDDDEDFISST) and the amino acid H112 of TrkA in this interaction. Interestingly, this blocking peptide reduces tumor growth and metastatic load. Furthermore, we showed that CD44 inhibition does not affect the binding of other TrkA/CD44 signaling molecules. We then deciphered the TrkA/signaling molecule interaction and showed that an inhibitor of this interaction blocks the migration of triple negative cancer cells. In conclusion, our studies revealed the role of TrkA/CD44/signaling molecule interactions in breast cancer aggressiveness and resistance to TrkA inhibitors. This suggests that if current TrkA phosphorylation inhibitors are not effective in TNBC, novel inhibitors disrupting TrkA/CD44 signaling could be effective new therapeutic strategies.

Valorisations

Article

Trouvilliez S, Cicero J, Lévêque R, Aubert L, Corbet C, Van Outryve A, Streule K, Angrand P-O, Völkel P, Magnez R, Brysbaert G, Mysiorek C, Gosselet F, Bourette R, Adriaenssens E, Thuru X, Lagadec C, de Ruyck J, Orian-Rousseau V, Le Bourhis X and Toillon R-A. **Direct interaction of TrkA/CD44v3 is essential to NGF-promoted aggressiveness of breast cancer cells. Journal of experimental and clinical cancer research. 2022, Mar, 41(1): 110.**

Conférences

Communications orales

Trouvilliez S, Cicero J, Giraud S, Van Outryve A, Toillon RA. Interaction TrkA/signaling partner: on the way of new TrkA inhibitors? 3eme Oncolille PhD day, Lille, **Mars 2022.**

Trouvilliez S, Cicero J, Streule K, Orian Rousseau V, Magnez R, Thuru X, Volkel P, Angrand PO, Bourette R, de Ruyck J, Toillon RA. Therapeutic potential of TrkA/CD44 interaction. GDR APPICOM, Lyon, **Novembre 2021**.

Trouvilliez S, Cicero J, Streule K, Orian Rousseau V, Magnez R, Thuru X, Volkel P, Angrand PO, Bourette R, de Ruyck J, Toillon RA. Therapeutic potential of TrkA/CD44 interaction. Séminaire Oncolille, **Octobre 2021.**

Trouvilliez S, Cicero J, Streule K, Orian Rousseau V, Magnez R, Thuru X, Volkel P, Angrand PO, Adriaenssens E, Bourette R, de Ruyck J, Toillon RA. Therapeutic potential of TrkA/CD44 interaction. 2nd Oncolille PhD day, Lille, **Mars 2021**.

Trouvilliez S, Streule K, Munoz Sagredo L, Orian Rousseau V, Toillon RA. Caracterization of the interactions between CD44 and the ERM, Karlsruhe (Allemagne), **Décembre 2020.**

Trouvilliez S, Cicero J, Magnez R, Thuru X, Volkel P, Angrand PO, Giraud S, Adriaenssens E, Bourette R, de Ruyck J, Toillon RA. Caracterization of the interactions between TrkA, CD44 and their signaling partners, KIT, Karlsruhe (Allemagne), **Octobre 2020.**

Trouvilliez S, Giraud Stéphan, Voelkel P, Angrand PO, Toillon RA. Therapeutic potential of the interactions between TrkA, CD44 and their signaling partners. Drug Discovery Day, Lille, **Décembre 2019.**

Communications par Poster

Trouvilliez S, Cicero J, Magnez R, Thuru X, Munoz Sagredo L, Orian Rousseau V, Toillon RA. Modulateur des signalisations de TrkA pour restaurer une réponse aux TKI. 14 ème journées du Cancéropole Nord-Ouest, Deauville, **Mai 2022.**

Trouvilliez S, Cicero J, Streule K, Orian Rousseau V, Magnez R, Thuru X, Volkel P, Angrand PO, Toillon RA. Therapeutic potential of TrkA/CD44 interaction. Membran Protein Meeting, Namur, **Décembre 2021**.

Trouvilliez S, Cicero J, Magnez R, Thuru X, Voelkel P, Angrand PO, Toillon RA. Potentiel thérapeutique de l'interaction TrkA/CD44 dans les cancers du sein triples négatifs. 13 ème journées du Cancéropole Nord-Ouest, Deauville, **Octobre 2021.** *Prix du meilleur poster.*

Trouvilliez S, Giraud S, Voelkel P, Angrand PO, Toillon RA. Therapeutic potential of TrkA/CD44 interaction Drug Discovery Day, Lille, **Décembre 2019.**

Trouvilliez S, Giraud S, Voelkel P, Angrand PO, Toillon RA. Potentiel thérapeutique des interactions entre TrkA, CD44 et les molécules de leur signalisation dans les cancers du sein triples négatifs. 12 ème journées du Cancéropole Nord-Ouest, Deauville, **Mai 2019.**

Trouvilliez S, Giraud S, Voelkel P, Angrand PO, Toillon RA. Potentiel thérapeutique des interactions entre TrkA, CD44 et les molécules de leur signalisation dans les cancers du sein triples négatifs. 1ère Oncolille PhD day, Lille, **2018.**

Communications « grand public »

Vanseuningen I, **Trouvilliez S**. Intervention pour la conférence "60 ans de recherche en cancérologie : comprendre les causes et facteurs pour mieux traiter les cancers" organisée par la Ligue, Lille, **Décembre 2021.**

Trouvilliez S. Intervention au lycée Jean Perrin, Lambersart, **Octobre 2021.**

Trouvilliez S, Herlédan M. Conférence grand public La recherche : une passion, un métier ? Lille, **Octobre 2021.**

Trouvilliez S. Fête de la science, Parc relais Nature Villeneuve d'Ascq, **Octobre 2021.**

Trouvilliez S. Interview radio-campus émission de la gazette, Villeneuve d'Ascq. **Octobre 2021.**

Trouvilliez S. Ma Thèse en 180 secondes finale régionale Hauts de France **2021. https://www.youtube.com/watch?v=mHSNZ1yhH4c**

Trouvilliez S, Cicero J, Toillon RA. Chercher pour guérir. « Comprendre les interactions entre les récepteurs de facteur de croissance, une piste pour le développement et l'amélioration des thérapies ciblées dans le cancer… » La ligue contre le cancer du nord, lettre trimestriel n°28, p6, **2019**. https://www.ligue-cancer.net/article/59164_comprendre-les-interactions-entre-les-recepteurs-de-facteur-de-croissance-une-piste.

Prix et distinctions

- Drug discovery day (2019) **1er prix** communication orale
- Oncolille phD days (2021) **1er prix** communication orale
- Journées du Cancéropole Nord Ouest (2021) **3eme prix** communication poster

Financements obtenus

- I-site, 2500 €, Caractérisation de l'interaction CD44v3/ERM dans les cancers du sein triple négatif, KIT Karlsruhe, Octobre-Décembre 2020.
- Cancéropole Nord Ouest, 2500 €, Caractérisation de l'interaction CD44v3/ERM dans les cancers du sein triple négatif, KIT Karlsruhe, Octobre-Décembre 2020
- Ligue contre le cancer, 4ième année de thèse

Sommaire

Remerciements 1

Résumé 6

Abstract 7

Valorisations 8

Table des figures 13

Table des tableaux 14

Abréviations 15

Introduction 19

1. Les cancers du sein triple négatifs 19

1.1. Les cancers du sein : une pathologie hétérogène 19

1.1.1. Épidémiologie et étiologie *19*

1.1.2. Carcinogenèse et développement *23*

1.1.3. Classification *26*

1.2. Les cancers du sein triple négatifs : un échec thérapeutique 28

1.2.1. De la classification au pronostic et choix thérapeutique *28*

1.2.2. Prise en charge, résistance et métastases *31*

2. Le récepteur TrkA 38

2.1. Le récepteur TrkA : un récepteur aux rôles pléiotropes 38

2.2. Rôle de l'axe NGF/TrkA dans les cancers 82

2.3. Ciblage de l'axe NGF/TrkA dans les cancers ..... **Error! Bookmark not defined.**

3. Le co-recepteur CD44 86

3.1. Découverte et synthèse 86

3.2. Structure-fonction ..... **Error! Bookmark not defined.**

3.3. Rôles des contenants v3 dans l'agressivité tumorale 89

4. Les molécules de la signalisation de TrkA/CD44v3 91

4.1. La protéine p115RhoGEF 91

4.1.1. Découverte *91*

4.1.2. Synthèse, structure, fonction cellulaire *91*

4.1.3. Rôles *95*

4.2. La protéine RhoA 96

4.2.1. Découverte *96*

4.1.2. Synthèse et structure *97*

Matériel et méthodes 102

1. Modélisation bioinformatique 102

1.1. Génération du modèle TrkA/CD44v3 102

1.2. Sélection du résidu cible pour la mutagénèse 102

1.3. Modélisation des structures peptidiques 103

2. Culture cellulaire 103

2.1. Entretien des celulles cancéreuses mammaires 103

2.2. Entretien des autres lignées celullaires 104

3. Amplification et vérification des plasmides 104
3.1. Constructions 104
3.2. Amplification des plasmides 105
3.3. Digestion 105

4. Transfection et validations 105
4.1. Electroporation (plasmides) 105
4.2. Lipofection (plasmides) 106
4.3. Interférine (siRNA) 106
4.4. Extraction d'ARN 106
4.5. qPCR 107
4.6. Extraction protéique 107
4.7. Western blot 108

5. Étude des associations protéiques *in cellulo* 108
5.1. Traitement des cellules en vue d'une lyse protéique 108
5.2. Immunoprécipitation 109
5.3. Duolink 109
5.4. Co-localisation 110

6. Étude des interactions protéiques *ex vitro* 111
6.1. Thermophorèse 111
6.1.1. Interaction TrkA/peptides de CD44 111
6.1.2 Interaction TrkA/CD44v3 111
6.1.3. Effet de CD44v3 sur l'affinité de TrkA pour le NGF 111
6.2. Biolayer Interferometry 112

7. Étude des signalisations 112
7.1. Biosenseur 112
7.2. Western blot 113

8. Études fonctionnelles 113
8.1. Test de clonogénicité 113
8.2. Test de blessure (IBIDI) 113
8.3. Test d'invasion (transwell) 114

9. Études *in vivo* 114
9.1. Croissance tumorale *in vivo* 114
9.2. Métastases *in vivo* 114

4. Résultats 116

Article 1 116

Article 2 184

Article 3 228

Discussion/Perspectives 261

Bibliographie 294

Table des figures

Figure 1 : Incidence et mortalité des cancers du sein dans le monde et en France.

Figure 2 : Facteurs de risque des cancers du sein.

Figure 3 : Carcinogenèse et développement des cancers du sein.

Figure 4 : Profil des patients diagnostiqués avec un TNBC.

Figure 5 : Prise en charge des cancers du sein triple négatifs.

Figure 6 : Molécules utilisées en clinique pour le ciblage de l'axe NGF/TrkA.

Figure 7 : CD44 : du gène aux effets cellulaires.

Figure 8 : p115RhoGEF : du gène à la protéine.

Figure 9 : Interactome de p115RhoGEF.

Figure 10 : Dynamique d'activation des protéines Rho.

Figure 11 : Objectifs scientifiques de la thèse.

Table des tableaux

Tableau 1 : Classifications des cancers du sein.

Tableau 2 : Répartition des cancers du sein triple négatifs entre les diffèrents stades TNM et grades SBR.

Tableau 3 : Caractéristiques moléculaires, traitements préconisés et pronostics associés à différents sous-types de cancer du sein.

Tableau 4 : Corrélation de l'expression de contenant v3 avec différents paramètres cliniques dans les cancers.

Abréviations

A

ADN(c) : Acide DésoxyriboNucléique (complémentaire)
ALK : Anaplastic Lymphoma Kinase
ANS : Agence Nationale de la Santé
AR : Androgen Receptor
ARN : Acide RiboNucléique
AREG : Amphireguline
ASR : Age-Standardised Rate
ATCC : American Type Culture Collection
ATM : Ataxia Telangiectasia Mutated
ATU : Autorisation Temporaire d'Utilisation

B

BCA : Bicinchronic Acid
BDNF : Brain Derived Neurotrophic Factor
BET : Bromure d'EThidium
BL1/2 : Basal-Like 1/2
BSA : Bovin Serum Albumin
BT-549 : Breast Tumor 549

C

CD44(v3) : Cluster of Differentiation 44 (variant 3)
CHEK2 : CHEckpoint Kinase 2
CryoEM : Cryo Microscopie Electronique

D

Dbl : Diffuse B cell lymphoma
DDR : DNA Damage Response
DH : Dbl Homology
DMSO : DiMéthylsulfoxyde

E

EDTA : EthyleneDiamineTetraacetic Acid
EphA2 : Ephrin A2
EGFR : epidermal Growth Factor Receptor
EMEM : Eagle's Minimum Essential Medium
EMT : Epithelial-Mesenchymal Transition
ER : Estrogen Receptor
ERM : Ezrin Radixin Moesin

F

FERM : Four-point-one, ezrin, radixin, moesin
FGF : Fibroblast Growth Factor
FGFR : Fibroblast Growth Factor Receptor

FISH : Fluorescence In Situ Hybridization
FRET : Fluorescence Resonance Energy Transfert

G

G418 : généticine
GF : Growth Factor
GPCR : G Protein Coupled Receptor

H

H112A : Mutation de l'histidine 112 en alanine
HA : Hyaluronic Acid
HEPES : Acide 4-(2-hydroxyethyl) -1-pipérazine éthane sulfonique
HER2 : Human Epidermal Growth Factor 2
His : Histidine

I

IA : Inhibiteur d'Aromatase
IHC : ImmunoHistoChimie
IgG : Immunoglobuline de type G
IGF : Insulin Growth Factor
IM : ImmunoModulatory
IMC : Indice de Masse Corporelle
IMD62 : IMmunoDeficience 62
INCa : Institut National du Cancer
IP : Immuno-Précipitation

K

KD : Kinase Dead
KI67 : marqueur de prolifération

L

LAR : Luminal Androgen Receptor
LB : Luria Broth
LPA : LisoPhosphatidic Acid

M

M : Mesenchymal
MDA-MB-231 : MD Anderson Malignant Breast 231
MEC : Matrice ExtraCellulaire
MMP : Matrix MetaloProtease
MSL : Mesenchymal Stem-Like

N

NGF : Nerve Growth Factor
NT-3/4/5 : Neurotrophin-3/4/5
NTRK(1) : NeuroTrophin Receptor Kinase (1)

O

OMS : Organisation Mondial de la Santé

P

PBS : Phosphate Buffered Saline
PC12 : PheoChromocytoma
pCMV : promoter CytoMegaloVirus
PDB : Protein DataBank
PDL1 : Programmed cell Death protein 1
PH : Plextrin Homology
PLA : Proximity Ligation Assay
PMSF : Phenyl Methyl Sulfonyl Fluoride
PR : Progesteron Receptor
PTEN : Phosphatase and TENsin homologue
PVDF : PolyVinylidene DiFluoride

R

RH : Rgs Homology
Rho : Ras homology
RhoGEF : Rho Guanine Exchanger Factor
RIN : Réseau d'Interaction Résiduel
ROCK : Rho-associated kinase
ROS : Reactive Oxygen Species
RPM : Rotation Par Minute
RT-qPCR : Reverse Transcriptase-quantitative Polymerase Chain Reaction

S

SDS : Sodium Dodecyl sulfate
SI : Système Immunitaire
siRNA : small interferent RNA
S.O.C. : Super Optimum broth
SUM-159-PT : Steve Ethier's lab University of Michigan
SVF : Sérum de Veau Fœtal

T

TBE : Tris Buffer EDTA
TBST : Tris Buffer Saline-Tween 20
TIM : T-cell immunoglobulin and mucin domain
TKI : Tyrosine Kinase Inhibitor
TNBC : Triple Negative Breast Cancer
TP53 : Tumor Protein 53
TrkA : Tropomyosine receptor kinase A

U

UV : Ultra violet

W

WHO : World Health Organization
Wnt : Wingless-related integration site

Y

Y490 : Tyrosine 490
Y490F : Mutation de la Tyrosine 490 en Phénylalanine

Introduction

1. Les cancers du sein triples négatifs

1.1. Les cancers du sein : une pathologie hétérogène

1.1.1. Épidémiologie et étiologie

Le cancer du sein, à l'échelle mondiale, affecte environ **2,1 millions** de femmes tous les ans (WHO 2018). Il peut également toucher les hommes, néanmoins le cancer du sein chez l'homme représente moins de 1 % des cancers du sein et moins de 1 % des cancers chez l'homme (Sanguinetti *et al*., 2016). Le nombre de décès estimés en 2018 est d'environ **627 000** soit environ 15 % des décès par cancer (WHO 2018). Le cancer du sein est ainsi le **premier cancer féminin** en termes **d'incidence** et de **mortalité dans le monde** (graphiques circulaires ; **Figure 1**). Toutefois, l'incidence et la mortalité varient selon les pays indépendamment du vieillissement de la population (carte des taux normalisés à l'âge ; **Figure 1**). Cette hétérogénéité résulte probablement de différences socio-économiques. En effet, d'une part, dans les pays à bas revenus les taux de mortalité sont plus élevés, notamment chez les patientes de moins de 50 ans. D'autre part, dans les pays à hauts revenus, l'incidence est plus élevée et en augmentation (**Figure 1**; Bellanger *et al.*, 2018). En France, en particulier, l'incidence a augmenté de 0,6 % par an entre 2010 et 2018 (moyenne) pour atteindre **58 459 nouveaux cas** (INCa 2018). Le cancer du sein est ainsi le cancer féminin le plus fréquent en France. Il est également le plus meurtrier (**12 146** décès estimés en 2018, INCa) et ce malgré une diminution de la mortalité (- 1,3 % par an entre 1990 et 2018). A l'échelle nationale, il existe néanmoins une disparité inter-régionale (**Figure 1**). La région des Hauts-de-France présente une incidence proche de la moyenne nationale (rapport standardisé d'incidence de 1,06 %) mais une **surmortalité importante.** En particulier, les départements du Nord et du Pas-de-Calais avec des taux respectivement 27 % et 33 % au-dessus de la moyenne nationale sont particulièrement touchés (INCa 2019). Ces taux plus élevés s'expliquent notamment par l'hygiène de vie (tabagisme et consommation d'alcool plus importante).

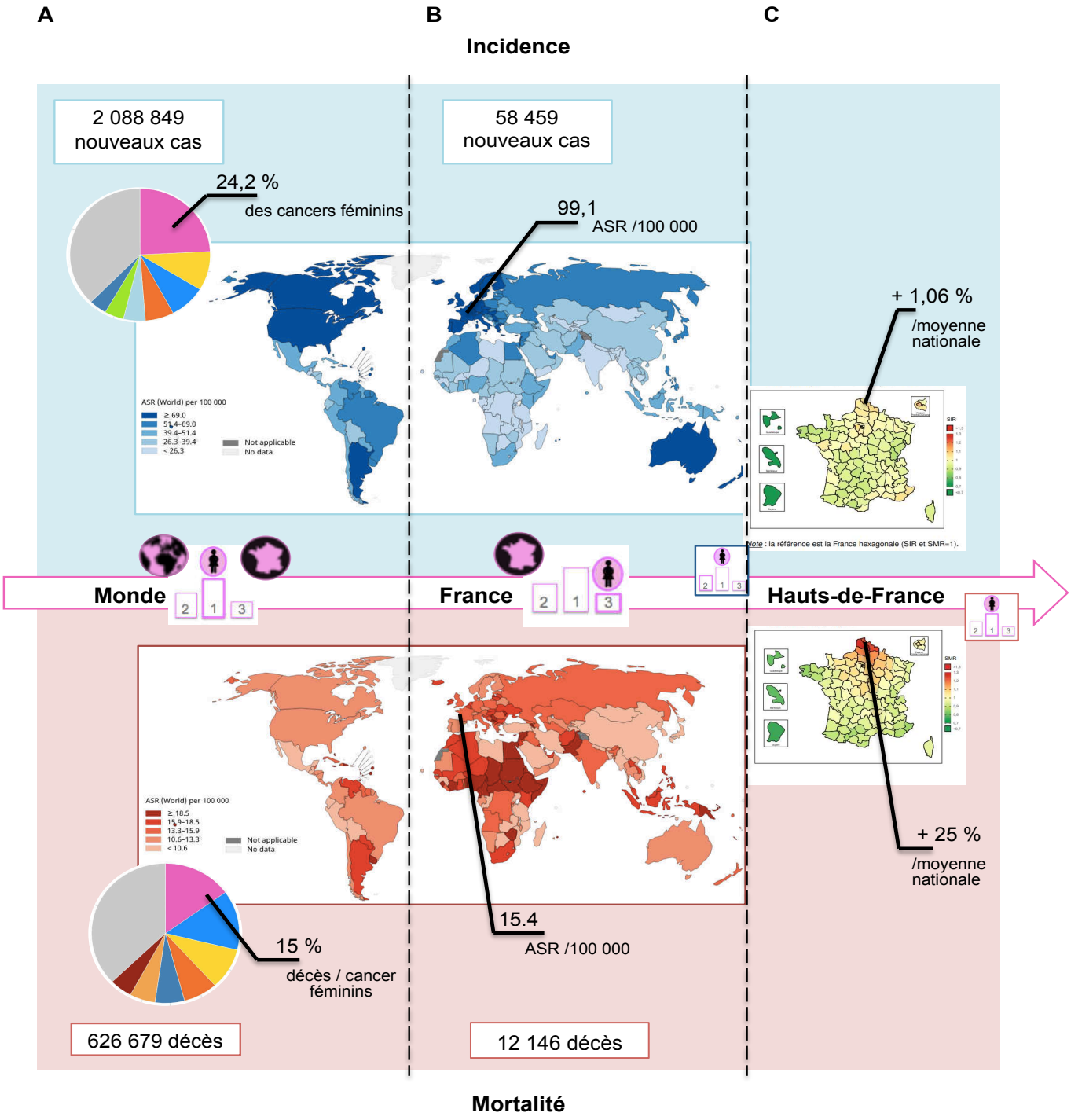


Figure 1 : Incidence et mortalité des cancers du sein dans le monde et en France par an. Le cancer du sein est le premier cancer féminin dans le monde et en France (A) en termes d'incidence (bleu) et de mortalité (rouge). Ces taux sont hétérogènes à l'échelle mondiale (A et B). La France figure au 3ième rang mondial (B) avec une disparité entre les territoires (C). En particulier, la région des Hauts-de-France présente une surmortalité de 25 % par rapport à la moyenne nationale (C). D'après le WHO (2018) et l'INCa (2015 et 2018).

Le cancer du sein est une **maladie multifactorielle** dont certains **facteurs de risque** sont contrôlables par l'individu (facteurs extrinsèques) et d'autres non (facteurs intrinsèques). Les facteurs **intrinsèques** sont : l'âge, la génétique, l'âge de survenue des premières règles et de la ménopause mais aussi la densité des seins (**Figure 2**). Seul environ 10 % des cancers du sein

sont d'origine génétique et sont, le plus souvent, dus à une ou des mutations des gènes impliqués dans la réparation de l'ADN *BRCA1* et *2* (BReast CAncer 1 et 2). La fréquence de mutation de ces gènes est plus élevée dans certaines populations (Daly *et al.*, 2016). Des gènes qui régulent le cycle cellulaire, comme T*P53* et *PTEN,* augmentent également le risque de cancer du sein. En plus de ces gènes à haute pénétrance, d'autres mutations de gènes ont été associées aux cancers du sein dont *ATM ou CHEK2* (Daly *et al.*, 2016). Les facteurs de risques **extrinsèques** peuvent être liés à **l'environnement** comme, par exemple, l'exposition aux pesticides ou à la pollution mais aussi au **mode de vie** (**Figure 2**): consommation d'alcool, le tabac, les contraceptifs et traitements hormonaux, l'âge de la première maternité (risque accru après 35 ans), l'allaitement, la sédentarité ou le surpoids/obésité (IMC>25) (Hsieh *et al.*,1984; Zbuk and Anand, 2012). Par exemple, la consommation d'alcool, excessive (>60 g d'alcool pur/jour ; environ 6 verres) mais aussi moyenne (entre 40 et 60 g d'alcool pur/jour ; 4-6 verres) et faible (de 0 à 20 g d'alcool pur ; environ 2 verres), est responsable d'environ 15 % des cancers du sein (2015) (Shield *et al.*, 2018). D'autres paramètres associés à l'occidentalisation ont également été mis en cause plus récemment tels que le manque de vitamine D, l'exposition à la lumière la nuit (perturbation cycles circadiens), les produits chimiques (cosmétiques, produits d'entretien, alimentation, exposition professionnelle). L'évolution de notre société semble ainsi avoir contribuée à l'augmentation de l'incidence des cancers du sein.

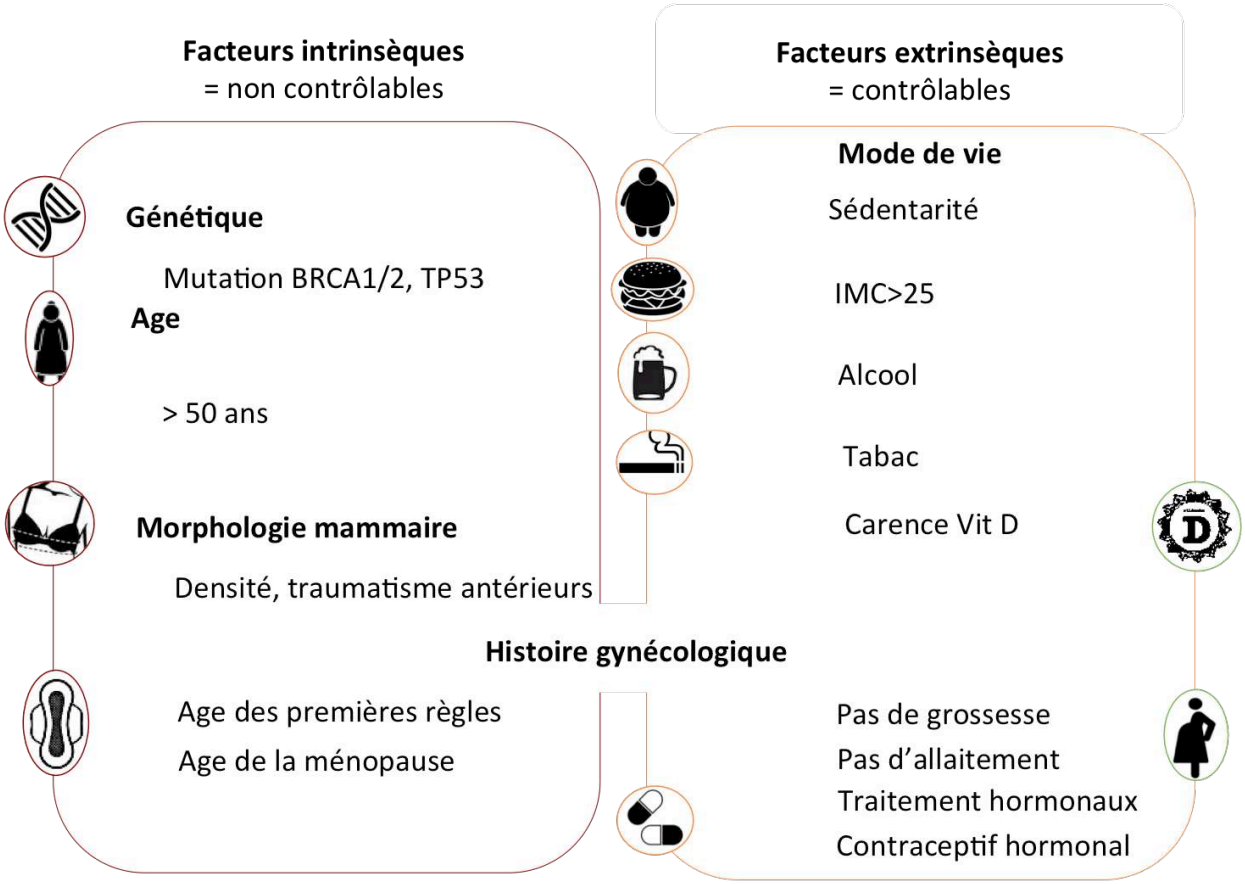


Figure 2: Facteurs de risques des cancers du sein. Chaque individu présente un risque global de développer un cancer du sein qui dépend de facteurs de risques intrinsèques (âge, génétique…) et extrinsèques (alimentation…). Les facteurs intrinsèques ne peuvent pas être modifiés par l'individu mais le pronostic et le risque global peuvent être limités par des mesures de suivi ou en minimisant les risques extrinsèques. Les risques extrinsèques résultent de comportements ou de l'environnement de l'individu qui peut ainsi au moins les limiter.

La mise en place de mesures « simples » à l'échelle individuelle mais aussi collective permettrait ainsi de réduire l'incidence de ces cancers (**Figure 2**). Dans ce but, l'OMS (Organisation Mondiale de la Santé) préconise d'ores et déjà certaines pratiques (activité physique etc.) qu'il appartient à chacun de suivre ou non. Néanmoins, les disparités socio-économiques entre les territoires peuvent s'avérer un frein à leurs mises en application. De plus, certains risques environnementaux sont difficiles voire impossibles à contrôler à l'échelle individuelle. En effet, il est possible de limiter son exposition à certains cancérigènes contenus dans les produits de notre quotidien (produits d'entretien, cosmétiques…) mais pas à ceux présents dans l'environnement (pesticides utilisés pour l'agriculture à la campagne, pollution en ville). En plus de mesures pour prévenir la hausse de l'incidence, des mesures peuvent être prises pour limiter la mortalité. Dans ce but, la France a mis en place des programmes de dépistage qui permettraient un diagnostic à des stades moins avancés (**Figure 2**). Dans ce sens, une étude récente montre que les taux de

cancer *in situ* et localisés sont plus importants dans le groupe des patientes ayant participé à un programme de dépistage. De plus, pour celles avec un cancer métastatique, elles présentent moins de métastases que celles du groupe non suivi (Lefeuvre *et al.*, 2019). Néanmoins, ces campagnes sont sujettes à contreverses et certains remettent en question leur rapport bénéfice/coût. Une des limites à ces campagnes est l'inclusion ou non selon l'âge des patientes. En effet, si l'âge est un facteur de risque, il ne permet pas d'identifier les patientes plus sujettes à développer un cancer du sein agressif/métastatique. Or, c'est pour ces patientes que la détection précoce pourrait en particulier permettre d'améliorer la prise en charge et le pronostic.

L'évolution de l'incidence et de la mortalité des cancers du sein est donc conditionnée par de nombreux facteurs contrôlables ou non par les individus. Or, en 2040, le WHO estime qu'en raison de la croissance démographique, le cancer du sein pourrait causer environ 1 000 000 décès supplémentaires par an dans le monde (WHO 2018). La prévention et la détection précoce des cancers du sein, en particulier ceux qui sont agressifs, constituent ainsi des enjeux de société grandissant. Afin d'identifier des marqueurs d'agressivité et/ou de la formation de métastases il est nécessaire de parfaire notre connaissance des mécanismes impliqués dans l'émergence et le développement des cancers du sein.

1.1.2. Carcinogenèse et développement

La glande mammaire est une glande exocrine d'origine ectodermique et mésodermique. Elle assure la production du lait grâce à des modifications structurales qui surviennent lors de la puberté (croissance canalaire) puis de la grossesse (différenciation alvéolaire) (Javed and Lteif, 2013; Sternlicht, 2006). La glande mammaire subit un dernier remodelage au cours de la ménopause. Cette évolution structurale et fonctionnelle tout au long de la vie est sous le contrôle d'hormones et de facteurs du microenvironnement dont des facteurs de croissances ou de molècules de la matrice extracellulaire (MEC) comme l'acide hyaluronique (HA) (Sternlicht, 2006). Au cours du développement embryonnaire, la liaison du FGF10 (Fibroblast growth Factor-

10) au FGFR2-IIIb (Fibroblast Growth Factor Receptor-IIIb) permet la formation des placodes mammaires à partir des crêtes mammaires. Puis, au cours de la puberté, l'IGF1 (Insulin-like Growth Factor 1) *via* son récepteur stimule la prolifération des cellules épithéliales (Macias and Hinck, 2012). De plus, au niveau des cellules stromales, la fixation de l'AREG (Amphireguline) conduit à son hétérodimérisation avec HER2/3 (Human Epidermal Growth Factor Receptor-2/3) qui promeut la production de FGF (McBryan *et al.*, 2008). L'interaction de ce FGF avec son récepteur est responsable de la croissance canalaire. Puis, l'épithélium subit une évolution/involution à chaque cycle menstruel. Cette évolution de la glande mammaire est rendue possible par un remodelage de la MEC contrôlé par les métalloprotéines (MMP) et leurs inhibiteurs (TIM). De plus, l'acide hyaluronique, un constituant majeur de la MEC, module l'effet des facteurs de croissance. En effet, il a été montré que le HA de faible poids moléculaire (10 kDa) favorise la croissance induite par l'EGF (Epidermal Growth Factor) tandis que la forme de haut poids (500 kDa) l'inhibe (Tolg *et al.*, 2017). Ce remodelage, plus intense durant la grossesse, reposerait sur une expression plus importante des récepteurs à l'HA dont CD44 (Cluster of Differentiation 44). De plus, la glycoprotéine CD44 est principalement exprimée dans les cellules myoépithéliales et est essentielle à l'établissement de l'identité des cellules dans la glande mammaire au cours du développement (*i.e.* cellules myoépithéliales ou luminales) (Louderbough *et al.*, 2011).

Dans 95 % des cas, les cancers du sein sont issus des cellules épithéliales du tissu glandulaire (canaux ou lobules) et sont ainsi des adénocarcinomes (**Figure 3 A**)**.** Les 5 % restant sont des formes rares de diverses origines et incluent les sarcomes, les lymphomes, les kystes hodgkiniens, les métastases mammaires (INCa, 2014). La carcinogenèse mammaire d'un point de vue histologique est un processus continu et multi-étapes. Elle débute par la **prolifération anarchique** de cellules épithéliales suite à des modifications épigénétiques et/ou génétiques. L'excroissance tissulaire est appelée **hyperplasie** (**Figure 3 A**). Les cellules peuvent alors commencer à se dédifférencier ce qui conduit à la formation d'une lésion pré-cancéreuse (ou **dysplasie**). L'accumulation de **mutations génétiques** va

alors faire évoluer la lésion encore bégnine en carcinome *in situ* (lésion localisée ; **Figure 3 B**). L'acquisition de propriétés pro-migratoires et invasives va alors permettre aux cellules cancéreuses de **franchir la lame basale et d'envahir le tissu conjonctif**. On parle alors de **carcinome infiltrant ou invasif** (**Figure 3 B**). Lorsque les cellules atteignent les ganglions lymphatiques, elles peuvent entrer dans la **circulation sanguine (intravasation)** puis en ressortir (**extravasation**) pour coloniser d'autres organes (Vargo-Gogola and Rosen, 2007). Les systèmes lymphatique et nerveux permettent également aux cellules cancéreuses de rejoindre d'autres organes (Li *et al.*, 2013; Rahman and Mohammed, 2015). La multiplication des cellules cancéreuses dans ces organes conduit à la formation de tumeurs secondaires (**métastases ; Figure 3 C**).

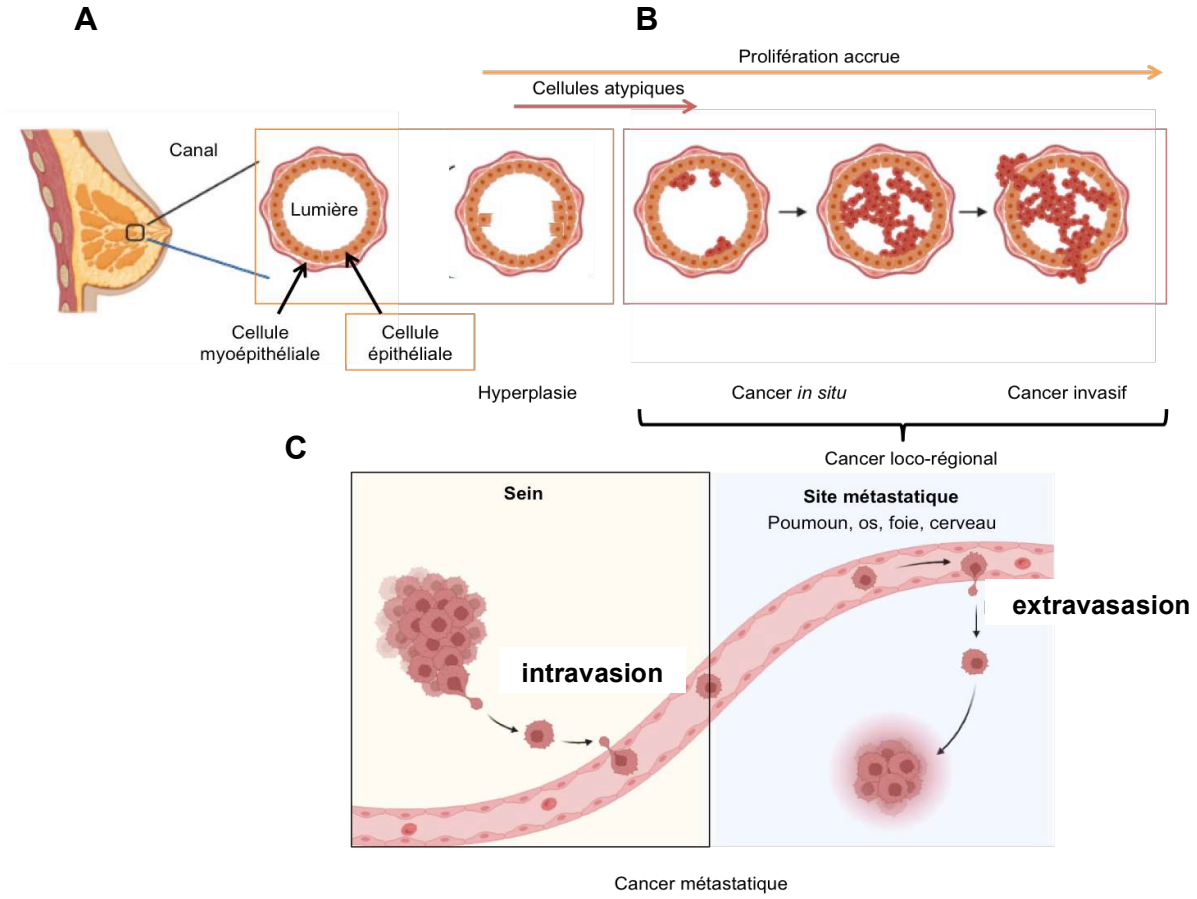


Figure 3 : Carcinogenèse et développement des cancers du sein. Les cancers du sein sont en majorité des adénocarcinomes et proviennent de cellules épithéliales de la glande mammaire (canaux ou lobules ; **A**). Au départ, la prolifération de ces cellules génère une hyperplasie bégnine (**A**). L'accumulation de mutation conduit au cancer dit *in situ* puis invasif une fois la lame basale franchie (**B**). Les cellules peuvent ensuite passer dans la circulation (intravasasion) puis en sortir (extravasasion) pour coloniser de nouveaux organes et former des métastases (**C**).

Si le type cellulaire à l'origine du cancer du sein est connu, les mécanismes cellulaires impliqués sont encore mal connus. Une meilleure connaissance des mécanismes cellulaires mais aussi moléculaires impliqués dans l'émergence et le développement des cancers du sein est donc nécessaire pour améliorer la prévention et la prise en charge. Dans ce sens, des classifications des cancers du sein ont été réalisées. En effet, les cancers du sein présentent une forte **hétérogénéité tumorale**. Or, selon le stade du diagnostic, il existe une forte **hétérogénéité pronostic** (survie à 5 ans de 98,3 % pour un diagnostic à un stade local contre 23,3 % pour un stade métastatique ; données INCa, 2015).

1.1.3. Classification

La classification stade **TNM** (Tumor Node Metastasis), première à avoir été utilisée pour le cancer du sein (adoptée en 1953), repose sur l'**examen clinique** de 3 paramètres : la **taille de la tumeur primaire** et son extension aux tissus et organes voisins, l'**invasion ganglionnaire,** la présence de **métastases** ou non (**Tableau 3 A**)**.** Cette classification ne permet cependant pas de récapituler toute l'hétérogénéité des cancers du sein. Dès 1957, l'examen clinique est complété par une analyse **histologique** des cancers infiltrants. Le grade **SBR** (Scarff-Bloom-Richardson) est obtenu grâce à l'évaluation de 3 paramètres : la **formation de tubules, le pléomorphisme nucléaire et le nombre de mitoses** (**Tableau 3 B**). La somme des scores de ces 3 paramètres correspond à un score total qui permet d'établir le grade (**Tableau 3 C**).

A **Classification TNM**

Stade	T	Tumeur	N	Ganglion	M	Métastases
0	Tis	in situ	N0	Absence	M0	Absence
IA	T1	≤ 2 cm	N0	Absence	M0	Absence
IB	T0 ou T1	Abs ou ≤ 2 cm	N1	Homolatérale axillaire	M0	Absence
IIA	T0 ou T1	in situ ou ≤ 2 cm	N0	Absence	M0	Absence
	T2	2 cm≤ T ≤ 5 cm	N0	Absence	M0	Absence
IIB	T2	2 cm ≤ T ≤ 5 cm	N1	Homolatérale axillaire	M0	Absence
	T3	≥ 5 cm	N0	Absence	M0	Absence
IIIA	T0 à T3	abs à ≥ 5 cm	N2	un ou plusieurs	M0	Absence
	T3	≥ 5 cm	N1	Homolatérale axillaire	M0	Absence
IIIB	T4	invasion locale	N0 à N2	Abs à un ou plusieurs	M0	Absence
IIIC	T0 à T4	abs à invasion locale	N3	sous claviculaire	M0	Absence
IV	T0 à T4	abs à invasion locale	N0 à N3	Abs à sous claviculaire	M1	Présence

B

Score	Formation de tubules	Pléomorphisme nucléaire	Nombre de mitoses
1	≥ 75 % surface tumeur	noyaux réguliers et monomorphes	0 ou 1
2	10 à 75 % surface tumeur	atypie cyto-nucléaire modérée	2 ou 3
3	≤ 10 % surface tumeur	noyaux pléomorphes avec atypie marquée	> 3

somme

C **Classification SBR**

Score total	Grade
3-5	1
6-7	2
8-9	3

Tableau 3 : Classifications des cancers du sein. L'examen clinique (A) et histologique (B) de la tumeur permet de déterminer respectivement le stade TNM (A) et le grade SBR (C). Ces stades et grades correspondent à des niveaux d'agressivité croissants illustré par les couleurs vert pâle, vert, rose et rouge.

En 1896, **George Thomas Beatson**, montre le rôle des hormones dans le cancer du sein en guérissant 2 femmes atteintes d'un cancer du sein par castration. Néanmoins, ce n'est qu'en 1958 que **Eldwood Jensen** décrit le récepteur aux oestrogènes de type alpha (**ER**) dans le cancer du sein. De cette découverte naitra la première thérapie ciblée : le tamoxifène. En 1974, **Horwitz et McGuire** identifie le récepteur à la progestérone (**PR**), un autre récepteur hormonal, dans les cancers sein. Enfin, le gène de l'Human Epidermal Growth Factor Receptor 2 (**HER2**) fut identifié entre 1982 et 1984 puis fut l'objet d'un ciblage (Trastuzumab). Perou *et al*. proposent ainsi dans les années 2000 une **classification moléculaire** reposant sur le profil d'expression notamment de ces 3 biomarqueurs protéiques : le sous-type **« luminal-like »** qui exprime les récepteurs aux oestrogènes (ER+) et/ou le récepteur à la progestérone (PR+) ; le **« HER2+ »** qui sur-exprime HER2 ; le **« basal like »** qui n'exprime ni ER (ER-) ni PR (PR-) et ne sur-exprime pas HER2 (HER2-) (Perou *et al.*, 2000). Ce dernier est également caractérisé par l'expression des cytokératines 5/6 et/ou l'EGFR.

Par la suite, des tests pronostics reposant sur des **signatures transcriptomiques**, tel que l'**OncotypeDX**, ont permis d'affiner cette classification et de faciliter le choix thérapeutique (Brenton *et al.*, 2005). Néanmoins, ces tests n'identifient pas l'ensemble des patientes pour lesquelles une stratégie thérapeutique plus agressive serait nécessaire pour éviter la formation de métastases. En effet, ceci resulte du fait que ces tests sont réalisés non seulement sur les cellules tumorales mais aussi du microenvironnement tumoral. Or, une étude menée dans les cellules cancéreuses spécifiquement montre qu'**une augmentation de la signalisation mammalian-enabled (Mena)-cofilin high »**) est associée à une **dissémination accrue** (Karagiannis et al., 2016).

Malgré ces efforts pour stratifier les patientes, les TNBC, en raison de leur potentiel accru à récidiver et former des métastases, restent encore particulièrement meurtriers (Lehmann *et al.*, 2011).

1.2. Les cancers du sein triple négatifs : un échec thérapeutique

1.2.1. De la classification au pronostic et choix thérapeutique

Les TNBC représentent **15-20 %** de l'ensemble des cancers du sein chez la femme. Il est à noter que le sous-type basal semble moins fréquent chez l'homme (5-6 % ; **Figure 4 A** ; Plasilova *et al.*, 2016; Yu *et al.*, 2013). Le diagnostic chez la femme survient plus tôt avec un âge médian de 50 ans. De plus, la fenêtre d'âge de diagnostic est large : de 20 à plus de 90 ans (**Figure 4 B;** Fayaz *et al.*, 2019; Kassam *et al.*, 2009). De façon intéressante, ce sous-type affecte plus fréquemment des femmes jeunes ou au contraire plus âgées (**Figure 4 B;** Kolečková *et al.*, 2017). Chez les patientes âgées de moins de 50 ans ce sous-type est associé à un mauvais pronostique (survie globale). Or, si les récidives surviennent en générale rapidement pour ce sous-type, 5 % des patientes sans récidives à 5 ans développeront des récidives par la suite (Reddy *et al.*, 2018). Les TNBC représentent également la majorité des cancers du sein chez les femmes âgées de plus de 90 ans (50 % ; Kolečková *et al.*, 2017). Ces 2 tranches d'âge ne sont pas concernées par les campagnes de dépistages ce qui contribue à une détection plus tardive.

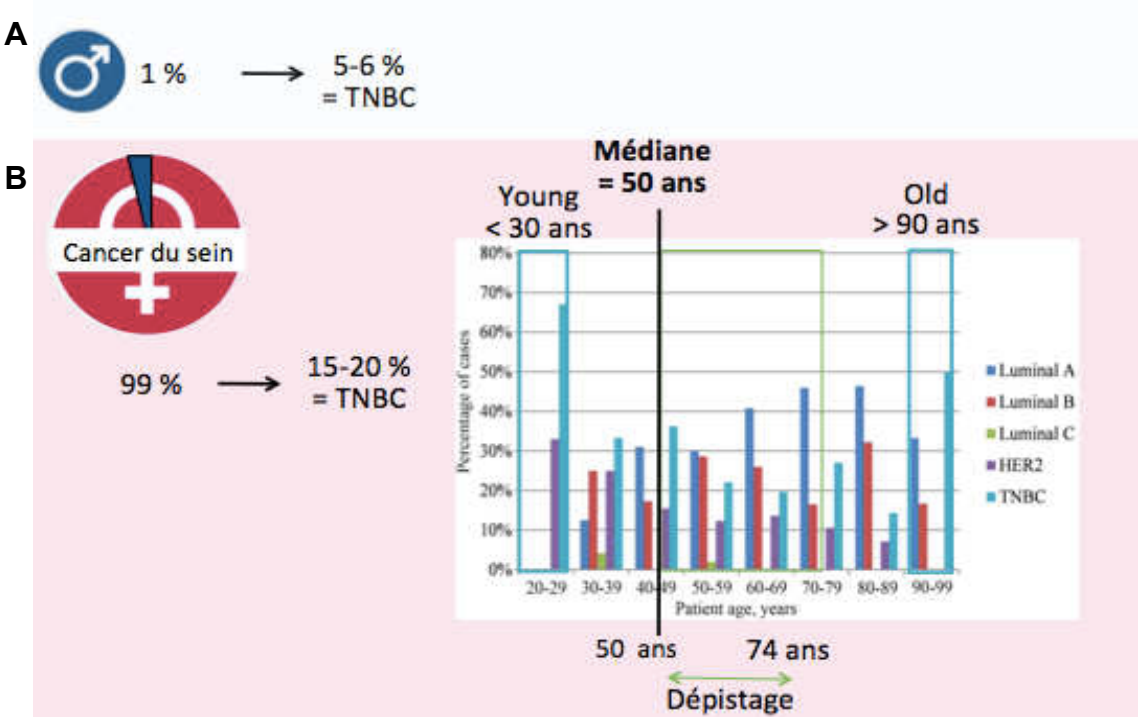


Figure 4 : Profil des patients diagnostiqués avec un TNBC. Les TNBC affectent les hommes et les femmes mais sont plus fréquents chez les femmes. Ils touchent des femmes de tout âge mais constitue le sous-type majoritaire pour les femmes de moins de 30 ans et de plus de 90 ans (d'après Kolečková et al., 2017).

Les TNBC sont dans **95 %** des cas des **carcinomes invasifs**. Ils sont majoritairement de **stade II,** et ce, indépendamment du pays d'origine (**Tableau 2**). Néanmoins, bien que moins abondants, ce sont les TNBC de stades III et IV, qui sont les plus problématiques. En effet, ils sont associés à une diminution de la survie (Park *et al.*, 2011)**.** Ces stades se distinguent des stades I et II notamment par une infiltration nodale (**Tableau 2**). Or, il a justement été montré qu'elle constitue un marqueur pronostic de moindre survie (Urru *et al.*, 2018). De plus, d'un point de vue histologique, ils sont peu différenciés et de haut grade (grade 3) (Park *et al.*, 2011). Ce haut grade est également associé à une diminution de la survie (globale et sans récidive) et est notamment du à leur potentiel prolifératrice accru (Kim *et al.*, 2012). Ce haut taux de prolifération se traduit par un marquage Ki67 élevé et constitue un marqueur pronostic de mortalité (Urru *et al.*, 2018). Les TNBC présentent également souvent une nécrose centrale et une vascularisation importante.

	Origine	Corée Park *et al.* 2011	Singapour Tang *et al.* 2019	Brésil Gonzalez et al. 2018	Italie Uru *et al.* 2018
Stade TNM	I	33,20%	27,20%	14,90%	25,10%
	II	**56,80%**	**42,60%**	**49,30%**	42,70%
	III	10%	21,40%	35,80%	19,10%
	IV	NI	8,70%	NI	1,20%
	ND	0%	0%	0%	11,90%
Grade SBR	1	3,20%	2%	20,90%	1,30%
	2	24,30%	15,60%	40,70%	20,10%
	3	**72,50%**	**73,30%**	38,40%	71,30%
	ND	0%	9%	0%	7,30%

Tableau 2 : Répartition des cancers du sein triple négatifs entre les diffèrents stades TNM et grades SBR. Les 4 cohorts de patientes correspondent à des patientes d'origines géographiques diffèrentes et donc des systèmes socio-économiques distincts. Dans l'ensemble de ces études, le stade TNBC (accolade noir) II représente environ la moitié des cas (ligne du tableau en vert). Pour le grade SBR (accolade grise), les études menées en Corée, Singapour et l'Italie présentent environ 70 % de grade 3. La cohorte de patientes du Brésil présente une répartition légèrement diffèrente avec d'avantage de stade I et II.

Au niveau moléculaire, les TNBC se caractérisent par une absence ou un **très faible marquage** en immunohistochimie des récepteurs **ER, PR et**

HER2 (Brenton *et al*., 2005). Les seuils d'inclusion sont fixés par l'American Society of Clinical Oncology, l'American College of Pathology et Saint Gallen Guidelines à moins de 1 % pour les ER et PR (IHC) et entre 0 et 1 % pour HER2 (IHC) ou une absence d'amplification du gène HER2 (FISH). Cependant, dans des publications plus anciennes des taux plus élevés des récepteurs (jusqu'à 10 %) étaient acceptés (Wolff *et al*., 2013) et sont encore d'usage en France. La majorité des TNBC appartiennent ainsi au type « basal-like » précédemment décrit (Bidard *et al*., 2007). Néanmoins, les TNBC constituent une pathologie très hétérogène d'un point de vue moléculaire et pronostique.

Leheman *et al*. ont en particulier montré grâce à l'analyse transcriptomique de 587 tumeurs l'existence de **6 sous-types** avec des profils moléculaires diffèrents (Lehmann *et al*., 2011; **Tableau 3**, ligne profil moléculaire). L'utilisation de molécules qui ciblent les caractéristiques de chaque sous-type est ainsi proposée pour améliorer la prise en charge des TNBC (Lehmann *et al*., 2011; **Tableau 3**, ligne traitement). Tout d'abord, les sous-types BL1 et 2 **(« Basal-Like » 1 et 2)** sont caractérisés par une **prolifération cellulaire intense**. Cette prolifération intense est associée à la surexpression des gènes impliqués dans le cycle cellulaire et la division cellulaire (*Myc*, *NRas*) pour les tumeurs BL1 et les gènes des facteurs de croissance (*EphA2*, *EGFR*) et du métabolisme du glucose (glycolyse et néoglucogenèse) pour les tumeurs BL2. Ces 2 sous-types peuvent ainsi être traités avec du **cisplatine**, un agent alkylant des bases azotées de l'ADN (qui empêche la réplication et transcription). Le sous-type **IM** (« Immunodulatory ») pour lequel on observe l'expression de gènes exprimés dans les cellules du système immunitaire. Les sous-types **M** (« Mesemchymal ») et **MSL** (« Mesenchymal Like ») sont 2 sous-types dont le **potentiel métastatique est accru**. En effet, les tumeurs **M** expriment d'avantage les gènes impliqués dans la mobilité cellulaire, la différenciation, la croissance cellulaire (protéines Rho, signalisation Wnt). Pour le sous-type **MSL** les gènes en lien avec des facteurs de croissance, l'angiogenèse mais aussi des marqueurs souches et d'EMT (transition myoépithéliale) sont également surexprimés (*EGFR*, *GPCR*, *VEGFR*, *TIE1*). Les tumeurs du sous-

type MSL sont ainsi moins proliféatrices que celles du sous-type M. Les cellules cancéreuses MDA-MB-231 font parties de ce sous-type. Ces 2 sous-types peuvent être traités avec du NVP-BEZ235 ou du Dazatinib qui inhibent respectivement la PI3-Kinase et Src. Enfin le sous-type **LAR** (« Luminal Androgen Receptor ») constitue le sous-type le plus diffèrent. Malgré l'absence de surexpression de l'ER, les gènes impliqués dans la régulation hormonale sont surexprimés. Le Bicalutamide, un anti-androgène, peut ainsi être utilisé pour traiter les tumeurs LAR.

(Sous-)type	Luminal		HER2+	Triple négatif					
	A	B		BL1	BL2	IM	M	MSL	LAR
Profil moléculaire	ER+, PR+		HER2+	ER-, PR-, HER2-					
	HER2-, Ki-67-	HER2+/-, Ki-67+		Gènes DDR+, prolifération+	Marqueurs myoépithélials +, Gènes GF+	Gènes SI +	Gènes EMT+	Gènes EMT+, prolifération -	Gènes AR+
Traitement	Tamoxifen	Tamoxifen +IA	Herceptin	Cisplatine			NVP-BEZ235 ou Dasatinib		Bicalutamide
Pronostic	Bon	Moins bon	Moyen	Mauvais					
Références	Brenton *et al.*, 2005			Lehmann *et al.*, 2011					

Tableau 3 : Caractéristiques moléculaires, traitements préconisés et pronostics associés à différents sous-types de cancer du sein. *Les « + » et les « – » désignent respectivement la présence et l'absence d'expression du gène à l'exception de HER2 où ils traduisent la sur-expression ou non. BL1/2 : Basal-Like 1/2 ; IM : « ImmunoModulatory » ; M : « Mesenchymal » ; MSL : « Mesenchymal Stem-Like » ; LAR : « Luminal AR » ; KI67 : marqueur de prolifération ; DDR : « DNA Damage Response » ; GF : « Growth Factor » ; SI : Système Immunitaire ; EMT : « Epithelial-Mesenchymal Transition » ; AR : Androgen Receptor. IA : Inhibiteur d'aromatase ; NVP-BEZ235 : inhibiteur PI3K/mTOR ; Dasatinib : inhibiteur abl/src ; Bicalutamide : AR antagoniste.*

Malgré les efforts de stratification pour identifier les tumeurs les plus agressives et adapter la stratégie thérapeutique, la prise en charge des patientes présentant un TNBC se limite majoritairement à la chirurgie, la radiothérapie et la chimiothérapie. Or, en plus de leur efficacité limitée (efficace dans moins de 50 % des cas), ces techniques ne sont pas spécifiques et nuisent à la qualité de vie de la patiente.

1.2.2. Prise en charge, résistance et métastases

Si les hormonothérapies et les anti-HER2 ont permis d'améliorer le pronostic des cancers du sein luminaux et HER2+, les TNBC n'y sont pas

sensibles en raison de leur profil moléculaire (ER-,PR-, HER2-) (Brenton *et al.*, 2005). La prise en charge des patientes avec un TNBC repose ainsi sur la chirurgie, la chimiothérapie et la radiothérapie. Le schéma thérapeutique peut comprendre l'ensemble ou une partie de ces techniques selon le stade au diagnostic (**Figure 5**).

La **chirurgie** consiste en une ablation partielle (chirurgie conservatrice ou tumorectomie) ou totale du sein (mastectomie) et des ganglions et tissus épidermiques sous-jacents (mastectomie radiale modifiée). Malgré leur haut grade et leur agressivité, l'ablation partielle peut-être une option choisie par la patiente lorsque les paramètres histo-clinico-pathologiques de la tumeur y sont propices. En effet, il a été montré que le taux de récidive locorégionale à 5 ans n'est pas plus élevé que dans les autres sous-types suite à une **chirurgie conservatrice** (Freedman *et al.*, 2010). En plus de la chirurgie locale, certaines métastases peuvent également être reséquées. De plus, pour éliminer les cellules restantes et éviter les récidives locorégionales la chirurgie peut être suivie d'une **radiothérapie adjuvante** (**Figure 5**).

La **radiothérapie** classique consiste en plusieurs irradiations de 2 Gy de l'ensemble du sein correspondant à une dose totale d'environ 45-50 Gy (Demaria and Formenti, 2012). Elle semble particulièrement recommandée suite à une chirurgie conservatrice afin d'éliminer les cellules residuelles. En effet, elle réduit le risque de récidives pour des TNBC à des stades peu avancés (T1-2 N0) (Abdulkarim *et al.*, 2011). De plus, elle améliore également la survie des patientes (globale et spécifique), en particulier pour les stades avancés (T3-T4) (Yao *et al.*, 2019). Une **chimiothérapie adjuvante** peut également être réalisée pour éviter les récurrences locorégionales mais aussi en thérapie palliative pour les TNBC métastatiques (**Figure 5**).

La **chimiothérapie** est la seule thérapie systématiquement utilisée pour les TNBC. La chimiothérapie repose sur une combinaison de molécules : les antimétabolites qui remplacent des métabolites normaux (5-Fluorouracile, méthotrexane, la capécitabine ou la gemcitabine), les **anthracyclines qui** s'intercalent dans l'ADN (doxorubicine et l'épirubicine) les agents alkylants qui

incorporent un groupement alkyle dans certaines bases de l'ADN (cyclophosphamide) et les poisons du fuseau mitotique qui empêchent la polymérisation de la tubuline (vinorelbine, taxanes, eribuline). La composition de la chimiothérapie dépend du profil de la tumeur. Pour les TNBC, la chimiothérapie comprend classiquement des anthracyclines et des taxanes (paclitaxel, doxétaxel). La chimiothérapie peut être réalisée après l'exérèse pour éliminer les cellules cancéreuses restantes (chimiothérapie adjuvante) notamment pour les tumeurs de **bas grade** (**Figure 5**). Les effets de l'administration d'une chimiothérapie adjuvante pour les TNBC de bas grade semblent néanmoins controversés (Fu *et al.*, 2020). Son effet peut être maximisé en optimisant le délai chirurgie-chimiothérapie (moins de 30 jours) ou par l'addition d'une thérapie ciblée (Li *et al.*, 2018). En particulier, l'ajout d'un traitement avec des « **Cytokine inducer killer »** (immunothérapie) à la chimiothérapie adjuvante a montré des résultats prometteurs pour traiter des TNBC de stades peu avancés (Zhang *et al.*, 2019). De plus, une étude montre que l'addition de capécitabine à une chimiothérapie classique (taxane et anthracycline) permet d'augmenter la survie sans récidive. Néanmoins, cette amélioration reste modeste (86,3 % vs 80,4 %; Li *et al.*, 2020). Dans le cas des TNBC de **haut grade**/avancés, la chimiothérapie pourra être réalisée avant la chirurgie (néoadjuvante ; **Figure 5**) afin de réduire la taille de la tumeur et d'améliorer le pronostic. En effet, en raison de leur haut pouvoir prolifératrice, les TNBC présentent une sensibilité accrue aux **chimiothérapies néoadjuvantes** par rapport aux autres types de cancers du sein. Elle diminue ainsi le risque de récidive locorégionale dans les 5 ans (Abdulkarim *et al.*, 2011). En revanche elle ne permet une réponse complète que pour environ 20 % des patientes (Liedtke *et al.*, 2008). Cette réponse est conditionnée par la séquence de traitement mais aussi le sous-type défini par Leheman *et al.* Par exemple dans une étude comparative menée par Liedtke *et al.*, l'administration pendant une semaine toutes les 3 semaines de paclitaxel/doxorubicine suivie de fluorouracile, doxorubicine, et cyclophosphamide s'est avérée la meilleure stratégie (taux de réponse complète de 28 %) (Liedtke *et al.*, 2008). De plus, les patientes avec un TNBC BL (1 ou 2) présentent un pourcentage de réponse aux thérapies à base de taxanes respectivement 2 et 4 plus élevé que pour les sous-types

MSL et LAR. Néanmoins, Masuda *et al.* ont montré qu'il existe une hétérogénéité de réponse entre le sous-type BL1 et 2. Les BL1 présentent le taux de réponse complète à la chimiothérapie néoadjuvante (absence de détection de carcinome invasif et d'envahissement ganglionnaire) le plus élevé (52 %) tandis que le sous-type BL2 ne présentait pas de réponse dans cette étude (Masuda *et al.*, 2013). Afin d'améliorer les taux de réponses des TNBC, la chimiothérapie néoadjuvante a été associée à d'autres composés notamment les sels de platine. Tous sous-types confondus, l'association carboplatine/paclitaxel augmente le taux de réponse complète mais pas la survie sans progression (Pandy *et al.*, 2018). Cette association semble particulièrement efficace pour les tumeurs mutées BRCA pour lesquelles l'association est synergique. Afin d'étendre ce type d'approches combinées, des études similaires avec des thérapies ciblant des récepteurs membranaires surexprimés ou leur ligand ont été menées.

La combinaison nab-paclitaxel avec l'**atezolizumab** (Tecentriq®), un anticorps monoclonal ciblant PDL1, a ainsi fait l'objet d'un essai clinique de phase III sur des TNBC métastatiques PDL1–positif. Cette immunothérapie combinée à la chimiothérapie améliore significativement et durablement la survie sans progression sur des patientes (Schmid *et al.*, 2018). Cette combinaison est ainsi approuvée par la FDA depuis décembre 2019 pour les TNBC locaux avancés non opérables et les TNBC métastatiques. En France, ce traitement a bénéficié d'une autorisation temporaire d'utilisation (ATU). Néanmoins, le résultat mitigé de l'étude a mené à la suspension de son utilisation pour les TNBC locaux avancés non opérables et les TNBC métastatiques. D'autre part, le ciblage du VEGFR, avec le **Bevacizumab** (anticorps monoclonal) est approuvé par l'ANS (Agence Nationale de la Santé) pour les TNBC métastatiques. D'autres RTK surexprimés dans les TNBC, font l'objet d'un ciblage dont l'EGFR. De façon intéressante, le **Cetuximab** en combinaison avec une chimiothérapie (paclitaxel) ou en monothérapie a montré des effets notables lors d'études pré-cliniques et cliniques (Liao *et al.*, 2019; Sabatier *et al.*, 2019). **Néanmoins, ni le Bevacizumab ni le Cetuximab n'améliorent significativement la survie globale**. De plus, les thérapies ciblées sont associées à des **mécanismes de**

résistance innés ou acquis. Ces mécanismes peuvent résulter de mutations, plus fréquentes dans les TNBC en raison de leur forte instabilité génétique. Toutefois, ces mécanismes génétiques ne permettent pas d'expliquer l'ensemble des résistances. En effet, des études génomiques ont montré que certaines patientes ne répondant pas aux thérapies ne présentent pas de mutations. De plus, même diagnostiquées précocement (stade I/II) 50 % des patientes sont victimes d'une récidive et 37 % décèdent dans les 5 ans suivant la chirurgie (Liedtke *et al.*, 2008). Les récidives et les décès sont en particulier associés à la formation de métastases. En effet, dans les TNBC le taux survie relative des patientes avec métastases est de 11 % contre 91 % pour un stade local (American Cancer Society, chiffres 2010-2015). Ainsi, il est encore aujourd'hui nécessaire de mieux comprendre les mécanismes impliqués dans le processus métastatique et les résistances aux thérapies pour améliorer la prise en charge des TNBC.

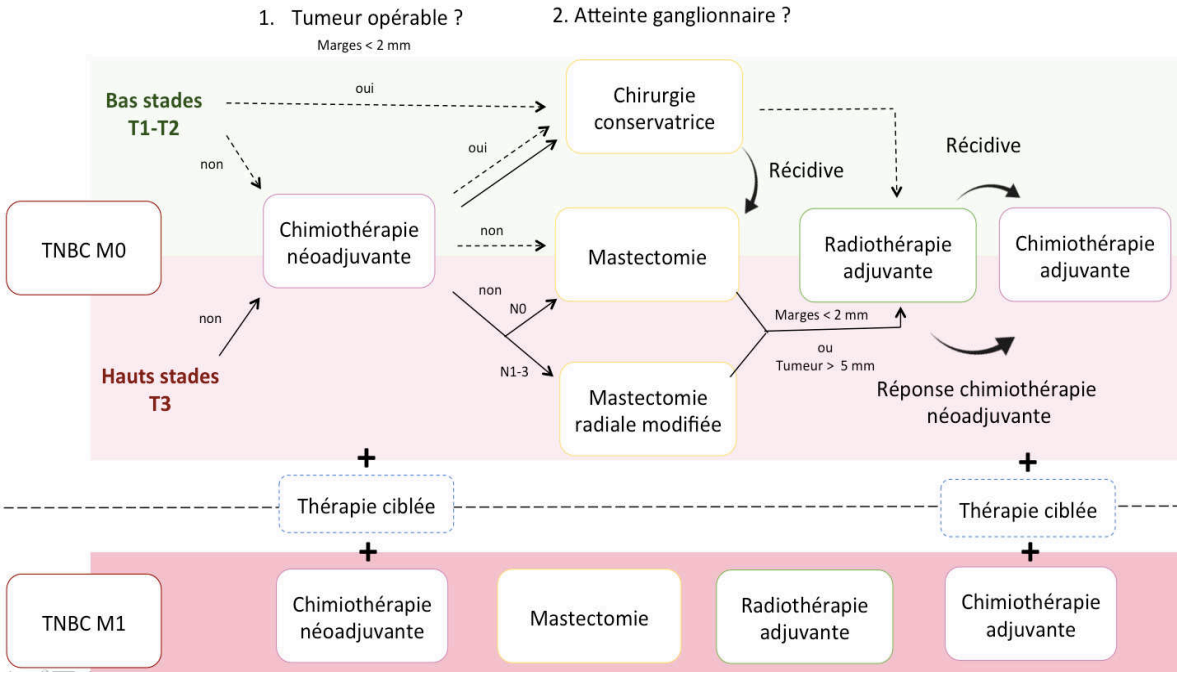


Figure 5 : Prise en charge des cancers du sein triple négatifs. Le schéma thérapeutique pour la prise en charge des TNBC dépend du stade au diagnostic. Dans le cas de TNBC non métastatique (M0), une chimiothérapie néoadjuvante pourra être réalisée pour réduire la taille de la tumeur avant la chirurgie. Différentes chirurgies plus ou moins invasives peuvent être proposées à la patiente, avant d'entreprendre une radiothérapie et éventuellement une chimiothérapie. Dans le cas des TNBC métastatiques, une chimiothérapie néoadjuvante suivie d'une mastectomie (+ résections éventuelles des métastases) puis d'une radiothérapie et d'une chimiothérapie adjuvante seront réalisés pour lutter contre le cancer primaire et les métastases.

Les **métastases** peuvent apparaître après la prise en charge de la patiente ou être présentes au diagnostic. Les récidives métastatiques sont plus fréquentes pour ce sous-type et peuvent survenir parfois de nombreuses années plus tard (Haffty *et al.*, 2006). De plus, en raison de leur fort potentiel prolifératrice, les TNBC sont moins souvent dépistés grâce aux mammographies de contrôle par rapport aux autres sous-types. Les TNBC sont ainsi diagnostiqués à des stades plus avancés que les cancers du sein hormono-dépendants et les métastases au diagnostic sont également plus fréquentes. De façon intéressante, il a été montré que les cancers du sein présentent un tropisme métastatique qui différent selon les sous-types. Ainsi, les cancers hormonaux-dépendant métastasent dans les os, les poumons, le foie et dans une moindre mesure le cerveau. Les cancers **HER2+ et les TNBC métastasent d'avantage au niveau du foie** (31 % pour les HER2+ et 22 % pour les TNBC contre 15 % pour les « luminal » A) **et du cerveau** (HER2+ 8% et TNBC 9% contre 4% pour les « luminal » A) (Wu *et al.*, 2017). Dans le cas des récidives, le cerveau et les poumons sont les sites les plus fréquents (Lin *et al.*, 2012). Les métastases sont particulièrement problématiques car elles génèrent des défaillances multi-viscérales qui touchent notamment le foie et le poumon. Les métastases osseuses génèrent quant à elles des douleurs chroniques et des fractures (Tsuzuki *et al.*, 2016). Enfin, les **métastases cérébrales** sont plus fréquentes que dans les cancers du sein hormono-dépendants (Wu *et al.*, 2017). En effet, on estime qu'environ **un tiers des patientes** ayant un cancer du sein triple négatif développe une métastase cérébrale. Ces métastases causent des troubles neurologiques (sensoriels et cognitifs) et altèrent ainsi grandement la qualité de vie de la patiente (Quigley *et al.*, 2013). De plus, le taux de mortalité lors de leur diagnostique peut aller jusqu'à 80 % dans l'année suivante (Lv *et al.,* 2021). Ceci s'explique notamment par le fait que la barrière hémato-encéphalique empêche le passage de certains traitements ce qui limite grandement l'arsenal thérapeutique. Or, les acteurs et les mécanismes moléculaires mis en jeu sont encore mal connus.

Les TNBCs constituent ainsi un sous-type de cancers du sein hétérogène, résistant et métastatique pour lesquels l'arsenal thérapeutique

est extrêmement limité et aspécifique. Ainsi pour améliorer la prise en charge des patientes atteintes d'un cancer du sein tiple négatif, il est nécessaire d'identifier de nouvelles cibles thérapeutiques pour mettre au point de nouvelles thérapies ciblées. Or, notre laboratoire a montré que le récepteur à activité tyrosine kinase TrkA est surexprimé (à l'échelle de la protéine) et phosphorylé dans les cancers du sein (Lagadec *et al.*, 2009). De plus, la surexpression de TrkA dans des cellules cancéreuses mammaires triples négatives MDA-MB-231 restaure un taux d'expression similaire à celui trouvé chez les patientes et favorise la croissance tumorale et le processus métastatique (Lagadec *et al.*, 2009). Le récepteur TrkA apparaît ainsi comme une cible thérapeutique potentielle pour empêcher la progression voire traiter les TNBC (formation et progression des métastases).

2. Le récepteur TrkA

2.1. Le récepteur TrkA : un récepteur aux rôles pléiotropes

2.1.1. Rôles physiologiques de TrkA

TrkA est le récepteur de haute affinité du Nerve Growth Factor, un facteur de croissance des cellules nerveuses. Le récepteur TrkA est majoritairement exprimé dans les cellules nerveuses où il joue un rôle majeur lors du développement embryonnaire mais aussi dans le maintien du fonctionnement physiologique du système nerveux après la naissance.

Durant le développement embryonnaire, l'expression de TrkA dans les **ganglions des racines dorsales**, nerfs émergents de la moelle épiniaire, varie. En effet, chez la souris il a été montré que TrkA est peu exprimé avant le jour 10,5 contraiment à TrkB et TrkC. Puis, entre le jour **10,5 et 13,5**, son **expression augmente**. Du jour 13,5 à la naissance, la majorité des neurones des racines dorsales expriment TrkA (Phillips & Armanini, 1996). Pour expliquer cette augmentation d'expression de TrkA, il fût initialement proposé que celle-ci résulterait de l'exposition des neurones sensoriels au NGF produit par les cellules cibles de ces neurones. Néanmoins, des souris n'exprimant pas le NGF présentent une expression normale de TrkA au niveau des ganglions trigéminaux, ganglions situés à la base du crâne sur la face antéropostérieure. Ces observations suggèrent donc l'implication d'autres facteurs dans l'augmentation d'expression de TrkA (Davis *et al.*, 1995). De plus, la fixation du NGF sur TrkA, **après le jour E13,5**, assurent la **survie des neurones sensoriels**. Le récepteur TrkA, à l'âge adulte, intervient ainsi dans les perceptions sensorielles dont la perception de la douleur. Dans ce sens, des mutations perte de fonction de TrkA, observées chez les patients atteints de syndrôme d'insensibilité à la douleur, provoquent une altération des capacités à percevoir les changements de température et la douleur. Ces mutations vont, en effet, altérer la phosphorylation de TrkA induite par la fixation du NGF et ainsi déréguler les voies de signalisation sous-jacentes.

2.1.1. Activation de TrkA et de ses signalisations

TrkA est un récepteur à activité tyrosine kinase (RTK). Comme les autres RTKs le modèle classique de transactivation a été proposé pour expliquer l'activation des signalisations sous-jacentes : fixation du ligand, changement de conformation, phosphorylation. Dans une revue intitulée « **TrkA, behind the myth of RTK transactivation model** », nous revenons sur les limites de ce modèle pour expliquer la complexicité de la régulation de la phosphorylation de TrkA et de ses voies de signalisation.

TrkA: behind the myth of the RTK transactivation model

Trouvilliez Sarah[1], Toillon Robert-Alain[1, *].

[1] Univ. Lille, CNRS, INSERM, CHU Lille, UMR9020-U1277 - CANTHER - Cancer Heterogeneity Plasticity and Resistance to Therapies, F-59000 Lille, France

*** Corresponding author:** Prof. Robert-Alain Toillon, UMR9020-U1277 - CANTHER - Cancer Heterogeneity Plasticity and Resistance to Therapies, Bâtiment SN3, 3ème étage, Cité Scientifique, Université de Lille, 59655 Villeneuve d'Ascq, France. Phone: +33 (0)3 20 43 65 59
E-mail: robert-alain.toillon@univ-lille.fr

Keywords: TrkA – RTK – Signaling - Structure

Abstract

The NGF–TrkA axis has been shown to be involved in various physiopathological contexts. Nevertheless, despite considerable progress made in understanding NGF and TrkA functions since their discovery, many aspects of this axis need to be elucidated. Therefore, a trans-autophosphorylation model has been proposed to explain the TrkA structure–function relationship, but this model is imperfect. In fact, this model does not explain the diversity of the biological functions (survival, migration, and differentiation) triggered by TrkA activation in different cellular contexts (the brain, immune cells, etc.). In this review, to explain the diversity of TrkA functions, we revisit the classical RTK structure–function relationship. After recapping the main aspects of NGF and its receptors, we discuss the limits of the trans-autophosphorylation model in explaining TrkA activation. Then, we explore how genetic mechanisms can diversify TrkA function. We also describe the role played by the microenvironment in TrkA activation and function.

Introduction

Our understanding has been profoundly advanced since Rita Levi-Montalcini discovered nerve growth factor (NGF) and later with the discovery its receptors; however, many aspects of NGF action remain unclear. Therefore, the complexity and diversity of cellular responses induced by TrkA and its ligands indicate that an on/off model imperfectly recapitulates TrkA action. Indeed, this type of model fails to explain how TrkA activation can result in the diversity of biological functions attributed to TrkA, including cell survival, migration, and differentiation. In this review, to explain the diverse effects of TrkA function, we revisit the initial explanation of the RTK structure–function relationship. After describing the main aspects of NGF and its receptors explained in the 70 years since their discovery, we discuss the limits of the classical RTK model of TrkA activation. Then, we explore how genetics can lead to diverse TrkA functions. We also describe the role played by the microenvironment in TrkA activation and function.

1. TrkA activation: more than a classical RTK activation model

1.1- Seventy years have passed since the discovery of NGF.

Nerve growth factor (NGF) was discovered in the early 1950s by Rita Levi Montalcini[1]. In fact, Rita Levi-Montalcini and Stanley Cohen received the Nobel Prize in Physiology and Medicine for this discovery in 1986. Nevertheless, many other works have explained the structure and function of NGF (**Figure 1**). For example, initial observations were described by Hamburger, who showed that the amputation of a wing bud induced the death of motor neurons[2]. Hamburger concluded a differentiating factor was lost with the wing bud removal. Four years later, Levi-Montalcini reproduced Hamburger's experiments and proposed that the neuronal death in this context was due to the absence of a trophic factor produced by peripheral tissues[3,4]. Then, Bueker performed experiments with tumor xenografts in chick embryos indicated, which an increase in the number of lymph nodes near a tumor, and he hypothesized that a peripheral factor of differentiation was involved in this change[5]. Levi-Montalcini resumed observed that fibers

invade the viscera and blood vessels and concluded that this invasion results in humoral factor production by tumor cells[1]. Through collaboration between Levi-Montalcini and Stanley Cohen, the factor was purified from sarcoma[6] and snake venom[7] and named “NGF” for nerve growth factor. Then, Angeletti contributed to the analysis by reporting the spectrum of NGF action in the peripheral nervous system and the mechanism of immunological sympathectomy development during early postnatal life[8]. Next, different groups contributed to descriptions on the NGF structure. The first, Shooter and Varon groups defined the activity of a high-molecular-weight complex called 7S NGF[9]. In addition, a smaller active compound was discovered by Piero Angeletti and Vincenzo Bocchini (called 2.5S NGF)[10]. Then, the primary structure of NGF was resolved with Nuclear Magnetic Resonance (NMR) by Ruth Hogue Angeletti and Ralph Bradshaw[11]**.** Although Levi-Montalcini had previously described invasion by macrophages, Aloe was the first to clearly demonstrate that NGF not only acts on neuronal cells but also on other cell types, especially immune cells such as mast cells. Aloe found that injecting NGF into animals increases the number and size of mast cells. He explained that targeting NGF showed therapeutic potential not only for neurodegenerative diseases but also for inflammation.

NGF is a member of the neurotrophin family that also includes brain-derived neurotrophin factor (BDNF), neurotrophin-3 (NT-3) and NT 4-5. Neurotrophins share approximately 50% sequence identity, but only NGF, not pro-NGF or NT-3, bind TrkA. NGF is encoded by a gene located on chromosome 1p22 and spans more than 45 kb. *NGF* includes 4 exons: IA-B; II; IIIA-B; and IV. *NGF* transcription results in 4 different transcripts because of 2 promoters and alternative splicing[13]. NGF is produced as a pre-proneurotrophin that during maturation undergoes two cleavage events to produce mature NGF[14], lead to sequential elimination of the signal peptide (pre) and then the prodomain. ProNGF spontaneously homodimerizes *via* noncovalent bonds. The prodomain is a flexible region that interacts with and stabilizes the mature part of NGF. Then, a second cleavage event at the Arg-Ser-Lys/Arg-Arg motif inside the cell or in the extracellular medium of the prodomain (103 amino acids) results in the production of mature NGF (118 amino acids). An NGF dimer has a molecular weight of approximately 27 kDa. The monomers are

composed of 7 B-strands in 2 sheets and are connected by 3 disulfide bonds. Two monomers interact in an antiparallel manner *via* noncovalent bonds. NT-3 is encoded by NTF3, which is located on chromosome 12p13[15]. Two isoforms are produced by alternative splicing. Similar to NGF, NT-3 is synthetized as a pre-pro-NT-3 that is cleaved twice to produce the mature form. The signal peptide has a length of 18 amino acids, the prodomain comprises 120 amino acids, and the mature NT-3 comprises 119 amino acids. An NT-3 homodimer has a molecular weight of approximately 27 kDa. The monomers exhibit a structure and spatial organization that are identical to those of NGF[16].

The NGF tyrosine kinase receptor, TrkA, was discovered in 1973, Barnajee *et al.* that showed that NGF binds to the cell membrane at specific binding sites. In 1986, an other NGF receptor was discovered: P75[NTR17,18], which is the common low-affinity receptor of neurotrophins and is part of the super family of death receptors, and TrkA, which had been originally discovered by Pulciani *et al.* (1982)[19] as *Onc D* and isolated later by Martin-Zanca *et al*. (1986) in colon cancer. Specifically, Martin-Zanca *et al*. identified *NTRK1* as an oncogene due to the translocation of a tropomyosin (the first 7 exons) fused to a tyrosine kinase (*TPM3*); therefore, it was renamed tropomyosin receptor kinase (Trk)[20]. The structure of TrkA was described in 1989, and TrkA was assumed to a member of the receptor tyrosine kinase (RTK) family[21] and, more precisely, to be a high-affinity receptor for NGF[22,23] that also binds NT-3 and NT-4[24,25]. TrkB, which shows sequence analogy with TrkA[23] and is a BDNF receptor, was also discovered[26,27]. TrkC, the final Trk family member to be identified, was discovered to be an NT-3 receptor[28]. The 3 aforementioned receptors share the same 3-domain organization as other RTKs: extracellular, transmembrane and intracellular domains. Each domain is associated with a specific function: the extracellular domain controls ligation, the transmembrane part controls signal transduction and the intracellular part activates specific signaling cascades (**Figure 2**). These domains are subdivided into structural subdomains. Exon 1 encodes the signal peptide and a cysteine-rich motif, and exons 2-4 encode 3 leucine-rich motifs (LRMs). The 3 LRMs are also called domains D1, D2 and D3. Exon 5 is

a cysteine-rich motif, exons 6 and 7 constitute immunoglobulin-like domain 1 (IgC1 = D4), and exon 8, at least, encodes is immunoglobulin-like domain 2 (IgC2 = D5) (**Figure 2**). Exons 10 and 11 encode the transmembrane domain. In the intracellular domain, exon 12 encodes the juxtamembrane region, exons 13 to 17 encode the catalytic kinase domain, and exon 17 encodes the end of the Trk cytoplasmic tail. Even though Trk receptors share important sequence homology, the primary sequence of the juxtamembrane region differs [29,30]. The juxtamembrane region in Trk receptors also differs in spatial arrangement after ligand stimulation. These observations highlight the importance of these regions to the specificity among Trk receptors but does not explain the diversity of TrkA functions in organisms. Therefore, the diversity of TrkA functions has been attributed to the formation of 3 isoforms, TrkA-I, II and III, which are expressed in specific tissues. Nevertheless, these isoforms do not explain the diversity of TrkA-I or TrkA-II function. In fact, TrkA-II, expressed in neuronal cells, can promote both cell survival and differentiation depending on the ligands to which it binds. That is, TrkA is the high-affinity receptor of NGF, but it can also bind 2 other (pro)-neurotrophins: proNGF and NT-3. TrkA is involved in critical physiological processes implicated in both the development and homeostasis of the nervous and immune systems. TrkA is a microenvironmental sensor that transduces environmental and paracrine signals. As for others RTKs, a classical TrkA transactivation model has been proposed: Upon NGF binding, TrkA dimerizes, leading to a conformational change and phosphorylation of tyrosine residues in the kinase domain *via* trans-autophosphorylation. Then, the phosphorylated kinase domain phosphorylates other intracellular tyrosine residues, enabling the full activation of TrkA and downstream signaling pathways, resulting in a specific cellular response.

Canonical RTK trans-autophosphorylation theory suggests that TrkA activation follows a 3-step process: 1) NGF binds to the receptor, 2) NGF undergoes dimerization/conformational change and 3) intracellular tyrosine-carrying proteins are trans-autophosphorylated. However, increasing evidence demonstrates that this model does not properly explain TrkA action,

and these clues need to be considered to properly understand the mechanisms underlying the activation of TrkA in cells.

1.2. Ligand-specific activation

TrkA phosphorylation is partially dependent on the nature and concentration of the ligand. Indeed, TrkA can bind NGF, ProNGF, and NT-3.

1.2.1 NGF

The IgC1 and IgC2 domains in TrkA had been initially proposed to be critical for the binding of NGF. NGF interaction with IgC2 (TrkA-D5) involves 2 amino acid patches in NGF. The first patch (amino acids 14-23) is highly conserved across neurotrophins. The second patch is composed of amino acids in the N-terminal region (2-13) and confers binding specificity. The most important residues in the N-terminal patch are His-4 and Ile-6, which are embedded into a hydrophobic canyon [31]. Site-directed mutagenesis has been performed, leading to the identification of the TrkA-D5 residues involved in direct and indirect interactions with NGF[32], and the structure of the IgC2–NGF complex has been resolved by NMR[33]. Nevertheless, *in cellulo* experiments indicated that other molecular determinants of TrkA are potentially implicated in TrkA–NGF binding. Therefore, a site of low TrkA binding in the LRM domain has been proposed. Indeed, Scatchard experiments performed with extracts of TrkA-overexpressing HEK-293 cells showed that the measured Kd was tenfold higher than that obtained with a chimeric protein consisting of TrkB carrying the IgC2 domain of TrkA (1.91 nM and 0.29 nM, respectively) [34]. Moreover, Windisch and colleagues showed that a peptide corresponding to the LRM region (97-120 in TrkA) interacted with NGF with nanomolar affinity similar to the full extracellular portion of TrkA[35]. As NGF does not bind the 92-125 or 100-120 amino acid regions, this group suggested that amino acids between these 2 regions are necessary for NGF–TrkA binding. Interestingly, for full TrkA, a second binding site is not always found. The second site has been proposed to be dependent on $P75^{NTR}$ *in cellulo*. Two models have been proposed to explain the effect of P75NTR on the increase in TrkA affinity: $P75^{NTR}$ may present NGF to TrkA (**Figure 3** - model 1) or interact with TrkA (**Figure 3** - model 2). Certain clues tend to validate the

ligand-passing model hypothesis (model 1) involving $P75^{NTR}$. For instance, the NGF^{R100W} mutant discovered in congenital insensitivity to pain disease bound to TrkA not to $p75^{NTR}$ [36]. Nevertheless, the $P75^{NTR}$ passing model does not fit the interaction perfectly. In fact, Windich and colleagues noted that the full extracellular TrkA portion and the LRM domain binds NGF with the same affinity. Moreover, Scatchard experiments with cells expressing only TrkA but not $P75^{NTR}$ revealed that the TrkA Kd was the same as that in cells expressing both receptors [23,37].

1.2.2 ProNGF

TrkA IgC2 residues have been implicated in differences between NGF and proNGF affinities. For instance, Trp-21 in NGF bound His-353 in TrkA, while in proNGF, these two residues did not interact, as Trp21 was inaccessible because of proNGF prodomain steric hindrance[38]. In addition, mass spectrometry analysis of the ProNGF structure has led to refinements in the model of the ProNGF and TrkA association. Authors proposed that lower affinity results in an interaction between the pro- and mature portion of NGF (Arg-41–Phe-33)[39]. Moreover, a study showed that mutated NGF Arg221, which binds IgC2 residues, affects the NGF–TrkA interaction, subsequent signaling and changes in biological responses[40]. Interestingly, both NGF and ProNGF (variant A) promoted survival and differentiation, but TrkA inhibition did not block the effects of ProNGF[41]. This outcome has been attributed to ProNGF variant A, in contrast to NGF, promoting survival *via* $P75^{NTR}$ but not *via* TrkA. Moreover, ProNGF variant (called B)[41] action depended on the TrkA:$P75^{NTR}$ receptor ratio, probably because the binding affinity of ProNGF for TrkA was lower than that of NGF (Kd= 14 nM and 1.8 nM, respectively)[42, 43]. In addition, proNGF binds to sortilin *via* its prodomain and presents proNGF to TrkA to activate proNGF and induce signaling[44] (**Figure 4**).

1.2.3-NT-3

In addition to binding NGF, TrkA can bind NT-3, which is necessary for sympathetic axon growth and target innervation [34]. Indeed, *NT-3*- and *NGF*-null mouse sympathetic neurons died when they expressed high levels of TrkA and low levels of TrkC[45,46]. Moreover, an NT-3 variant that activated

TrkC but not TrkA did not support the survival of sympathetic neurons [47]. This finding suggests that both NGF and NT-3 bound TrkA and that NT-3 binding to TrkA leads to the transduction of a specific signal that differs from that transduced by TrkC. In addition, Ivanenisenic *et al.* demonstrated that NT-3 binds to IgC1 (D4) and IgC2 (D5) to promote full TrkA activation. Because NT-3 could bind only one of these 2 aforementioned sites, the activation of TrkA is low. Moreover, even with IgC2 in an NGF binding site, NT-3 binding shows an additive effect. NT-3 affinity is increased in neuronal cells after alternative splicing of exon 9. The resulting isoform, called TrkA-II, includes 6 more amino acids than TrkA-I (Val-Ser-Phe-Ser-Pro-Val) (**Figure 5**)[48]. This insert is called "an insert of specificity" (**Figure 5**, yellow; Barker *et al*., 1993). Although TrkA-I and TrkA-II exhibit a similar global organization in the extracellular, transmembrane and intracellular domains (**Figure 5**), differences contribute to their distinct physiological functions[50]. In fact, the level of TrkA activation differs on the basis of the type of ligand stimulant. NT-3-induced activation of TrkA (isoform I) was 10-fold less than that induced by NGF [47]. Interestingly, this reduced activation level is sufficient to induce cell differentiation, but activated NT-3 is 20-40-fold less efficient than activated NGF in promoting cell survival [47]. Moreover, the cellular response is not only due to differences in the response magnitude but also to differences in the localization of the signal. Hence, the association of NT-3 with TrkA is lost under acidic conditions, such as in endosomes, in contrast to NGF–TrkA. As a result, NT-3 is less effective in inducing retrograde survival than NGF, which produced signals when inside endosomes [51].

1.3-Stoichiometry and conformation of TrkA

1.3.1- Is TrkA a preformed dimer?

The stoichiometry of the TrkA complex before NGF binding is still debated. All 3 TrkA ligands bind as active homodimers; therefore, it has been hypothesized that TrkA receptors dimerize as homodimers with NGF acting as a bridge. Nevertheless, the observation that the deletion of the TrkA-D5 domain results in TrkA dimerization does not fit this theory. TrkA-D5 deletion results in constitutive activation and transformation of Rat-1 cells, indicating

that the TrkA-D5 NGF-binding site contributes to the maintenance of ligand-dependent TrkA activation (at an autoinhibiting site)[52]. Therefore, TrkA may predimerize at the plasma membrane in the absence of NGF, as observed for the first time by Mischel *et al*. (2002) studying the ectopic expression of TrkA in *Xenopus laevis* oocytes with freeze-fracture. Other studies also contribute to the support of this hypothesis through different approaches; for example, Shen and Maruyama used bimolecular fluorescence complementation and firefly luciferase fragment complementation[53] and Ahmed et Hirstova (2018) performed *Förster* resonance energy transfer (FRET). In addition to these experiments in the assessment of an TrkA-overexpressing system, TrkA association in the absence of NGF is confirmed through a cross-linking experiment. However, all TrkA, including intracellular TrkA, is cross-linked. Hence, Marechetti *et al.* (2013), using ACP–TrkA conjugated to an organic fluorophore, questioned the existence of a TrkA dimer at the plasma membrane. In summary, NGF binding is critical for TrkA receptor immobilization and dimer formation. However, some observations may suggest that TrkA forms dimers before NGF activation or forms them, not at the plasma membrane, but in an intracellular compartment(s).

1.3.2- Does TrkA undergo only a conformational change in the transmembrane region?

The TrkA transmembrane domain is 26 amino acids in length, and its rotation promotes phosphorylation of the tyrosine kinase domain, which leads to the phosphorylation of other intracellular tyrosine residues[54]. Franco *et al.* confirmed that TrkA activation undergoes juxtamembrane and transmembrane domain rotation (Franco *et al*., 2019). They also demonstrate that TrkA residues Ala-421, Ala-425 and Ala-428 (especially Ala-428) rotate and engage in phosphorylation[56]. Ahmed *et al.* showed that this conformational change affects the intracellular juxtamembrane region of TrkA. Interestingly, in contrast to TrkA (and TrkB), ligand binding to TrkC does not affect the conformation of the juxtamembrane region but affects the C-terminal region of TrkC. Therefore, the 3 Trk proteins undergo a

conformational change in the intracellular part after ligand binding, which may result in activation of specific signaling cascades (**Figure 6**).

1.4. Phosphorylation of TrkA

1.4.1- Does signaling depend solely on tyrosine kinases?

The recruitment of signaling partners by TrkA depends on its tyrosine residues, their phosphorylation state and the nature of the neighboring residues (motifs)[57]. The juxtamembrane region includes one tyrosine residue (Tyr-490), and it is in the NPXY motif. The NPXY motif is critical for Shc recruitment when Tyr-490 is phosphorylated and promotes survival (**Figure 7**). Interestingly, this phosphotyrosine residue also binds another adaptor protein, Frs2, which promotes differentiation[59] (**Figure 7**). This parallel activity suggests that Tyr-490 plays a role in the control of the differentiation/survival balance. In addition, other residues in this region play an important role in TrkA signaling; these residues include Cys-436, which is involved in the degree of signaling partner recruitment to the Tyr-490 residue in TrkA. Therefore, the mutation of this residue affects TrkA signaling kinetics[60]. The kinase domain includes 3 tyrosine residues (Tyr-670, Tyr-674, Tyr-675), which is very highly conserved in the Trk family. Hence, TrkA inhibitors that target this region inhibit TrkB and TrkC phosphorylation. Finally, the C-terminal tail in TrkA includes additional phosphorylated tyrosine sites (Tyr-751 and Tyr-785). Notably, Tyr-751 is included in the consensus motif YXXM, and its phosphorylation promotes the recruitment of the p85/subunit of PI3K [61]. phosphorylated Tyr-785 recruits PLCγ1 to promote differentiation (**Figure 7**). In addition, this residue promotes differentiation *via* the recruitment of CHK thanks the CHK SH2 domain[62]. Biarc *et al*. proposed that for certain Trk partners do not readily associate with a tyrosine residue and that the effect of the Tyr-490 mutation can be reversed by binding to Tyr-785[63].

1.4.2- TrkA phosphorylation: an on/off mechanism?

Notably, studies on TrkA phosphorylation suggested that the diversity of signaling is a result of not only differences in TrkA tyrosine specificity but also of specific binding preference differences among tyrosine residues. In fact,

phosphorylation is not an on/off mechanism; in contrast, it is dynamic in time and magnitude. The kinetics of activation are affected by different intracellular actors, which include not only kinases but also phosphatases. protein phosphatase 2A (PP2A), a heterotrimeric Ser/Thr phosphatase composed of scaffolding, catalytic, and regulatory subunits, has been identified through studies based on pharmacological or short interfering RNA (siRNA) inhibition to control the degree of TrkA phosphorylation (Tyr-490). Interestingly, the inhibition of PP2A impaired TrkA long-lasting activation of Akt and Erk signaling but not the degree of their respective phosphorylation[64]. Zhang and colleagues (2016) showed that a tyrosine phosphatase called PTP-MEG2 (**Figure 7**) colocalized with TrkA and dephosphorylated TrkA (at Tyr-490 and Tyr-674/Tyr-675)[65]. In addition to soluble phosphatases, certain membrane receptors have been shown to control TrkA activation. For example, the protein tyrosine phosphatase receptor PTPRZ suppressed autophosphorylation of Trk receptors. PTPRZ overexpression in PC12 cells increased Trk phosphorylation and impaired neurite outgrowth[66]. Similarly, PTP1B transfection resulted in a decrease in TrkA phosphorylation of ERK and affected neurite outgrowth[67]. Hence, phosphatases are key regulators of TrkA phosphorylation signaling kinetics. Nevertheless, TrkA signaling does not rely solely on the kinase/phosphatase feedback loops. Notably, the Lemmon group reported that the purified kinase domain of TrkA did not maintain a phosphorylated state even in the absence of phosphatase[68]. The conservation of this mechanism among RTKs may indicate the importance of mechanism(s) that function independent of phosphorylation.

1.4.3- Locoregional dynamic activation by GTPases

Rac1, Cdc42 or RhoA**,** 3 GTPase proteins activated by specific RhoGEFs (not kinases), have been immunoprecipitated with TrkA. As demonstrated by studies based on the siRNA approach and the expression of constitutively activated Rac1, a GTPase was necessary and sufficient for retrograde transport and neuronal survival[51]. Moreover, Rac1 was critical for RhoA inhibition and blocked ROCK recruitment. As a result, Rac1 impaired differentiation mediated by RhoA[69]. In addition, in a yeast two-hybrid system, NOMA-GAP (ARGAP33) has been shown to interact directly with the N-

terminal region (residues 279–782; **Figure 7**). Upon NOMA-GAP binding and phosphorylation, the tyrosine phosphatase SHP2 was recruited and activated. Thus, it sustained the activation of ERK5 and tempered Cdc42/PAK signaling pathway activity (**Figure 7**). Clearly, these mechanisms promote neurite outgrowth[70]. Interestingly, kinases, phosphatases and GTPases are primarily localized in the cytoplasm, but following different extracellular stimuli, including NGF stimulation, they localize to the plasma membrane, where they are activated. Hence, these molecules can interact both directly and indirectly with TrkA.

2. What do genetics tell us about TrkA?

The *NTRK1* gene was originally described as a unique gene of 23 kb located on the 1q21-q22 chromosome and composed of 16 introns and 17 exons[71]. Nevertheless, further investigations have shown complex organizational variations of *NTRK1*.

2.1. Different isoforms are produced via different initiation sites

Luberg and colleagues (2015), using reverse transcription–polymerase chain reaction (RT–PCR) and rapid amplification of 5' complementary DNA ends analyses, highlighted that human *NTRK1* is overlapped by two other genes (INSRR and SH2D2A) and spans 67 kb[50]. Transcription and translation produce various isoforms resulting from different initiation sites. An *in-silico* analysis suggested that *NTRK1* has different transcription initiation sites. In addition to the initiation sites in exon 1, transcription initiation in exon 10 and many different nucleotides within exon 8 has been detected. An RT–PCR analysis has confirmed various transcripts in human adult and embryo samples. Interestingly, isoform expression depends on tissue type and is mutually exclusive. These isoforms form unique TrkA structures and exhibit different catalytic activities, subcellular localizations and functions in organisms.

2.2. A constitutively activated isoform: TrkA III

Similar to TrkA-I and II, the splicing isoform (exons 6-7) TrkA-III includes the 3 main domains, but the extracellular domain of Ig-like 2 is truncated. In contrast to TrkA-I and TrkA-II, TrkA-III is not N-glycosylated due to the deletion of the extracellular D4 Ig-like domain that includes certain N-glycosylation sites, and, therefore, is localized only to intracellular compartments. Notably, TrkA-III is found in pre-Golgi membranes, centrosomes, mitochondria and endosomes. This TrkA isoform is constitutively activated and induces TrkA signaling. Moreover, the expression of this isoform is restricted to embryonic and postnatal thymic epithelial cells, thymocytes and neural progenitor cells. TrkA-III protects these cells against stress through ligand-independent activation[72]. Tacconelli *et al*. showed that under thymic cell hypoxic conditions, TrkA-III and TrkA-I/II expression was decreased. In contrast, normoxic conditions reversed this expression profile[72].

2.3. A transcription factor?

Interestingly, Luberg and colleagues demonstrated that the spliced isoform (exons 7-8-9) which is 40 kDa and is called TrkA-K was translocated into the nucleus. These authors proposed that the translocation resulted from the recognition of the TrkA N-terminal by importin-7. Nevertheless, the molecular mechanism of TrkA-K translocation remains unclear, and further investigations are needed. In addition, the relative level of TrkA-K expression was low in comparison to that of TrkA-I and TrkA-II. Moreover, intracellular TrkA and phosphorylated TrkA in the nucleus have been observed in liver cells[73] and melanocytic tumors, respectively[74]. Nevertheless, the role played by nuclear TrkA remains unclear.

TrkA-III and TrkA-I/TrkA-II appear to display not only distinct functions in the body but also antagonist effects on the cell response to microenvironmental variations (medium composition, stress, etc.). This observation indicates the importance of not only the kinase function of TrkA but also the extracellular function in biological responses. TrkA isoforms show distinct patterns of expression in the body and different cells because of their different structures. TrkA-III presents a very different structure–function

relationship than TrkA-I or TrkA-II. These differences are related to different posttranslational modifications and subcellular locations.

3. A microenvironmental adaptable model

3.1- TrkA subcellular localization: a pre-transcription event?

N-glycosylation and ubiquitination control TrkA folding, exocytosis and recycling, and these post-translational events affect the level of TrkA at the cell membrane and in endosomes, where it mediates the transduction of extracellular signals after ligand binding. The extracellular domain of 85-kDa TrkA protein undergoes N-glycosylation during its trafficking through the endoplasmic reticulum (the N-terminus is located in the ER lumen) and the Golgi apparatus, leading to the development of a 110-kDa form. The fully glycosylated form is found at the plasma membrane (140 kDa) because this protein is glycosylated in exocytic vesicles[75]. These 13 N-glycosyl groups are necessary for membrane expression of TrkA and have been suggested to prevent ligand-independent activation of TrkA[76]. The constitutive activation of nonglycosylated TrkA leads to activation of the Pi3K/Akt and PLCg/PKC pathways but not to MAPK activation[76]. In addition to N-glycosylation, the addition of glucose to a Lys residue has been described during aging and results in a 3-fold reduction in NGF affinity and reduced neurite outgrowth [77]. Interestingly, a 180-kDa form of TrkA has been reported and suggested to be a hyperglycosylated consecutively activated form of TrkA[50,78]. This supposition has reinforced the idea that glycosylation plays a key role in controlling TrkA activity. Nevertheless, to date, research focusing on this form has not been published, and the evidence indicating a 180-kDa TrkA form has been obtained only by western blot analysis. Further investigations may be interesting to understand the mechanisms regulating TrkA activation.

TrkA-I has been observed in signaling endosomes after ubiquitination. NGF-induced mono- or polyubiquitination of TrkA promotes TrkA internalization into cells *via* classical clathrin-mediated endocytosis or pincher-mediated macropinocytosis[79–81]. However, early endosomes exhibit different

functions depending on the type of protein ubiquitination. The polyubiquitination of the PPXY motif (Leu-784 and Val-790) in the C-terminal tail of TrkA by TRAF6 leads to endocytosis and retrograde signaling of TrkA. Endosomes carrying signaling molecules are retroactively transported through dynein from axon to neuronal cell body, where they promote neuron survival and development[82]. These signaling endosomes evade lysosomal degradation due to coronin-1 expression. In contrast, the E3 ubiquitin ligase *Nedd4*-2 (TRAF4) monoubiquitinated the K(485)FG motif of the juxtamembrane region of TrkA, which facilitated TrkA lysosomal degradation, reducing the level of membrane TrkA[84]. This event followed NGF stimulation *in vitro* and *in vivo*[85,86]. Interestingly, the P785S TrkA mutant**,** which does not undergo ubiquitination, not only showed impaired internalization but also compromised lateral movement at the plasma membrane after NGF stimulation [87]. In addition, mutation in the TrkA kinase domain (K547N) resulted in altered membrane localization and trafficking into the cell. Interestingly, NT-3 binding did not induce TrkA ubiquitination or internalization but promoted its phosphorylation. Moreover, TrkA endocytosis can also be mediated *by* sortilin, a TrkA coreceptor. Sortilin is preferentially localized in intracellular compartments (90%), including the trans-Golgi network, endosomes, dendrites, axons, immature secretory granules, and synaptic vesicles[88]. Approximately 10 % of Sortilin is exposed at the cell surface. The sortilin–TrkA association at the plasma membrane permits TrkA anterograde transport[89] *via* 3 TrkA motifs: YSVL (792-795 amino acids), DSDED (824-828 amino acids), and LL (829-830 amino acids)[88,90]. This suggests that TrkA function can be modulated not only by posttranslational modifications but also by other modifications.

3.2- Is ligand composition the only way to control TrkA activation?

The pH and ionic composition of the local environment of cells affect ligand binding and are important parameters affecting the cellular response. Indeed, NT-3 binding results in TrkA phosphorylation at neutral pH, and in contrast to NGF, is thus affected by acidic conditions. As a result, TrkA phosphorylation is induced by NGF under acidic conditions, but the effect is

weaker[51]. Moreover, following proton challenge, the intracellular store of TrkA at the plasma membrane is mobilized and promotes neuronal sensitivity to NGF[91]. Interestingly, under acidic conditions (pH = 6.5), this mechanism depends on $Ca^{2+,}$ whereas at pH 7.4, KCl-induced depolarization is sufficient to mobilize membrane TrkA. Moreover, inorganic compounds contribute to controlling TrkA activation. The first clues indicating that inorganic compounds are important for TrkA signaling were discovered by Biarc *et al*. (2013), who performed elegant experiments by carefully ensuring that the activity was not triggered by NGF in the medium. That is, medium with chelated serum was replaced with medium containing nonchelated serum to ensure that the response was indicative of cellular NGF activation. Then, Pandini *et al.* demonstrated that zinc and copper were crucial for TrkA activation and internalization[92]. In addition, TrkA activation has been shown to contribute to the control of ion flux. The phosphorylation of Tyr-785 led to PLCγ1 recruitment, subsequent PiP2 hydrolysis, IP3/DAG production and endoplasmic reticular calcium liberation, which stimulated PKC and CAMK.

Different inflammatory factors have been shown to modulate the activity of TrkA. For example, IL-2 permits the expression of TrkA and thus promotes inflammation *via* cell degranulation NGF induction of natural killer (NK) cells[93]. In monocytes, TrkA expression has been associated with maturation into macrophages, and NGF stimulation of this mast cells increased their production of proinflammatory mediators, including histamine[94]. In rat mast cells, histamine stimulation resulted in a NGF response mediate through PLC/PKC and Pi3K/Akt pathway activation but not MAPK pathway activation[95]. In addition, NK cells have been shown to harbor different membrane TrkA species depending on the microenvironment, resulting in different NGF responses. For instance, in bone marrow, NK cells exhibit higher TrkA expression levels than NK cells in blood. This difference explains the reason that the NK cell subpopulation in blood has lower cytokine secretion ability[96]. In some immune cells, TrkA activation is affected by harmful conditions. For example, in monocytes, NGF stimulation led to anti-inflammatory effects only after TLR activation. Thus, TrkA activation induced Akt, which inhibited glycogen synthase kinase 3 or IkB phosphorylation and

subsequent p65 NF-kB nuclear translocation but increases p50 NF-kB nuclear binding[97]. Interestingly, this NGF effect on the production of inflammatory cytokines has been identified only in TLR-activated monocytes and at high NGF concentrations (maximal effect at 100 ng/ml), suggesting roles played by others membrane receptors in TrkA function in immune cells.

In addition to protein–protein interactions, protein–lipid interactions have been shown to play a role in RTK regulation. Lysophosphatidylcholine (LPC) is a bioactive lipid that can be produced via hydrolytic degradation of phosphatidylcholine from the plasma membrane and lipoprotein. In PC12 cells, LPC enhanced Akt and MAPK activation NGF-induced. This mechanism depended on the extracellular domain of TrkA but did not affect TrkA dimerization. Taken together, these observations suggest that the membrane-proximal D5 subdomain of TrkA undergoes allosteric changes that modulate the affinity and/or stability of the TrkA–NGF complex. Alternatively, LPC may affects TrkA activity by modulating the properties of lipid rafts[98]. In fact, NGF binding to TrkA induces TrkA localization to lipid rafts[99], a subcompartment of the membrane enriched with sphingolipids and cholesterol. However, TrkA does not present CARC or GXXXG-like domains and therefore may interact with cholesterol. Moreover, variations in cholesterol concentration have led to no clear effect on TrkA dimerization[100]. Taken together, these observations suggest that the TrkA response may be modulated only in a lipid-dependent fashion but not by cholesterol.

G protein-coupled receptors (GPCRs), which are seven-transmembrane receptors that interact with inactive heterodimeric G proteins (associated with GDP), can transactivate TrkA. Upon ligand binding to GPCR, the GPCR conformation changes, which that activates (associated with GTP) and cleaves the G protein into 2 parts. This free G protein activates various signaling partners, such as TrkA, through GTP hydrolysis. In PC12 cells derived from adrenal medullary tumors of rats, the A2a receptor was active by adenyl cyclase to activate TrkA, which promoted Akt, ERK1/2 and SAPK/JNK activation but not p38 MAPK activation. Interestingly, this mechanism is calcium-dependent (Lee and Chao, 2001; Malek et al., 1999). In addition,

other GPCR ligands have been reported to support TrkA transactivation in PC-12 cells; these ligands included pituitary adenylate cyclase-activating protein (PACAP) and lysophosphatidate 1 (LPA1). In NG108 cells, a hybrid cell with characteristics of neuroblastoma and glioma cells, the angiotensin 2 (AT2) receptor was activated by Ang II, which induced TrkA phosphorylation. TrkA activation resulted in sustained activation of MAPK (p42/p44), which promoted neurite outgrowth[103]. Interestingly, the MAPK activation mechanism did not rely on PKA activation; in contrast, it relied on Fyn (a member of the Src family kinases) activation[104]. TrkA transactivation by GPCR induced MAPK activation, which is profoundly delayed compared with MAPK activation induced by NGF or the subsequent activation of other RTKs, including EGFR.

Discussion/perspectives

In this review, we highlighted some limits of the RTK activation model in explaining TrkA function and described it's the functional diversity of TrkA. First, cell fate is regulated by the nature and concentration of the ligand to drive the specific kinetics and localization of TrkA and promote signaling activation. Second, different isoforms, including but not exclusively TrkA-I and TrkA-II, contribute to the diverse structure–function relationships exhibited by different forms. Third, the microenvironment controls TrkA localization and ligand affinity. Various factors, including pH and inflammatory factors, as well as co-receptors ($P75^{NTR}$, sortilin, and GPCR) and TrkA interactions with lipids, play key roles in TrkA activation. Moreover, herein, we focused on mechanisms that contribute to the diversity of TrkA tyrosine kinase activity. Nevertheless, certain cues indicate that TrkA can transduce signals in a phosphorylation-independent way. However, very few investigations have been performed on this mechanism. In addition, even though we focused on TrkA in this review, similar considerations can be applied to other RTKs. For example, EGFR is bound by other ligands, in addition to EGF, including epiregulin (EREG). Notably, EGF and EREG do not induce the same EGFR dimer conformation, and therefore, they do not cause the same signaling and cell fates. In fact, EREG induces a weaker interaction between the 2 EGFRs constituting a dimer, as indicated by phosphorylation assay results and the

induction of MCF-7 differentiation, whereas EGF promotes a stronger interaction between EGFR monomers forming the dimer, leading to transient activation and proliferation[105]. Moreover, similar to the mechanism suggested to explain TrkA activation, EGF may bind to preformed EGFR dimers to promote transmembrane rotation, as suggested by Moriki and colleagues [106]. In addition, different tyrosine residues in EGFR can be phosphorylated, similar to TrkA, and result in the activation of different signaling pathway and acquisition of different phenotypes. The phosphorylation can be promoted in a ligand-independent manner. EGFR can also be transactivated by GPCR [107]. We emphasized that genetic differences contribute to TrkA structure–function diversity and that these results are not solely due to differences of strucures among the 3 TrkA isoforms. This important diversity of isoforms is observed in other RTKs, such as EGFR. Moreover, although role played by the nuclear TrkA isoform has not yet been solved, EGFR is known to be a transcriptional co-activator of different genes, including cyclin D1[108]. We investigated the importance of the microenvironment on the TrkA structure-function relationship. First, we found that the environment affected TrkA structure by modulating ubiquitination and glycosylation. Glycosylation exerts a large impact not only on TrkA subcellular localization but also on its ligand affinity. Glycosylation has also been shown to be critical for binding of molecules, especially ligands, to the EGFR ectodomain[109]. All these considerations are important not only to the field of neurobiology but also to many other research fields. In fact, the descriptions of TrkA mechanisms of action in neuron cells may also be apply to other cell types, including immune cells. The acquisition of similar phenotypes and activation of different pathways triggered by TrkA activation have been reported in the literature, suggesting that, upon phosphorylation, different tyrosine residues in TrkA may activate distinct signaling cascades, similar to the effect of TrkA activation in neuronal cells. Nevertheless, activation of specific pathways on the basis of tyrosine activation has not been convincingly demonstrated. Moreover, the NGF concentration that promotes the acquisition of a particular phenotype may differ by cell type. For example, in the nervous system, NGF stimulation leads to the acquisition of different phenotypes based on ligand concentration. NGF promoted the differentiation through MAPK and p90rsk activation in B cells,

similar to its effect in neuronal cells, but at a 10-fold lower concentration (400 pg/ml) in the B cells[110]. In contrast to dendritic cells, other immune cells express and release NGF, inducing *via* positive feedback loop. In addition, this released NGF is a chemoattractant of dendric cells and, thus, promotes pain. These findings suggest that the NGF–TrkA axis is involved in a complex dialog between immune cells and the nervous system; this dialog is important in different diseases, including neurodegenerative diseases. NGF–TrkA axis activation is downregulated in different neurodegenerative diseases, including Alzheimer's disease. In fact, downregulation of this axis results in neuronal death. Therefore, positive modulation of NGF *via* pharmacological or genetic approaches has been tested as a means to restore a healthy cellular balance. For example**,** NGF gene therapy and NGF agonists have been shown to activate neurons in Alzheimer's disease (AD) patients[111]. Nevertheless, NGF can also bind to $P75^{NTR}$ and cause pain. Therefore, producing a TrkA agonist that does not bind $P75^{NTR}$ remains an important area of research. Another challenge to the application of TrkA agonists is the blood–brain barrier (BBB); the drug must permeate the barrier and enter the targeted area. For example, D3 could be directed to bind TrkA but not activate $P75^{NTR}$ and be delivered using MRI-guided focused ultrasound to permit transient and selective entry into the brain. D3 has been shown to be an efficient treatment in a mouse model of AD[112]. Moreover, to induce TrkA activation without inducing pain, the modulation of the NT-3–TrkA was examined. In the context of spinal cord injury, a biodegradable material that released NT-3 over 14 days led to recovery of motor and sensory functions in a monkey[113]. In addition, this approach may be useful not only to treat diseases affecting the nervous system but also to attenuate inflammatory diseases. Notably, in juvenile idiopathic arthritis, TrkA expression was downregulated in monocytes, which promoted the production of inflammatory cytokines [97]. In cancers, upregulated TrkA expression has been generally associated with a poor prognosis, particularly in breast, prostate or head and neck squamous cell carcinoma (HNSCC). This upregulated expression of TrkA promotes cancer cell aggressiveness and drug resistance[114,115]. For example, in HNSCC, TrkA phosphorylation was involved in erlotinib failure[116]. In this review, we depicted the reasons that the classical transactivation model does not adequately

explain all TrkA phosphorylation-dependent effects. Specifically, TrkA effects do not seem to be solely dependent on phosphorylation. For example, our team reported that the association of TrkA with EphA2 and CD44 promoted breast cancer aggressiveness *via* a phosphorylation-independent signaling pathway[44,117,118]. This finding suggests that RTKs may exert effects through mechanisms not only phosphor-dependent.

Abbreviations

BBB: Blood–brain barrier

BDNF: Brain-derived neurotrophic factor

CAMK: Ca^{2+}/calmodulin-dependent protein kinase

Cdc42: Cell division control protein 42

CD44: Cluster of differentiation 44

CR: Cysteine-rich

EGFR: Epidermal growth factor receptor

EphA2: Ephrin type-A receptor 2

EREG: Epiregulin

FBS: Fetal bovine serum

FGF: Fibroblast growth factor

FRET: Fluorescence resonance energy transfer

GPCR: G protein-coupled receptor

HB-EGF: Heparin-binding EGF-like growth factor

HER2: Human epidermal growth factor receptor 2

HGF/SF: Hepatocyte growth factor/scatter factor

HNSCC: Head and neck squamous cell carcinoma

Ig: Immunoglobulin

LPC: Lysophosphatidylcholine

LRR: Leucin-rich region 1

MAPK: Mitogen-activated protein kinase

MIP1b: Macrophage inflammatory protein 1β

MCF-7: Michigan Cancer Foundation-7

MST: Microscale thermophoresis

NTF3: Neurotrophin 3

NGF: Nerve growth factor

NK: Natural killer

NOMA-GAP: Neurite outgrowth multiadaptor-GTPase-activating protein

NT-3: Neurotrophin-3

NTRK1: Neurotrophin tyrosine receptor kinase 1

PACAP: Pituitary adenylate cyclase-activating protein

PC12: Pheochromocytoma 12

PKC: Protein kinase C

PLCγ1: Phospholipase C, gamma 1

$P75^{NTR:}$ P75 neurotrophin receptor

Rac1: Ras-related C3 botulinum toxin substrate 1

RhoA: Ras homolog gene family member A

ROCK: Rho-associated coiled-coil kinase

RTK: Receptor tyrosine kinase

SCID: Severe combined immunodeficiency

TLR: Toll-like receptor

TRAF: TNF receptor-associated factor

TN: Triple Negative

TNBC: Triple negative breast cancer

TrkA: Tropomyosin kinase A

Declarations

Consent for publication

All the participants of this study consented to the publication of this work.

Competing interests

The authors declare that they have no competing interests.

Funding

This work was supported by “La ligue contre le cancer” (« comité du Nord, du Pas de Calais et de l’Aisne »), cancéropole Nord-Ouest, I-site “Université Lille Nord-Europe” and Contrat de Plan Etat-Région CPER Cancer 2015-2020. ST was funded by “conseil régional Hauts de France”, Lille University and “La Ligue contre le cancer”.

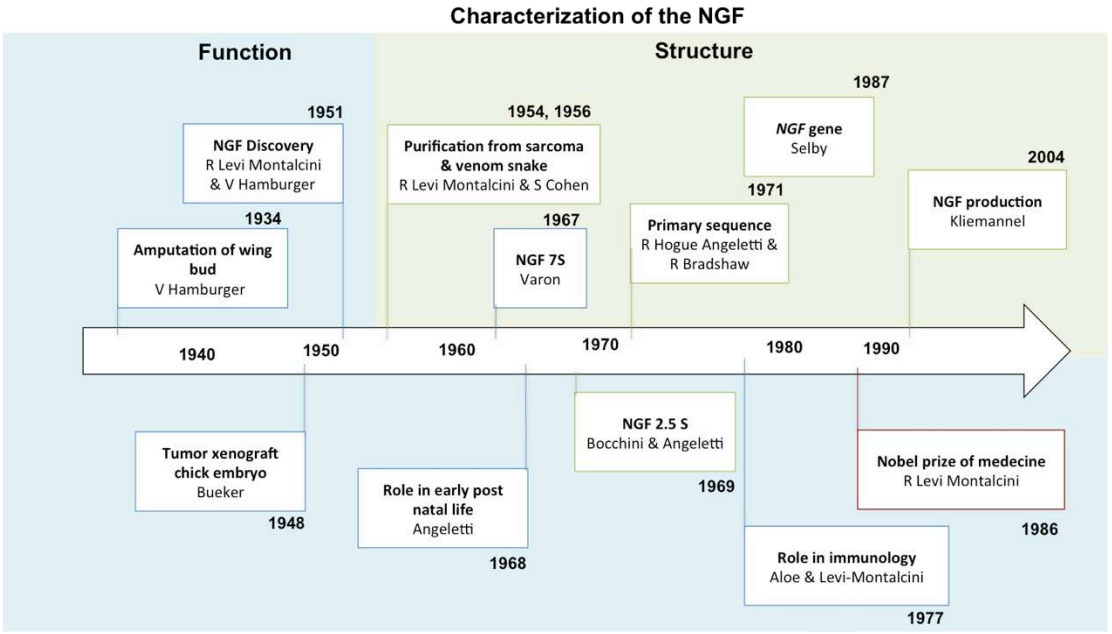


Figure 1: Time line of NGF history.

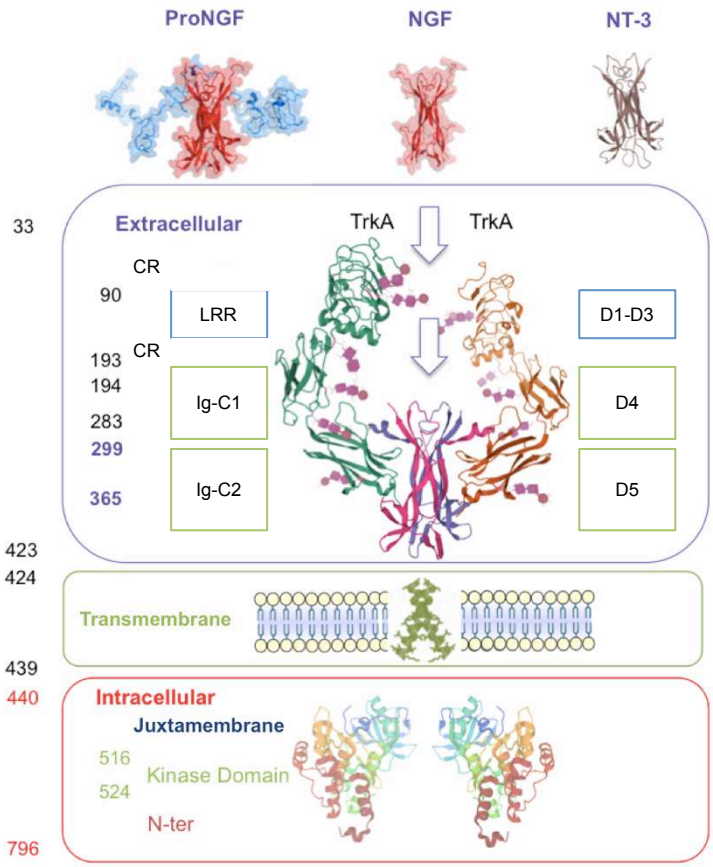


Figure 2: Structure of TrkA. TrkA is divided into 3 domains: extracellular, transmembrane and intracellular. The structure of the extracellular, the transmembrane and the intracellular part of TrkA have been solved respectively by X-Ray (2IFG), NMR (2N90) and X-Ray (5KMO without ligand). The extracellular domain presents 3 LRM (Leucine Rich Motif) that composed the Leucine Rich Region (LRR), 2 Cysteine Rich (CR) motifs and 2 Immunoglobulin-like domains. The transmembrane is composed of a-helix. At least, the intracellular domain can be divided into 3 parts: the juxta-membrane, the kinase and the N-ter region.

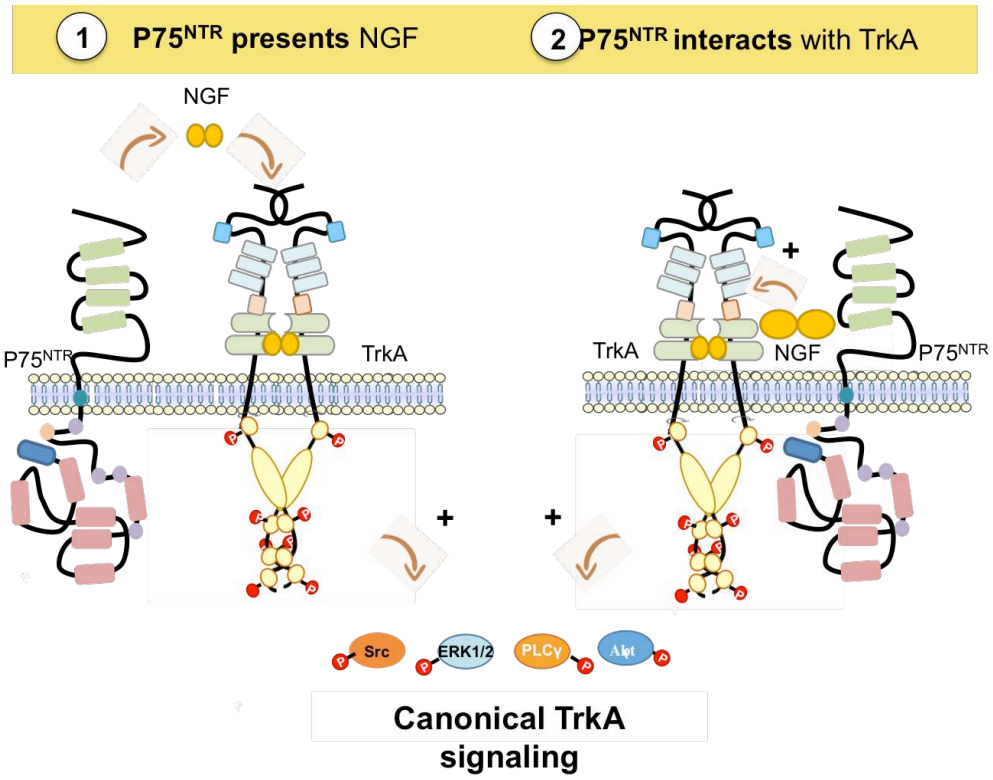


Figure 3: Models of the mechanistic by which P75^{NTR} increases NGF affinity to TrkA. Two models have been proposed to explain P75^{NTR} increase NGF affinity to TrkA. NGF binds on P75^{NTR} that present it to TrkA (ligand-passing model; 1). Another model proposed that P75^{NTR} interacts with TrkA to promote NGF affinity (2).

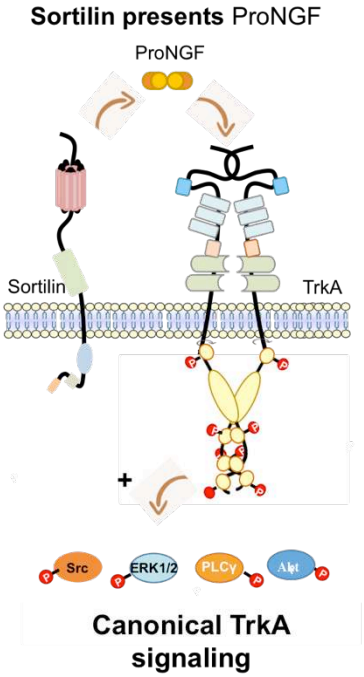


Figure 4: Model of ProNGF presentation by the Sortilin. The ProNGF can bind on the Sortilin. Then, Sortilin presents ProNGF to TrkA and promote the activation of canonical TrkA signaling.

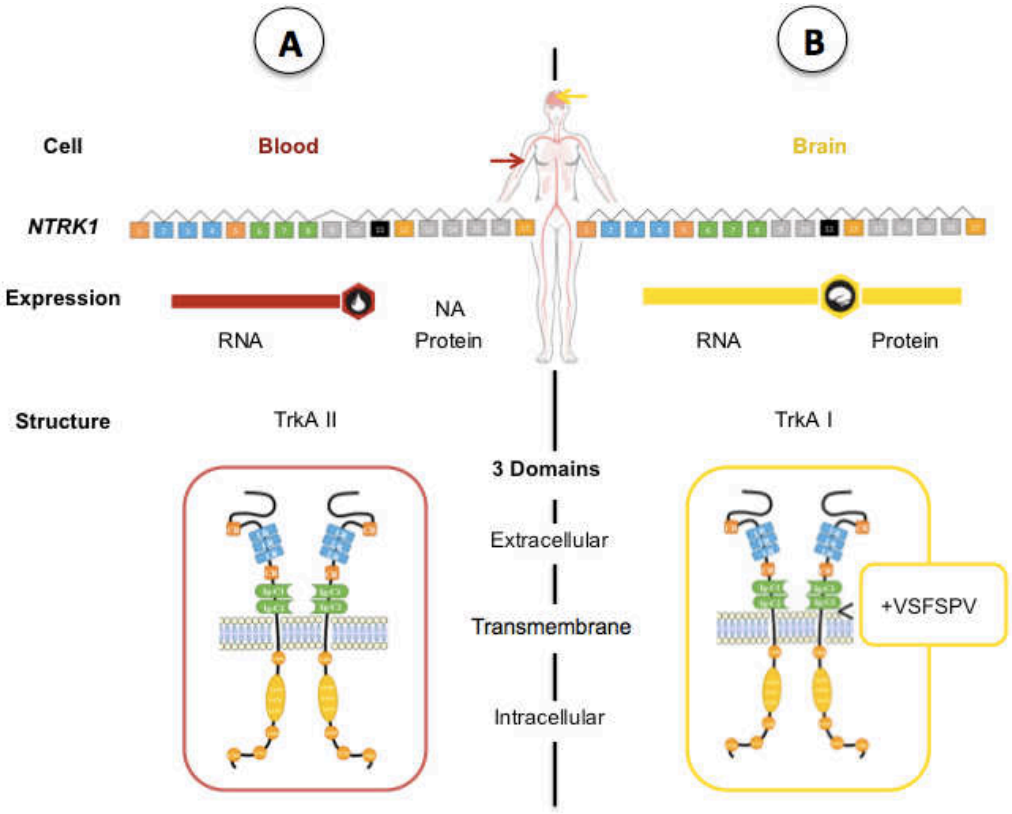


Figure 5: The two TrkA isoforms. TrkA-I and TrkA-II are not expressed in the same cell types (cell). TrkA-I is expressed especially in blood cells whereas TrkA-II is found in neuronal cells. TrkA-I and TrkA-II are expressed by *NTRK1*. An alternative splicing of the exon 9 results in 6 additional amino acids in the extracellular domain of TrkA-II, called insert of specificity (structure). This insert promotes NT-3 affinity to TrkA.

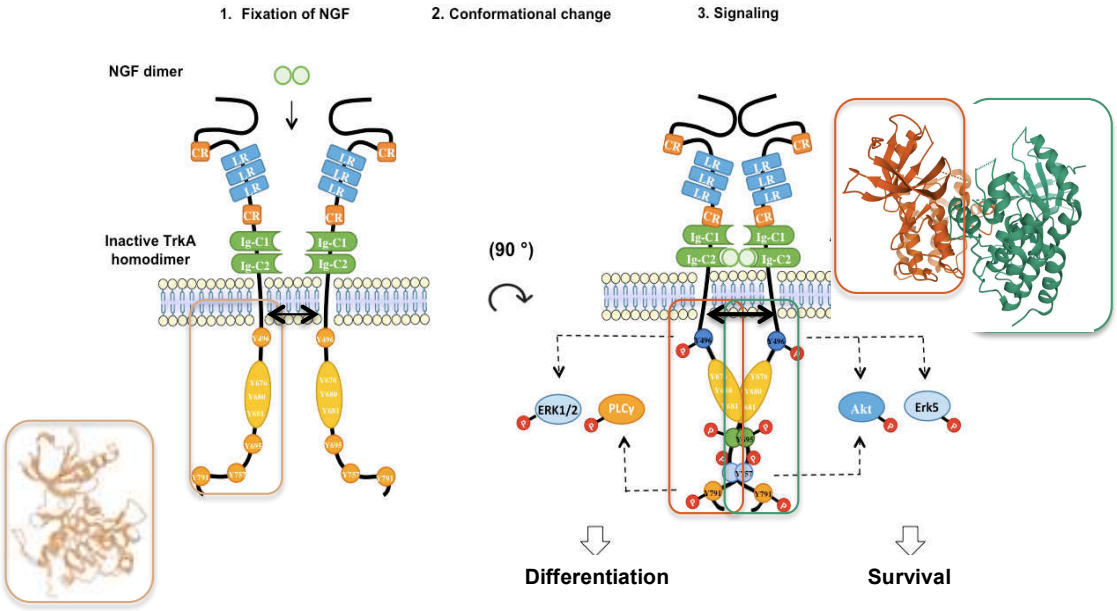


Figure 6: Mechanism of TrkA activation by NGF. The receptor TrkA is composed of 3 domains that interplay to transduce extracellular signal. Preformed TrkA homodimer has an inactive intracellular domain (ID: 1WWA). When extracellular stimulation occurs, here NGF fixation on TrkA homodimer (1), following a rotation of the transmembrane domain (2) a conformation change of the intracellular domain occurs (3) (ID: 6IQN). This conformational change increases the distance between the 2 juxtamembrane region. This activated TrkA homodimer is phosphorylated on different residues tyrosine.

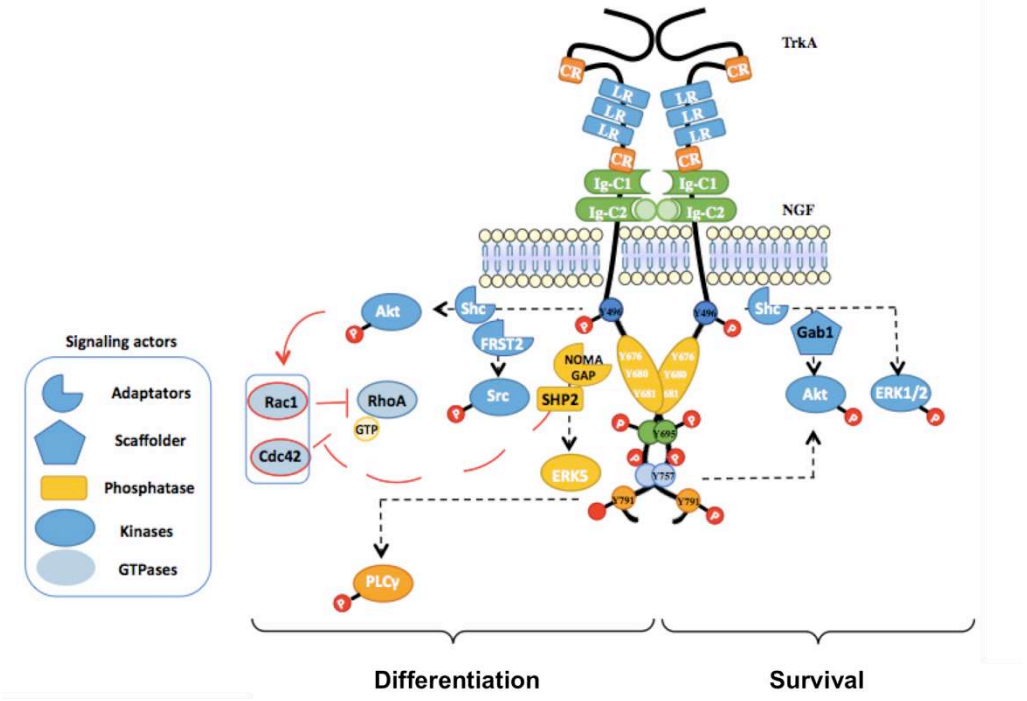


Figure 7: TrkA signaling to a dynamic regulation of cell fate. Different types of signaling actors (phosphatases, kinases, GTPases…) control the kinetic and the localization of TrkA activation. Moreover, each TrkA tyrosine activate specific signaling that promote differentiation or survival in neuronal cells.

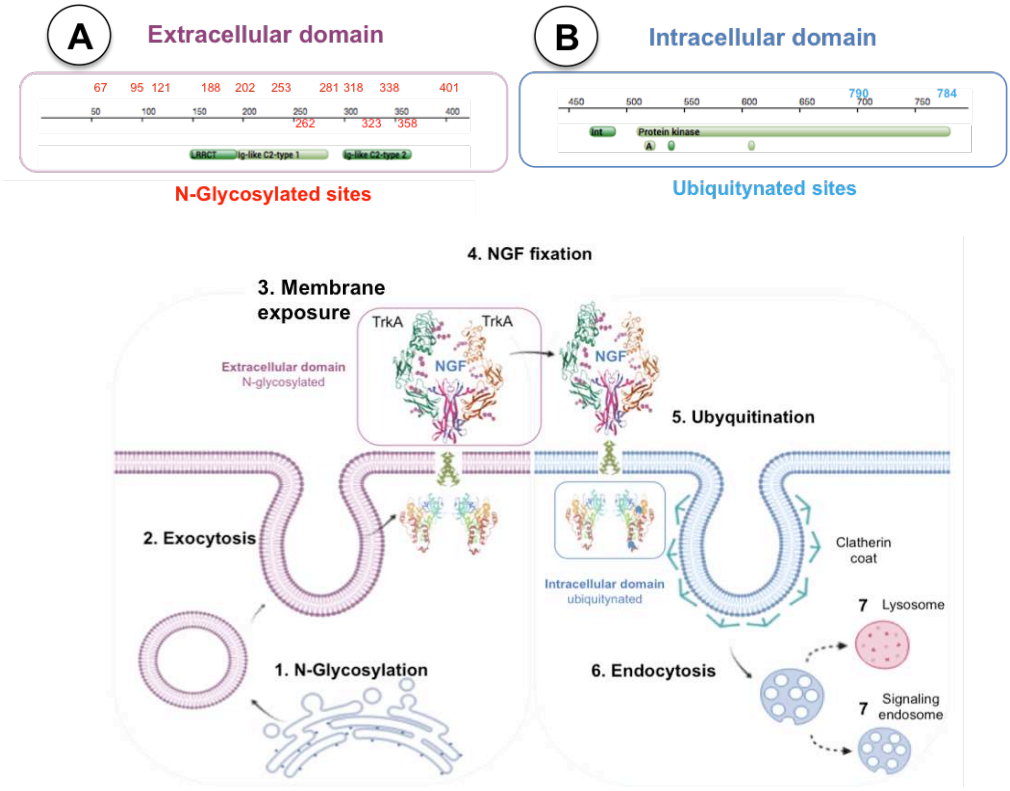


Figure 8: TrkA glycosylations and ubiquitination control TrkA localization and pattern of activation. The extracellular domain is N-glycosylated during trafficking (1) and permits TrkA folding and cell surface exposition (2-3). When NGF fixation occurs (4), upon the ubiquitination of TrkA and it clathrin-dependent internalization (6). Then TrkA will be degraded (7 lysosome) or not (7 signaling endosome). The signaling endosome is retrogradely transport (axon-cell body) and leads to the activation of TrkA signaling in cell body.

References

1. Levi-Montalcini R. & Hamburger V. Selective growth stimulating effects of mouse sarcoma on the sensory and sympathetic nervous system of the chick embryo. *J. Exp. Zool.* (1951).

2. Hamburger V. The effects of wing bud extirpation on the development of the central nervous system in chick embryos. *J. Exp. Zool.* **68**, 449–494 (1934).

3. Levi-Montalcini R. & Levi G., Arch. Biol. Liège 54, 183-206, 1943.

4. Hamburger V. & Levi-Montalcini R. Proliferation, differentiation and degeneration in the spinal ganglia of the chick embryo under normal and experimental conditions. *J. Exp. Zool.* **111**, 457–501 (1949).

5. Bueker E. D. Implantation of tumors in the hind limb field of the embryonic chick and the developmental response of the lumbosacral nervous system. 511–524 (1948).

6. Cohen S., Levi-Montalcini R. & Hamburger V. a Nerve Growth-Stimulating Factor Isolated From Sarcom As 37 and 180. *Proc. Natl. Acad. Sci.* **40**, 1014–1018 (1954).

7. Cohen S. & Levi-Montalcini R. a Nerve Growth-Stimulating Factor Isolated From Snake Venom. *Proc. Natl. Acad. Sci.* **42**, 571–574 (1956).

8. Angeletti R. H. Studies on the nerve growth factor(NGF) from snake venom molecular heterogeneity. *J. Chromatogr. A* **37**, 62–69 (1968).

9. Varon S., Nomura J. & Shooter E. M. The Isolation of the Mouse Nerve Growth Factor Protein in a High Molecular Weight Form*. *Biochemistry* **6**, 2202–2209 (1967).

10. Bocchini V. & Angeletti P. U. The nerve growth factor: purification as a 30,000-molecular-weight protein. *Proc. Natl. Acad. Sci. U. S. A.* **64**, 787–794 (1969).

11. Bradshaw R. A., Angeletti R. A. H. & Wade R. D. Subunit structure and amino acid composition of mouse submaxillary gland nerve growth factor. *Biochemistry* **10**, 463–469 (1971).

12. Aloe L. & Levi-montalcini R. Mast cells increase in tissues of neonatal rats injected with the nerve growth factor. *Cell* **133**, 358–366 (1977).

13. Selby M. J., Edwards R., Sharp F. & Rutter W. J. Mouse nerve growth factor gene: structure and expression. *Mol. Cell. Biol.* **7**, 3057–3064 (1987).

14. Kliemannel M. *et al.* The mature part of proNGF induces the structure of its pro-peptide. *FEBS Lett.* **566**, 207–212 (2004).

15. Maisonpierre P. C. *et al.* Human and rat brain-derived neurotrophic factor and neurotrophin-3: Gene structures, distributions, and chromosomal localizations. *Genomics* **10**, 558–568 (1991).

16. Butte M. J., Hwang P. K., Mobley W. C. & Fletterick R. J. Crystal Structure of Neurotrophin-3 Homodimer Shows Distinct Regions Are Used To Bind Its Receptors,. *Biochemistry* **37**, 16846–16852 (1998).

17. Johnson D. *et al.* Expression and structure of the human NGF receptor. *Cell* **47**, 545–554 (1986).

18. Radeke M. J., Misko T. P., Hsu C., Herzenberg L. A. & Shooter E. M. Gene transfer and molecular cloning of the rat nerve growth factor receptor. *Nature* **325**, 593–597 (1987).

19. Pulciani S. *et al.* Oncogenes in solid human tumours. *Nature* **300**, 539–542 (1982).

20. Martin-Zanca D., Hughes S. H. & Barbacid M. A human oncogene formed by the fusion of truncated tropomyosin and protein tyrosine kinase sequences. *Nature* **319**, 743–748 (1986).

21. Martin-Zanca D., Oskam R., Mitra G., Copeland T. & Barbacid M. Molecular and biochemical characterization of the human trk proto-oncogene. *Mol. Cell. Biol.* **9**, 24–33 (1989).

22. Kaplan D. R., Martin-Zanca D. & Parada L. F. Tyrosine phosphorylation and tyrosine kinase activity of the trk proto-oncogene product induced by NGF. *Nature* **350**, 158–160 (1991).

23. Klein R., Jing S., Nanduri V., O'Rourke E. & Barbacid M. The trk proto-oncogene encodes a receptor for nerve growth factor. *Cell* **65**, 189–197 (1991).

24. Cordon-cardo C. *et al.* NIH Public Access. **66**, 173–183 (2009).

25. Klein R., Lamballe F., Bryant S. & Barbacid M. The trkB tyrosine protein kinase is a receptor for neurotrophin-4. *Neuron* **8**, 947–956 (1992).

26. Soppet D. *et al.* The neurotrophic factors brain-derived neurotrophic factor and neurotrophin-3 are ligands for the trkB tyrosine kinase receptor. *Cell* **65**, 895–903 (1991).

27. Squinto S. P. *et al.* trkB encodes a functional receptor for brain-derived neurotrophic factor and neurotrophin-3 but not nerve growth factor. *Cell* **65**, 885–893 (1991).

28. Lamballe F., Klein R. & Barbacid M. trkC, a new member of the trk family of tyrosine protein kinases, is a receptor for neurotrophin-3. *Cell* **66**, 967–979 (1991).

29. Furuya N., Momose T., Katsuno K., Fushimi N. & Muranaka H. Bioorganic & Medicinal Chemistry Letters The juxtamembrane region of TrkA kinase is critical for inhibitor selectivity. **27**, 1233–1236 (2017).

30. Su H. P. *et al.* Structural characterization of nonactive site, TrkA-selective kinase inhibitors. *Proc. Natl. Acad. Sci. U. S. A.* **114**, E297–E306 (2017).

31. Wlesmann C., Ultsch M. H., Bass S. H. & De Vos A. M. Crystal structure of nerve growth factor in complex with the ligand- binding domain of the TrkA receptor. *Nature* **401**, 184–188 (1999).

32. Settanni G., Cattaneo A. & Carloni P. Molecular dynamics simulations of the NGF-TrkA domain 5 complex and comparison with biological data. *Biophys. J.* **84**, 2282–2292 (2003).

33. Shoemark D. K. *et al.* Design and nuclear magnetic resonance (NMR) structure determination of the second extracellular immunoglobulin tyrosine kinase a (trkaig2) domain construct for binding site elucidation in drug discovery. *J. Med. Chem.* **58**, 767–777 (2015).

34. Ivanisevic L., Zheng W. H., Wo S. B., Neet K. E. & Saragovi H. U. TrkA receptor 'hot spots' for binding of NT-3 as a heterologous ligand. *J. Biol. Chem.* **282**, 16754–16763 (2007).

35. Windisch J. M., Marksteiner R. & Schneider R. Nerve growth factor binding site on TrkA mapped to a single 24-amino acid leucine-rich motif. *J. Biol. Chem.* **270**, 28133–28138 (1995).

36. Capsoni S. *et al.* Taking pain out of ngf: A 'painless' ngf mutant, linked to hereditary sensory autonomic neuropathy type v, with full neurotrophic activity. *PLoS One* **6**, (2011).

37. Jing S., Tapley P. & Barbacid M. Nerve growth factor mediates signal transduction through trk homodimer receptors. *Neuron* **9**, 1067–1079 (1992).

38. Kliemannel M., Golbik R., Rudolph R., Schwarz E. & Lilie H. The pro-peptide of proNGF: Structure formation and intramolecular association with NGF. *Protein Sci.* **16**, 411–419 (2007).

39. Trabjerg E., Kartberg F., Christensen S. & Rand K. D. Conformational characterization of nerve growth factor- reveals that its regulatory pro-part domain stabilizes three loop regions in its mature part. *J. Biol. Chem.* **292**, 16665–16676 (2017).

40. Resende-Lara P. T., Perahia D., Scott A. L. & Braz A. S. K. Unveiling functional motions based on point mutations in biased signaling systems: A normal mode study on nerve growth factor bound to TrkA. *PLoS One* **15**, 1–25 (2020).

41. Soligo M. *et al.* Different responses of PC12 cells to different pro-nerve growth factor protein variants. *Neurochem. Int.* **129**, 104498 (2019).

42. Demont Y. *et al.* Pro-nerve growth factor induces autocrine stimulation of breast cancer cell invasion through tropomyosin-related kinase A (TrkA) and sortilin protein. *J. Biol. Chem.* **287**, 1923–1931 (2012).

43. Clewes O. *et al.* Human ProNGF: Biological effects and binding profiles at TrkA, P75 NTR and sortilin. *J. Neurochem.* **107**, 1124–1135 (2008).

44. Lévêque R. *et al.* ProNGF increases breast tumor aggressiveness through functional association of TrkA with EphA2. *Cancer Lett.* **449**, 196–206 (2019).

45. Fagan A. M. *et al.* TrkA, but not TrkC, receptors are essential for survival of sympathetic neurons in vivo. *J. Neurosci.* **16**, 6208–6218 (1996).

46. Francis N. *et al.* NT-3, like NGF, is required for survival of sympathetic neurons, but not their precursors. *Dev. Biol.* **210**, 411–427 (1999).

47. Belliveau D. J. *et al.* NGF and neurotrophin-3 both activate TrkA on sympathetic neurons but differentially regulate survival and neuritogenesis. *J. Cell Biol.* **136**, 375–388 (1997).

48. Clary D. O. & Reichardt L. F. An alternatively spliced form of the nerve growth factor receptor TrkA confers an enhanced response to neurotrophin 3. *Proc. Natl. Acad. Sci. U. S. A.* **91**, 11133–11137 (1994).

49. Barker P. A. *et al.* Tissue-specific alternative splicing generates two isoforms of the trkA receptor. *J. Biol. Chem.* **268**, 15150–15157 (1993).

50. Luberg K., Park R., Aleksejeva E. & Timmusk T. Novel transcripts reveal a complex structure of the human TRKA gene and imply the presence of multiple protein isoforms. *BMC Neurosci.* **16**, 1–21 (2015).

51. Harrington A. W. *et al.* Recruitment of actin modifiers to TrkA endosomes governs retrograde NGF signaling and survival. *Cell* **146**, 421–434 (2011).

52. Arevalo J. C. *et al.* TrkA Immunoglobulin-Like Ligand Binding Domains Inhibit Spontaneous Activation of the Receptor. *Mol. Cell. Biol.* **20**, 5908–5916 (2000).

53. Shen J. & Maruyama I. N. Nerve growth factor receptor TrkA exists as a preformed, yet inactive, dimer in living cells. *FEBS Lett.* **585**, 295–299 (2011).

54. Reichardt, L. F. Neurotrophin-regulated signalling pathways. *Philos. Trans. R. Soc. B Biol. Sci.* **361**, 1545–1564 (2006).

55. Franco M.L., Nadezhdin K.D., Goncharuk S.A, Mineev K.S., Arsiniev A. S., Vilar M. Structural Basis and Mechanism of TrkA Activation by NGF through Ligand- Induced Rotation of Transmembrane Domain Dimers.

56. Franco M. L. *et al.* Structural basis of the transmembrane domain dimerization and rotation in the activation mechanism of the TRKA receptor by nerve growth factor. *J. Biol. Chem.* **295**, 275–286 (2020).

57. Smith M. J., Hardy W. R., Murphy J. M., Jones N. & Pawson T. Screening for PTB Domain Binding Partners and Ligand Specificity Using Proteome-Derived NPXY Peptide Arrays. *Mol. Cell. Biol.* **26**, 8461–8474 (2006).

58. Dikic I., Batzer A.G., Blaikie P., Obermeier A., Ullrich A., Schlessinger J., Margolis B. Shc binding to nerve growth factor receptor is mediated by the phosphotyrosine interaction domain.*J. Biol. Chem.* ; 270: 15125-15129 (1995).

59. Meakin S. O. & MacDonald J. I. S. A novel juxtamembrane deletion in rat TrkA blocks differentiative but not mitogenic cell signaling in response to nerve growth factor. *J. Neurochem.* **71**, 1875–1888 (1998).

60. Jiang H. *et al.* A double cystiene trkA mutant exhibiting reduced NGF binding and delayed Erk signaling. *J. Mol. Neurosci.* **17**, 293–302 (2001).

61. Obermeier A. *et al.* Identification of Trk binding sites for SHC and phosphatidylinositol 3'- kinase and formation of a multimeric signaling complex. *J. Biol. Chem.* **268**, 22963–22966 (1993).

62. Yamashita H., Avraham S., Jiang S., Dikic I. & Avraham H. The Csk homologous kinase associates with TrkA receptors and is involved in neurite outgrowth of PC12 cells. *J. Biol. Chem.* **274**, 15059–15065 (1999).

63. Biarc J., Chalkley R. J., Burlingame A. L. & Bradshaw R. A. Dissecting the roles of tyrosines 490 and 785 of TrkA protein in the induction of downstream protein phosphorylation using chimeric receptors. *J. Biol. Chem.* **288**, 16606–16618 (2013).

64. Van Kanegan M. J. & Strack S. The Protein Phosphatase 2A

Regulatory Subunits B′β and B′δ Mediate Sustained TrkA Neurotrophin Receptor Autophosphorylation and Neuronal Differentiation. *Mol. Cell. Biol.* **29**, 662–674 (2009).

65. Zhang D. *et al.* The protein tyrosine phosphatase MEG2 regulates the transport and signal transduction of tropomyosin receptor kinase A. *J. Biol. Chem.* **291**, 23895–23905 (2016).

66. Shintani T. & Noda, M. Protein Tyrosine Phosphatase Receptor Type Z Dephosphorylates TrkA Receptors and Attenuates NGF-dependent Neurite Outgrowth of PC12 Cells. *J. Biochem.* **144**, 259–266 (2008).

67. Shibata T. *et al.* A food-derived synergist of NGF signaling: identification of protein tyrosine phosphatase 1B as a key regulator of NGF receptor-initiated signal transduction. *J. Neurochem.* **107**, 1248–1260 (2008).

68. Artim SC, Kiyatkin A. L. M. Comparison of tyrosine kinase domain properties for the neurotrophin receptors TrkA and TrkB. *Biochem. J.* **176**, 139–148 (2020).

69. Nusser N., Gosmanova E., Zheng Y. & Tigyi G. Nerve growth factor signals through TrkA, phosphatidylinositol 3-kinase, and Rac1 to inactivate RhoA during the initiation of neuronal differentiation of PC12 cells. *J. Biol. Chem.* **277**, 35840–35846 (2002).

70. Rosário M., Franke R., Bednarski C. & Birchmeier W. The neurite outgrowth multiadaptor RhoGAP, NOMA-GAP, regulates neurite extension through SHP2 and Cdc42. *J. Cell Biol.* **178**, 503–516 (2007).

71. Indo Y. Structure and organization of the human trka gene encoding a high affinity receptor for nerve growth factor. *Jpn. J. Hum. Genet.* **42**, 343–351 (1997).

72. Tacconelli A. *et al.* TrkAIII expression in the thymus. *J. Neuroimmunol.* **183**, 151–161 (2007).

73. Bonacchi A. *et al.* Nuclear localization of TRK-A in liver cells. *Histol. Histopathol.* **23**, 327–340 (2008).

74. Flørenes V. A. *et al.* Expression of Activated TrkA Protein in Melanocytic Tumors. *Am. J. Clin. Pathol.* **122**, 412–420 (2004).

75. Ehlers M. D., Kaplan D. R., Price D. L. & Koliatsos V. E. NGF-stimulated retrograde transport of trkA in the mammalian nervous system. *J. Cell Biol.* **130**, 149–156 (1995).

76. Watson F. L., Porcionatto M. A., Bhattacharyya A., Stiles C. D. & Segal R. A. TrkA glycosylation regulates receptor localization and activity. *J. Neurobiol.* **39**, 323–336 (1999).

77. Bennmann D. *et al.* Glycation of the high affinity NGF-receptor and RAGE leads to reduced ligand affinity. *Mech. Ageing Dev.* **150**, 1–11 (2015).

78. Griffin N. *et al.* The receptor tyrosine kinase trka is increased and targetable in HER2-positive breast cancer. *Biomolecules* **10**, 1–13 (2020).

79. Beattie E. C., Howe C. L., Wilde A., Brodsky F. M. & Mobley W. C. NGF signals through TrkA to increase clathrin at the plasma membrane and enhance clathrin-mediated membrane trafficking. *J. Neurosci.* **20**, 7325–7333 (2000).

80. Grimes M. L., Beattie E. & Mobley W. C. A signaling organelle containing the nerve growth factor-activated receptor tyrosine kinase, TrkA. *Proc. Natl. Acad. Sci. U. S. A.* **94**, 9909–9914 (1997).

81. Shao Y. *et al.* Pincher, a pinocytic chaperone for nerve growth factor/TrkA signaling endosomes. *J. Cell Biol.* **157**, 679–691 (2002).

82. Heerssen H. M., Pazyra M. F. & Segal R. A. Dynein motors transport activated Trks to promote survival of target-dependent neurons. *Nat. Neurosci.* **7**, 596–604 (2004).

83. Dong S., Park J., Harrington A.W., Zweifel L.S., Mihalas S., Deppman C.D. Coronin-1 is a neurotrophin endosomal effector required for developmental competition for survival. **17**, 36–45 (2014).

84. Georgieva M. V., De Pablo Y., Sanchis D., Comella J. X. & Llovera M. Ubiquitination of TrkA by Nedd4-2 regulates receptor lysosomal targeting and mediates receptor signaling. *J. Neurochem.* **117**, 479–493 (2011).

85. Peng X., Greene L. A., Kaplan D. R. & Stephens R. M. Deletion of a conserved juxtamembrane sequence in Trk abolishes NGF-promoted neuritogenesis. *Neuron* **15**, 395–406 (1995).

86. Kiris E. *et al.* TrkA in vivo function is negatively regulated by ubiquitination. *J. Neurosci.* **34**, 4090–4098 (2014).

87. Amodeo R. *et al.* Molecular insight on the altered membrane trafficking of TrkA kinase dead mutants. *Biochim. Biophys. Acta - Mol. Cell Res.* **1867**, 118614 (2020).

88. Petersen C. M. *et al.* Molecular identification of a novel candidate sorting receptor purified from human brain by receptor-associated protein affinity chromatography. *J. Biol. Chem.* **272**, 3599–3605 (1997).

89. Vaegter C. B. *et al.* Erratum: Sortilin associates with Trk receptors to enhance anterograde transport and neurotrophin signaling. *Nat.*

Neurosci. **14**, 1217 (2011).

90. Nielsen M. S. *et al.* The sortilin cytoplasmic tail conveys Golgi-endosome transport and binds the VHS domain of the GGA2 sorting protein. *EMBO J.* **20**, 2180–2190 (2001).

91. Bray G. E. *et al.* Extracellular pH and neuronal depolarization serve as dynamic switches to rapidly mobilize trkA to the membrane of adult sensory neurons. *J. Neurosci.* **33**, 8202–8215 (2013).

92. Pandini G. *et al.* The inorganic side of NGF: Copper(II) and zinc(II) affect the NGF mimicking signaling of the N-terminus peptides encompassing the recognition domain of TrkA receptor. *Front. Neurosci.* **10**, 1–21 (2016).

93. Ralainirina N. *et al.* Mouse natural killer (NK) cells express the nerve growth factor receptor TrkA, which is dynamically regulated. *PLoS One* **5**, 1–9 (2010).

94. Ehrhard P. B., Ganter U., Bauer J. & Otten U. Expression of functional trk protooncogene in human monocytes. *Proc. Natl. Acad. Sci. U. S. A.* **90**, 5423–5427 (1993).

95. Štempelj M. & Ferjan I. Signaling pathway in nerve growth factor induced histamine release from rat mast cells. *Inflamm. Res.* **54**, 344–349 (2005).

96. Fu B. *et al.* CD11b and CD27 reflect distinct population and functional specialization in human natural killer cells. *Immunology* **133**, 350–359 (2011).

97. Prencipe G. *et al.* Nerve Growth Factor Downregulates Inflammatory Response in Human Monocytes through TrkA. *J. Immunol.* **192**, 3345–3354 (2014).

98. Wuhanqimuge Itakura A., Matsuki Y., Tanaka M. & Arioka M. Lysophosphatidylcholine enhances NGF-induced MAPK and Akt signals through the extracellular domain of TrkA in PC12 cells. *FEBS Open Bio* **3**, 243–251 (2013).

99. Limpert A. S., Karlo J. C. & Landreth G. E. Nerve Growth Factor Stimulates the Concentration of TrkA within Lipid Rafts and Extracellular Signal-Regulated Kinase Activation through c-Cbl-Associated Protein. *Mol. Cell. Biol.* **27**, 5686–5698 (2007).

100. Casarotto P. C. *et al.* Antidepressant drugs act by directly binding to TRKB neurotrophin receptors. *Cell* **184**, 1299-1313.e19 (2021).

101. Lee F. S. & Chao M. V. Activation of Trk neurotrophin receptors in the absence of neurotrophins. *Proc. Natl. Acad. Sci. U. S. A.* **98**, 3555–

3560 (2001).

102. Malek R. L., Nie Z., Ramkumar V. & Lee N. H. Adenosine A(2A) receptor mRNA regulation by nerve growth factor is TrkA- , Src-, and Ras-dependent via extracellular regulated kinase and stress- activated protein kinase/c-Jun NH2-terminal kinase. *J. Biol. Chem.* **274**, 35499–35504 (1999).

103. Plouffe B., Guimond M. O., Beaudry H. & Gallo-Payet N. Role of tyrosine kinase receptors in angiotensin II AT2 receptor signaling: Involvement in neurite outgrowth and in p42/p44mapk activation in NG108-15 cells. *Endocrinology* **147**, 4646–4654 (2006).

104. Guimond M.-O., Roberge C. & Gallo-Payet N. Fyn is involved in angiotensin II type 2 receptor-induced neurite outgrowth, but not in p42/p44mapk in NG108-15 cells. *Mol. Cell. Neurosci.* **45**, 201–212 (2010).

105. Freed D. M. *et al.* EGFR Ligands Differentially Stabilize Receptor Dimers to Specify Signaling Kinetics. *Cell* **171**, 683-695.e18 (2017).

106. Moriki T., Maruyama H. & Maruyama I. N. Activation of preformed EGF receptor dimers by ligand-induced rotation of the transmembrane domain. *J. Mol. Biol.* **311**, 1011–1026 (2001).

107. Parra-Mercado G. K. *et al.* CRF1 Receptor Signaling via the ERK1/2-MAP and Akt Kinase Cascades: Roles of Src, EGF Receptor, and PI3-Kinase Mechanisms. *Front. Endocrinol. (Lausanne).* **10**, 1–22 (2019).

108. Lin S. Y. *et al.* Nuclear localization of EGF receptor and its potential new role as a transcription factor. *Nat. Cell Biol.* **3**, 802–808 (2001).

109. Azimzadeh Irani M., Kannan S. & Verma C. Role of N-glycosylation in EGFR ectodomain ligand binding. *Proteins Struct. Funct. Bioinforma.* **85**, 1529–1549 (2017).

110. Franklin R. A. *et al.* Nerve growth factor induces activation of MAP-kinase and p90rsk in human B lymphocytes. *J. Immunol.* **154**, 4965 LP – 4972 (1995).

111. Malkki H. Alzheimer disease: NGF gene therapy activates neurons in the AD patient brain. *Nat. Rev. Neurol.* **11**, 548 (2015).

112. Xhima K. *et al.* Ultrasound delivery of a TrkA agonist confers neuroprotection to Alzheimer-associated pathologies. *Brain* awab460 (2021). doi:10.1093/brain/awab460

113. Rao J. S. *et al.* NT3-chitosan enables de novo regeneration and functional recovery in monkeys after spinal cord injury. *Proc. Natl. Acad. Sci. U. S. A.* **115**, E5595–E5604 (2018).

114. Kumar A., Raza, K., Nag, T. C., Srivastava, A. & Sehgal, R. Localization and hypersecretion of nerve growth factor in breast phyllodes tumors: Evidence from a preliminary study. *Cancer Rep.* **4**, 8–12 (2021).

115. Lagadec C. *et al.* TrkA overexpression enhances growth and metastasis of breast cancer cells. *Oncogene* **28**, 1960–1970 (2009).

116. Lin C. *et al.* Nerve growth factor (NGF)-TrkA axis in head and neck squamous cell carcinoma triggers EMT and confers resistance to the EGFR inhibitor erlotinib. *Cancer Lett.* **472**, 81–96 (2020).

117. Trouvilliez S. *et al.* Direct interaction of TrkA / CD44v3 is essential for NGF-promoted aggressiveness of breast cancer cells. *J. Exp. Clin. Cancer Res.* 1–21 (2022). doi:10.1186/s13046-022-02314-4

118. Aubert L. *et al.* NGF-induced TrkA / CD44 association is involved in tumor aggressiveness and resistance to lestaurtinib. **6** (2015).

Comme décrit dans la revue, le récepteur TrkA participe à de nombreuses fonctions biologiques dont la survie et la différenciation neuronale. De plus, il est également impliqué dans de nombreuses pathologies dont les cancers.

2.2. Rôle de l'axe NGF/TrkA dans les cancers

L'implication de l'axe NGF/TrkA a été démontrée dans de nombreux cancers dont les cancers du sein, de la prostate et des voies aerodigestives supérieures.

Notre laboratoire a montré que le NGF est surexprimé dans les cancers du sein. Néanmoins, cette surexpression n'a pas de valeur pronostique (Adriaenssens *et al.*, 2008). Son récepteur, TrkA, est également surexprimé et activé (phosphorylé) dans les cancers du sein (Lagadec *et al.*, 2009). De plus, l'expression de TrkA dans les tissus de patients est plus élevée que dans les cellules cancéreuses mammaires triples négatives MDA-MB-231. De façon intéressante, ces cellules métastasent peu au cerveau *in vivo* (xénogreffes en souris SCID) mais la surexpression de TrkA restaure un tropisme cérébrale. Dans les cancers des voies aerodigestives supérieures, l'axe NGF/TrkA favorise la transition épithélio-mésenchymateuse. Il est également impliqué dans l'inefficacité des inhibiteurs d'EGFR (Erlotinib) (Lin *et al.*, 2020). L'axe NGF/TrkA semble participer également participer à l'inefficacité des traitements anti-HER2 dans les cancers de la prostate (Festuccia *et al.*, 2009).

Dans diffèrents cancers, dont les cancers du sein, de la prostate ou des voies aérodigestives supérieures, l'axe NGF/TrkA semble donc favoriser l'agressivité tumorale *via* son rôle dans les cellules tumorales. Néanmoins, le NGF participe également à l'agressivité tumorale *via* son action sur les cellules du microenvironnement dont les cellules endothéliales ou nerveuses.

De façon intéressante, le NGF ne stimule pas les cellules épithéliales mammaires non cancéreuses mais *a contrario* promeut la croissance, la migration et l'invasion des cellules cancéreuses (Descamps *et al.*, 2001). Le

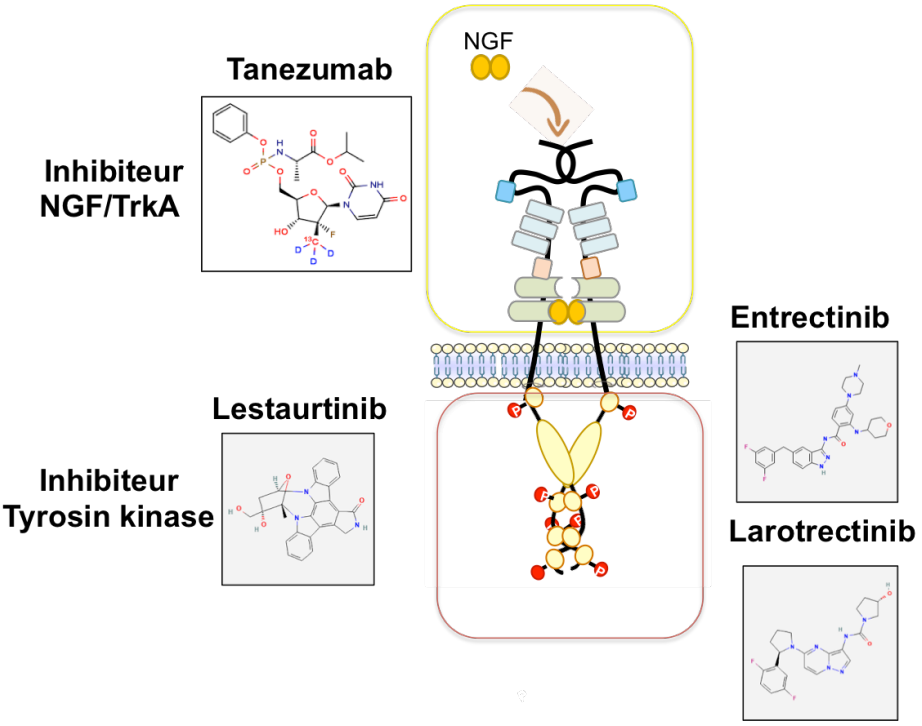
NGF contribue ainsi non seulement à la croissance tumorale mais aussi au processus métastatique. Le NGF favorise également l'enrichissement en cellules souches cancéreuses, mécanisme qui serait impliqué dans la formation des métastases et la résistance aux thérapies. En plus de son action sur les cellules cancéreuses mammaires, le NGF peut agir sur d'autres types cellulaires, ce qui concourt à l'évolution du cancer. Par exemple, le NGF favorise la survie et la différenciation des cellules nerveuses. Dans le cadre d'un cancer, ce mécanisme contribuerait aux douleurs associées au cancer et au processus métastatique. En effet, il a été montré que la neutralisation du NGF à l'aide d'un anticorps bloquant permet de réduire la douleur associée. De plus, le NGF favorise également la migration, l'invasion et la tubulogenèse des cellules endothéliales. *In vivo*, il promeut ainsi la vascularisation de la tumeur et contribue au processus métastatique.

Ces observations montrent l'importance de l'axe NGF/TrkA non seulement dans les cellules cancéreuses mammaires mais aussi les cellules du microenvironnement. Le ciblage de l'axe NGF/TrkA et en particulier de la phosphorylation de ce récepteur apparaît ainsi comme une piste thérapeutique de choix pour la prise en charge des cancers.

2.3. Ciblage de l'axe NGF/TrkA

Une première stratégie est de **bloquer la fixation du NGF** sur TrkA. Un anticorps monoclonal humanisé ciblant le NGF, le Tanezumab (**Figure 6**), a fait l'objet d'essais cliniques pour tester son effet sur les douleurs associées aux métastases osseuses et à l'arthrose du genou et de la hanche. Dans le cas de l'arthrose, l'Agence Européenne des Médicaments (AEM ; rapport de Septembre 2021) n'a rapporté aucun bénéfice du Tanezumab par rapport aux anti-inflammatoires non-stéroïdiens (traitement actuel) et des effets secondaires. Ainsi l'AEM n'a pas autorisé son utilisation pour l'arthrose. Dans le cas des douleurs associés aux métastases osseuses, les essaies cliniques de phase III ont montré un bénéfice du Tanezumab. Bien que ces résultats nécessitent d'être confirmés, il s'avère encourageants, ce qui soulignent l'importance de développer de nouveaux composés de ce type. Dans ce sens, des molécules compétitrices du NGF qui se fixent sur TrkA ont été

produites dont le peptide BVNP-0197 qui interagit avec la boucle II/IV (Kennedy *et al.*, 2017; Poole *et al.*, 2019). Néanmoins, ces composés n'ont pas d'effets anti-tumoraux. En effet, l'activation de TrkA ne résulte pas forcement de la fixation du ligand (NGF ou ProNGF). Ainsi, pour bloquer les effets pro-tumoraux de TrkA ligand-dépendants et indépendants, des inhibiteurs de la phosphorylation de TrkA ont été mis au point.



<u>Figure 6 :</u> Molécules utilisées en clinique pour le ciblage de l'axe NGF/TrkA. L'axe NGF/TrkA peut être ciblé à l'aide de molécules qui bloque l'interaction entre TrkA et son ligand. En particulier, le Tanezumab est un anticorps monoclonal humanisé (A). Il est également possible d'inhiber la phosphorylation de TrkA à l'aide d'inhibiteurs tyrosine kinase dont le Lestaurtinib, l'Entrectinib et le Larotrectinib.

L'Entrectinib et le Larotrectinib sont 2 **inhibiteurs de la phosphorylation** de TrkA (TKI ; **Figure 6**). Ces inhibiteurs se fixent au niveau du domaine kinase et jouent le rôle de compétiteurs vis à vis de l'ATP. Néanmoins, la séquence du domaine kinase de TrkA présente une forte homologie avec celle de TrkB et TrkC. Ces inhibiteurs ciblent ainsi également la phosphorylation de TrkB et TrkC. De plus, l'Entrectinib inhibe ALK (Anaplastic Lymphoma Kinase) et ROS1 (c-ros oncogen 1). Le Larotrectinib et l'Entrectinib sont approuvés par la FDA (Food and Drug Association) pour traiter les cancers qui présentent une fusion d'un gène *NTRK*. Néanmoins, les fusions NTRK sont des évènements rares et ces TKI ne présentent pas d'effet

dans le cas des autres altérations de TrkA dont les mutations ponctuelles mais aussi les surexpressions. De plus, malgré l'engouement initial pour ces composés, le récent rapport des Hautes Autorités de Santé (France) reporte un bénéfice modéré voir insuffisant pour ces composés même dans le cas de tumeurs présentant des fusions NTRK. Ces observations montrent l'importance de parfaire notre connaissance des voies de signalisation de TrkA et de leur implication dans l'inefficacité des TKI.

C'est dans ce contexte que notre équipe a montré qu'indépendamment de sa phosphorylation, TrkA peut s'associer à des co-récepteurs pour favoriser l'agressivité tumorale. Ces mécanismes pourraient ainsi contribuer à l'inefficacité des TKI notamment dans le cas de surexpression de TrkA. En particulier, la fixation du NGF sur TrkA favorise son association avec la glycoprotéine CD44, connue pour être impliquée dans la croissance tumorale, le processus métastatique et la résistance aux thérapies.

3. Le co-recepteur CD44

3.1. Découverte, synthèse, Structure-fonction

3.1.1. Découverte

CD44, pour « Cluster of Differentiation 44 », a été découvert en 1980 à la surface de différents types de cellules immunitaire : cellules thymiques, de la moelle osseuse, des monocytes, des lymphocytes des ganglions lymphatiques et des granulocytes (Dalchau *et al.*, 1980). La protéine CD44 est également exprimée dans d'autres types cellulaires dont les cellules endothéliales.

3.1.2. Synthèse, structure, fonction cellulaire

CD44 est une famille de glycoprotéines transmembranaire codée par un gène de **20 exons** localisé sur le **locus 11p13** (NCBI gene ID : 960). La transcription de *CD44* permet la production d'une forme standard constituée des exons 1 à 5 et des exons 6 à 10. La régulation par **épissage alternatif** des 10 exons centraux de *CD44* permet également la production de nombreux isoformes (Plus de 20) qui inclus les exons 2 à 10 (Ponta *et al.*, 2003 ; **Figure 7**).

La protéine CD44 est un récepteur membranaire de type I et est ainsi constituée d'une **partie extracellulaire, transmembranaire et intracellulaire**. Les parties transmembranaire et intracellulaire de CD44 présentent une conservation importante (à l'exception d'une insertion chez les oiseaux). La partie intracellulaire de CD44 présente différents sites impliqués dans la mise en place de ses voies de signalisation. Elle peut tout d'abord recruter les protéines **ERM** (Ezrine, Radixine et Moésine), 3 paralogues présents chez les Vertébrés. Les protéines ERM permettent de faire le lien entre la membrane plasmique et le cytossquelet d'actine de la cellule et joue ainsi un rôle clé dans différents mécanismes dont la migation et la division cellulaire ERM. Le recrutement des ERM par CD44, tout comme d'autres protéines membranaires dont les échangeurs sodium/hydrogènes NHERF-1/2, se fait *via* leur domaine FERM (**Figure 7 bleu**). Néanmoins, de façon intéressante, CD44 ne présente pas le motif de liaison aux ERMs

(MDW*XXXXX*(L/I) F*XX*(L/F)) identifié dans ces échangeurs. En revanche, la queue cytoplasmique de CD44 contient deux régions basiques impliquées dans l'interaction qui contiennent en particulier les acides aminés Q298,Q300 et G296,Q297 (Legg and Isacke, 1998). Par cristallographie de la partie cytoplasmique de CD44 (peptide) avec le FERM de la Radixine, il a été montré l'existence d'une interaction directe entre ces 2 protéines (Mori *et al.*, 2008). L'interaction entre la partie cytoplasmique de CD44 et la Moésine a également été mise en évidence grâce à cette méthode (Bradshaw ; PDB to be published). L'existence d'une interaction directe entre CD44 et l'Ezrine et ses déterminants moléculaires n'a en revanche pas été élucidée à ce jour. De plus, la fixation des ERM sur CD44 permet la mise place de signalisations sous-jacentes (**Figure 7, bleu**). Par exemple, il a été montré que suite à une stimulation au HGF (Human Growth Factor), l'activation de la voie de signalisation MEK/Erk par le récepteur Met (Mesenchymal-epithelial transition factor) nécessite la fixation des ERM sur CD44v6 (Orian-Rousseau *et al.*, 2002). Ce mécanisme favoriserait ainsi la migration des cellules cancéreuses de colon humaines HT29. *A contrario*, la fixation de la Merline (au même niveau de la partie intracellulaire de CD44 que les ERM), une protéine similaire aux ERM, en inhibant le clivage de l'ectodomaine de CD44 permet de bloquer la migration des cellules cancéreuses mammaires MDA-MB-231 (Hartmann *et al.*, 2015; **Figure 7, bleu**). De plus, de façon intéressante, dans des cellules neuronales de Schwann RT4-D6P2T surexprimant la Merline, la phosphorylation de la Merline par Akt favorise sa fixation aux phospholipides, ce qui bloque son activité pro-apoptotique et anti-migratoire dans des cellules neuronales de Schwann RT4-D6P2T (Okada *et al.*, 2009). La queue cytoplasmique de CD44 présente également un site de fixation pour les Ankyrines, une famille de protéines se fixant sur la spectrine. Ces protéines, comme les ERM constituent ainsi un lien entre la membrane plasmique et le cytosquelette. Les Ankyrines se fixent au niveau des acides aminés 306 à 320 (NGGNGT-VEDRKPSEL) de CD44 et permet par exemple l'adhésion induite par l'acide hyaluronique, ligand de haute affinité de CD44 (Lokeshwar *et al.*, 1994). La partie extracellulaire de CD44 peut être décomposée en 3 parties. Les 2 zones communes à toutes les isoformes sont codées par les 5 premiers exons et les exons 6 et 7. Entre les acides aminés 32 et 123, se

trouve la zone de liaison de l'acide hyaluronique. D'autres ligands, composants de la matrice extracellulaire, comme la fibronectine, peuvent s'y fixer. Cette zone est la seule de la partie extracellulaire de CD44 dont la structure a été caractérisée expérimentalement en raison de ses nombreuses O et N-glycosylations (**Figure 7 rouge**). Ces glycosylations jouent un rôle clé dans la conformation mais aussi la fixation de ses ligands. CD44 peut présenter différentes glycosylations selon les variants (Azevedo *et al.*, 2018; **Figure 7 rouge**). En particulier, le variant 3 présente un motif SGSG, qui fixe des facteurs de croissance dont l'HB-EGF (Heparin Binding-Epidermal Growth Factor) ou le FGF (Fibroblast Growth Factor). En revanche, l'affinité pour le NGF au niveau de ce motif est faible. De plus, le variant 6 permet lui la fixation du HGF. Ainsi, la liaison de Met et CD44v6 semble se faire indirectement *via* l'HGF.

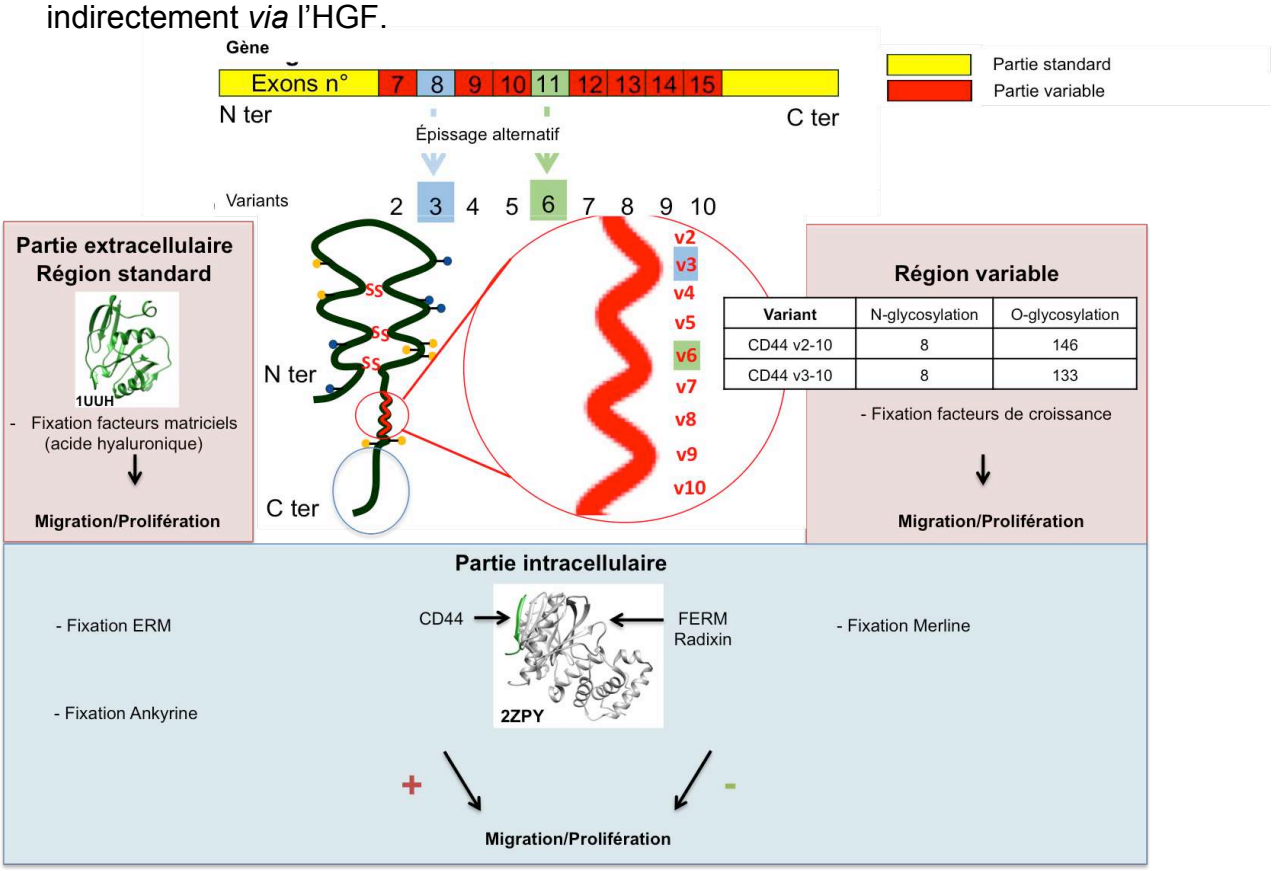


Figure 7 : Structure de CD44 : du gène aux effets cellulaires. CD44 est codée par un gène de **20 exons**. En plus de la forme standard constituée des exons 1 à 5 et des exons 6 à 10, l'épissage alternatif des 10 exons centraux de *CD44* permet la production d'isoformes qui inclus les exons variant 2 à 10. Cette région variable mais aussi la zone de fixation pour les ligands de CD44 dont l'acide hyaluronique contribue à ses effets pro-tumoraux. De plus, la partie intracellulaire présente des motifs permettant le recrutement des ERM, la Merline et l'Ankyrine qui jouent un rôle clé dans la régulation de la migration et la prolifération cellulaire.

Précédemment, notre équipe a observé que la fixation du NGF sur TrkA favorise son association avec CD44 dans différents modèles cellulaires : cellules de cancers du sein (PR-), de prostate (PC-3) et des voies aérodigestives supérieures (Cal-33, SCC9). Cette association se ferait en particulier *via* le variant 3. Néanmoins, la nature de cette association (interaction directe ou non), ses modalités moléculaires et son rôle nécessitait de plus amples investigations.

3.3. Rôles des contenants v3 dans l'agressivité tumorale

Dans différents cancers, il a été montré que les isoformes contenant le variant 3 (CD44v3) sont impliqués dans différents mécanismes pro-tumoraux dont la croissance tumorale, le processus métastatique et la résistance aux thérapies.

Dans les cancers des voies aérodigestives supérieures, CD44v3 est associé à la croissance tumorale et la migration (Wang *et al.*, 2007). Au contraire, dans le cancer de la prostate, l'expression de CD44v3 dans des cellules non cancéreuses de prostate conduit à une moindre adhésion aux cellules endothéliales et des capacités d'invasion réduites par rapport aux cellules cancéreuses de prostate PC-3 (Harrison M. *et al.*, 2006).

Chez les patients, CD44v3 est surexprimé et associé à diffèrents paramètres cliniques dont l'envahissement ganglionnaire dans diffèrents cancers (**Tableau 4**). Dans les cancers des voies aérodigestives supérieures, CD44v3 est surexprimé et corrélé avec l'envahissement ganglionnaire (Erika *et al.*, 2007; Wang *et al.*, 2007). Dans le cancer du sein, il a été montré que des isoformes contenant le variant 3 sont exprimés au niveau de la tumeur primaire et des ganglions lymphatiques mais pas dans les tissus mammaires normaux (Kalish *et al.*, 1999). Dans les cancers colorectaux, l'expression de CD44v3 est associée à la différenciation, à l'envahissement ganglionnaire et au stade TNM (**Tableau 4**). De plus, il est également corrélé à une moindre survie sans progression (Yan *et al.*, 2020). Les isoformes contenant le variant 3 seraient également impliqués dans la résistance à la chimio- et la radio-

thérapie. Dans les cancers de la vessie, par exemple, un anti-acide hyaluronique (4-MU) augmente la sensitivité à la chimiothérapie. D'autre part, dans les cancers des voies aérodigestives supérieures, l'isoforme v3-v10 contribue à la radio-résistance en modulant le cycle cellulaire (Al Bazaz *et al.*, 2020).

Cancer	Paramètre clinique	Référence
Sein	Envahissement ganglionnaire	Erika et al., 2007; Wang et al., 2007
Voies aérodigestives supérieures	Envahissement ganglionnaire Récurrence locale	Tsuruoka et al., 2011
Colorectaux	Diminution de survie sans progression Envahissement ganglionnaire Stade TNM	Yan et al., 2020
Poumon non à petites cellules	Envahissement ganglionnaire Stade (Stade III > Stade I-II)	Wu et al., 2003

Tableau 4 : Corrélation de l'expression de contenant v3 avec différents paramètres cliniques dans les cancers. Dans les cancers du sein, des voies aérodigestives supérieures, colorectaux ou encore du poumon non à petites cellules l'expression de CD44v3 est corrélée avec l'envahissement ganglionnaire.

L'expression des isoformes contenant le variant 3 est associée à l'agressivité tumorale dans différents modèles de cancérologie. Néanmoins, ces isoformes peuvent aussi contenir d'autres variants dont le variant 6. L'équipe du Pr. Véronique Orian Rousseau a ainsi montré, à l'aide d'un peptide mimétique de CD44v6 le rôle de l'association du variant 6 avec ses co-récepteurs (Met et VEGFR). Or, à ce jour, les études menées pour étudier le rôle du variant 3 dans la croissance tumorale et la métastase utilisent des outils (ex : siRNA) qui inhibent des isoformes contenant le variant 3 mais aussi le variant 6. Les résultats obtenus ne permettent donc pas de conclure sur le rôle du variant 3 dans la croissance tumorale et le processus métastatique. La compréhension du rôle spécifique du variant 3 nécessite donc de mettre au point de nouveaux outils pour inhiber spécifiquement les voies de signalisation du variant 3.

4. Les molécules de la signalisation de TrkA/CD44v3

4.1. La protéine p115RhoGEF

4.1.1. Découverte

La première RhoGEF (Rho Guanine Exchange Factor) découverte dans les années 80 est une RasGEF : *mcf2* (*CDC42 : Cell Division Control protein 42*). Découverte en tant qu'oncogène inconnu, CDC42 est par la suite isolée et séquencée. La comparaison de sa séquence à celle de la protéine Dbl montre qu'il s'agit de 2 versions du même oncogène (activation par des mécanismes différents)(Fasano *et al.*, 1984)**.** En 1991, Matthew J. Hart et ses collaborateurs montrent pour la première fois que cet oncogène est un facteur d'échange pour la protéine Ras (Noguchi *et al.*, 1988). En 1996, cette même équipe identifie un nouveau facteur d'échange pour les protéines Rho. Par purification d'affinité de lysats cellulaires avec une protéine Rho comme ligand, une GEF d'un poids moléculaire de 115 kDa est isolée. Elle est baptisée p115-RhoGEF (Hart *et al.*, 1991).

4.1.2. Synthèse, structure, fonction cellulaire

La protéine p115RhoGEF, aussi appelée RhoGEF1, est codée par le gène *ARHGEF1* situé au niveau du locus 19q13.2. Cette protéine est composée de 912 acides aminés pour un poids moléculaire de 115 kDa (**Figure 8**). La protéine p115RhoGEF possède 4 isoformes produits par épissage alternatif et 8 autres potentiels. Elle appartient à la famille des RhoGEF qui compte plus de 80 membres. Les protéines de cette famille par définition sont des facteurs d'échange GTP/GDP pour les protéines Rho. Cette famille peut être divisée en 2 sous-familles : une petite sous famille des DOCK protéines (11 membres) qui ne possède pas de similarité avec l'autre sous famille des protéines Dbl-like (70 membres) qui présente un domaine Dbl Homology dont fait partie p115RhoGEF (DH : acides aminés 416 à 605). En plus de ce domaine DH, p115RhoGEF possède 2 autres domaines fonctionnels : un domaine RH (RGS Homology ; acides aminés 41-232) et un domaine PH (Plextrin Homology ; acides aminés 647-760 ; **Figure 8**). Ces 3 domaines collaborent pour permettre l'activation de p115RhoGEF (passage

de la forme GDP à GTP) puis son interaction avec les protéines Rho. P115RhoGEF peut ainsi induire le changement de conformation des protéines Rho. Elle peut également subir des modifications post-traductionnelles dont la phosphorylation de résidus tyrosine ou sérine qui modulent son activité. Par exemple, la phosphorylation de la sérine 330 inhibe son activité et ainsi l'activation d'une de ses cibles, dont RhoA (Hart *et al.*, 1996). De plus, la phosphorylation de la tyrosine 738 par Jak2 suite à une stimulation avec de l'Angiotensine II permet l'activation de RhoA. Ce mécanisme contribuerait ainsi à l'hypertension dépendante de l'Angiotensine II (Guilluy *et al.*, 2010).

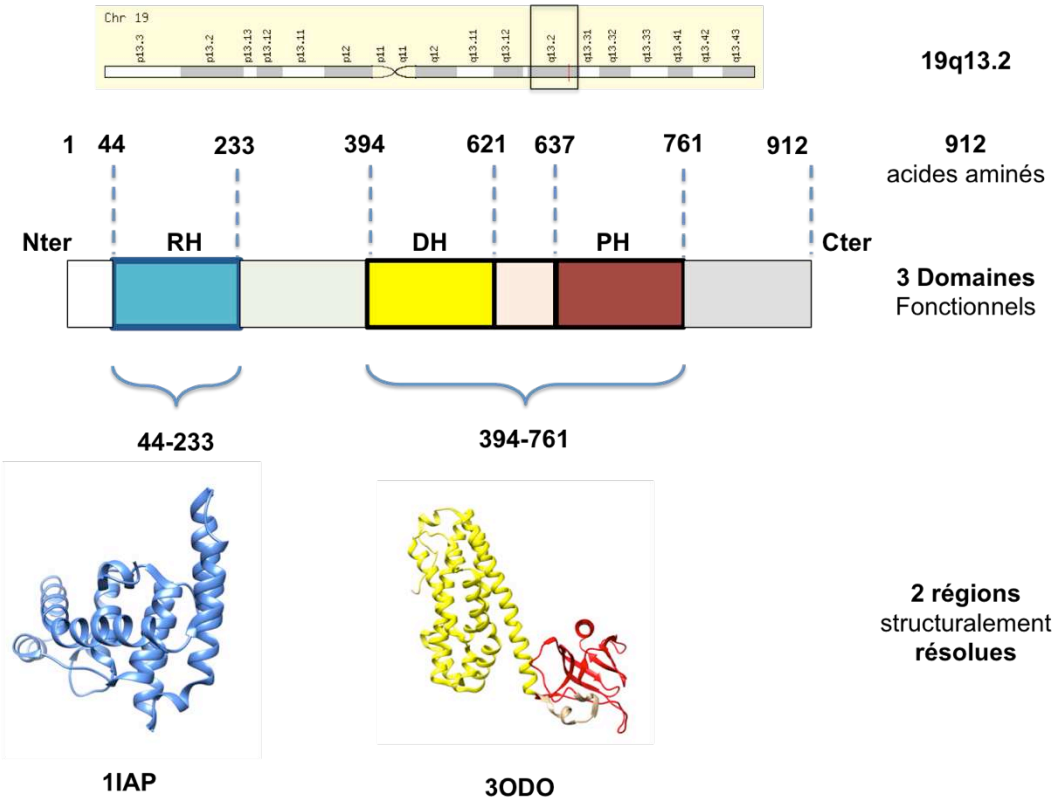


Figure 8 : p115RhoGEF : du gène à la protéine. Le gène ARHGEF1 localisé sur au niveau du locus 19q13.2 code pour la protéine p115RhoGEF. Cette protéine est constituée de 3 domaines fonctionnels (RH, DH, PH) dont la structure 3D est connue. Ces domaines sont reliés par des domaines de liaison.

La protéine p115RhoGEF est majoritairement localisée dans le cytoplasme où elle est sous forme inactive, c'est à dire couplée avec du GDP. Le passage sous la forme active (couplée au GTP) et sa relocalisation à la

membrane peut être induite par les protéines Gα12 et 13 activées. Suite à cette activation, par le LPA (LisoPhosphatidic Acid) par exemple, les GPCRw libèrent et activent la sous-unité α des protéines Gα12/13 qui s'associe avec le domaine RH de p115RhoGEF (**Figure 9**). Il faut préciser que les modalités des recrutements de p115RhoGEF par les protéines Gα12 et Gα13 sont différentes. En effet, une région acide en position N-terminale du domaine RGS de p115RhoGEF est nécessaire à son recrutement par la protéine Gα12 mais pas par la protéine Gα13 (Chow *et al.*, 2013). En effet, l'association et activation de p115RhoGEF avec et par la protéine Gα13 à la membrane plasmique nécessitent une protéine Rho ce qui n'est pas le cas pour Gα12. De plus, la relocalisation à la membrane mettrait en jeu, en plus du domaine RH, le domaine PH. En effet, la délétion d'un seul de ces domaines n'abolit pas la localisation membranaire. En revanche un domaine PH recombinant présente une localisation exclusivement cytoplasmique, ce qui suggère que ce domaine n'est pas suffisant à la localisation membranaire de p115RhoGEF (Wells *et al.*, 2001). Deux motifs du domaine DH (23-IIG et 27-EDEDF) contribuent également à son recrutement à la mebrane. En plus de cette activation GPCR-dépendante, il a été montré que p115RhoGEF peut être recrutée et activée de façon indépendante des protéines G.

P115RhoGEF peut également s'associer avec d'autres récepteurs membranaires dont les intégrines. Suite à une stimulation par la Fibronectine, p115RhoGEF est activée par les intégrines indépendamment des récepteurs couplés aux petites protéines G (GPCR) (Bhattacharyya *et al.*, 2009). P115RhoGEF peut également interagir avec CD44v3 suite à une stimulation avec la fibronectine ou l'acide huluronique *(*Dubash *et al.*, 2007; Bourguignon et al. 2003; **Figure 9**). Ces études, menées par immunoprécipitation, ne permettent néanmoins pas de conclure quant à la nature directe ou indirecte de cette association. De façon intéressante, dans ces études menées dans le même modèle cellulaire que nos travaux (cellules cancéreuses mammaires MDA-MB-231), l'association CD44v3/p115RhoGEF fait suite à une stimulation de CD44 par ses ligands et non le NGF (**Figure 9**). Or, une analyse en spectrométrie de masse du récepteur TrkA dans des cellules de

neuroblastome SH-SY5Y stimulées avec du NGF a révèlé que p115RhoGEF fait partie de l'interactome de TrkA (Emdal *et al.*, 2015). De plus, notre équipe a précédement montré que la protéine p115RhoGEF est immunoprécipitée avec TrkA dans des cellules MDA-MB-231 stimulées avec du NGF (Aubert *et al.*, 2015). Or, dans cette même étude Aubert *et al.* ont montré que le NGF favorise l'association TrkA/CD44. Ainsi, dans l'état actuel de nos connaissances, il est impossible de dire si le recrutement de p115RhoGEF repose sur TrkA et/ou CD44.

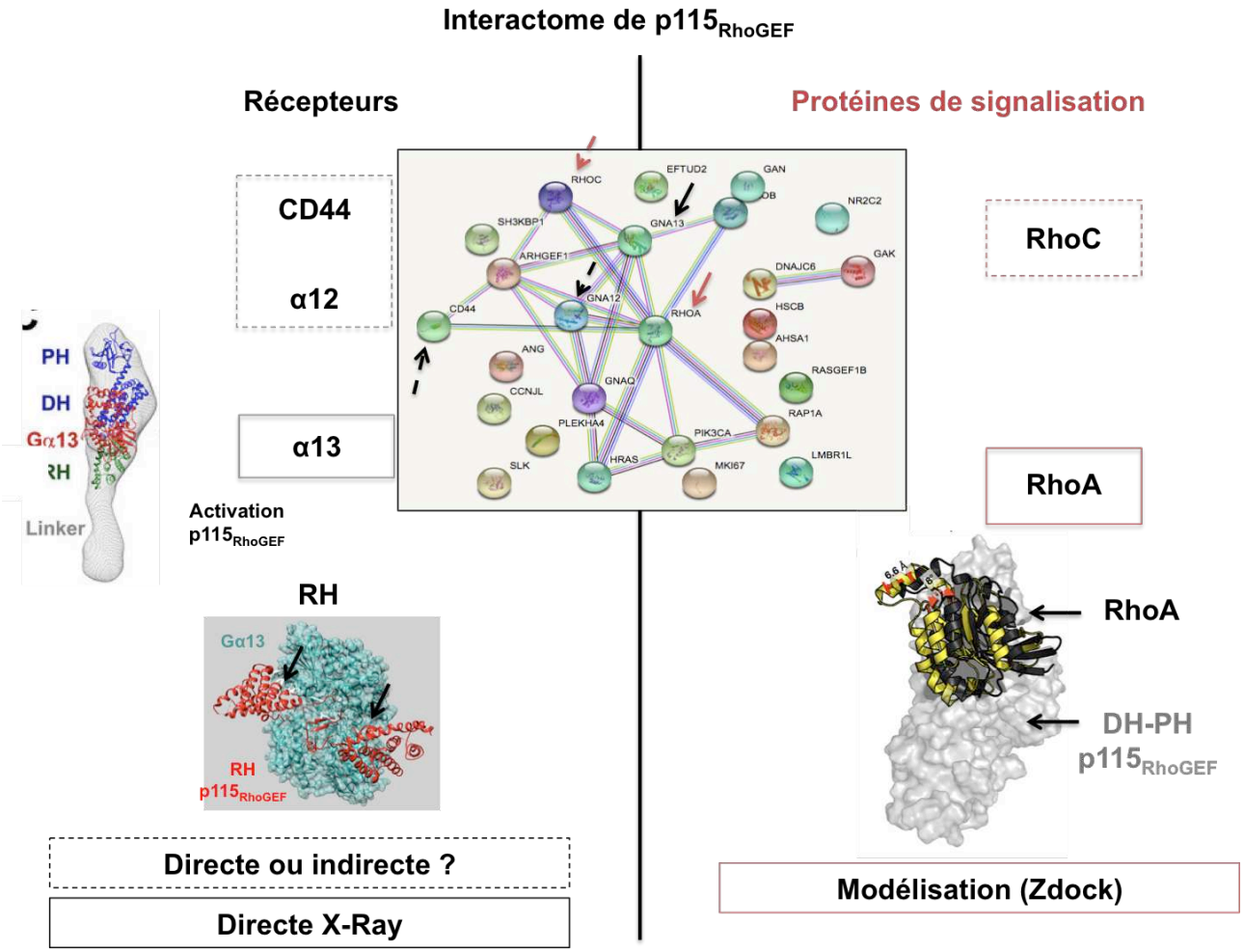


Figure 9 : Interactome de p115RhoGEF. P115RhoGEF présente une interaction fonctionnelle avec de nombreuses protéines membranaires et cytoplasmiques. Elle interagit en particulier *via* son domaine RH avec la protéine Gα13 et *via* ses domaines DH-PH avec la protéine RhoA. P115RhoGEF est également immuno-précipitée avec CD44.

Cette RhoGEF peut également, *via* sa partie C-terminale, s'homodimériser mais pas s'hétérodimériser contrairement à d'autres RhoGEF telle que LARG (Chikumi *et al.*, 2004). Cette homodimérisation

inhibe son activité GEF. Ceci explique probablement que sa surexpression conduit à un moindre potentiel migratoire (Kher *et al.*, 2014). Certaines modifications post-traductionnelles modulent également son activation dont la phosphorylation de résidus sérine ou tyrosine. La phosphorylation de la sérine 330 (localisée dans la hinge region, domaine de liaison entre le RH et le DH) favorise une conformation inactive de p115RhoGEF et donc une moindre activation de RhoA (Chikumi *et al.*, 2004). Au contraire, la phosphorylation de résidus tyrosines sur p115RhoGEF favorise l'activation de la GTP-ase Rac-1 dans des cellules musculaires d'aortes humaines (Chow *et al.*, 2013). La phosphorylation de p115RhoGEF, qui conditionne son état d'activation, dépend de tyrosines kinases dont les protéines de la famille de Src et FAK, mais aussi de phosphatases dont Shp2 (Src Homology Phosphatase 2) (Singh *et al.*, 2017; Xu *et al.*, 2020). L'activation de p115RhoGEF est donc conditionnée non seulement par le milieu extracellulaire mais aussi des acteurs intracellulaires pouvant être recrutés par les récepteurs membranaires dont TrkA. Lors de son activation, p115RhoGEF va pouvoir activer les protéines Rho et en particulier la protéine RhoA. *Via* ses DH-PH domaines, P115RhoGEF interagirait en effet directement avec RhoA (**Figure 9**). Néanmoins, cette interaction n'a pu être que prédite à ce jour en raison de la nature désordonnée des régions impliquées dans leur association (Gheyouche *et al.,* 2021). L'interaction p115RhoGEF/RhoA contribue à de nombreux mécanismes cellulaires dont la prolifération, migration ou l'invasion. Les interactions p115RhoGEF/RhoA et récepteurs membranaires/p115RhoGEF jouent ainsi un rôle clé dans de nombreux mécanismes physio-pathologiques et constituent de nouvelles cibles potentielles pour différentes maladies dont l'immunodéficience, l'hypertension ou les cancers.

4.1.3. Rôles

P115RhoGEF est exprimée dans de nombreux organes : le foie, les muscles, la peau, le sang, la moelle osseuse, l'intestin, la rate, les poumons, le système nerveux, les yeux, le cœur, les glandes salivaires, les nœuds lymphatiques et les cellules du système immunitaire.

Au niveau du système nerveux, il a été montré que p115RhoGEF est impliquée dans la perte d'intégrité de la barrière hémato-encéphalique. En effet, une stimulation avec du LPA (LisoPhosphatidic Acid) ou du TNFα (Tumor Necrosis Factor) accroit l'activation de RhoA *via* p115RhoGEF ce qui réduit la perméabilité de la barrière hémato-encéphalique (Peng *et al.*, 2011; Xiaolu *et al.*, 2011). Dans des cellules dendritiques dérivant de moelle osseuse, il a été montré que l'activité de p115RhoGEF, *via* l'activation des protéines Rho, contribue à la migration induite par le LPS (LipoPolySaccharide). De plus, p115RhoGEF est également impliquée dans le système cardio-vasculaire où il permet notamment la prolifération et la migration (Peng *et al.*, 2011; Xiaolu *et al.*, 2011). Au niveau du système digestif, une déficience en p115RhoGEF conduit à un défaut d'innervation et des troubles moteurs. Ces phénotypes résulteraient d'un taux d'expression de NGF réduit. Les maladies associées à P115RhoGEF peuvent également résultées de l'expression de variants. Par exemple, l'IMD62 (immunodéficience62) est une maladie autosomale récessive qui résulte de l'introduction d'un codon STOP prématurément dans la séquence de p115RhoGEF ce qui génère une protéine instable et cause un défaut d'activation de RhoA, de la dynamique du cytosquelette d'actine et altère ainsi la motilité des lymphocytes (Singh *et al.*, 2017). Ce défaut des lymphocytes B et T provoque des troubles respiratoires et des bronchites chroniques.

La protéine p115RhoGEF intervient ainsi dans de nombreux mécanismes physio-pathologiques tout comme TrkA. Cette pléiotropie de fonction peut en particulier s'expliquer par le fait que p115RhoGEF régule l'activation spatio-temporelle des protéines Rho dont RhoA (Sjöblom *et al.*, 2006). Or, ces protéines Rho sont impliquées dans de nombreux mécanismes cellulaires dont la migration, l'invasion ou encore la survie.

4.2. La protéine RhoA

4.2.1. Découverte

Les protéines Rho ont été découvertes dans les années 80. Cette découverte fortuite a eu lieu en tentant de cloner un gène homologue de la

sous-unité α de la gonadotropine chorionique humaine dans des escargots de mer (*Aplysia)* (Madaule and Axel, 1985). Puis, Alan Hall et Anne Ridley montrèrent que l'expression d'une protéine RhoA constitutivement active dans des fibroblastes quiescents conduit à la formation de fibres de stress et de points d'adhésion focaux. De plus, dans des cellules 3T3, ils démontrent que l'acide lisophosphatidique provoque le même effet (Ridley & Hall, 1992). Ces travaux marquent un tournant majeur pour l'étude des protéines Rho qui était jusque là reléguée au second plan. Par la suite, Alan Hall et les membres de son laboratoire poursuivirent menèrent de nombreux travaux sur les protéines Rho permettant d'améliorer considérablement notre compréhension du rôle et de la régulation des protéines Rho.

4.1.2. Synthèse et structure

La famille des protéines Rho (Ras Homologous) appartient à la superfamille des petites protéines G monomériques Ras (Rat Sarcoma) qui compte plus de 150 membres chez l'Homme. Le génome humain présente 20 gènes codant pour des protéines Rho (Huttlin *et al.*, 2017). Ces protéines se caractérisent par la présence d'un domaine G, dont la séquence d'environ 160 acides aminés est impliquée dans la fixation de leurs cibles et de leurs régulateurs. En particulier, les protéines RhoA et RhoC, font partie de la sous-famille RhoA qui compte 3 membres (RhoA, RhoB, RhoC). Ces deux protéines, codées par deux gènes distincts, présentent une forte homologie de séquence (92 %).

Ces protéines sont des GTPases qui jouent le rôle d'interrupteur moléculaire. Elles peuvent, en effet, passer d'un état inactif à actif par hydrolyse d'un GTP (**Figure 10**). Ce passage d'un état à l'autre est accéléré par les protéines GEF (dont p115RhoGEF). Au contraire, les protéines GAP favorise un échange GTP-GDP et donc l'inactivation des protéines Rho (**Figure 10**). Ce passage d'un état à l'autre, appelé cycle des protéines G, instaure un équilibre dynamique entre les 2 formes qui contrôle l'organisation du cytosquelette d'actine (Boureux *et al.*, 2007). La mise en place d'une activation dynamique et locale de l'actine dans la cellule par ce trio de

protéines participe ainsi à des processus cellulaires dynamiques : locomotion/adhérence et forme cellulaire. La dérégulation de cette dynamique, notamment lors de la surexpression de p115RhoGEF, a ainsi pour conséquence d'inhiber la migration cellulaire des cellules cancéreuses mammaires MDA-MB-231 (Kher *et al.*, 2014).

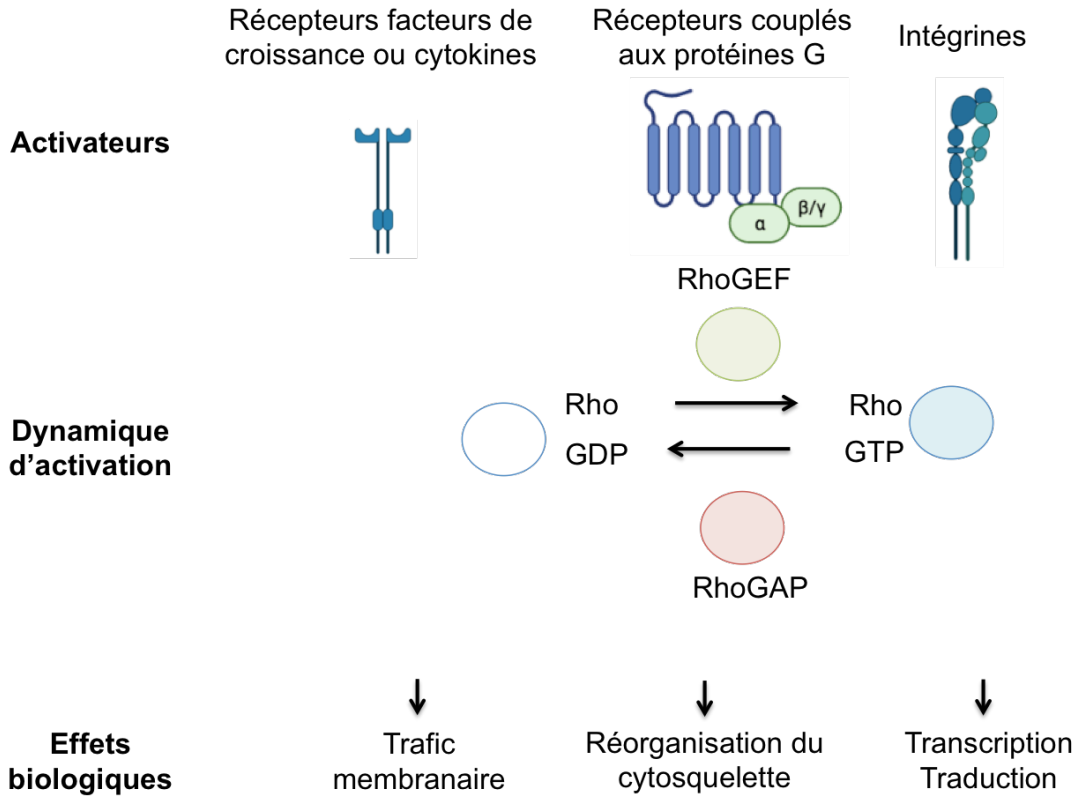


Figure 10 : Dynamique d'activation des protéines Rho. L'activation de différents récepteurs (facteurs de croissance, cytokines, GPCR, intégrines) permet l'activation de protéines RhoGEF. Les protéines RhoGEF (GTP exchanger factor) peuvent alors activer les protéines Rho par un échange GDP-GTP. Cet échange est associé à un changement conformationnel. Les protéines Rho peuvent au contraire être inactivées par les protéines RhoGAP (GTPase activating protein).

La protéine RhoA possède de nombreuses cibles dont la sérine/thréonine kinase ROCK1. La protéine ROCK1 phosphorylée peut elle-même phosphoryler de nombreuses protéines et intervient ainsi dans différents mécanismes cellulaires dont la migration. Par exemple, dans les leucocytes, l'activation de ROCK par RhoA permet le détachement de l'arrière de la cellule et ainsi sa migration (Hall, 1998). Dans les lymphocytes, il a été montré que l'axe Rho/ROCK régule la forme cellulaire et donc la migration *via*

la phosphorylation de la Thr567 de l'Ezrine, une ERM (Alblas *et al.*, 2001). De plus, la forme active de RhoA est relocalisée à l'arrière de la cellule et assurerait ainsi une migration orientée de la cellule.

La protéine RhoA est surexprimée dans différents cancers. C'est également le cas de RhoC mais pas la protéine RhoB. RhoA et RhoC interviennent toutes les 2 dans les processus métastatiques, néanmoins, il a été proposé qu'elles agissent par des mécanismes distincts. RhoC ne serait pas nécessaire à l'initiation tumorale mais interviendrait dans le processus métastatique en favorisant la vascularisation de la tumeur et l'extravasation des cellules (Lee *et al.*, 2004). RhoA quant-à-elle contribuerait à la formation de métastases *via* son rôle dans la migration et l'invasion. De plus, de façon intéressante, il a été montré que les macrophages induisent l'activation de RhoA dans les cellules cancéreuses mammaires MDA-MB-231 ce qui favorise la formation d'invadopode et leur extravasation vers les tissus (Hakem *et al.*, 2005; Miles *et al.*, 2008).

Notre équipe a précédemment montré que la signalisation de TrkA/CD44 repose sur p115RhoGEF et RhoA/C. Néanmoins, les modalités du recrutement de p115RhoGEF et d'activation spatio-temporelle de RhoA/C n'avaient pas été étudiées. Ainsi, pour comprendre le rôle de TrkA et CD44 dans la mise en place de la signalisation phospho-indépendante et la bloquer spécifiquement des études de mutagenèse et de biosenseur FRET ont été réalisées respectivement pour p115RhoGEF et RhoA au cours de ma thèse.

Objectifs de la thèse

Les objectifs de ma thèse, illustrés en **Figure 11**, sont de caractériser d'un point de vue **moléculaire et fonctionnel** les **interactions** entre TrkA, CD44v3 et les molécules de leur signalisation. Pour cela, j'ai travaillé sur 3 axes :

1. Caractériser **l'association TrkA et CD44v3** (publication 1):
    - Identifier des déterminants moléculaires de TrkA et CD44v3
    - Étudier les modalités d'activation de RhoA par TrkA/CD44v3
    - Étudier son rôle *in vitro* et *in vivo*

2. Étudier le rôle de CD44v3 dans **l'inefficacité des TKI** (publication 2):
    - Étudier les effets d'inhibiteurs de TrkA dans le cas des surexpressions de TrkA
    - Comprendre le rôle de CD44v3 sur les voies de signalisation de TrkA phospho-dépendantes et phospho-indépendantes
    - Tester le rôle de CD44v3 dans l' « inefficacité » des TKI

3. Caractériser l'association **TrkA/p115RhoGEF** (publication 3):
    - Étudier les modalités du recrutement de p115RhoGEF par TrkA
    - Identifier des déterminants moléculaires impliqués dans l'association TrkA/p115RhoGEF
    - Étudier son rôle *in vitro*

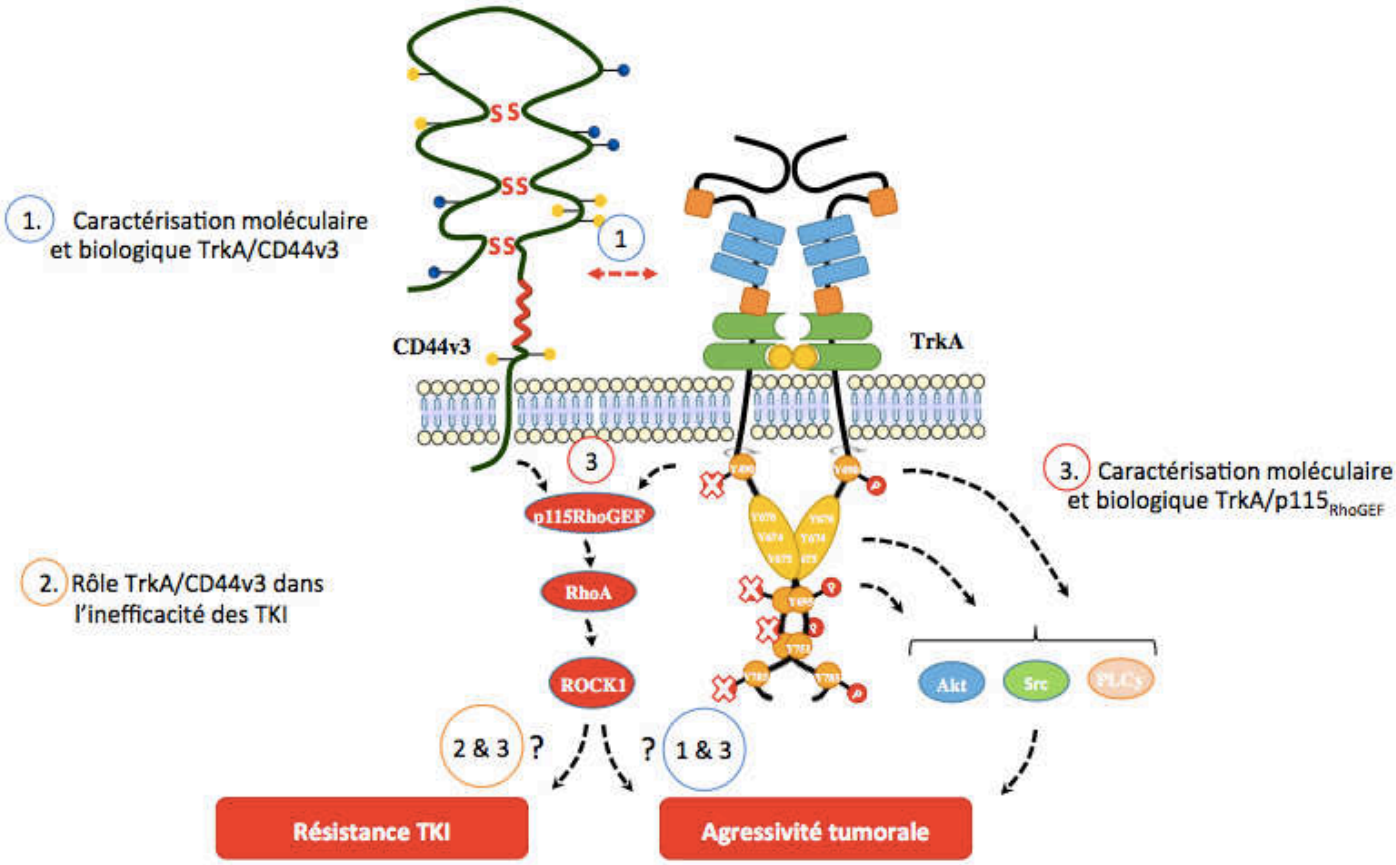


Figure 11 : Objectifs scientifiques de la thèse. Le but de ma thèse est de caractériser les interactions entre TrkA, CD44v3 et les molécules de la signalisation de TrkA/CD44. Pour cela sous-objectifs définis sont de 1) caractériser l'association TrkA/CD44v3 ; 2) comprendre les rôle de TrkA/CD44v3 dans l'inefficacité des TKI ; 3) caractériser l'association TrkA/p115RhoGEF.

Matériel et méthodes

1. Modélisation bioinformatique

1.1. Génération du modèle TrkA/CD44v3

La structure de TrkA disponible dans la Protein Data Bank (PBD ID : 2IFG ; résolution 3,4 Å) a été utilisée pour prédire l'interaction entre TrkA et un peptide de la région variable 3 de CD44. Le peptide de CD44v3, non glycosylé, a été généré par modélisation d'homologie. Le serveur web ClusPro2.020. a été utilisé pour générer plusieurs modèles qui ont été minimisés et notés (score).

1.2. Sélection du résidu cible pour la mutagénèse

Le modèle avec le meilleur score à fait l'objet d'une inspection visuelle de la structure afin d'identifier un résidu cible pour la mutagenèse. De plus, une analyse de la centralité d'interdépendance (BCA) a été réalisée en utilisant un réseau d'interaction résiduel (RIN) généré à partir du modèle et de la structure de TrkA seul. Un RIN est un réseau d'interactions entre les acides aminés d'une structure où les nœuds sont des acides aminés et les arêtes sont les interactions détectées entre les nœuds. Le RIN de cette étude a été généré à l'aide d'un programme C interne (UGSF), et les contacts résidu-résidu ont été sélectionnés lorsque la distance entre eux était comprise entre 2,5 Å et 5 Å. La BCA a été réalisée à l'aide de l'application RINspector de Cytoscape, et les scores $Z \geq 2$ ont été considérés comme des résidus centraux. Puis, les résidus jugés centraux pour le complexe d'interaction d'après la BCA et qui ne l'étaient pas dans la structure de TrkA seul ont été recherchés. Le résidu His112 a ainsi été sélectionné pour la mutagenèse. La mutation His-112-Ala a été modélisée pour s'assurer qu'elle ne modifiait pas la structure locale de TrkA.

1.3. Modélisation des structures peptidiques

Pour chaque peptide, la structure a été produite *de novo* avec le serveur web PEP-FOLD 3.5. La séquence d'acides aminés de chaque peptide a été utilisée comme entrée. La modélisation a été effectuée en utilisant les paramètres standards. La représentation du meilleur modèle a ensuite été visualisée et colorée à l'aide du logiciel Chimera.

2. Culture cellulaire

Les cellules épithéliales cancéreuses du sein MDA-MB-231 et BT-549 utilisées proviennent de l'ATCC® (American Type Culture Collection®). Ce sont des cellules triples négatives (ER -, PR - et HER2 -). Les cellules HA-TrkA sont obtenues par transfection d'un vecteur pDisplay permettant l'expression de TrkA couplé à son extrémité N-terminale avec une étiquette HA (YPYDVPDYA). Les cellules sont ensuite sélectionnées (2 semaines) à l'aide de la généticine (G418). Les cellules HA-TrkA + myc-p115RhoGEF (delta) ont été obtenues par transfection de cellules HA-TrkA avec des plasmides d'expression de myc-p115RhoGEF et séléction avec de l'hygromycine pendant 2-3 semaines. Ces plasmides co-expriment la GFP afin de valider par microscopie l'expression du plasmide. Les cellules de phéochromocytome PC-12 proviennent également de l'ATCC® (American Type Culture Collection®). Les cellules épithéliales cancéreuses du sein triples négatives SUM-159-PT proviennent de BioIVT. Les cellules rénales de singe COS-7 ont été fournies par le Pr. Véronique Orian Rousseau.

2.1. Entretien des celulles cancéreuses mammaires

Les cellules MDA-MB-231 et BT-549 sont cultivées dans un milieu Eagles's Minimum Essential Medium (EMEM, Gibco™) supplémenté par 10% de Sérum de Veau Fœtal (SVF; HyClone™), 1% d'acides aminés non essenciels (Gibco™), 0,5 mg/ml de G418 (HyClone™), 40UI/ml penicilline/40μg/ml sptreptomycine (Gibco™), 1% de ZellShield 100X (Biovalley). Les cellules

SUM-159-PT ont été cultivées dans un milieu F12 supplémenté pat 5 % de sérum de veau fétal inactivé (FBS) (Hyclone, Belgium), 1 % HEPES, 100 UI/ml Penicilline/Streptomycine, 40 µg/mL Insuline and 1 µg/mL Hydrocortisone.

2.2. Entretien des autres lignées celullaires

Les cellules COS-7 sont cultivées dans du milieu Dulbecco's Minimal Essential Medium (DMEM) supplémenté avec 10 % de Sérum de Veau Fœtal (SVF), 1 % d'acides aminés non-essentiels, 40 UI/ml penicilline/Streptomycine and 40 µg/mL Gentamycine.

Les cellules PC12 sont cultivées dans du milieu Dulbecco's Minimal Essential Medium (DMEM) supplémentés avec 10 % de Sérum de Veau Fœtal (SVF), 5 % de Sérum de Cheval, 10 UI/ml Penicilline/Streptomycine.

Les cellules sont entretenues dans des flacons de culture de 75 cm^2 (Falcon, Beckton Dickinson) et incubées en atmosphère saturée en humidité à 5 % de CO_2 à 37°C. A confluence, les cellules sont décollées à l'aide de trypsine/EDTA (1 mL ; 0,05 %/0,25 % EDTA ; 37°C, 1 min) et passées au plus au $1/10^{ième}$ afin de conserver l'hétérogénéité de la population. Le nombre de passages est également limité à 20 après décongélation afin d'éviter les dérives phénotypiques.

3. Amplification et vérification des plasmides

3.1. Constructions

Les vecteurs d'expression HA-TrkA disponibles (Wild-type et Y490F) au laboratoire ont été générés par mutagenèse dirigée et clonage de la séquence de TrkA étiqueté HA (coté N-ter) dans le vecteur P-Display (Adgene). Le vecteur d'expression HA-TrkA muté H112A a été généré par mutagenèse dirigée au cours de cette étude. Les vecteurs d'expression de p115RhoGEF étiquetés myc (coté C-ter ; séquence : EQKLISEEDL) et tronqués ou non au niveau des domaine(s) RH (Rgs Homology), PH (Pleskstrin Homology) et/ou DH (Dbl Homology) ont été produits par la

société e-Zyvec à partir d'un vecteur commercial pCMV contenant la séquence de p115RhoGEF (ORIGENE, NM_199002).

3.2. Amplification des plasmides

Après incubation de 1 µL de plasmide avec 25 µL de bactéries (One Shot Top 10 ; Promega) (25 min, 4°C), un choc thermique est réalisé (42°C, 30s ; 4°C, 2 min) et 150 µL de milieu S.O.C. (invitogen™) sont ajoutés. Le mélange est incubé (1h, 37°C, 250 RPM, Forma Orbital Shaker Thermo) puis 30 µL sont étalés sur une boite LB agar (100 µg/ml ampicilline) (16 h, 37°C). Plusieurs colonies isolées et placées dans 5 ml de milieu LB (25g/L, sigma ; 100 µg/ml ampicilline). Les tubes de cultures sont incubés (24 h, 37°C, 250 RPM). Les vecteurs sont isolés et purifiés selon le protocole du kit QIAprep® Spin Miniprep (Qiagen) puis 1 µL d'échantillon est dosé par spectrophotométrie (nanodrop).

3.3. Digestion

Afin de valider les plasmides de p115RhoGEF (delta), 500 ng de chaque est incubé dans un mélange réactionnel contenant les enzymes de restriction XhoI et SalI (1 µL XhoI ; 1 µL SalI, ; 2 µL tampon D 10X ; 0,3 µL BSA 100X ; Promega ; dans 20 µL de QSP d'eau) (1h, 37°C). Vingt microlitres de la digestion sont complétés par 5 µl de « dye » 5X Quiagen. Quinze microlitres de ce mélange sont alors déposés dans un puits pour une migration sur gel (agarose 1 % p/v (Euromedex) ; 1 goutte de BET (Euromedex), 100V, 1h30). Le profil de digestion est observé après migration à l'aide d'un banc UV (Uvitech, 264 nm).

4. Transfection et validations

4.1. Electroporation (plasmides)

Pour la transfection par electroporation des plasmides (delta P115RhoGEF), les cellules à 80 % de confluence sont trypsinisées afin d'obtenir une suspension cellulaire contenant 10^6 cellules. Après centrifugation (300 g, 10 min), le culot cellulaire est repris dans 100 µL de nucleofactor™ et 2 µg de

plasmides sont ajoutés puis le mélange est placé dans une cuve de transfection (kit AMAXA® V, Lonza).

4.2. Lipofection (plasmides)

Pour les transfections par lipofection (pour générer les lignées surexprimant HA-TrkA et myc-p115RhoGEF), le kit JetOPTIMUS a été utilisé. Des cellules à 50 % de confluence sont transfectées à l'aide 4 µg de plasmide mélangé à 500 µL de JetOPTIMUS buffer et 5 µL de JetOPTIMUS reagent préalablement incubé 10 min (à température ambiante).

4.3. Interférine (siRNA)

Pour la transfection des siRNA, 500 µL de milieu 10 % SVF, 20 µL d'interferin™ et 20 µM de siARN (siCTRL, siCD44v3, siTrkA) est laissé à incuber (20 min, 20°C). Pendant ce temps, les cellules ensemencées (Boite de pétri diamètre 100) sont lavées avec 5 mL de milieu et replacées dans 9,5 mL de mileu EMEM (10 % SVF). Le mélange de transfection est déposé sur les cellules puis le tout est incubé 48 h (5 % de CO_2, 37°C) avant la lyse. Les séquences des siRNA utilisés sont :
siCD44v3 (poll) : UGAAGAUGAAAGAGACAGACA et AGGCAUUGAUGAUGAUGAAGA, siCD44 : GUAUGACACAUAUUGCUUC, SiGFP (=siCTRL) : GAUGAACUUCAGGGUCAGC.

4.4. Extraction d'ARN

Les cellules sont soumises à une lyse alkaline réalisée par 600 µL de tampon de lyse RLT (RNeasy mini kit; Qiagen) et 1 % β-mercapto-éthanol (Sigma®) par boite diamètre 100 (Greiner Bio-One). Les boites sont placées au -80°C une nuit. Après décongélation sur glace et ajout de 600 µL d'éthanol (70 % (v/v), H_2O) l'échantillon est placé dans une colonne d'affinité puis centrifugé (8000 g, 15 s). Après lavage et centrifugation (700 µL tampon RW1, 10 500 g, 1 min), les ADN sont éliminés à l'aide d'un mélange contenant de la DNase (70 µL tampon RDD et 10 µL de DNase). Puis 3 séries de lavage/centrifugation sont effectuées (700 µL tampon RW1, 10 500 g, 1 min puis 2 fois 500 µL tampon RPE, 10500 g, 1 min) ainsi qu'une dernière centrifugation à sec (11500 g, 5 min). Les ARN sont élués en 2 fois avec 40

µL H_2O RNase free au total. La concentration et qualité des ARN sont testées par dosage spectrophotométrique (MultiskanGo ou NanoDrop 2000, Thermoscientific). Ces ARN sont ensuite utilisés pour tester l'efficacité des siRNA par qPCR.

4.5. qPCR

Les ARN (1 µg) sont incubés avec un mix contitué de 4 µL iScript Reaction Mix, 1 µL iScript Reverse Transcriptase, QSP H_2O 20 µL; iScript™ cDNA Synthesis Kit, Bio-Rad). Les ADNc sont produit grâce au programme suivant : 5 min à 25°C, 25 min à 46°C et 1 min à 95°C (Mastercycle personal, Eppendorf). Les ADNc sont ensuite stockés à -20°C. Des triplicats sont réalisés dans des plaques 96 puits (Multiplate PCR Plates 96-well, Bio-Rad) avec 2 µL d'ADNc, 5 µL de QuantiFast SYBR Green Mix 2X (Qiagen), 0,1 µL d'amorces sens 100 µM de *NTRK1* (TGGACTACGGCACCAACTTC) ou *PUM-1* (GATTATTCAGGCACGCAGGT), 0,1 µL d'amorces anti-sens 100 µM de *NTRK1* (TAGAAGCCTTTGCGGGTGAG) ou *PUM-1* (AGCAGCGCTGATGATGTATGG) et 2,8 µL H_2O RNase free. Après 5 min à 95°C, 40 cycles de 10 s à 95°C et 30 s à 60°C sont réalisés (CFX96 Real-Time System C1000 Touch Thermal Cycler). Les $2^{\Delta Ct(TrkA)-\Delta Ct(Pum1)}$ sont calculés pour comparer l'expression de *NTRK1* ou *CD44v3* dans les cellules transfectées avec les vecteurs d'expression HA-TrkA mutés (Y490F et KD) ou non (HA) et les cellules non transfectées (WT). Le gène *PUM-1* sert de gènes de référence.

4.6. Extraction protéique

Les cellules sont ensemencées en boite de Pétri (diamètre 100 ; Greiner). A 80 % de confluence, les cellules sont rincées (EMEM 0,1 % SVF), puis lavées 2 fois au PBS 1X (137 mM NaCl ; 2,7 mM KCl ; 10 mM Na_2HPO_4 ; 1,38 mM KH_2PO_4 ; pH 7,4) et lysées avec un tampon de lyse (40 mM HEPES pH 7,5 ; 1 mM EDTA ; 120 mM NaCl ; 10 mM NaPPi ; 50 mM NaF ; 1,5 mM Na_3VO_4 ; 1% Triton X-100 ; 0,1% SDS ; 1 mM PMSF ; 10 min, 4°C). Les lysats sont récupérés par raclage, centrifugés (10 min, 15 800 g, 4°C). Puis le surnageant est récupéré et stocké à -80°C. Les protéines sont dosées par la méthode BCA selon les recommandations du fabricant. Les concentrations

sont déterminées par mesure de l'absorbance en triplicat et comparées à une gamme étalon de BSA (de 0 à 800 µg/µl) à 560 nm (photomètre Multiskan FC). Les échantillons sont ensuite utilisés pour valider l'expression du HA-TrkA ou myc-p115RhoGEF par western blot.

4.7. Western blot

Les extraits protéiques sont dilués à 1 µg/µL dans un tampon de Laemmli 5X (63 mM Tris HCl, 10 % glycérol, 2 % SDS, 5 % de β-mercaptoéthanol, 0,025 % de Bleu de Bromophénol, pH 6,8 ; 7 min ; 95°C ; sous agitation) puis déposées (40 µg/puits) et séparées sur gel de polyacrylamide (7,5 %, 200 V constant, 45 min, sur glace). Les protéines sont transférées (tampon transfert Tris Base 25 mmol/L, glycine 192 mmol/L, 15 % de méthanol, H_2O) sur membrane PVDF (100 V, 1h15). Les membranes sont ensuite saturées dans une solution Tris Buffer Saline Tween 20 0,1 % (TBST 0,1 %) + 5 % BSA (p/v ; 1 h, 20°C, sous agitation) ou + 5 % lait écrémé (p/v ; anti-myc) puis incubées avec les anticorps primaires anti-HA (BioLegend, clone 16B12), myc (9B11 Cell signaling) ou anti-βactine (A2066, Sigma-Aldrich, 1/10 000ième) dilués dans les solutions de saturation (16 h, 4°C, sous agitation). Après lavages (TBST 0,1 %, 5x5 min, 20°C), les membranes sont incubées avec l'anticorps secondaire dilué dans le TBST 0,1 % (anti-IgG de lapin ou souris, Jackson ImmunoResearch, 1/5000ième ; 1h15, 20°C, sous agitation) puis à nouveau lavées (TBST 0,1%, 5x5 min, 20°C). La révélation par chimiluminescence (West Pico ou Femto, ThermoScientific) est détectée à l'aide d'un appareil de révélation (FUJIFILM LAS-4000 ou Fusion FX) et analysée avec le logiciel MultiGauge ou Fusion.

5. Étude des associations protéiques *in cellulo*

5.1. Traitement des cellules en vue d'une lyse protéique

Les cellules sont ensemencées en boite de Pétri (diamètre 100 ; Greiner). A 80 % de confluence, les cellules sont rincées (EMEM 0,1 % SVF), puis sevrées dans du milieu EMEM supplémenté par 0,1 % SVF (SVF; HyClone™), 1 % d'acides aminés non essenciels (Gibco™), 40UI/ml penicilline/40mg/ml sptreptomycine (Gibco™), 1 % de ZellShield 100X

(Biovalley). Après 3h de sevrage (EMEM 0,1 % SVF), les cellules sont traitées ou non avec un inhibiteur de la phosphorylation de TrkA (Larotrectinib ou Entrectinib) ou le peptide mimétique de p115RhoGEF couplé à une séquence TAT (TATP13 ; 50 ng/mL) ou son contol (TATSP) puis 1h plus tard les cellules sont traitées avec 100 ng de NGF (Alomone) (5 ou 30 min) ou non (0 min). Le peptide mimétique de CD44v3 P4 (50 ng/mL) ou son contrôle est ajoutés 3h30 après le début du sevrage. Les traitements sont réalisés dans un incubateur pour éviter les stress mécaniques et thermiques. Les cellules sont ensuite placées sur glace pour procéder à la lyse comme décrit précédement.

5.2. Immunoprécipitation

Les protéines (1 mg dans 400 µl de tampon de lyse) sont incubées (1h, 4°C, 10 RPM, sur roue) avec 100 µL de billes G (Protein G Agarose, Upstate) et 10 µL d'IGg2 (0,5 µg/µL). Après centrifugation (5 min, 4°C, 13 800g) le surnageant est incubé (2h, 4°C, 10 RPM, sur roue) avec 12,5 µL d'AC anti-HA (0,4 µg/µL ; Roche 12CA5). Des billes G (100 µL, Protein G Agarose, Upstate) sont ajoutées puis le surnageant est remis à incuber (16 h, 4°C, 10 RPM, sur roue). Après 3 lavages dans le tampon de lyse par centrifugation (5 min, 4°C, 13 800 g). Les complexes protéiques sont récupérés dans le culot par ajout du tampon de Laemmli 2X (25,2 mM Tris HCl, 4 % glycérol, 0,8 % SDS, 2 % de β-mercaptoéthanol, 0,01 % de Bleu de Bromophénol, pH 6,8 ; 7 min ; 95°C ; sous agitation).
Des western blot avec les anticorps anti-p115RhoGEF (3669S, Cell Signaling, 1/1000ième), anti-HA (BioLegend, clone 16B12) et anti-myc (Cell Signaling) sont ensuite réalisés.

5.3. Duolink

Les cellules sont ensemencées (6 000 cellules/puits) sur des lames compartimentées Nunc™ Lab-tek™ 8 puits (ThermoScientific) coatées au collagène de type 1 (50 µg) puis mises à incuber à 37°C pendant 24 h. Après 4 h de sevrage (milieu 0,1 % SVF), les cellules sont traitées avec 16 nM de NGF (0, 5, 15, 30 min). Deux rinçages au PBS sont réalisés puis les cellules sont fixées avec une solution de paraformaldéhyde (4% (p/v) dans PBS pH

7,4) (10 min ; 20°C). Une solution de Glycine (100 mM) permet de bloquer les résidus aldéhydes libres (3 x 5 min). Une solution de PBS + 4 % SVF permet de saturer les sites aspécifiques (60 min, 20°C, sous agitation) avant d'incuber (16 h, 4°C, sous agitation) dans une solution de PBS + 4 % SVF contenant les anticorps primaires (p115RhoGEF, Cell Signaling, 1/50ième). Après la saturation, les cellules sont incubées (16 h, 4°C, sous agitation) avec les anticorps primaires (CD44, Cell signaling 1/100ième ; TrkA sc-118, Santa Cruz, 1/50$^{ième)}$. Les cellules sont incubées avec des sondes plus (anti-rabbit) et minus (anti-mouse) du kit Duolink *in situ* (Sigma-Aldrich), diluées au 1/5ème dans du PBS + 4% BSA (1h, 37°C). Puis, les cellules sont mises en présence de la ligase diluée au 1/40ème dans le tampon de ligation dilué au 1/5ème dans de l'eau (30 min, 37°C). L'amplification est alors réalisée avec une solution contenant la polymérase diluée (1/80ième) dans le tampon d'amplification dilué (1/5ième) dans de l'eau (100 min, 37°C). Après 2 lavages, une contre-coloration est réalisée avec du Hoechst 33258 (1mM, 30 min, 20°C, à l'obscurité) puis la lame est à nouveau rincée (PBS, 3x5min). Les lames sont alors montées au fluoromount (Dako).

5.4. Co-localisation

Le début du protocole est le même que celui des Duolink. Après lavages, les cellules sont incubées avec les anticorps secondaires Alexa Fluor 488 et 546 (Invitrogen, 1/4000ième) dilués dans du PBS + 5 % SVF (1h30, 20°C, sous agitation). Puis une contre coloration est effectuée au Hoechst 33258 (1 mM, 30 min, sous agitation) ainsi que 2 lavages (PBS, 5 min, 20°C). Les lames sont alors montées au fluoromount (Dako). Les marquages sont visualisés à l'aide d'un microscope confocal et les images sont analysées à l'aide du logiciel Fiji. La colocalisation est évaluée à l'aide d'une matrice de colocalisation.

6. Étude des interactions protéiques *in vitro*

6.1. Thermophorèse

6.1.1. Interaction TrkA/peptides de CD44

La protéine TrkA-His taguée (partie extracellulaire ; Ala 34-Gly423) (9966-TK-050 ; R&D Systems, Royaume-Uni), diluée à 200 nM dans le tampon PBS-T (fourni par le vendeur), a été marquée à l'aide d'un kit de marquage Monolith His-Tag avec RED-Tris-NTA (Nano Temper). Le colorant RED-Tris-NTA a été dilué dans du PBS-T à 100 nM. Le mélange a été incubé à température ambiante dans l'obscurité pendant 30 minutes. Puis les peptides ont été ajoutés. Les capillaires ont été remplis individuellement et chargés dans l'instrument pour réaliser le binding check avec un Pico MST NT.115 A (Nano Temper Technologies GmbH).

6.1.2 Interaction TrkA/CD44v3

Pour tester la liaison de CD44v3 à TrkA, des extraits de cellules COS-7 transfectées avec un plasmide d'expression de CD44v3-his ont été marqué puis une dilution en série avec la protéine recombinante TrkA-His (ECD), ou le NGF ont été réalisés pour tester la fixation de TrkA et le NGF sur CD44v3. Puis, une dilution en série du NGF dans un mix extraits COS-7 CD44v3 marqué : TrkA (1 :1) a été réalisé pour tester l'association de CD44v3 à dans la conformation TrkA avec le NGF. Les capillaires ont été remplis individuellement et chargés dans l'instrument. Les données ont été analysées à l'aide du logiciel MO Control (Nano Temper).

6.1.3. Effet de CD44v3 sur l'affinité de TrkA pour le NGF

Comme précédemment, la protéine TrkA-His taguée, diluée à 200 nM dans le tampon PBS-T, a été marquée à l'aide d'un kit de marquage Monolith His-Tag avec RED-Tris-NTA (Nano Temper). Le colorant RED-Tris-NTA a été dilué dans du PBS-T (100 nM). Le mélange a été incubé à température ambiante dans l'obscurité pendant 30 minutes. Puis un mix peptide ou extrait de COS-7 exprimant ou non (contrôle négatif) CD44v3-his ont été réalisés (1 :1). Les

extraits sont préparés à l'aide du protocole décrit ci-après. Puis, une dilution en série du NGF a été réalisée, les capillaires remplis individuellement ont été chargés dans l'instrument. Les données ont été analysées à l'aide du logiciel MO Control (Nano Temper).

6.2. Biolayer Interferometry

L'interaction p115RhoGEF/TrkA est mesurée par interférométrie. Les courbes d'association et de dissociation ont été effectuées en présence de la protéine p115RhoGEF recombinante purifiée et des peptides TrkA wild-type biotinylé (TrkA-WT-biot) (QGHIIENPQ**Y**FSDAC-biotine) ou mutant Y490G biotinylé (TrkA-mt-biot) (QGHIIENPQ**G**FSDAC-biotine) comparé au tampon seul (tp/p115).

7. Étude des signalisations

7.1. Biosenseur

Les cellules sont ensemencées (5 000 cellules/puits ; ovn, 37°C) dans des chambres à fond de verre (Lab-Tek®) coatées avec du collagène de type I (100 µg/mL ; Corning). Ces cellules ont été transfectées avec le plasmide pBabe-puro-RhoA (0,15 µg ; Addgene plasmid #12602) à l'aide du système JetOPTIMUS®. Trois heures avant l'acquisition d'images, les cellules exprimant le biosenseur RhoA ont été sevrées (0,1% de SVF) dans un milieu sans rouge de phénol. L'acquisition des images, se fait en chambre thermostatée à 37°C, 5 % de $C0_2$ et humidifiée (papier humidifié). Les images ont été réalisées à l'aide d'un microscope confocal ZEISS LSM 880 avec un objectif plan-apochromatique 63×/1.4 à contraste interférentiel différentiel (DIC). Le laser à argon était réglé pour émettre des lignes laser de 458 nm et 514 nm à travers un filtre d'émission passe-bande de 470 à 500 nm (BP470-500) pour la détection du CFP et un filtre d'émission passe-longueur de 530 nm (LP530) pour la détection du YFP. L'émission des canaux CFP, FRET et YFP a été enregistrée. Les rapports d'émission de fluorescence ont été calculés à l'aide du logiciel Fiji.

7.2. Western blot

Les western blot sont réalisés comme décrit précedement. Les anticorps primaires utilisés sont : anti-phospho Y685/6 de TrkA (Cell Signaling, 1/1000ième), pAkt (D9E Cell Signaling, 1/1000ième), Akt (11E7 Cell Signaling, 1/1000ième) et anti-βactine (A2066, Sigma-Aldrich, 1/10 000ième).

8. Études fonctionnelles

8.1. Test de clonogénicité

Vingt-quatre heures après la transfection des siRNA (siCTRL ou sip115RhoGEF), les cellules sont ensemencées en plaque 6 puits (500 cellules/puits) dans du milieu à 2% de SVF puis remises à incuber (5 % de CO_2, 37°C). Les cellules sont traitées 2 h et 24 h post-ensemencement avec du NGF (16 nM) puis incubées pendant 7 jours. Le milieu est changé au bout de 5 jours. Les puits sont rincés (PBS) puis incubés avec une solution de paraformaldéhyde (4% (p/v) dans PBS pH 7,4 ; 30 min, 20°C, sous agitation, à l'obscurité). Puis, 2 rinçages sont réalisés (PBS) avant de colorer les cellules avec une solution de crystal violet (0,1 % (p/v), 30 min, 20°C, sous agitation). Enfin, après 3 rinçages (eau distillée), les plaques sont laissées à sécher à l'air libre puis les colonies sont comptées.

8.2. Test de blessure (IBIDI)

Les cellules sont ensemencées en plaque 6 puits (400 000 cellules/mL) dans lesquels a été préalablement placé un système IBIDI (1/puits). Les cellules sont incubées 24 h (10 % SVF, 5 % de CO_2, 37°C). Le système IBIDI est retiré puis après un rinçage (milieu 0,1% SVF, 1mL/puits), les blessures sont photographiées (2/blessure) et les cellules sont sevrées 1h (milieu 0,1% SVF). Les cellules sont ensuite traitées avec un inhibiteur de la phosphorylation de TrkA (LOXO-101 ou Entrectinib, 250 nM, 1h) et/ou un peptide (P4 inhibiteur TrkA/CD44v3 ou TAT-P13 inhibiteur TrkA/p115RhoGEF, 30 min) puis stimulées avec du NGF (16 nM). Vingt heures plus tard des photographies sont réalisées (au même endroit qu'à 0h)

à l'aide du microscope Eclipse TiU, Nikon (objectif 4X) et du logiciel NIS element BR 2.30 (Nikon). La distance entre les fronts de migration est quantifiée à l'aide du logiciel Fidji.

8.3. Test d'invasion (transwell)

10^6 cellules sevrées 3h30 (0,1 % dans le milieu SVF) ont été ensemmencées sur la partie supérieure de transwell coatés avec du collagène I (8 mm ; Corning, Life Sciences) et incubées (10 min, 37°). Le traitement avec un peptide (50 ng/mL ; 30 min) puis le NGF (16 nM) a été ajouté dans la chambre inférieure. Après 24 h, les cellules ont été fixées avec du méthanol (10 min, RT) et colorées avec du Hoechst 33258 (1 mg/mL ; 30 min). Les cellules qui ont envahi la surface inférieure à travers les pores des inserts ont été comptées automatiquement avec le logiciel ImageJ (plug-in développé en interne) à partir de photographies prises sous un microscope inversé.

9. Études *in vivo*

9.1. Croissance tumorale *in vivo*

Des cellules MDA-MB-231 (3 x 10^6) surexprimant HA-TrkA ou non sont injectées en sous-cutané dans le flanc de souris immunodéficientes (CB-17/Icr-Prkdc scid/Rj, Janvier Labs) de 7-8 semaines. Environ un mois plus tard, les souris sont randomisées et réparties dans 2 (Scramble peptide ou PBS et peptide P4) ou 4 groupes (Control, peptide P4, LOXO-101 ou Entrectinib, LOXO-101 ou Entrectinib + P4). Le peptide P4 (20 μg/injection) est injecté en péritumoral et les inhibiteurs (LOXO-101 100 mg/kg ; Entrectinib 50 mg/kg) administrés par gavage oral 5 fois tous les 2-3 jours. Le poids des souris et le volume tumoral (length (l) and width (w) and calculated as p/6 x 1 x w x (1+w) /2) sont également suivis jusqu'au sacrifice des animaux. Les animaux sont sacrifiés à des tailles de tumeurs similaires.

9.2. Métastases *in vivo*

Les foies, poumons et cerveaux sont récupérés et placés pour moitié dans l'azote (ARN), l'autre moitié est placé dans le PAF 4% frais pour d'éventuelles

coupes histologiques ou marquage en iDISCO. Les organes sont ensuite décongelés sur glace et placés dans des tubes Precellys avec du QIAzol (1 mL). Une lyse mécanique et thermique des organes sont ainsi réalisées à l'aide d'un Cryolysis (3x60s). Les ARN sont ensuite extraits à l'aide du kit Qiagen RNAeasy Mini Kit. Les ARNs (1,25 ug) sont rétrotranscrits à l'aide du kit Sensifast. Puis, des PCR sont réalisées à partir de 5 µl cDNA selon les instructions du kit Promega GoTaq (GoTaq Buffer, dNTP, 10 µM primer, and GoTaqPol). Les cycles suivants sont réalisés avec un thermocycler TC-5000 : 95°C, 2 min ; 40 cycles à 95°C 30 s, 60°C 30 s, 72°C 30 s ; 72°C, 2 min. Une migration sur gel d'agarose (2 %, BET) des cDNA est réalisée pour étudier la présence (amplicon) ou non de métastase dans chaque organe.

Article 1

Trouvilliez S, Cicero J, Lévêque R, Aubert L, Corbet C, Van Outryve A, Streule K, Angrand P-O, Völkel P, Magnez R, Brysbaert G, Mysiorek C, Gosselet F, Bourette R, Adriaenssens E, Thuru X, Lagadec C, de Ruyck J, Orian-Rousseau V, Le Bourhis X and Toillon R-A.

Direct interaction of TrkA/CD44v3 is essential to NGF-promoted aggressiveness of breast cancer cells.

Journal of experimental and clinical cancer research. 2022, Mar, 41(1) : 110.

Démarche expérimentale

Les travaux du laboratoire ont montré que TrkA s'associe à CD44 (Aubert et al., 2015). Néanmoins de nombreux variants de CD44 sont exprimés et peuvent agir spécifiquement avec les facteurs de croissance ou leurs récepteurs. Des résultats préliminaires obtenus tendent à impliquer le variant 3 de CD44. L'objectif de cette première partie du travail était donc de confirmer les résultats obtenus et de pleinement caractériser l'association TrkA/CD44v3. Pour se faire, la nature directe de l'interaction entre TrkA et CD44v3 a été vérifiée par Thermophorèse à Micro-échelle. Puis, nous avons recherché les motifs d'interaction sur TrkA et CD44v3 par modélisation, mutagenèses dirigées et par l'emploi de peptide mimétique. Enfin les effets biologiques associés à TrkA/CD44v3 ont été caractérisés *in vitro* (survie, migration, invasion) et in vivo (croissance tumorale et métastases). De plus, la fromation du complexe chez les patients et sa valeure pronostique a été étudié par « duolink » sur des échantillons de patients en « tissue micro-arrays ».

Ainsi, dans cet article, nous montrons pour la première fois l'existence d'une interaction directe entre un variant de CD44 (variant 3) et un RTK (TrkA). De plus, nous avons montré que cette interaction nécessite les 10 derniers acides aminés du variant 3 (C-ter) et le résidu H112 de TrkA. De façon intéressante cette association permet l'activation de RhoA indépendamment de la phosphorylation de TrkA, en particulier au niveau des fronts de migration des cellules cancéreuses triples négatives surexprimant un TrkA non phosphorylable. De plus, le ciblage de TrkA/CD44v3 décroit la migration, l'invasion, la croissance tumorale et la charge métastatique *in vivo*. Enfin, le complexe TrkA/CD44v3 est inversement corrélé à l'expression des récepteurs à la progestérone.

Cet article a été publié dans la revue : Trouvilliez S, Cicero J, Lévêque R, Aubert L, Corbet C, Van Outryve A, Streule K, Angrand P-O, Völkel P, Magnez R, Brysbaert G, Mysiorek C, Gosselet F, Bourette R, Adriaenssens E, Thuru X, Lagadec C, de Ruyck J, Orian-Rousseau V, Le Bourhis X and Toillon R-A. Direct interaction of TrkA/CD44v3 is essential to NGF-promoted aggressiveness of breast cancer cells. **Journal of Experimental and Clinical Cancer Research**. 2022, Mar, 41(1): 110.

Direct interaction of TrkA/CD44v3 is essential for NGF-promoted aggressiveness of breast cancer cells

Sarah Trouvilliez [1,#], Julien Cicero [1,2,#], Romain Lévêque [1], Léo Aubert [1], Cyril Corbet [1], Alexandre Van Outryve [1], Karolin Streule [3], Pierre-Olivier[1]Angrand, Pamela Völkel [1], Romain Magnez [1], Guillaume Brysbaert [4], Caroline Mysiorek [2], Fabien Gosselet [2], Roland Bourette [1], Eric Adriaenssens [1], Xavier Thuru [1], Chann Lagadec [1], Jérôme de Ruyck [4], Véronique Orian-Rousseau [3], Xuefen Le Bourhis [1] & Robert-Alain Toillon [1, *].

[1] Univ. Lille, CNRS, INSERM, CHU Lille, UMR9020-U1277 - CANTHER - Cancer Heterogeneity Plasticity and Resistance to Therapies, F-59000 Lille, France
[2] Univ. Artois, UR 2465, Laboratoire de la Barrière Hémato-Encéphalique (LBHE), F-62300 Lens, France
[3] Karlsruhe Institute of Technology, Institute of Toxicology and Genetics, 76344 Eggenstein-Leopoldshafen, Germany
[4] Univ. Lille, CNRS, UMR 8576 - UGSF - Unité de Glycobiologie Structurale et Fonctionnelle, F-59000 Lille, France

These authors equally contributed to this work.

* Corresponding author: Prof. Robert-Alain Toillon, Université de Lille, Faculté des Sciences et Technologies, UMR CNRS 9020- INSERM U1277 - CANTHER - Cancer Heterogeneity Plasticity and Resistance to Therapies, Bâtiment SN3, 3ème étage, Cité scientifique, 59655 Villeneuve d'Ascq, France. Phone: +33 (0)3 20 43 65 59. E-mail: robert-alain.toillon(at)univ-lille.fr

Abstract

Background

CD44 is a multifunctional membrane glycoprotein. Through its heparan sulfate chain, CD44 presents growth factors to their receptors. We have shown that CD44 and Tropomyosin kinase A (TrkA) form a complex following nerve growth factor (NGF) induction. Our study aimed to understand how CD44 and TrkA interact and the consequences of inhibiting this interaction regarding the pro-tumoral effect of NGF in breast cancer.

Methods

After determining which CD44 isoforms (variants) are involved in forming the TrkA/CD44 complex using proximity ligation assays, we investigated the molecular determinants of this interaction. By molecular modeling, we isolated the amino acids involved and confirmed their involvement using mutations. A CD44v3 mimetic peptide was then synthesized to block the TrkA/CD44v3 interaction. The effects of this peptide on the growth, migration and invasion of xenografted triple-negative breast cancer cells were assessed. Finally, we investigated the correlations between the expression of the TrkA/CD44v3 complex in tumors and histo-pronostic parameters.

Results

We demonstrated that isoform v3 (CD44v3), but not v6, binds to TrkA in response to NGF stimulation. The final 10 amino acids of exon v3 and the TrkA H112 residue are necessary for the association of CD44v3 with TrkA. Functionally, the CD44v3 mimetic peptide impairs not only NGF-induced RhoA activation, clonogenicity, and migration/invasion of breast cancer cells in vitro but also tumor growth and metastasis in a xenograft mouse model. We

also detected TrkA/CD44v3 only in cancerous cells, not in normal adjacent tissues.

Conclusion

Collectively, our results suggest that blocking the CD44v3/TrkA interaction can be a new therapeutic option for triple-negative breast cancers.

Keywords: CD44v3, TrkA, NGF, breast cancer, metastasis

Background

Breast cancer is the most prevalent cancer in women worldwide. With a slight increase in annual incidence, it is estimated that 1 in 8 women will be affected in her lifetime. Despite significant progress in both patient care and treatments, more than 684,000 women died of breast cancer in 2020[1]. These deaths are largely attributable to metastatic progression[2]. Among the main breast cancer subtypes (luminal, Her2-positive and triple-negative (TN) subtypes), the TN subtype is the most aggressive. Metastasis of TN breast cancer (TNBC) is associated with an overall survival 3.5-fold lower than that of luminal breast cancer[3]. This low overall survival is probably related to a higher metastasis rate. As Paget described, breast cancer metastasis is not a random mechanism[4] as described by the seed and soil theory; it involves crosstalk between tumor cells and microenvironmental factors such as the extracellular matrix and growth factors. Among these factors, hyaluronan, a major component of the extracellular matrix, binds to the CD44 glycoprotein, which is the main hyaluronan receptor. CD44 is involved in various physiological functions, including cell proliferation, migration, invasion, and the immune response. Since this discovery, many studies have underlined the importance and expression of CD44 in different cancers[5]. The diversity of CD44 functions is due to the multiplicity of CD44 ligands (e.g., hyaluronan and osteopontin), posttranslational modifications (such as glycosylation) or isoform expression. Of the 20 CD44 gene exons, 12 are variable splicing exons, allowing the formation of more than 700 isoforms. However, not all combinations are expressed[6], and at least 20 CD44 isoforms have been described to date. These variants exhibit specific functions and pattern

expression[7]. The most abundant isoform is the CD44 standard transcript, but several variants of CD44 have been shown to be involved in CD44 responses. In cancers, two specific alternative splicing variants of CD44, variants 3 (CD44v3) and 6 (CD44v6), containing variable exons 8 and 11, respectively, interact with numerous tyrosine kinase receptors[8,9]. Hence, the discovery of the differential expression of CD44 variants in cancer biology explained the role of variant 6 in the metastatic processes of rat tumors[10]. CD44v6 is a coreceptor in MET activation by MET ligands HGF/SF[11]. Furthermore, we recently emphasized that cells express different CD44 variants, including CD44v6, to orchestrate the response of epidermal growth factor (EGFR) after it binds to its cognate ligands. Additionally, we highlighted that the CD44v6/EGFR complex is correlated with lymph node metastasis and the human epidermal growth factor receptor 2 (HER2) breast cancer subtype and is inversely correlated with TN status[12]. CD44v3 was the second variant identified to interfere with growth factor signaling. CD44v3 effects are mainly due to its ability to bind heparin-binding growth factors such as macrophage inflammatory protein-1β[13], hepatocyte growth factor/scatter factor[14], fibroblast growth factor (FGF)[15], and heparin binding EGF like growth factor (HB-EGF)[16]. In a relevant study, we showed that NGF induces the complex-forming association of CD44 with the tyrosine kinase receptor TrkA, resulting in the activation of various signaling cascades that promote survival or migration/invasion[17]. However, to date, the identity of the CD44 variant that interacts with TrkA and precise mechanisms of this interaction and the intracellular action of this TrkA-binding CD44 variant are unknown. Therefore, in this study, we sought to determine whether CD44 variant 3 binds TrkA. We

found that NGF induces direct binding between CD44v3 and TrkA. Additionally, we found that CD44v3 binds TrkA via the interaction of the CD44v3 C-terminal region and leucine-rich region 1 (LRR1) of TrkA. In a most unusual finding, we observed that CD44v3 cannot act as a coreceptor because it does not bind NGF. Specifically, using a CD44v3 C-terminal-mimicking peptide, we demonstrated that the interaction of CD44v3 with TrkA is critical for nerve growth factor (NGF)-induced phospho-TrkA-independent RhoA activation. Through a thorough investigation, we determined that the inhibition of the CD44v3-mimic/TrkA complex decreased tumor growth and metastasis *in vivo*. This outcome suggests that the CD44v3/TrkA interaction may be leveraged in breast cancer therapy because only cancer cells, not their normal counterparts, express this complex.

Methods

Cell culture

MDA-MB-231, SUM159-PT, T47-D, BT-474 and HCC-1954 breast cancer cell lines were purchased from the American Type Culture Collection (ATCC, Manassas, VA, USA). The COS-7 cell line (African green monkey kidney) was obtained from Pr. V. Orian-Rousseau (Karlsruhe Institute of Technology [KIT], Karlsruhe, Germany). MDA-MB-231 cells were cultured in Eagle's minimal essential medium (EMEM), and COS-7 cells were cultured with Dulbecco's minimal essential medium (DMEM) supplemented with 10% inactivated fetal bovine serum (FBS) (HyClone, Belgium), 1% nonessential amino acids, 40 UI/ml of penicillin/streptomycin and 40 µg/mL of gentamycin. SUM159-PT cells were cultured in F12 medium supplemented with 5% inactivated FBS

(HyClone, Belgium), 1% HEPES, 100 UI/mL of penicillin/streptomycin, 40 µg/mL of insulin and 1 µg/mL of hydrocortisone. T47-D cells were cultured in RPMI+GlutaMAX supplemented with 10% inactivated FBS (HyClone, Belgium), 1% nonessential amino acids, 40 UI/mL of penicillin/streptomycin, 40 µg/mL of gentamycin and 10 µg/mL of insulin. BT-474 cells were cultured in RPMI supplemented with 40 UI/mL of penicillin/streptomycin and 10 µg/mL of insulin. HCC-1954 cells were cultured in RPMI supplemented with 10% inactivated FBS (HyClone, Belgium) and 40 UI/mL of penicillin/streptomycin. All the cell lines were incubated at 37°C in a humidified atmosphere containing 5% CO_2. The cells were amplified after acquisition and cultured for no more than 25 passages. Before treatment, the cells were rinsed twice with trypsin/EDTA, cultured for 24 h in medium supplemented with 0.1% FBS, and then treated with recombinant human β-NGF (referred to as NGF and administered at 100 ng/ml in all experiments) (Alomone Labs, Israel) for the indicated times.

Plasmids

To obtain plasmids containing the CD44 variant 3 or variant 6 sequence, the sequences were inserted into a pcDNA3.1/Hygro plasmid by polymerase chain reaction (PCR)-based mutagenesis. The plasmid carrying CD44v3 with a tagged histone (N-terminal) was produced by e-Zyvec. The pBabe-Puro-RhoA FLARE.sc biosensor was a gift from Klaus Hahn (Addgene plasmid # 12602; http://n2t.net/addgene:12602; RRID, Addgene_12602)[18]. The cloning procedure is available upon request. Transient transfections were performed by electroporation using Amaxa® Nucleofector® technology (Lonza, Switzerland) according to the manufacturer's instructions.

In situ proximity ligation assay (PLA)

Cells (10,000 cells per well) were grown on acid-washed eight-well glass slides (Thermo Scientific) in the appropriate medium supplemented with 10% FBS for 24 h. After NGF treatment, paraformaldehyde (PAF)-fixed cells were incubated with 4% bovine serum albumin (BSA) or 5% FBS (for 1 h at 20°C), followed by overnight incubation with primary antibodies (rabbit anti-TrkA or rabbit anti-IgG + mouse anti-pan-CD44; mouse anti-CD44v3; mouse anti-CD44v6; mouse anti-IgG2a; mouse anti-IgG2b; or mouse anti-IgG1). PLA was performed following the manufacturer's instructions in the assay kit (Duolink PLA; Sigma–Aldrich). To obtain the correct representation of the PLA signal for each condition, 30 fields per condition were observed using a fluorescence microscope (Eclipse TiU; Nikon, Japan). The PLA signals (red dots) were automatically quantified using ImageJ software (with an in-house-developed plug-in). After PLA, statistical analyses were performed using GraphPad Prism software to determine the mean dot intensity in the cells.

Paraffin-embedded sections of breast tumors were obtained from US BioMax (HBre-Duc150Sur01). The sections were rinsed twice in Tris-buffered saline (TBS; 0.01 M Tris, pH 7.4; 0.15 M NaCl; and 0.05% Tween 20) and incubated with blocking solution (20% FBS in TBS for 1 h at room temperature [RT]). The slices were incubated with the same primary antibodies as those used for immunocytochemistry (cited above, diluted 1:50 in 1% FBS and incubated overnight at 4°C).

Protein extraction

Subconfluent cells were washed twice with ice-cold PBS and lysed (40 mM HEPES, pH 7.5; 120 mM NaCl; 1 mM EDTA; 1% Triton X-100; 0.1% SDS;

10% glycerol; 10 mM sodium pyrophosphate; 50 mM sodium fluoride; 1.5 mM sodium orthovanadate; and 1 mM PMSF, supplemented with a protease inhibitor cocktail) (Sigma–Aldrich, France). The cell lysates were cleared by centrifugation (6000 × g for 10 min at 4°C) and stored at -80°C until analysis. The supernatants were collected, and the protein concentration was determined using the bicinchoninic acid assay (Sigma–Aldrich).

Microscale thermophoresis (MST)

MST was conducted using an NT.115 A Pico MST instrument (Nano Temper Technologies GmbH) equipped with red and blue filter sets. The TrkA-His tagged extracellular domain protein (Ala 34-Gly423) (9966-TK-050; R&D Systems, United Kingdom), diluted to 200 nM in PBS-T buffer (supplied by the vendor), was labeled using a Monolith His-Tag Labeling Kit with RED-Tris-NTA (Nano Temper). The RED-Tris-NTA dye was diluted in PBS-T to 100 nM. The mix was incubated at RT in the dark for 30 min. Next, an extract expressing CD44v3-labeled protein (CD44v3-His) and ligand and/or TrkA was mixed at a 1:1 ratio and incubated at RT in the dark for 15 min. For the binding check, peptides and TrkA-His were used. Capillaries were filled individually and loaded into the instrument. The data were acquired using high MST power and 100% LED. The data were analyzed using MO Control Software (Nano Temper).

Production of the interaction model

Because the TrkA crystal structure is available, we directly retrieved it from the Protein Data Bank (PBD ID: 2IFG) at a resolution of 3.4 Å[19]. This structure was used to predict the interaction between TrkA and the peptide CD44v3, for which we generated many 3D structures. The interaction model was finally

obtained using a protein–protein algorithm and, more specifically, the ClusPro2.0 webserver[20]. The subsequently obtained docking poses were minimized and scored.

Selection of the residue target for mutagenesis

The residue target for mutagenesis was selected based on a visual inspection of the structure of the docking model with the best score and betweenness centrality analysis (BCA) was performed using a residual interaction network (RIN) generated from the PDB of the docking model form and native structure of TrkA. An RIN is defined as a network of interactions between the amino acids of a structure; thus, nodes are amino acids, and edges are the interactions detected between nodes. The RIN in this study was generated using an in-house C program, and residue-residue contacts were selected when the distance between them was between 2.5 Å and 5 Å. BCA was performed using the RINspector app[21,22] of Cytoscape[23], and Z scores ≥ 2 were considered central residues. We focused on the residues at the interface of the protein that were deemed central to the interaction complex based on BCA but were not in the native TrkA structure, with the former criterion considered indicative of the essentiality of the residue for the interaction; only His112 fit this criterion. Therefore, His112 was selected for mutagenesis.

Modeling of the peptide structures

For each peptide, the structure was produced *de novo* using the PEP-FOLD 3.5 webserver. The amino acid sequence of each peptide was used as input. Modeling was performed using standard parameters. The representation of the best model was then visualized and colored using Chimera software.

Clonogenicity assay

The clonogenicity assay was performed to assess cell survival. MDA-MB-231 cells (250 cells/mL) were seeded into 6 plate wells (2% FBS medium; 2 mL/well). When the cells attached (within 3 h), they were treated with the peptide (scramble or P4; 50 ng/mL) or no peptide (control) and incubated for 24 h. The next day, a second-round treatment was performed. Three days later, the medium was changed, and the cells were incubated for another 5 days. After 10 days of culture, the medium was removed, and the cells were washed twice (PBS 1×), fixed (4% PAF for 30 min at RT), colored (violet crystal 2%; 30 min; RT) and washed twice (distilled water). Representative pictures of one well were taken, and the colonies were counted.

Scratch/wound migration assay

Scratch/wound migration assays were performed using inserts (Ibidi, Germany). MDA-MB-231 cells (4×10^5 cells/mL) were seeded onto each side of the chamber and incubated overnight at 37°C until they reached the subconfluent stage. Next, the inserts were removed, and the cells were rinsed and starved (1 mL of 0.1% FBS medium for 1 h). Images of the initial wound were obtained using an inverted microscope, and the cells were incubated with or without the peptide (scramble or P4; 50 ng/mL) for 30 min and stimulated with NGF (100 ng/ml). After 24 h, images (2/wound) were obtained of the same place on the wound as those initially taken. The distance between the 2 migration fronts was measured using ImageJ software.

Cell invasion assay

Transwell invasion assays were performed to assess cancer cell invasion in a Transwell chamber containing a collagen I-coated membrane (12-wells with inserts and 8 mm pore size membranes; Corning, Life Sciences). A total of

1×10^6 starved cells (0.1% in SVF medium) were plated in the top chamber and incubated for 10 min before treatment with a peptide (50 ng/mL for 30 min); NGF was added to the lower chamber. After 24 h, the cells were fixed with methanol for 10 min and stained with Hoechst 33258 (1 mg/mL) for 30 min, and the cells that invaded the lower surface through the pores of the inserts were automatically counted under an inverted microscope with ImageJ software (with an in-house-developed plug-in).

Förster resonance energy transfer (FRET)

MDA-MB-231 native or KD cells were seeded (5,000 cells/well; ovn, 37°C) in a chambered coverglass system (Lab-Tek®) coated with a type I collagen matrix (100 µg/mL; Corning). These cells were transfected using the pBabe-puro-RhoA plasmid (0.15 µg; Addgene plasmid #12602) diluted in a buffer solution (JetOPTIMUS® buffer) and a transfection agent (TA; 10 min). The mixture was incorporated into the culture medium (4 h; 37°C). Two to three hours before image acquisition, the cells expressing the RhoA biosensor were starved in fresh EMEM containing 0.1% FBS and no phenol red. During image acquisition, the cells were maintained at 37°C and with 5% CO_2 in an incubation chamber installed under a microscope. Images were collected using a ZEISS LSM 880 confocal microscope with a plan-apochromat 63×/1.4 oil differential interference contrast (DIC) objective. The argon laser was tuned to emit 458 nm and 514 nm laser lines through a 470 to 500 nm bandpass emission filter (BP470-500) for CFP detection and a 530 nm longpass emission filter (LP530) for YFP detection. The emission of the CFP, FRET and YFP channels was recorded. The fluorescence emission ratios were

computed using ImageJ software, which was also used to generate a report showing the FRET efficiency and intensity signal for each channel.

Tumor xenograft growth in SCID (immunodeficient) mice

MDA-MB-231 cells (2×10^6) were subcutaneously injected into the flanks of six-week-old female SCID mice. One month after injection, the mice were randomized into 2 groups and injected near the tumor with CD44v3 mimetic peptide 4 (P4) or not (control) five times in a 3-day interval. Tumor volume was determined throughout the experiment by measuring the length (l) and width (w) and was calculated as $\pi/6 \times l \times w \times (1+w)/2$. Animals were sacrificed using isoflurane anesthesia when the tumors reached a similar size, and the organs were immediately removed and stored in liquid nitrogen.

RNA extraction from organs

Each organ was placed in a Precellys tube with QIAzol (1 mL) for lysis using a Precellys machine (3×). Next, RNA was extracted following the instructions of the Qiagen RNAeasy Mini Kit. All the procedures were performed on ice to prevent RNA degradation.

Reverse transcription PCR

cDNA (5 μl) was mixed with Promega GoTaq kit components (GoTaq Buffer, dNTP, 10 μM primer, and GoTaqPol). After spinning down the contents, PCR cycles (95°C for 2 min; 40 cycles of 95°C for 30 s, 60°C for 30 s, 72°C for 30 s; 72°C for 2 min; holding at 4°C) were performed using a TC-5000 thermocycler. After the addition of the dye (6×), cDNA was separated in an agarose gel (2%).

Statistical analyses

Statistical analyses were performed using GraphPad Prism 5.01 software. Analyses were performed using one-way analysis of variance (ANOVA) for the PLA, clonogenicity and Transwell assay data followed by Bonferroni's posttest. For the wound assay, analyses were performed using two-way ANOVA with Bonferroni's posttest. Tumor growth was analyzed by T test.

Results

CD44 variant 3 is involved in the TrkA/CD44 interaction following NGF stimulation.

In our previous studies, we demonstrated that NGF induces the association between TrkA and CD44 in cancer cells[17]. The CD44v3- and CD44v6-containing isoforms expressing respectively exon 8 and 11(Figure 1A) can interact with growth factor receptors. Using COS-7 cells with low CD44 and TrkA expression (Supplementary Figure 1A-D), we differentially expressed TrkA and CD44s or a CD44 variant, either CD44v3 or CD44v6 (Figure 1B, supplementary Figure 2). PLA revealed greater TrkA/CD44 variant associations within a complex (Figure 1B). Notably, only the expression of CD44 variant 3 with TrkA increased the PLA-detected TrkA/CD44v3 signal in the plasma membrane of COS-7 cells following NGF stimulation. Additionally, formation of the TrkA/CD44v3 complex was transient and decreased 30 min after NGF stimulation (Figure 1B). Neither wild-type COS-7 cells nor COS-7 cells transfected with TrkA and the CD44s or CD44v6 isoform showed the formation of the dynamic TrkA/CD44 complex in PLA, indicating that these two isoforms are not involved in complex formation (Supplementary Figure 2A-C). Moreover, in MDA-MB-231 breast cancer cells, flow cytometric

analysis also revealed that NGF increased the plasma membrane level of CD44v3 but not CD44v6 (Supplementary Figure 3A-D). Additionally, we evaluated the expression of TrkA and CD44v3 at the membrane level or in cells by immunofluorescence in MDA-MB-231 cells. The level of CD44v3 increased at the membrane until 15 minutes of NGF treatment and then decreased (Supplementary Figure 3E & F). Interestingly, the membrane level of TrkA followed the same trend. Additionally, the overall fluorescence intensities for TrkA and CD44v3 increased globally in the cell, suggesting that after internalization, the proteins were not degraded (Supplementary Figure 3G & H).

The complex formation mechanism was then further examined. Because CD44v3 binds growth factors, we tested the ability of CD44v3 to bind NGF by microscale thermophoresis (MST). In contrast to FGF-1 (Supplementary Figure 4), NGF did not bind to CD44v3. Additionally, TrkA binding to CD44v3 was not detected in the absence of NGF but was observed in the presence of NGF (Kd=9.47 nM) (Figure 1C). Taken together, these data suggested a direct interaction between TrkA in complex with NGF and CD44v3, but neither NGF nor TrkA alone could bind CD44v3.

To further investigate the interaction between TrkA and CD44v3, molecular modeling was performed using the available structure of TrkA complexed with NGF to identify amino acid residues involved in TrkA/CD44v3 complex formation (Figure 1D). Because no structure of variant exon 3 was available, the CD44v3 sequence was cut into 4 domains of approximately 10 amino acid residues (zone 1, STSSNTISAG; zone 2, WEPNEENEDE; zone 3, RDRHLSFSGSG; and zone 4, IDDDEDFISST), and we scanned each peptide

to locate the putative binding sequence. Visual examination of the TrkA-CD44v3 poses suggested that TrkA His112 binds to the C-terminal region of exon v3 (ID**D**[34]DED**F**[38]ISST) (Figure 1D & E). Statistical BCA confirmed that His112 in zone 4 of CD44v3 is likely a key residue for the interaction of this variant with TrkA (Supplementary Figure 5A). This histidine residue was critical in all TrkA isoforms (I, II and III) (Figure 1F) but not in TrkB or C (Figure 1G). In the latter two receptors, His112 was replaced with either a leucine or alanine, and subsequent analysis indicated that His112 is highly specific to TrkA. Notably, His112 is a polar amino acid that can form a hydrogen bond with the C-terminal region of CD44v3 (Asp4 and Phe38) while leucine or alanine in TrkB and TrkC are non-polar (Figure 1H). Interestingly, multiple sequence alignment with sequences of various mammals also showed that His112 is highly conserved among mammals (Supplementary Figure 5B-D). Additionally, replacing this histidine with arginine in rabbits and mice, in which the TrkA sequence is similar, did not abolish the CD44v3-TrkA interaction. Therefore, the conservation of this histidine residue was investigated more extensively through phylogenic analysis (Supplementary Figure 5E). TrkA is conserved across vertebrates; therefore, Trk sequences in species of each vertebrate taxon were aligned to its more distant ancestor, DTrk (*Drosophila melanogaster*). In vertebrates and *D. melanogaster*, histidine is replaced by 1 of 3 different polar residues (lysine, glutamine, or glycine), which can form a hydrogen bond (glutamine in *Danio rerio* and *Gallus*; lysine in *Branchiostoma floridae;* and glycine in *D. melanogaster*). These observations indicated the positive selection of histidine 112 and its physiological importance. Additionally, alignment analysis of the CD44v3

sequence with that of CD44v6 showed that a region of CD44v6 shared 42% identity with the C-terminal region of CD44v3. Interestingly, when the residues corresponding to Asp34 and Phe38 were replaced by glutamate, a weaker hydrogen bond was formed, and when they were replaced with proline, no hydrogen bond was formed, explaining the absence/weak association of TrkA/CD44v6 indicated by PLA (Supplementary Figure 2C). These data indicated that TrkA H112 and the CD44v3 C-terminal region are likely crucial for the biological function of these respective proteins. Therefore, using COS-7 cells, we first tested the effect of the TrkA H112A mutation on TrkA/CD44v3 complex formation (Figure 2A & B). In the TrkA H112A mutant cells, TrkA binding to CD44v3 was lost, as indicated by the lack of a PLA signal in COS-7 cells, compared with TrkA wild-type cells, as detected by PLA, confirming the essential role of H112 in the TrkA-CD44v3 interaction (Figure 2A & B). The involvement of the CD44v3 C-terminal region (IDDDEDFISST) in TrkA/CD44v3 complex formation was then tested. To complete this test, expression vectors of CD44v3 lacking its C-terminal region (IDDDEDFISST) or neighboring region (RDRHLSFSGSG), constructs named CD44v3_Δ3 and CD44v3_Δ4, respectively (Figure 2C), were cotransfected into COS-7 cells with TrkA. The number of TrkA/CD44v3 complexes in these transfected COS-7 cells was then quantified by PLA (Figure 2D & E). The CD44v3_Δ4 mutant could not bind TrkA because no signal was detectable by PLA, while CD44v3_Δ3 could bind TrkA following NGF stimulation to an extent similar to that of CD44v3 (Figure 2D & E). Taken together, these results suggest that the C-terminal region of variant 3 is involved in TrkA binding and this is a

general mechanism because it can be observed in breast cancer cells but also in cos7 in which we have induced the expression of TrkA and CD44.

The C-terminal mimetic peptide of CD44v3 disrupts the TrkA-CD44v3 association.

To block the TrkA-CD44v3 association, 4 mimetic peptides of CD44v3 were designed corresponding to zone 1 [(K) STSSNTISAG], zone 2 (WEPNEENEDE), zone 3 (RDRHLSFSGSG) and zone 4 (IDDDEDFISST) (Figure 2F & G). The binding capacities of the CD44v3 mimetic peptides to TrkA were then measured by MST (Figure 2H). As expected, neither peptide 1 (KSTSSNTISAG) nor peptide 2 (WEPNEENEDE) could bind TrkA, while mimetic peptide 4 (IDDDEDFISST) corresponding to the C-terminal region of CD44v3 could bind TrkA. To confirm mimetic peptide 4 binding, we assessed its ability to bind TrkA using nanoscale differential scanning fluorimetry (nanoDSF; Supplementary Figure 6A & B). We observed that mimetic peptide 4 (but not a scramble peptide) bound TrkA, but we did not detect CD44v3/P4 binding (Supplementary Figure 6C).

Unexpectedly, the RDRHLSFSGSG peptide (P3) corresponding to CD44v3 zone 3 also bound TrkA. Therefore, the abilities of peptides 3 and 4 to disrupt TrkA/CD44v3 complex formation were evaluated in the COS-7 cell line (Figure 2I & J). As observed in CD44v3 mutants, only peptide 4 corresponding to zone 4 of CD44v3 could decrease NGF-induced TrkA/CD44v3 complex formation in COS-7 cells. However, peptide 3 did not inhibit TrkA/CD44v3 complex formation.

Collectively, our results demonstrated that the interaction of TrkA and CD44v3 was blocked by mimicking peptide 4 (IDDDEDFISST), which corresponds to the C-terminal region of exon variant 3 of CD44.

The TrkA-CD44v3 interaction is involved in NGF-induced migration and invasion of MDA-MB-231 TNBC cells.

We previously showed that NGF is implicated in breast cancer aggressiveness because it enhances cell migration/invasion[17,24]. Therefore, in this study, we assessed TrkA binding to CD44v3 in MDA-MB-231 cells, which were used as TNBC model cells. First, PLA was performed using anti-CD44 variant 3- (Figure 3A and Supplementary Figure 7) or anti-CD44 variant 6-specific antibodies (Figure 3B). NGF induced TrkA/CD44v3 complex formation in MDA-MB-231 cells at the plasma membrane within 5 min to 30 min of administration (Figure 3A and Supplementary Figure 7) but did not induce TrkA/CD44v6 complex formation (Figure 3B). Next, we tested the ability of CD44v3 mimetic peptides to block TrkA/CD44v3 complex formation in MDA-MB-231 cells (Figure 3C-E). Similar to the results observed with COS-7 cells, neither a scramble peptide (Figure 3C) nor mimetic peptide P3 (Figure 3D) inhibited TrkA/CD44v3 complex formation following NGF treatment. Only mimetic peptide 4 (Figure 3E) and the H112A mutation (Supplementary Figure 8A) could disrupt TrkA/CD44v3 complex formation in MDA-MB-231 cells. Therefore, we evaluated the physiological consequences of TrkA/CD44v3 complex dissociation induced by CD44v3 mimetic peptide 4 on MDA-MB-231 cell phenotypes (Figure 4). We first examined the effect of mimetic peptide 4 on clonogenic cell growth. For this experiment, MDA-MB-

231 cells were grown in the presence of 2% FBS for 3 weeks in the presence or absence of CD44v3 mimetic peptide 4 (Figure 4A and B). Under these conditions, CD44v3 mimetic peptide 4 reduced the proportion of MDA-MB-231 colony forming units by two-thirds compared with its effect on control cells or that of the scramble peptide. The same observations were made in SUM-159PT, another triple-negative cell line (Supplementary Figure 9 A & B). Next, we tested the inhibitory effect of CD44v3 mimetic peptide 4 on the migration and invasion of MDA-MB-231 breast cancer cells (Figure 4C-K). We first determined the effect of CD44v3 on the length-to-width (l/w) ratio of the cells (elongation factor) (Figure 4C-E). NGF induced the acquisition of a fibroblast phenotype by MDA-MB-231 cells, which exhibited a significant increase in the l/w ratio (Figure 4D-E). This effect of NGF was inhibited by the addition of CD44v3 mimetic peptide 4. Hence, MDA-MB-231 cell migration ability was assessed after NGF treatment in a wound healing test (Figure 4H & I). Following NGF treatment, the migration of MDA-MB-231 cells was increased, as indicated by complete wound closure 24 h after treatment. This effect was not inhibited using the scramble CD44v3 mimetic peptide, while CD44v3 mimetic peptide 4 completely blocked NGF-dependent wound closure, indicating that CD44v3 mimetic peptide 4 inhibited the NGF-induced migration of MDA-MB-231 cells. We also confirmed the effects of CD44v3 mimetic peptide 4 on migration in SUM-159-PT cells (Supplementary Figure 9 C & D). The MDA-MB-231 cell invasive capacity was then investigated using Boyden chambers (Figure 4J & K). As observed in the pictures of the underside of the Transwell membrane (Figure 4J), more NGF-treated cells than untreated cells invaded the collagen substrate. In the presence of CD44v3 mimetic peptide 4,

a decrease in both basal levels and NGF-induced invasion was observed in MDA-MB-231 cells. These observations were confirmed by counting the cells that had invaded the Transwell membrane and were apparent on its underside (Figure 4K). These effects on invasion were also observed in the MDA-MB-468 triple-negative breast cancer cell line (Supplementary Figure 9 E). Additionally, the expression of TrkA-H112A also reduced migration and invasion compared with that of wild-type TrkA in MDA-MB-231 cells (Supplementary Figure 8 B-E).

To determine the role of CD44v3 in NGF-induced phenotype acquisition, the effect of short interfering RNA (siRNA) targeting CD44v3 (siCD44v3) was assessed (Supplementary Figure 10). siCD44v3 reduced the clonogenicity of MDA-MB-231 and SUM-159-PT cells (Supplementary Figure 10 A & B) and MDA-MB-231 migration and invasion (Supplementary Figure 10 C-E).

Our results indicated that NGF also induced TrkA/CD44v3 complex formation in MDA-MB-231 breast cancer cells. Additionally, we depicted for the first time that the inhibition of TrkA/CD44v3 complex formation by CD44v3 mimetic peptide 4 is associated with the decreased clonogenic cell growth and migration/invasion abilities of MDA-MB-231 cells.

TrkA/CD44v3 activates RhoA independently of TrkA phosphorylation.

To further elucidate the mechanism of action of CD44v3 mimetic peptide 4, we studied its effect on the TrkA signaling pathway. First, we performed western blot analysis to determine the effect of mimetic peptide 4 on TrkA phosphorylation (Figure 5A). Interestingly, CD44v3 mimetic peptide 4 did not inhibit TrkA phosphorylation induced by NGF (Figure 5A), indicating that disruption of TrkA/CD44v3 complex formation did not influence TrkA

phosphorylation. Notably, we previously showed that NGF may enhance RhoA activity in breast cancer cells to promote migration/invasion independent of TrkA phosphorylation[17]. Therefore, we performed acceptor (photo)bleaching (AB)-FRET to examine the effect of CD44v3 mimetic peptide 4 on NGF-induced RhoA activity in MDA-MB-231 cells transfected with a RhoA FRET biosensor[18] (Figure 5B). In MDA-MB-231 cells, NGF increased the FRET signal in the presence of the scramble peptide but not with CD44v3 mimetic peptide 4 (Figure 5C). Additionally, to confirm that this effect was independent of TrkA phosphorylation, we measured RhoA activation in MDA-MB-231 cells expressing dead TrkA kinase, which cannot be phosphorylated (Figure 5D). In these cells, we determined the ratiometric value of active (RhoA-GTP-to-yellow fluorescent protein (YFP) fluorescence) and inactive RhoA (RhoA-GTP-to-cyan fluorescence protein (CFP) fluorescence) after NGF stimulation (after 0, 25 and 45 min) and categorized the effect into five intensity categories (from low intensity, indicated in blue, to high intensity, indicated in white). We observed that NGF increased the proportion of active RhoA after 45 min in the presence of the scramble peptide (Figure 5E) but not CD44v3 mimetic peptide 4 (Figure 5F). Furthermore, we observed the relocation of activated RhoA to the migration front of the control cells with the scramble peptide after 25 min of NGF treatment but not with CD44v3 mimetic peptide 4 (Figure 5E & F, Supplementary Figure 11A). Furthermore, a similar decrease in RhoA activation was obtained using the TrkA-H112A mutation, which also prevents the formation of the TrkA/CD44v3 complex in the absence or presence of the TrkA kinase inhibitor k252A (Supplementary Figure 11B & C, Supplementary Video 1 & 2).

Taken together, our results indicated that CD44v3 mimetic peptide 4 inhibits TrkA phosphorylation-independent RhoA activation induced by NGF.

TrkA/CD44v3 is involved in tumor growth and MDA-MB-231 cell metastasis.

To assess the role of TrkA/CD44v3 *in vivo*, SCID mice were injected with MDA-MB-231 cells to generate xenografts. Primary tumor development and metastasis (to the lung, brain and liver) were analyzed (Figure 6). To determine the effects of TrkA/CD44v3, tumor cell growth was compared after treatment with mimetic peptide 4 and PBS (Figure 6A-C). We first observed that CD44v3 mimetic peptide 4 did not affect the overall body weight of the mice (Figure 6B). The development of primary tumors was measured throughout the experiments. CD44v3 peptide 4 injections were performed when the mean tumor volume reached 100 mm^3 (Figure 6C). The CD44v3 mimetic peptide significantly inhibited the growth of MDA-MB-231 cells in xenograft tumors. This result confirmed our preliminary clonogenic assay results, indicating that CD44v3 mimetic peptide 4 decreased the long-term growth of MDA-MB-231 cells both in vitro and *in vivo*. We also assessed the metastatic burden. Because CD44 mimetic peptide 4 blocked primary development, we chose to inject the CD44v3 mimetic peptide into the mice harboring the largest tumors. Hence, the mice were sacrificed when the primary tumors reached the same size (Figure 6D). Micrometastases were detected at the end of the experiment by PCR of human microglobulin in xenograft mice treated with or without the CD44v3 mimetic peptide (Figure 6E). Similar to previously reported results[17], our experiments showed that wild-type MDA-MB-231 cells colonized the lung and liver and, to a lesser

extent, the brain. Interestingly, CD44v3 mimetic peptide 4 decreased the metastatic burden at each analyzed location. These results indicated that MDA-MB-231 cell metastasis in these three organs was blocked by CD44v3 mimetic peptide 4. To confirm the implication of the TrkA/CD44v3 complex in metastasis, we also performed xenograft experiments using MDA-MB-231 HA-TrkA H112A cells (Figure 6F). We confirmed that HA-TrkA cells (control) appeared more metastatic than MDA-MB-231 cells[24], but MDA-MB-231 cells overexpressing TrkA H112A xenografted mice seemed to exhibit less metastasis in the brain and liver. These results suggested that the TrkA/CD44v3 association could be implicated in metastasis and that CD44v3 mimetic peptide 4 might impair metastasis development.

The TrkA/CD44v3 complex is differentially detected in breast cancer cells and tumors.

NGF induced TrkA/CD44v3 complex formation in MDA-MB-231 cells, which are the gold standard models of TNBC. We also examined the expression and induction of TrkA/CD44v3 in breast cancer cell lines corresponding to different breast cancer subtypes (Figure 7 A-D). Four cell lines were assessed: SUM159-PT (TN; i.e., ERα-, PR-, and Her2-) cells, T47-D (luminal A; i.e., ERα+, PR+, and Her2-) cells, BT-474 (luminal B; ERα+, PR+, and Her2+) cells and HCC-1954 (Her2-like; ERα-, PR-, and Her2+) cells. Under these conditions, NGF induction of CD44v3/TrkA complex formation was observed in SUM-159PT (TN) and HCC-1954 (Her2) cells. By contrast, T47-D cells (luminal A) expressed the TrkA/CD44v3 complex at a lower rate, and NGF induction was insufficient to modulate TrkA/CD44v3 complex formation in BT-

474 (luminal B) cells, which are known to express a very low level of complex (compared with background noise in PLA). Therefore, TrkA/CD44v3 complex formation was likely induced differently among breast cancer cell lines. The TrkA/CD44v3 complex formation rate and activity level appeared higher in breast cancer cell lines, representing various breast cancer subtypes that did not express the progesterone receptor (PR). Therefore, TrkA/CD44v3 complex formation was assessed in breast cancer tissue microarrays to determine the level to which it correlated with clinical-biological parameters of breast tumors (i.e., estrogen receptor, PR and HER2 expression) (Figure 7E & F). Complex formation was detected by PLA and scored ranging from no staining (0) (Figure 7, E2) to high intensity staining (3) (Figure 7, E3). Interestingly, we observed that the TrkA/CD44v3 complex was absent in "normal adjacent tissue" (Figure 7, E1), indicating that TrkA/CD44v3 complex staining was specific to cancer cells. Using our scoring method, PR-negative tumors exhibited significantly higher TrkA/CD44v3 complex levels (mean staining: 2.607) than progesterone-positive tumors (mean staining: 2.188) (Figure 7F). These results indicated that TrkA/CD44v3 complex formation is inversely correlated with PR. TrkA/CD44v3 staining in PLA was more intense in estrogen receptor-negative cells than in estrogen receptor-positive cells and in triple-negative cells than in non-TN cells; these correlations were at the limit of significance ($p=0.0657$ and 0.0528, respectively).

Discussion

With more functions than those of a membrane receptor, CD44 is a multifunctional platform implicated in numerous physiological and disease mechanisms. In cancer, it has many functions (e.g., adhesion, migration/invasion, growth, differentiation, and resistance to therapies) depending on the splice variant expressed, corresponding ligands, posttranscriptional modifications, and association with growth factors and different membrane proteins. In the present study, we demonstrated, for the first time, the role played by CD44v3 in association with TrkA in the survival, migration, invasion, tumor growth and metastasis of breast cancer cells. After in-depth analysis, we described CD44v3 binding to TrkA as an original mechanism. The protein core of CD44v3 may bind directly to TrkA, and this binding does not involve a heparan sulfate moiety (Figure 8). Hence, 10 amino acids in the C-terminal region of CD44 variant 3 likely engage the His112 residue in the LRR1 of TrkA. To our best knowledge, no description of the interaction between TrkA and/or its ligands with CD44v3 or other CD44 variants has been described. As recently shown, homophilic interactions of the CD44 protein in adjacent cancer cells are involved in the aggregation and metastasis of breast cancer cells. Amino acid residues from position 21 to 97 in the nonvariable region of CD44 were identified as critical for CD44 interactions[25]. The unique direct interaction of the protein core of CD44 with a growth factor receptor has been reported by Bourguignon *et al.* (1997)[26]. They reported that Her2 may be linked to the standard form of CD44 because of interchain disulfide bridge formation between the two receptors. More commonly, CD44v3 acts as a coreceptor that presents ligands to the

conjugate receptor. This presentation requires the heparan sulfate chain of CD44v3, which binds heparin-binding growth factors[14]. For example, Yu *et al.* (2002) showed that the heparan sulfate chain of CD44v3 is involved in the formation of Hb-EGF, MMP7 and the ErbB4 complex at the cell surface[16]. However, NGF likely did not bind directly with CD44v3. This result aligns with the finding that, in contrast to other growth factors, NGF does not bind heparin[27]. Furthermore, the heparan sulfate-binding branch sequence is SGSG[28], which is located in CD44v3 region 3 (RDRHLSFSGSG**),** and we showed that the deletion of this region (CD44v3_Δ3) does not impede the NGF-induced association between CD44v3 and TrkA. Additionally, indirect effects were assessed by MST. A zone 3 mimetic peptide of CD44v3 (P3), which was not glycosylated, bound TrkA but did not abolish complex formation. Taken together, these findings suggest that CD44v3 glycosylation may not be involved in the TrkA-CD44v3 interaction.

CD44 is the main hyaluronan receptor, and it is permissive of interactions between cells and the extracellular matrix. However, CD44v3 recruitment of membrane proteins and receptors triggers multiple actions. As we highlighted in our previous study, CD44v3 may act as a signaling scaffold protein for TrkA. Specifically, we showed that NGF-induced CD44v3 binding to TrkA is necessary to activate RhoA GTPase at the leading edge of the cells and may be involved in directing migration[29].

As previously reported, TrkA overexpression enhanced the metastasis of MDA-MB-231 cells[24,30]. This effect is attributed to the phosphorylation of TrkA, as NGF induced TrkA phosphorylation and subsequent signaling potentially involved in migration/invasion, and TrkA overexpression induced ligand-

independent phosphorylation. Interestingly, the results presented herein seemed to invalidate these previous findings. In the present study, we showed that 1) CD44v3 mimetic peptide 4, which did not inhibit TrkA phosphorylation but blocked TrkA/CD44v3 complex formation, impeded tumor growth and metastases and that 2) RhoA activation was probably dependent not only on TrkA phosphorylation but also on complex formation by recruiting RhoA, as indicated by experiments in which we used kinase-dead TrkA (Figure 8). These observations are interesting because they confirm that TrkA may be critical for breast cancer cell metastasis, not only through phosphorylation but also likely through its ability to heterodimerize with CD44v3.

Furthermore, our tissue microarray revealed that TrkA/CD44v3 is expressed only in cancer cells and not in normal epithelial cells. This finding is consistent with normal breast epithelial cells not expressing CD44v3[31] but low levels of TrkA[24]. This first observation indicates that we could consider a treatment that targets the complex (similar to peptide 4) because it is specific to cancer cells and not normal cells. Furthermore, we determined that TrkA/CD44v3 complex formation is higher in PR-negative than PR-positive tumors, and a strong tendency ($p=0.0528$) exists for the presence of the complex to correlate with triple-negative status in breast cancer and inversely correlate with the estrogen receptor ($p=0.0657$). Thus, in Her2-positive cells, a subpopulation of PR-positive (luminal B) cells exists and the expression of Her2-positive cells does not allow the correlation of TrkA/CD44v3 formation with TN status. This inverse correlation between the presence of the TrkA/CD44v3 complex and progesterone receptor is consistent with the inverse correlation of TrkA expression with PR expression[17]. Additionally, CD44v3-containing isoforms

are mainly associated with tumorigenesis[32] and breast cancer aggressiveness[33,34]. Batsché *et al*.[35] also dissected the mechanism of CD44 variant inclusion and splicing and showed that variant inclusion is increased during tumor progression and metastasis in breast cancer.

In conclusion, we revealed a newly discovered mechanism of action of CD44v3 that is independent of its heparan sulfate chain. Additionally, the direct interaction between CD44v3 and TrkA leads to TrkA signaling that is independent of tyrosine phosphorylation. More specifically, the CD44v3-TrkA interaction is critical for breast cancer cell tumor development and metastasis *in vivo,* as indicated by the results showing that inhibition of TrkA/CD44v3 formation was sufficient to decrease the tumor burden and metastasis in SCID mice. Additionally, using CD44v3 mimetic peptide 4, therapeutic intervention is possible and may be a novel and interesting way to target TrkA oncogenic effects in tumors. Furthermore, developing bispecific antibodies targeting the complex or the treatment combination of TrkA and CD44v3 inhibitors is warranted. In breast cancer, TrkA/CD44v3 complex formation is inversely correlated with PR expression and is associated with TN status. In this latter subtype, only sacituzumab govitecam passed through drug process development and was recently approved by the Food and Drug Administration and European Medecines Agency[36]. Similar to sacituzumab govitecam, our fundamental discovery may highly impact the development of new treatments based on TNBC-specific membrane receptor targeting.

Conclusion

Our results are highly original because CD44v3 binds to TrkA independently of its heparan sulfate and diversifies TrkA signaling through a TrkA phosphorylation-independent signaling pathway. Together, these results demonstrate that the oncogenic action of TrkA is linked to its association with CD44v3. Therefore, our therapeutic strategies to inhibit these receptor platforms must be reviewed.

Abbreviations

BCA: Betweenness Centrality Analysis

BSA: Bovine Serum Albumin

CFP: Cyan Fluorescent Protein

CD44v: CD44 variant

DMEM: Dulbecco Minimum Essential Medium

EGFR: Epidermal Growth factor

EMEM: Earle's salt Minimum Essential Medium

FBS: Fetal Bovine Serum

FGF: Fibroblast Growth Factor

FRET: Fluorescence Resonance Energy Transfer

HB-EGF: Heparin Binding EGF Like Growth Factor

HER2: Human Epidermal growth factor Receptor 2

HGF/SF: Hepatocyte Growth Factor/Scatter factor

LRR1: leucin Rich Region 1

MIP1b: Macrophage inflammatory protein-1β

MST: MicroScale Thermophoresis

NGF: Nerve Growth Factor

PBS-T: phosphate-buffered saline – Tween 20

PLA: proximity Ligation Assay

RPMI: Roswell Park Memorial Institute

SCID: Severe Combined ImmunoDeficiency

SD: Standard Deviation

TBS: Tris-buffered saline

TN: Triple Negative

TNBC: Triple Negative Breast Cancer

TrkA: Tropomyosin kinase A

YFP: Yellow Fluorescent Protein

Declarations

Ethics approval and consent to participate

Animal studies were performed according to the regulations. The study protocol was approved by the regional ethics committee and submitted by RB. It considers animal welfare and the need to reduce and/or replace the use of animals for experimental purposes as much as possible.

Consent for publication

All the participants of this study consented to the publication of this work.

Availability of data and material

The data and materials generated in this study are available upon reasonable request from the corresponding author:

Prof. Robert-Alain Toillon, Université de Lille, Faculté des Sciences et Technologies, UMR CNRS 9020- INSERM U1277 - CANTHER - Cancer

Heterogeneity Plasticity and Resistance to Therapies, Bâtiment SN3, 3ème étage, Cité scientifique, 59655 Villeneuve d'Ascq, France. Phone: +33 (0)3 20 43 65 59. E-mail: robert-alain.toillon(at)univ-lille.fr

Competing interests

The authors declare that they have no competing interests.

Funding

This work was supported by “La ligue contre le cancer” (« comité du Nord, du Pas de Calais et de l’Aisne »), cancéropole Nord-Ouest, I-site “Université Lille Nord-Europe” and Contrat de Plan Etat-Région CPER Cancer 2015-2020. ST was funded by “conseil régional Hauts de France”, Lille University and La ligue contre le cancer.

Author contributions

ST, JC, RL, LA, CC, AVO, KS, P-O A, PV, RM, GB, XT, JdR & R-AT conceived experiments, performed experiments and collected data. ST, JC, EA, RB, and R-A T designed and performed *in vivo* experiments. FG, CM, XT, CL, XLB, V-OR and R-A T provided funding acquisition, resources and supervised research project. ST and R-AT wrote the manuscript in consultation with JdR, XT, VO-R.

References

1. Sung H., Ferlay J., Sieggel R.L., Laversanne M., Soerjomataram I., Jemal A., and bray F. Global Cancer Statistics 2020: GLOBOCAN Estimates of Incidence and Mortality Worldwide for 36 Cancers in 185 Countries. CA Cancer J Clin. 71: 209-49 (2021).

2. Xie H.Y., Shao Z.M. and Li D.Q. Tumor microenvironment: driving forces and potential therapeutic targets for breast cancer metastasis. Chin. J. Cancer. 36(1):36 (2017).

3. Chen W., Hoffmann A.D., Liu H. and Liu X. Organotropism: new insights into molecular mechanisms of breast cancer metastasis. NPJ Precis. Oncol. 2(1):4 (2018).

4. Paget S. Distribution of secondary growths in cancer of the breast. The Lancet. 571-3 (1889).

5. Chen C., Zhao S., Karnad A. and Freeman J.W. The biology and role of CD44 in cancer progression: therapeutic implications. J. Hematol. Oncol. 11(1):64 (2018).

6. Naor D., Wallach-Dayan S.B., Zahalka M.A. and Sionov R.V. Involvement of CD44, a molecule with a thousand faces, in cancer dissemination. Seminars in Cancer Biology. 18(4):260-7 (2008).

7. Ponta H., Wainwright D. and Herrlich P. The CD44 protein family. Int. J. Biochem. Cell. Biol. 30(3):299-305 (1998).

8. Orian-Rousseau V. and Ponta H. Adhesion proteins meet receptors: a common theme? Adv Cancer Res. 101:63–92 (2008).

9. Chaudhry G., Akim A., Zafar M.N., Safdar N., Sung Y.Y. and Muhammad T.S.T. Understanding Hyaluronan Receptor (CD44) Interaction, HA-CD44 Activated Potential Targets in Cancer Therapeutics. Adv Pharm Bull. 11(3):426-38 (2021).

10. Günthert U., Hofmann M., Rudy W., Reber S., Zöller M., Haussmann I., *et al*. A new variant of glycoprotein CD44 confers metastatic potential to rat carcinoma cells. Cell. 65(1):13-24 (1991).

11. Orian-Rousseau V., Chen L., Sleeman J.P., Herrlich P. and Ponta H. CD44 is required for two consecutive steps in HGF/c-Met signaling. Genes Dev. 16(23):3074–86 (2002).

12. Morath I., Jung C., Lévêque R., Linfeng C., Toillon R.A., Warth A. and Orian-Rousseau V. Differential recruitment of CD44 isoforms by ErbB ligands. Oncogene. 37(11):1472-84 (2018).

13. Tanaka Y., Adams D.H., Hubscher S., Hirano H., Siebenlist U. and Shaw S. T-cell adhesion induced by proteoglycan-immobilized cytokine MIP-1 beta. Nature. 361(6407):79-82 (1993).

14. Bennett K.L., Jackson D.G., Simon J.C, Tanczos E., Peach R., Modrell B. *et al.* CD44 isoforms containing exon V3 are responsible for the presentation of heparin-binding growth factor. J. Cell Biol. 128(4):687-98 (1995).

15. Sherman L., Wainwright D., Ponta H. and Herrlich P. A splice variant of CD44 expressed in the apical ectodermal ridge presents fibroblast growth factors to limb mesenchyme and is required for limb outgrowth. Genes Dev. 12(7):1058-71 (1998).

16. Yu W.H., Woessner J.F., McNeish J.D. and Stamenkovic I. CD44 anchors the assembly of matrilysin/MMP-7 with heparin-binding epidermal growth factor precursor and ErbB4 and regulates female reproductive organ remodeling. Genes Dev. 16(3):307-23 (2002).

17. Aubert L., Guilbert M., Corbet C., Génot E., Adriaenssens E., Chassat T. *et al.* NGF-induced TrkA/CD44 association is involved in tumor aggressiveness and resistance to lestaurtinib. Oncotarget. 6(12):9807-19 (2015).

18. Pertz O., Hodgson L., Klemke R.L., Hahn K.M. Spatiotemporal dynamics of RhoA activity in migrating cells. Nature. 440(7087):1069-72 (2006).

19. Wehrman T., He X., Raab B., Dukipatti A., Blau H., and Garcia K.C. Structural and mechanistic insights into nerve growth factor interactions with the TrkA and p75 receptors. Neuron. 53(1), 25-38 (2007).

20. Kozakov D., Hall D.R., Xia B., Porter K.A., Padhorny D., Yueh C., Beglov D. and Vajda S. The ClusPro web server for protein-protein docking. Nature Protocols. 12(2):255-78 (2017).

21. Brysbaert G., Lorgouilloux K., Vranken W., and Lensink M.F. RINspector: a Cytoscape app for centrality analyzes and DynaMine flexibility prediction. Bioinformatics. 34(2):294-6 (2018).

22. Brysbaert G., Mauri T., de Ruyck J., and Lensink, M.F. (2019). Identification of Key Residues in Proteins Through Centrality Analysis and Flexibility Prediction with RINspector. Curr. Protoc. Bioinformatics. 65, e66 (2018).

23. Shannon P., Markiel A., Ozier O., Baliga N.S., Wang J.T., Ramage D. *et al*. Cytoscape: a software environment for integrated models of biomolecular interaction networks. Genome Res 13, 2498-504 (2003).

24. Lagadec C., Meignan S., Adriaenssens E., Foveau B., Vanhecke E., Romon R., *et al*. TrkA overexpression enhances growth and metastasis of breast cancer cells. Oncogene. 28(18):1960–70 (2009).

25. Liu X., Taftaf R., Kawaguchi M., Chang Y.F., Chen W., Entenberg D. *et al.* Homophilic CD44 Interactions Mediate Tumor Cell Aggregation and Polyclonal Metastasis in Patient-Derived Breast Cancer Models. Cancer Discov. 9(1):96-113 (2019).

26. Bourguignon L.Y., Zhu H., Chu A., Iida N., Zhang L. and Hung M.C. Interaction between the adhesion receptor, CD44, and the oncogene product, p185HER2, promotes human ovarian tumor cell activation. J. Biol. Chem. 272(44):27913-8 (1997).

27. Martino M.M., Briquez P.S., Ranga A., Lutolf M.P. and Hubbell J.A. Heparin-binding domain of fibrin(ogen) binds growth factors and promotes tissue repair when incorporated within a synthetic matrix. PNAS. 110(12). 4563-8 (2013).

28. Vela E., Hilari J.M., Delclaux M., Fernandez-Bellon H. and Isamat M. Conservation of CD44 exon v3 functional elements in mammals. BMC Res. Notes. 1 :57 (2008).

29. Tripathi B.K., Grant T., Qian X., Zhou M., Mertins P., Wang D. *et al.* Receptor tyrosine kinase activation of RhoA is mediated by AKT phosphorylation of DLC1. J. Cell Biol. 216(12): 4255-70 (2017).

30. Di Donato M., Galasso G., Giovanneli P., Sinisi A.A., Migliaccio A. and Castoria G. Targeting the Nerve Growth Factor Signaling Impairs the

Proliferative and Migratory Phenotype of Triple-Negative Breast Cancer Cells. Front. Cell Dev. Biol., 9:676568 (2021).

31. Auvinen P., Tammi R., Tammi M., Johansson R. and Kosma V.M. Expression of CD44s, CD44v3 and CD44v6 in benign and malignant breast lesions: correlation and colocalization with hyaluronan. Histopathology. 47(4): 420-8 (2005).

32. Prochazka L., Tesarik R. and Turanek J. Regulation of alternative splicing of CD44 in cancer. Cellular Signalling. 26: 2234-9 (2014).

33. Kaufmann M., Heider K.H., Sinn H.P., von Minkwitz G., Ponta H. and Herrlich P. CD44 variant exon epitopes in primary breast cancer and length of survival. The Lancet, 345: 615-9 (1995).

34. Wu X.J., Li X.D., Zhang H., Zhang X., Ning ZH, Yin Y-M, *et al*. Clinical significance of CD44s, CD44v3 and CD44v6 in breast cancer. J. Int. Med. Res., 43(2) 173-9 (2015).

35. Batsché E., Yi J., Mauger O., Kornobis E., Hopkins B., Hanner-Lloyd C. and Muchardt C. CD44 alternative splicing senses intragenic DNA methylation in tumors via direct and indirect mechanisms. Nucleic Acid Research, 49(11): 6231-7 (2021).

36. Bravaccini S. and Maltoni R. Trop-2 therapy in metastatic Triple-Negative breast cancer in Italy: Clinical opportunity and Regulatory Pitfalls. J. Pers. Med., 11(11): 1211 (2021).

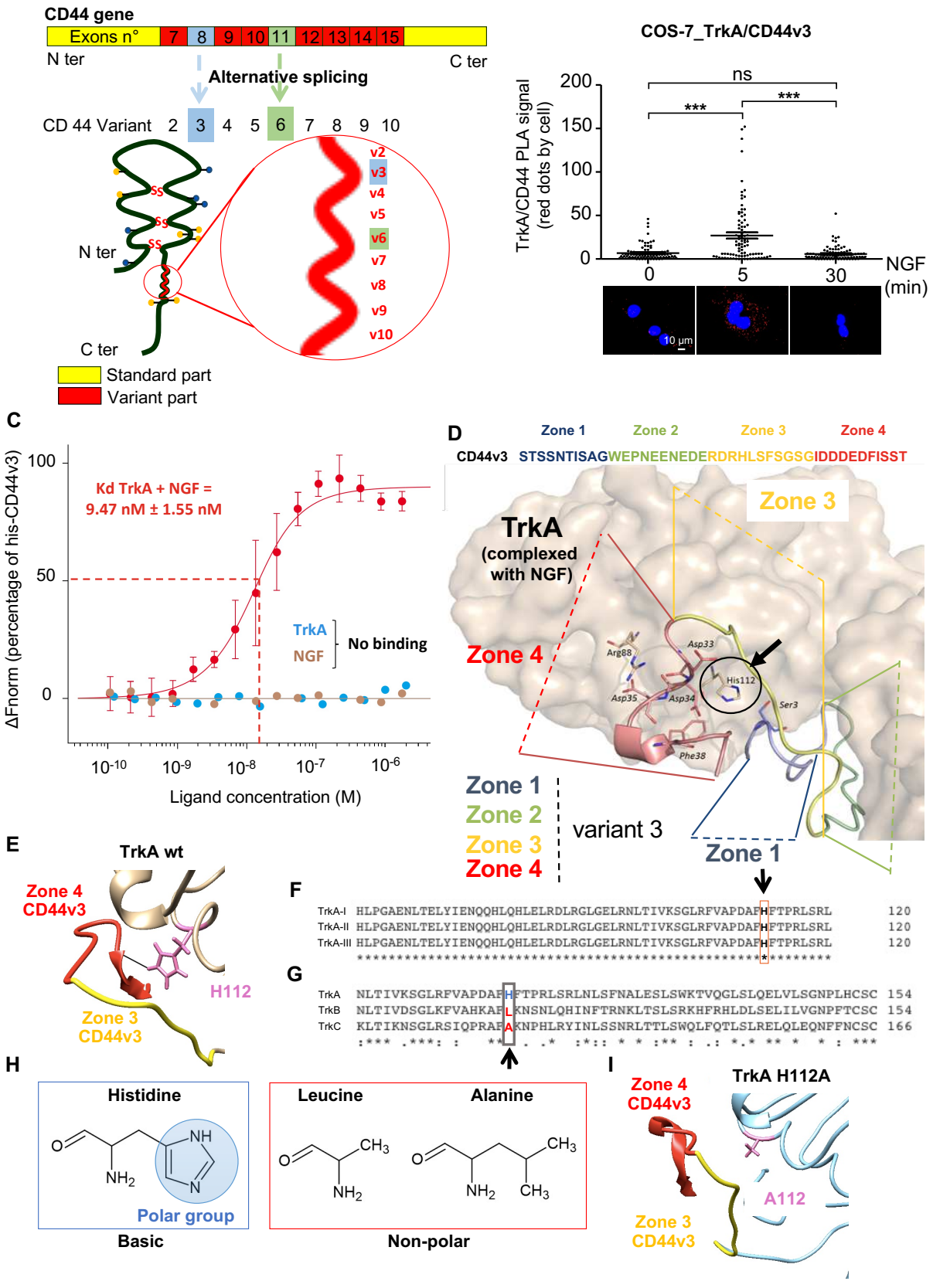


Figure 1, Trouvilliez *et al.*

Figure 1: The C-terminal region of CD44 variant 3 binds to TrkA. (A) Schematic representation of the CD44 gene and protein structure. Alternative

splicing leads to the expression of CD44 variants, thus the insertion of exon 8 leads to the expression of a CD44 protein containing variant 3 (CD44v3) and the insertion of exon 11 leads to the expression of a CD44 containing variant 6 (CD44v6) **(B)** TrkA/CD44v3 complex formation in COS-7 cells expressing TrkA and CD44v3 was detected by the proximity ligation assay (PLA), which was performed 0, 5 and 30 min after the initiation of NGF (100 ng/ml) treatment. The images represent signals detected by PLA. Quantification of the red spots was performed by ImageJ software (30 randomly chosen fields per condition of three different experiments). Statistical analyses were performed using one-way ANOVA followed by Bonferroni's posttest. Error bars represent the standard error of the mean (S.E.M.); *** $p < 0.001$. ns, nonsignificant. **(C)** NGF and/or TrkA binding to CD44v3 was measured by microscale thermophoresis (MST). MST experiments were performed on whole cell extracts of COS-7 cells expressing CD44v3. (**D, E)** Modeling of TrkA and CD44 variant exon 3; sequence alignment of TrkA isoforms **(F)** or TrkA, TrkB and TrkC **(G)** using the Clustal Omega program. **(H)** Structure of histidine, leucine and arginine amino acids (ChemSketch software). **(I)** Modeling of TrkA H112A and CD44v3.

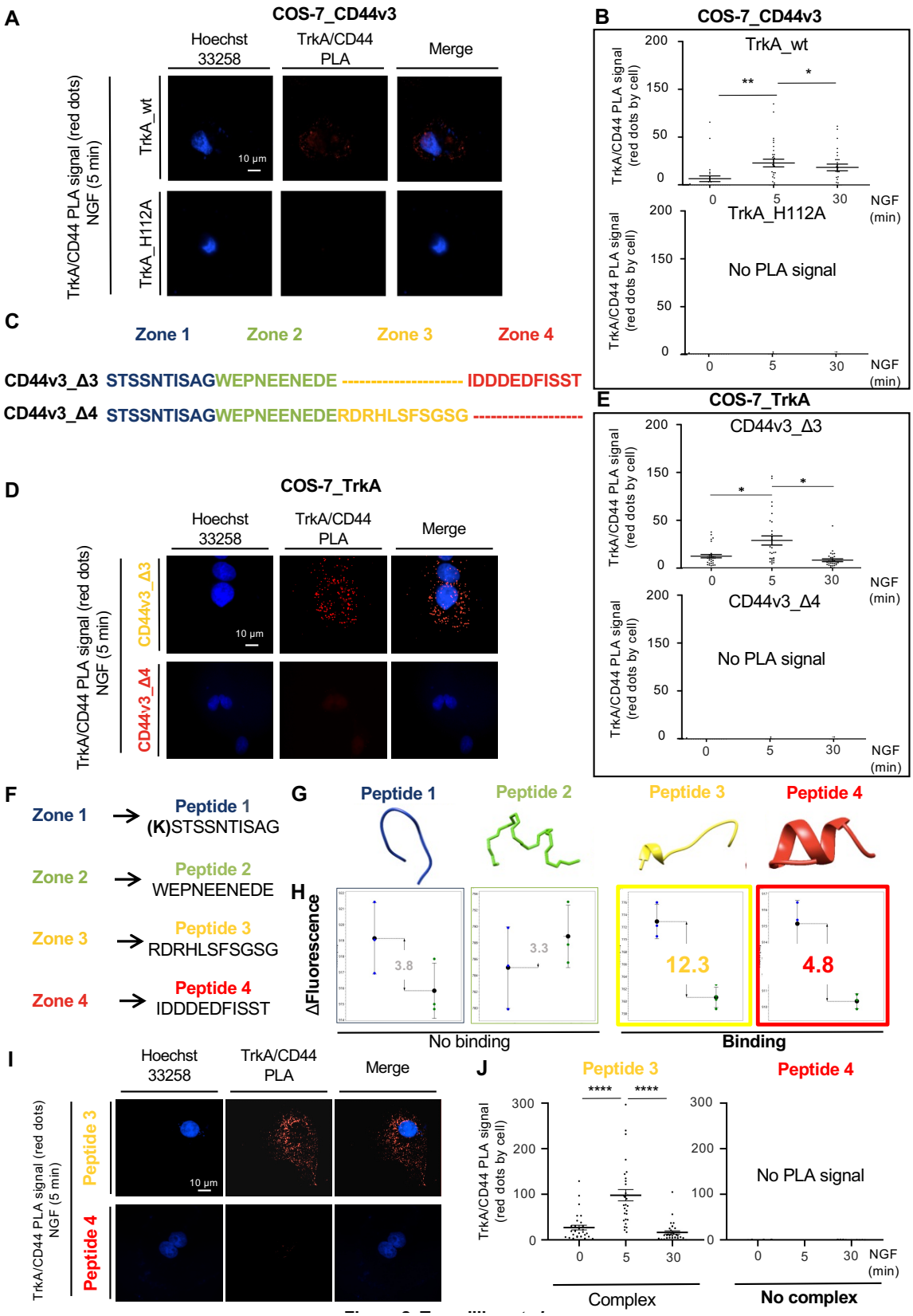


Figure 2: The C-terminal region of CD44v3 and the His112 residue of TrkA are involved in the CD44v3/TrkA interaction. TrkA/CD44v3 complex

association was detected by the proximity ligation assay (PLA) in wild-type TrkA- or TrkA_H112A- and CD44v3-expressing COS-7 cells. Proximity ligation assays were performed after 0, 5 and 30 min of NGF treatment (100 ng/ml). Representative images of signals detected by PLA **(A)** and their quantification **(B)**. Sequence of CD44 exon variant 3 and deletion mutant Δ3 or Δ4 **(C)**. TrkA/CD44v3 complex association was detected by PLA in wild-type TrkA and CD44v3 wild type or CD44v3 deleted mutant Δ3 or Δ4 expressing COS-7 **(D, E)**. Sequence of CD44v3 mimetic peptides **(F)** and structure **(G)**. TrkA binding to CD44v3 mimetic peptides by microscale thermophoresis **(H)** and effects of CD44v3 mimetic peptides 3 (RDRHLSFSGSG) and 4 (IDDEDFISST) on TrkA/CD44v3 complex formation **(I, J)**. Quantification of PLA was performed using ImageJ software (30 fields per condition of three different experiments). Statistical analyses were performed using one-way ANOVA followed by Bonferroni's posttest. The error bars represent the standard error of the mean (S.E.M.); * $p < 0.05$; ** $p < 0.01$.

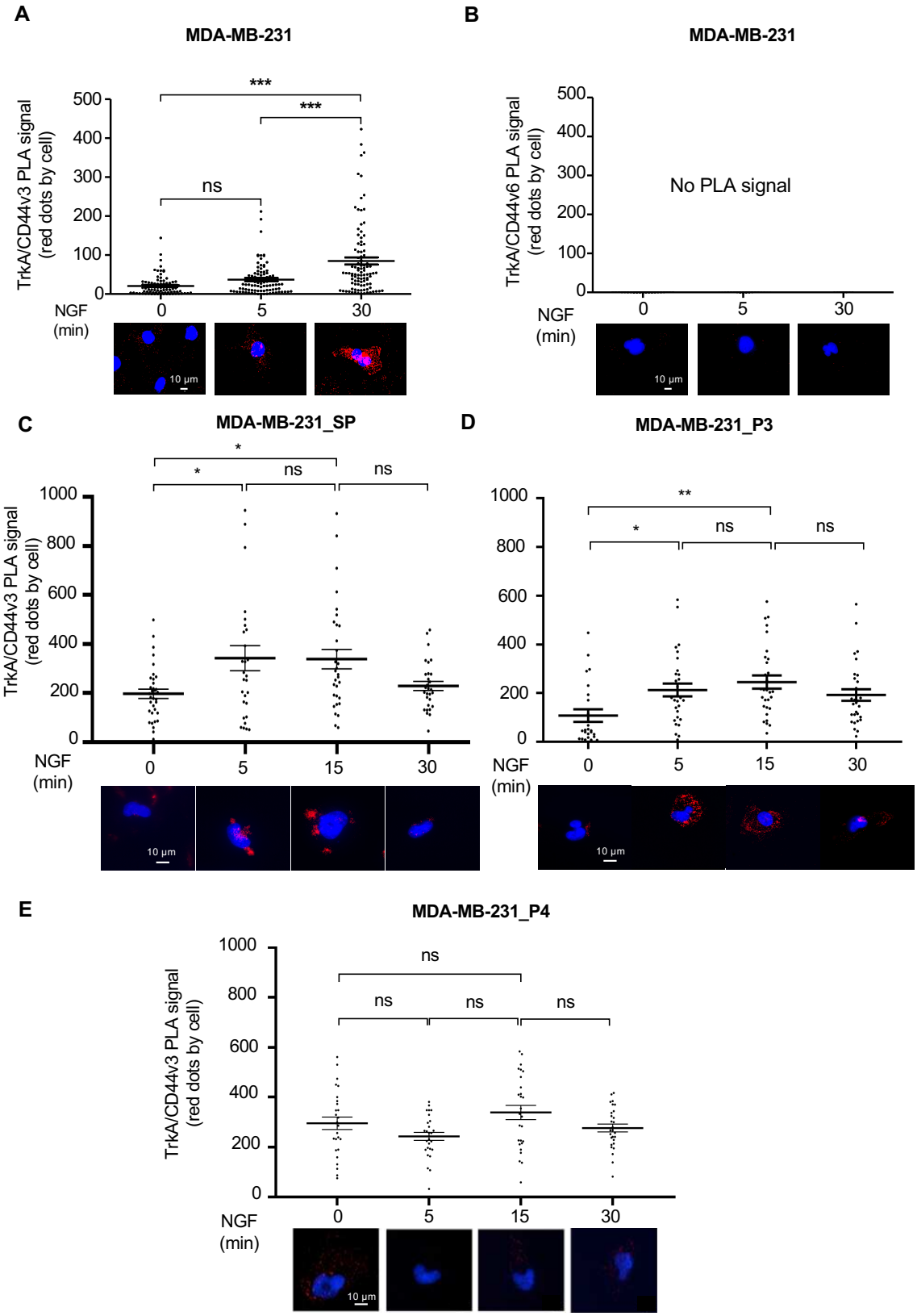


Figure 3: CD44v3 mimetic peptide 4 blocks the TrkA-CD44 association in MDA-MB-231 breast cancer cells. TrkA/CD44v3 **(A)** and TrkA/CD44v6 **(B)**

complex associations were detected by the proximity ligation assay (PLA) in MDA-MB-231 breast cancer cells. Effects of a scramble peptide (SP) **(C)**, CD44v3 mimetic peptide 3 (P3) and 4 (P4) **(D**) on TrkA/CD44v3 complex formation induced by NGF. Quantification of the PLA results was performed by ImageJ software (30 randomly chosen fields per condition of three different experiments). Statistical analyses were performed using one-way ANOVA followed by Bonferroni's posttest. The error bars represent the standard error of the mean (S.E.M.); * $p < 0.05$, ** $p < 0.01$, *** $p<0.001$; ns, not significant.

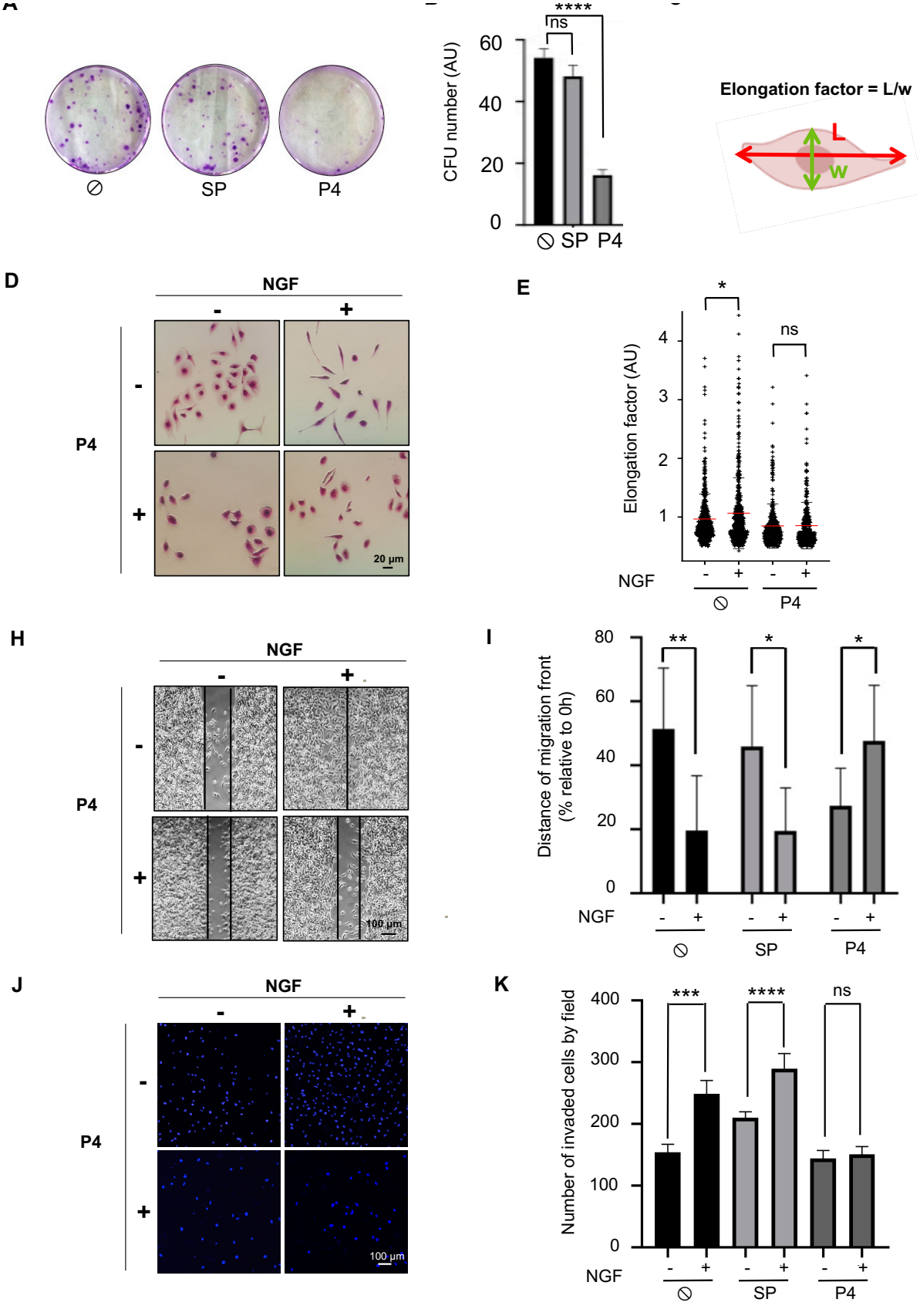

A
⊘
SP
P4
CFU number (AU)
60
40
20
0
****
ns
⊘ SP P4
Elongation factor = L/w
L
W
D
NGF
-
+
P4
20 µm
E
Elongation factor (AU)
4
3
2
1
*
ns
NGF
⊘
P4
H
100 µm
I
Distance of migration front (% relative to 0h)
80
60
40
20
0
**
*
*
⊘
SP
P4
J
100 µm
K
Number of invaded cells by field
400
300
200
100
0
***
****
ns

Figure 4: CD44v3 mimetic peptide 4 inhibits MDA-MB-231 breast cancer cell growth and migration/invasion. Clonogenic MDA-MB-231 cell growth was measured after 10 days in the presence of a scramble peptide (SP) or CD44v3 mimetic peptide (P4) **(A, B)**. The elongation factor (length-to-width ratio) was assessed after 10 days in the presence or absence of NGF (**C, D, E**). Migration assays were performed using Ibidi devices 24 h after treatment (**H, I**). Invasion through collagen 1 was measured by the Transwell assay 16 h after treatment (**J, K**). Statistical analyses were performed using one-way ANOVA followed by Bonferroni's posttest. The error bars represent the standard error of the mean (S.E.M.); * $p < 0.05$, ** $p < 0.01$, *** $p<0.001$, **** $p<0.0001$; ns, not significant.

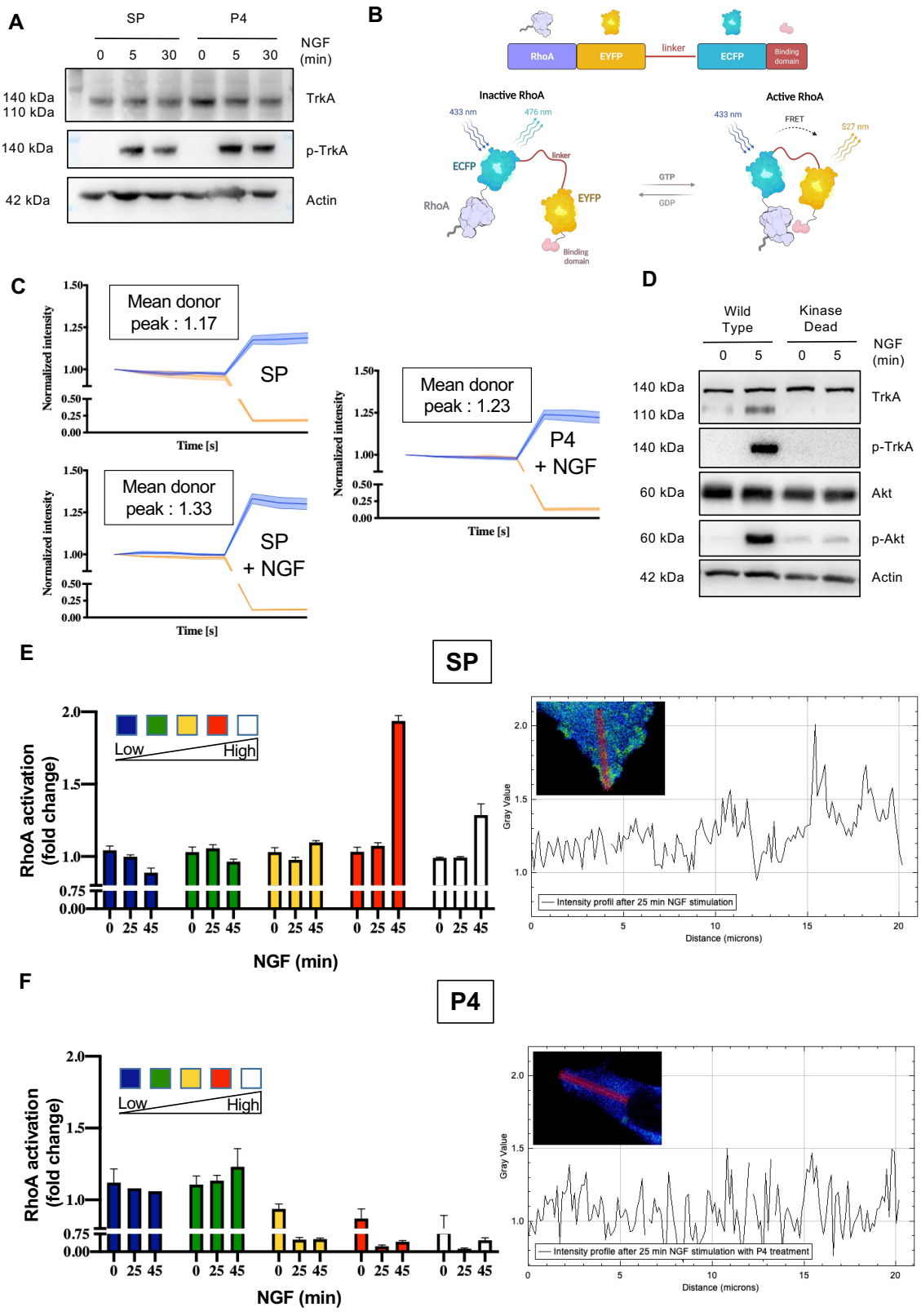
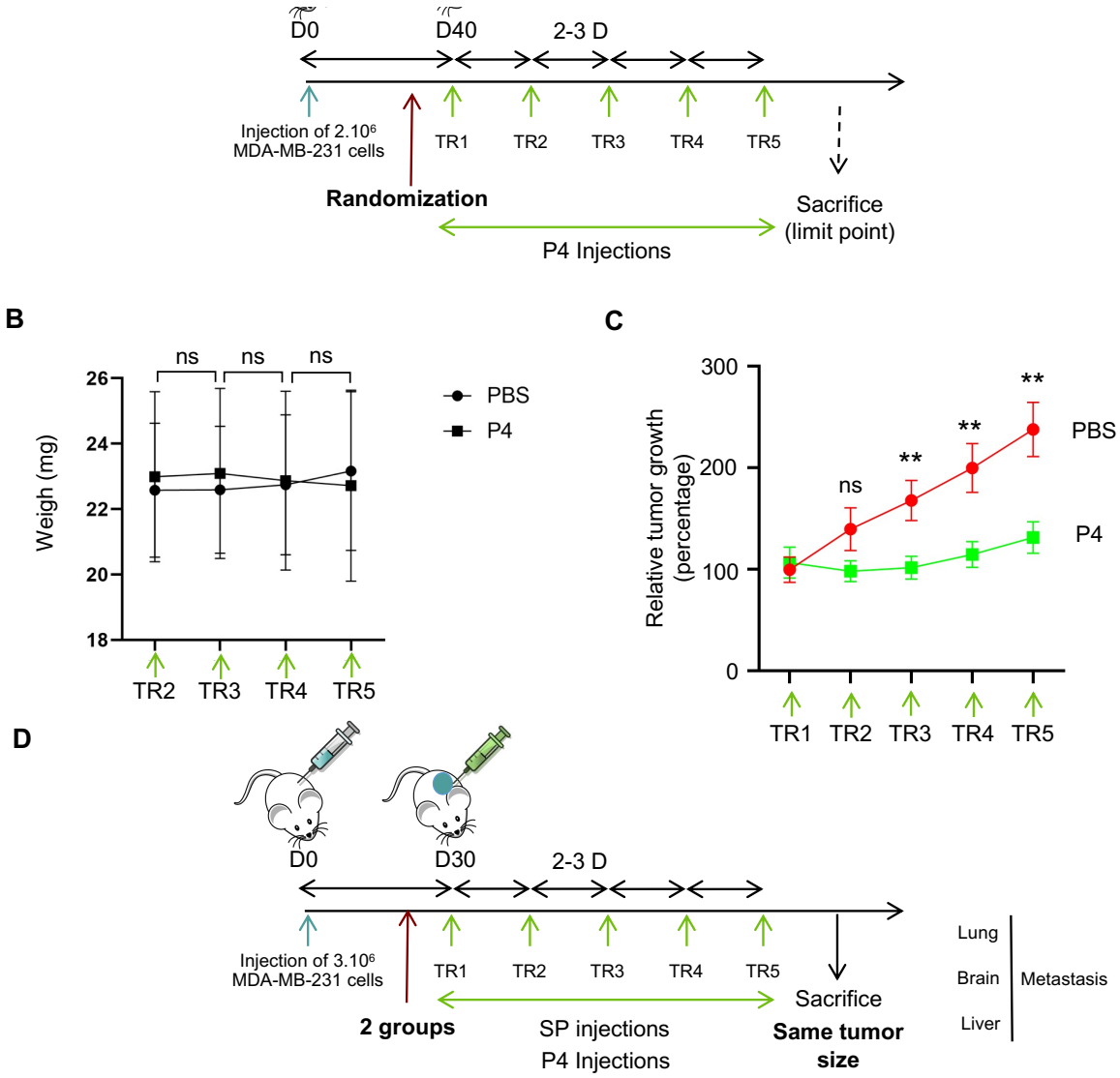


Figure 5: CD44v3 is implicated in the phospho-TrkA-independent activation of RhoA GTPase. Phosphorylation of TrkA was measured in the presence of a scramble peptide or CD44v3 mimetic peptide 4 (P4) in the

presence or absence of NGF **(A)**. Schematic representation of the Rho biosensor; **(B)**. AB-FRET measurement of RhoA activation induced by NGF in MDA-MB-231 cells in the presence of a scramble peptide or P4 **(C)**. Phosphorylation of TrkA and downstream Akt in wild-type MDA-MB-231 and MDA-MB-231 cells expressing kinase-dead TrkA, as determined by western blotting **(D)**. Measurement of RhoA activation using the RhoA biosensor by FRET 25 and 45 min after NGF treatment in cells expressing either a scramble peptide (SP) or CD44v3 mimetic peptide 4 (P4). Based on the FRET signal intensity from low to high, the cells were divided into five groups **(E, F)**. Localization of activated RhoA activation in MDA-MB-231 cells expressing kinase-dead TrkA **(G, H)**.



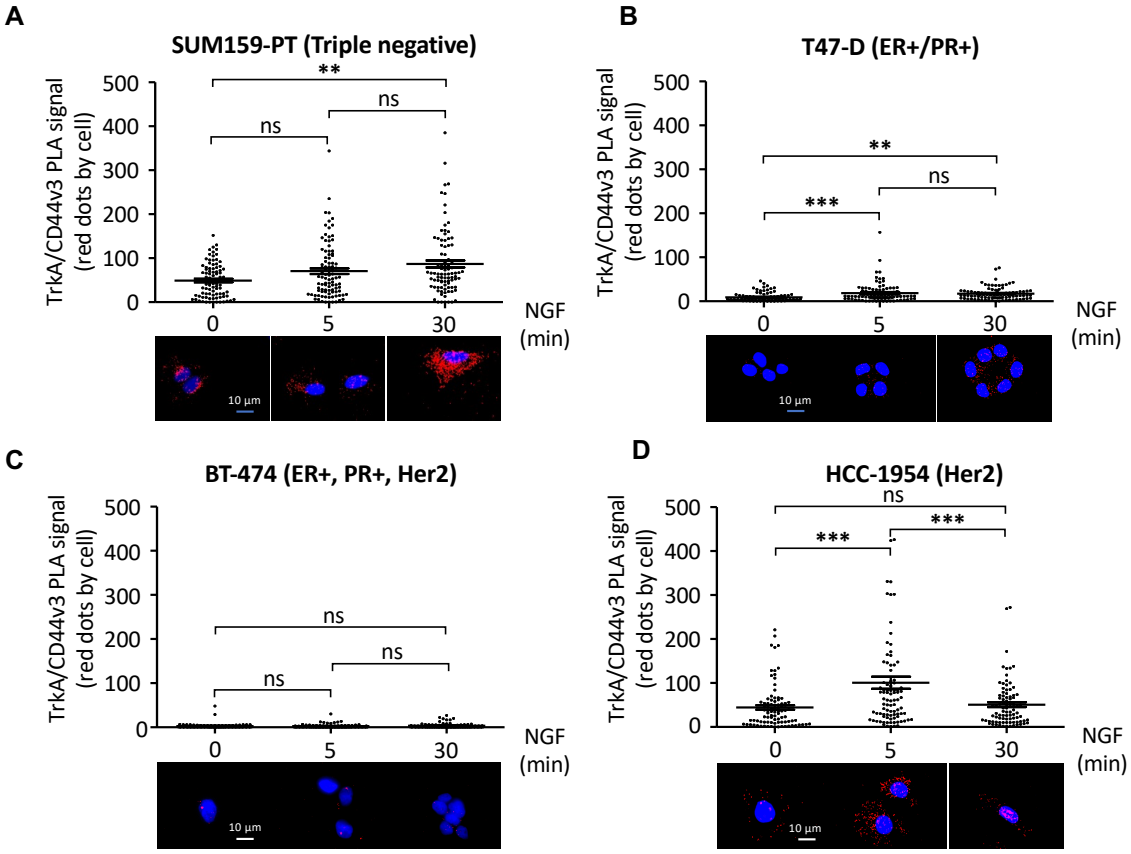
Organ	Lung	Brain	Liver
SP	100%	33,33%	66,66%
P4	**33%**	**0%**	**33%**

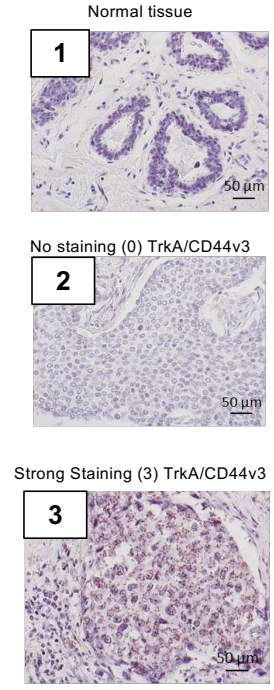
Organ	Lung	Brain	Liver
Control	100%	60%	100%
H112A	**100%**	**16%**	**66%**

Figure 6, Trouvilliez *et al.*

Figure 6: CD44v3 mimetic peptide 4 blocks MDA-MB-231 tumor growth

and metastasis. Schematic representation of the experimental setup for MDA-MB-231 tumor growth assessment in SCID mice **(A)**. Body weight **(B)** and tumor volume **(C)** were measured following CD44v3 mimetic peptide administration (10 mice per group). Schematic representation of the experimental setup for MDA-MB-231 metastasis assessment in SCID mice **(D)**. Percentage of metastasis-positive lungs, brains and livers **(E)** after scramble peptide or CD44v3 mimetic peptide 4 treatment (3 mice/group) or (**F**) after TrkA-H112 mutant treatment (6 mice) compared with HA-TrkA cells (5 mice). ** $p<0.01$; ns, nonsignificant. T test.





F

			Mean staining	p value
Total of patients		150	2.35	-
Mean age (years) at diagnosis		53.57 (29-83)	ND	-
Average Follow up (years)		9.3 (0.167-13.5)	ND	-
Estrogen receptor	Negative	46 (30.67%)	2.609	-
	Positive	96 (64%)	2.208	0.0657
	NA	8 (5.33%)	ND	-
Progesterone receptor	Negative	56 (37.33%)	2.607	-
	Positive	85 (56.67%)	2.188	**0.0445**
	NA	9 (6%)	ND	-
HER-2	Negative	94 (62.67%)	2.394	-
	Positive	49 (32.67%)	2.245	0.4877
	NA	7 (4.67%)	ND	-
Triple negative	Negative	118 (78.67%)	2.271	-
	Positive	22 (14.67%)	2.818	**0.0528**
	NA	10 (6.67%)	ND	-

Figure 7: The TrkA/CD44v3 complex is formed in PR-negative breast cancer cells and tumors. TrkA/CD44v3 complex formation was measured in SUM159-PT (triple negative—i.e., ERα-, PR-, and Her2-) cells **(A)**, T47-D

(luminal A—i.e., ERα+, PR+, and Her2-) cells **(B)**, BT-474 (luminal B—ERα+, PR+, and Her2+) cells **(C)**, HCC-1954 (Her2-like—ERα-, PR-, and Her2+) cells **(D),** and 150 tumor patient samples obtained from US BioMax (HBre-Duc150Sur01) **(E, F)** using the proximity ligation assay (PLA). For breast cancer cell lines, quantification of the PLA results was performed using ImageJ software (30 randomly chosen fields per condition of three different experiments). Statistical analysis was performed using one-way ANOVA followed by Bonferroni's posttest. The error bars represent the standard error of the mean (S.E.M.); * $p < 0.05$; ** $p < 0.01$; ns, not significant. Representative micrograph of PLA staining of normal tissue **(E, 1)** and breast tumors **(E, 2 and 3)**. For PLA, the signals were classified into 4 categories ranging from no signal **(E,2)** to a high intensity signal **(E,3)**. The scoring for TrkA/CD44v3 PLA staining is reported in Table (F) according to estrogen receptor, progesterone receptor, Her2 expression and triple-negative status (absence of estrogen receptor, progesterone receptor and Her2 overexpression). NA, information not available.

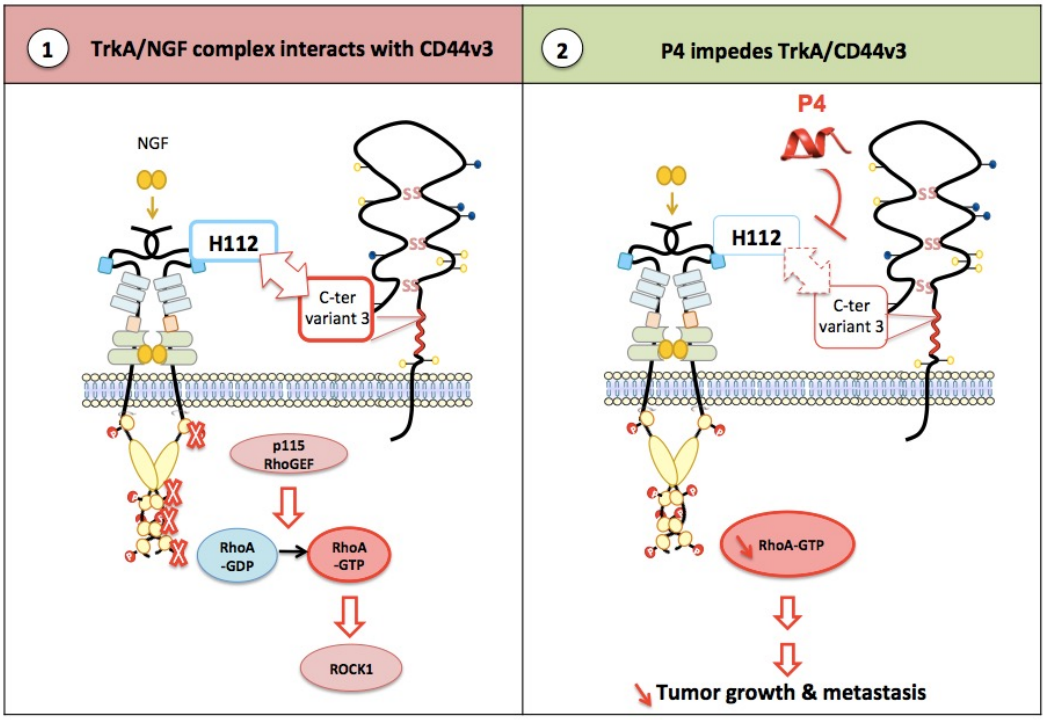
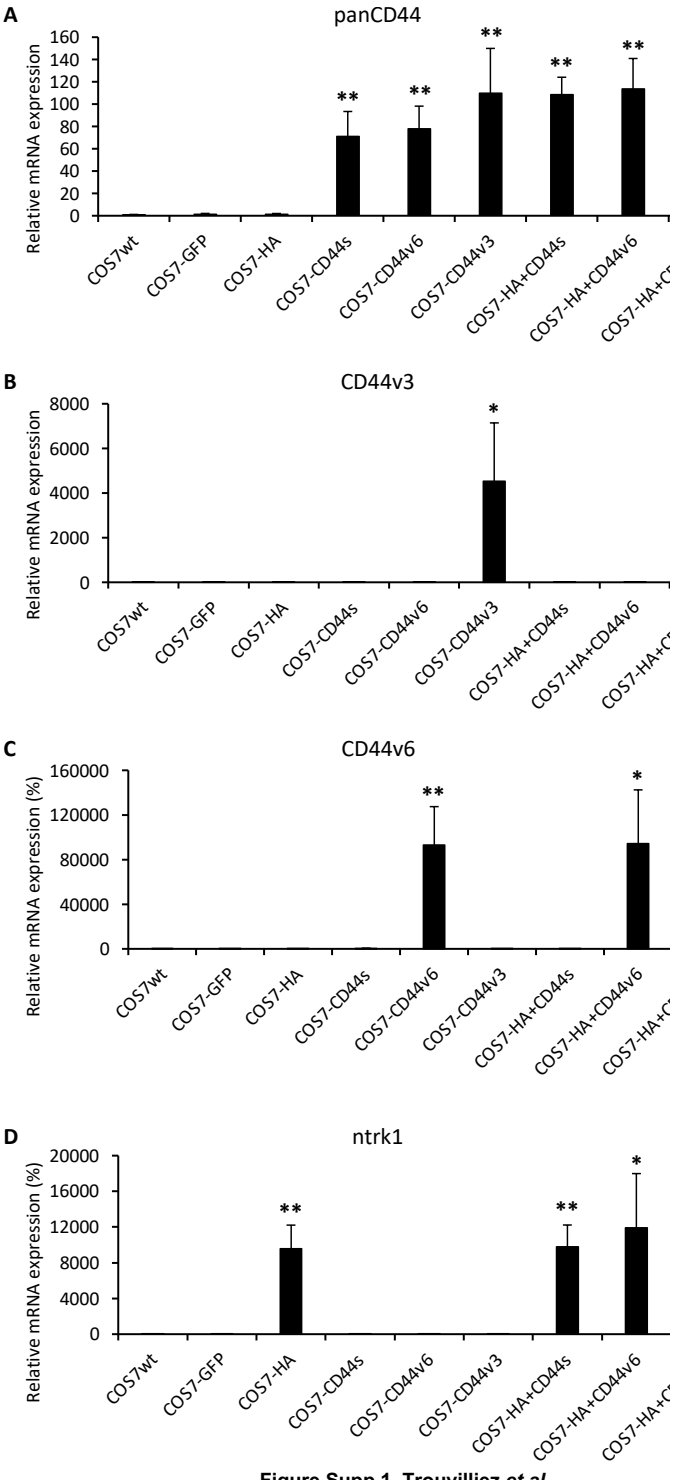


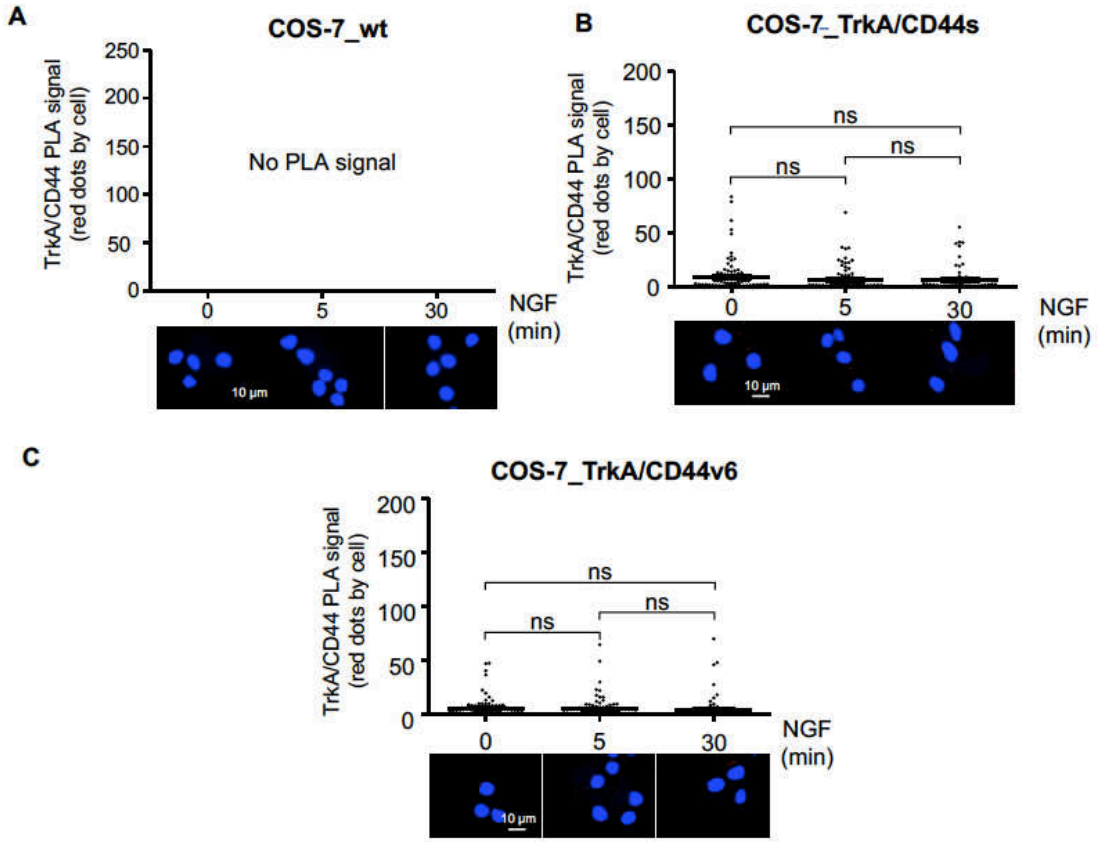
Figure 8: Schematic representation of the TrkA-CD44v3 interaction induced by NGF. (1) In the presence of NGF, TrkA interacts with CD44v3 variant 3 at histone residue H112. This interaction is the basis for phospho-independent TrkA signaling. It involves the p115 RhoGEF/RhoA/ROCK1 signaling cascade to induce tumor development. **(2)** In the presence of CD44v3 4 mimetic peptide (P4), the TrkA/CD44v3 complex cannot form, and phosphorescent-independent TrkA signaling through RhoA is inhibited. This results in decreased tumor development and metastatic capabilities.

Supplementary data:



Supplementary Figure 1: Validation of the ectopic expression of CD44 and/or TrkA in COS-7 cells. The expression of all CD44 isoforms **(A)**, CD44 variant 3 **(B)**, CD44 variant 6 **(C)** and TrkA (hyaluronan [HA]; **D)** was evaluated by RT–qPCR (normalized using PUM-1). No expression of CD44, CD44 variants (3 or 6) or TrkA was detected in COS-7 cells **(A-D)** compared

with that in cells transfected with the expression plasmid carrying each protein.



<u>Supplementary figure 2:</u> TrkA does not interact with CD44s or CD44v6. Wild-type cos7 cells **(A)** or CD44S- **(B)** or CD44v6 **(C)** cells transfected with TrkA were treated with 100 ng/ml NGF (0, 5 or 30 min) and fixed. Quantification of the PLA results was performed using ImageJ software (30 randomly chosen fields per condition of three different experiments). Statistical analyses were performed using one-way ANOVA followed by Bonferroni's posttest. The error bars represent the standard error of the mean (S.E.M.); ns, not significant.

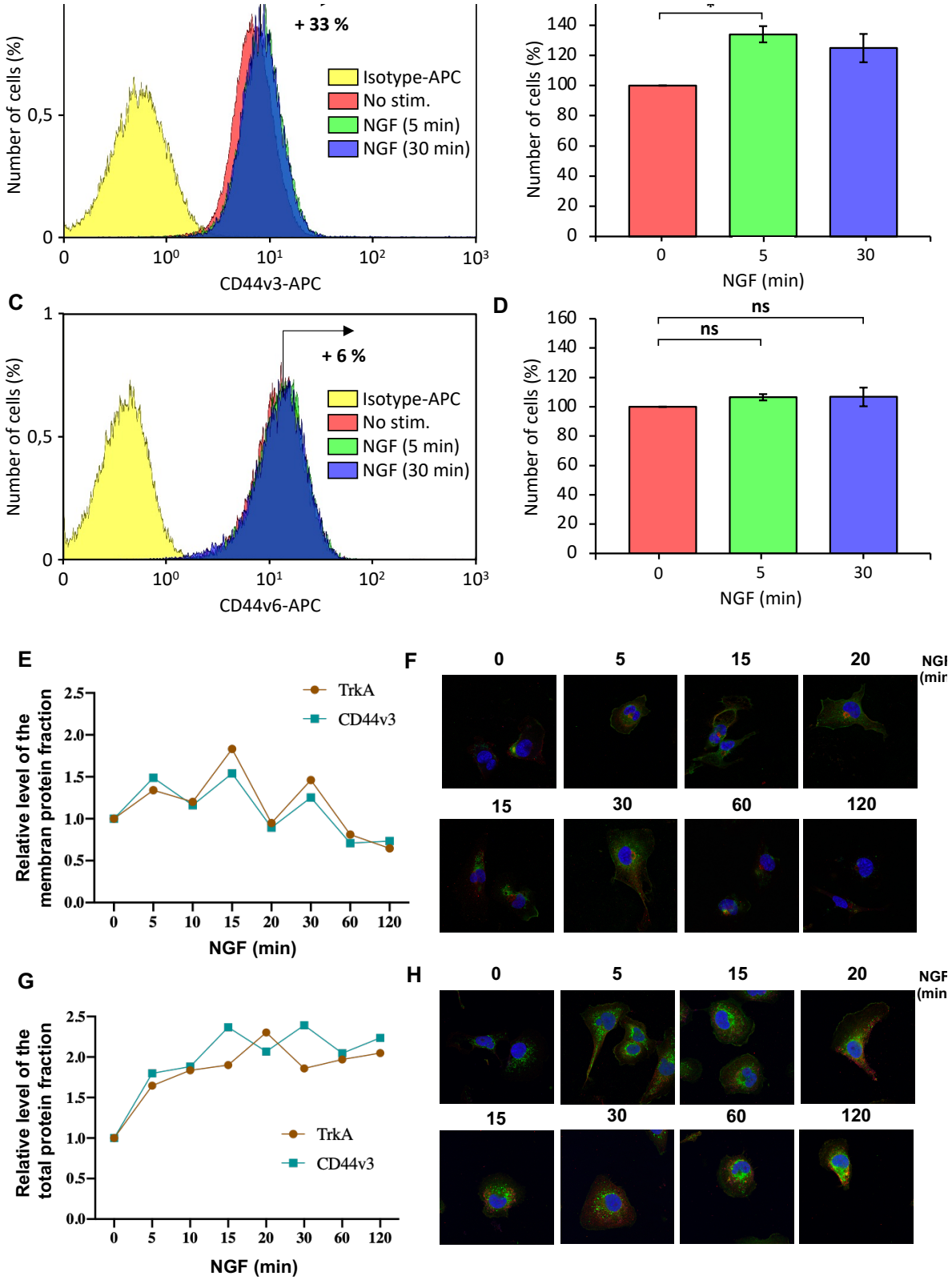
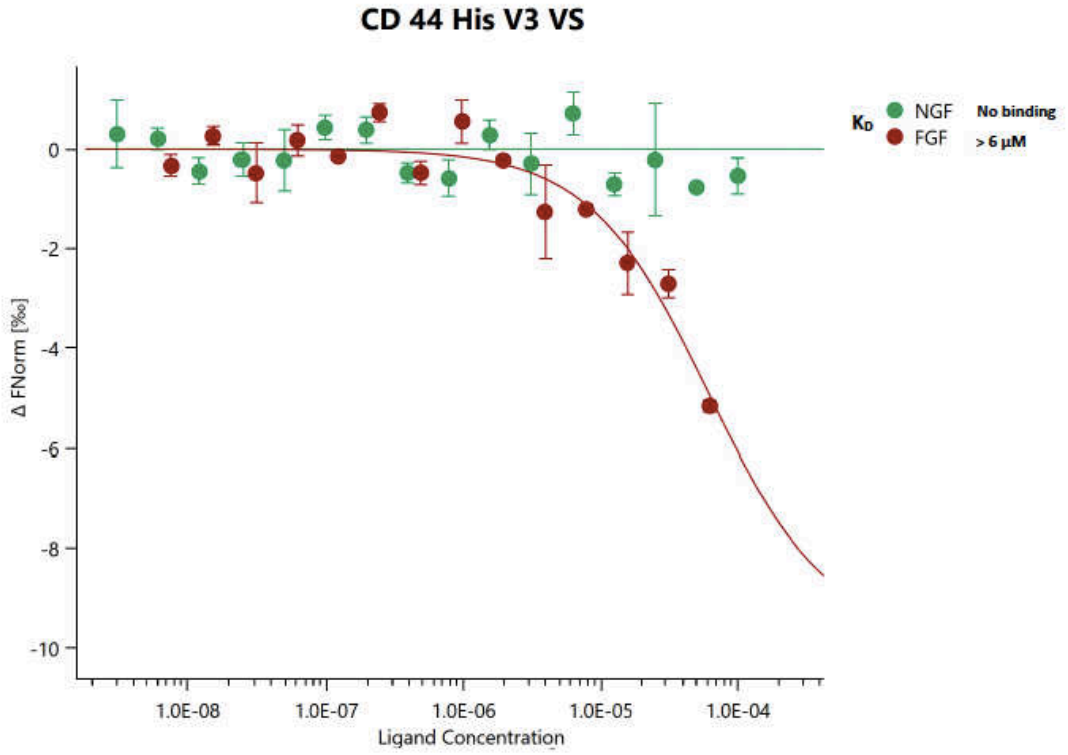


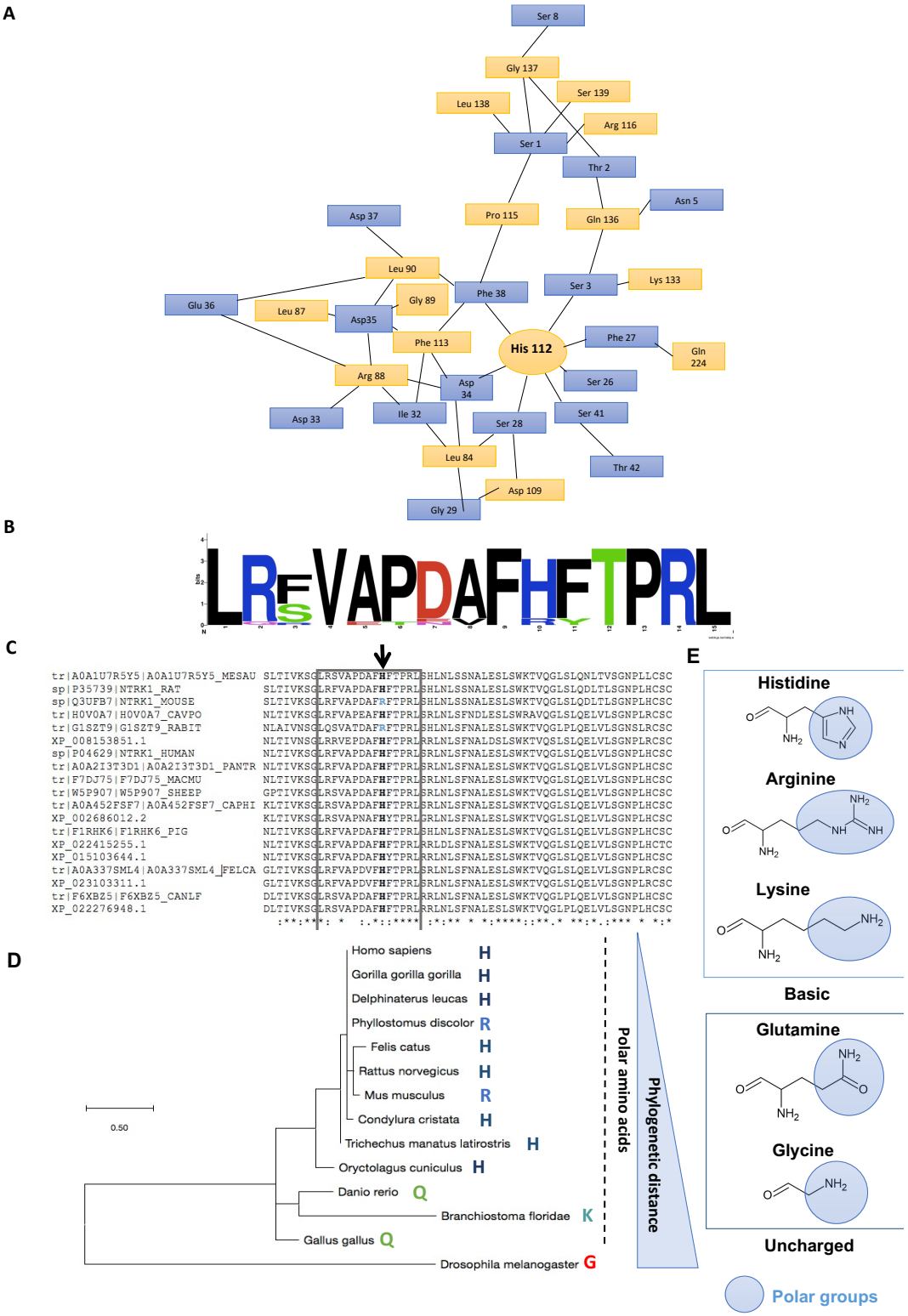
Figure Supp 2, Trouvilliez *et al.*

Supplementary Figure 3: CD44v3 and TrkA are recruited to the plasma membrane through NGF stimulation. CD44v3 and CD44v6 levels at the plasma membrane were assessed by flow cytometry **(A-D)**. The plasma

membrane and total TrkA and CD44v3 levels were also quantified by confocal microscopy **(E-H).** Statistical analyses were performed using one-way ANOVA followed by Bonferroni's posttest. The error bars represent the standard error of the mean (S.E.M.); * $p < 0.05$; ns, not significant.

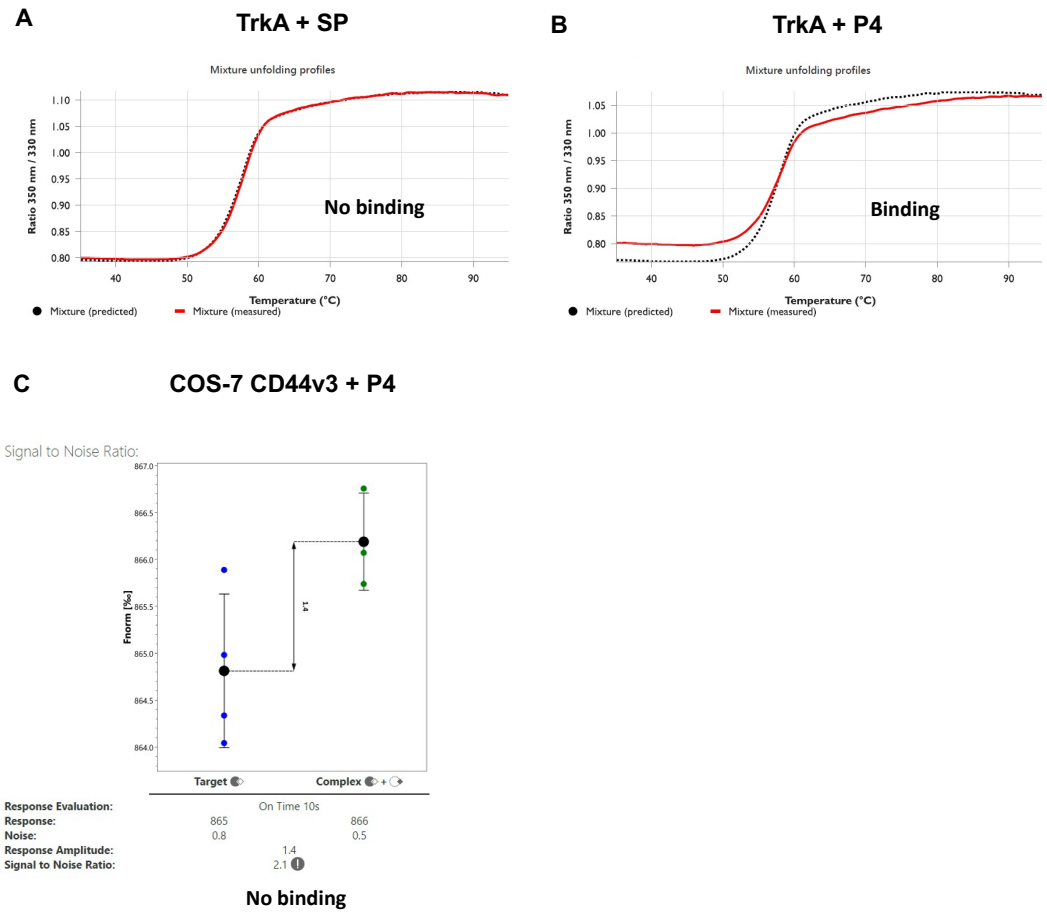


Supplementary Figure 4: NGF does not bind to CD44v3. The CD44v3/NGF interaction was evaluated using microscale thermophoresis (MST). FGF-2 (control) binding to CD44v3 but not to NGF was detected.

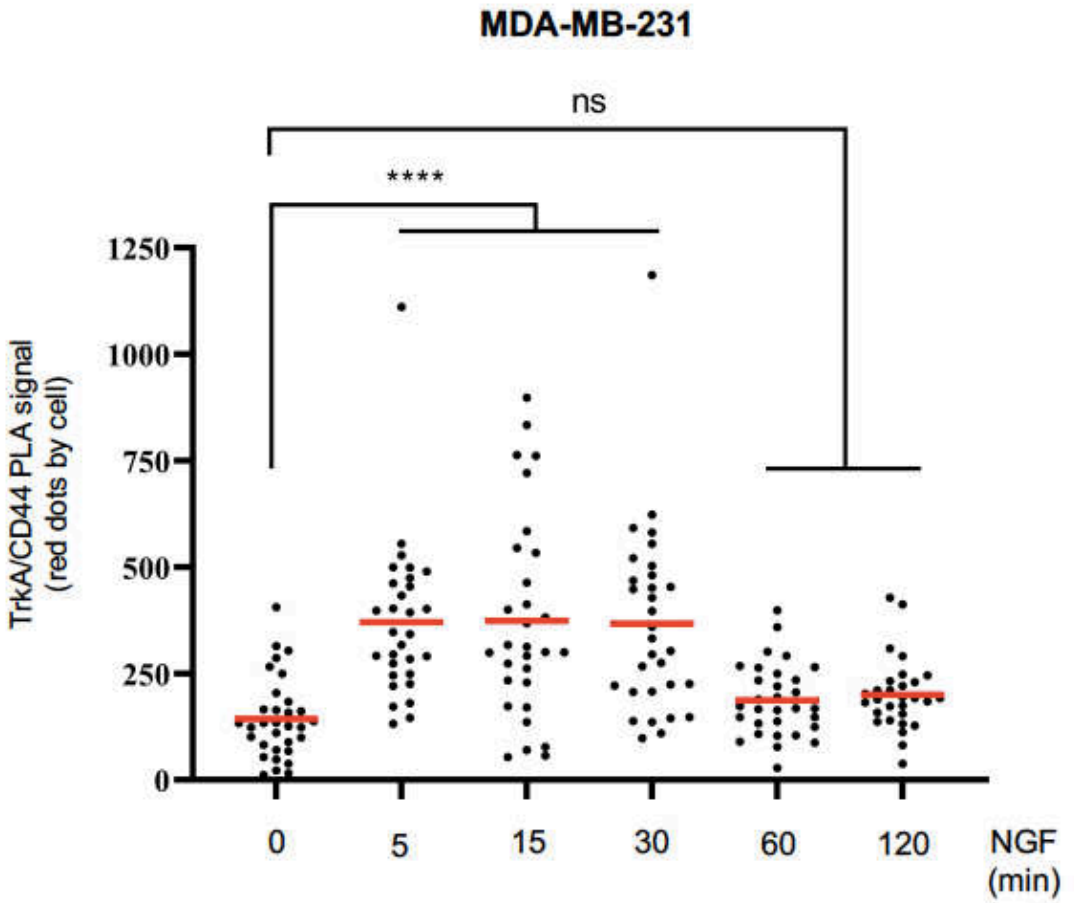


<u>Supplementary Figure 5:</u> His112 of TrkA is conserved across mammals. Graphical representation of the interactions between residue H112 of TrkA and CD44v3 using betweenness centrality analysis (BCA) **(A)**. Conservation of His112 across mammals was assessed by alignment analysis of TrkA sequences in different mammals using WebLogos **(B)** and the Clustal Omega

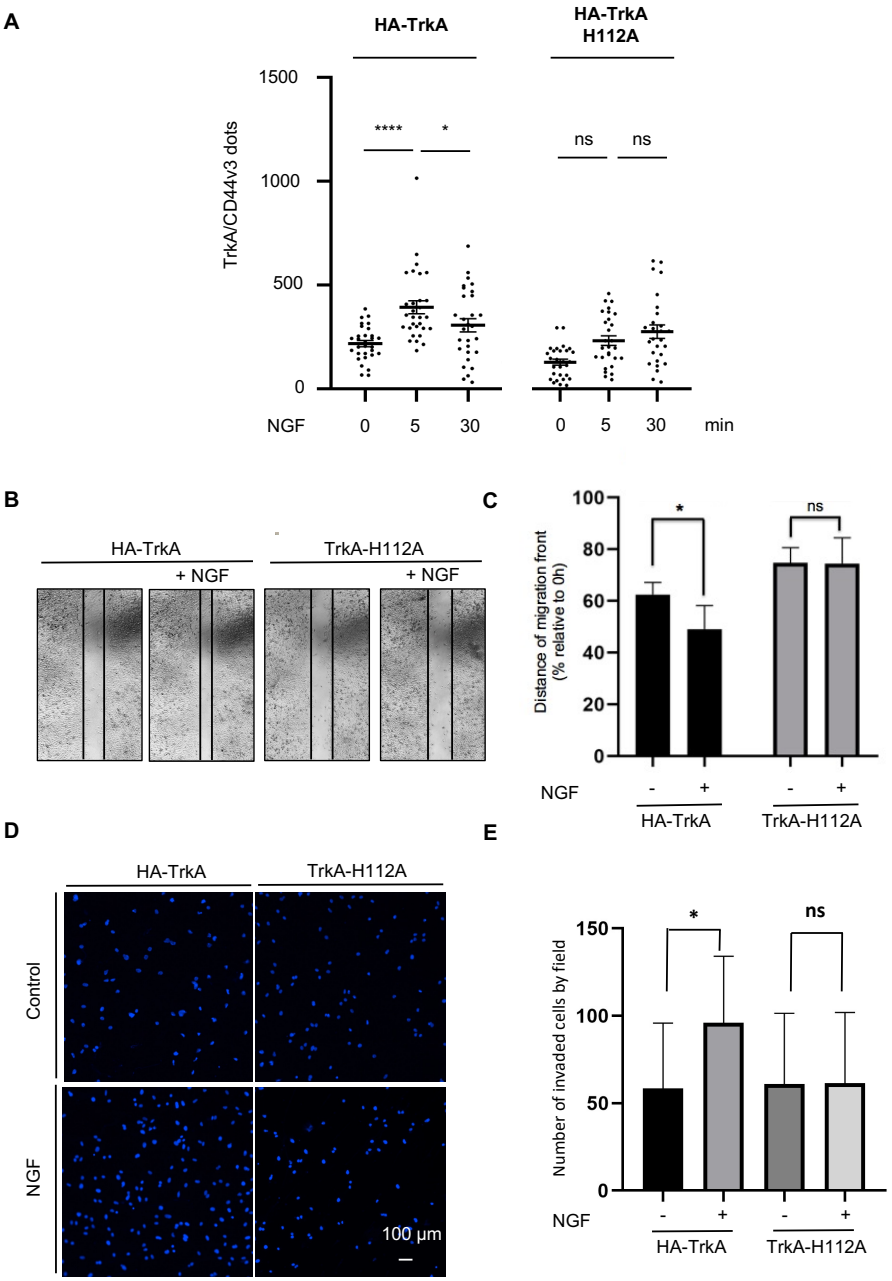
program **(C).** A phylogenetic tree using the neighbor-joining method constructed with the MegaX program shows the evolution of the TrkA His112 region across vertebrates. For each species, the residue corresponding to His112 was reported **(D)**. Schematic representation (ChemSketch) of the amino acid substitution of His112 across vertebrates **(E).**



<u>Supplementary Figure 6:</u> CD44v3 mimic peptide 4 (P4) binds to TrkA but not to CD44v3. Peptide binding (P4; **A**) or not (scramble protein [SP]; **B**) was validated by nanoscale differential scanning fluorimetry (NanoDSF). The CD44v3/P4 with TrkA interaction was evaluated using microscale thermophoresis (MST; binding determination analysis is shown in **C**.

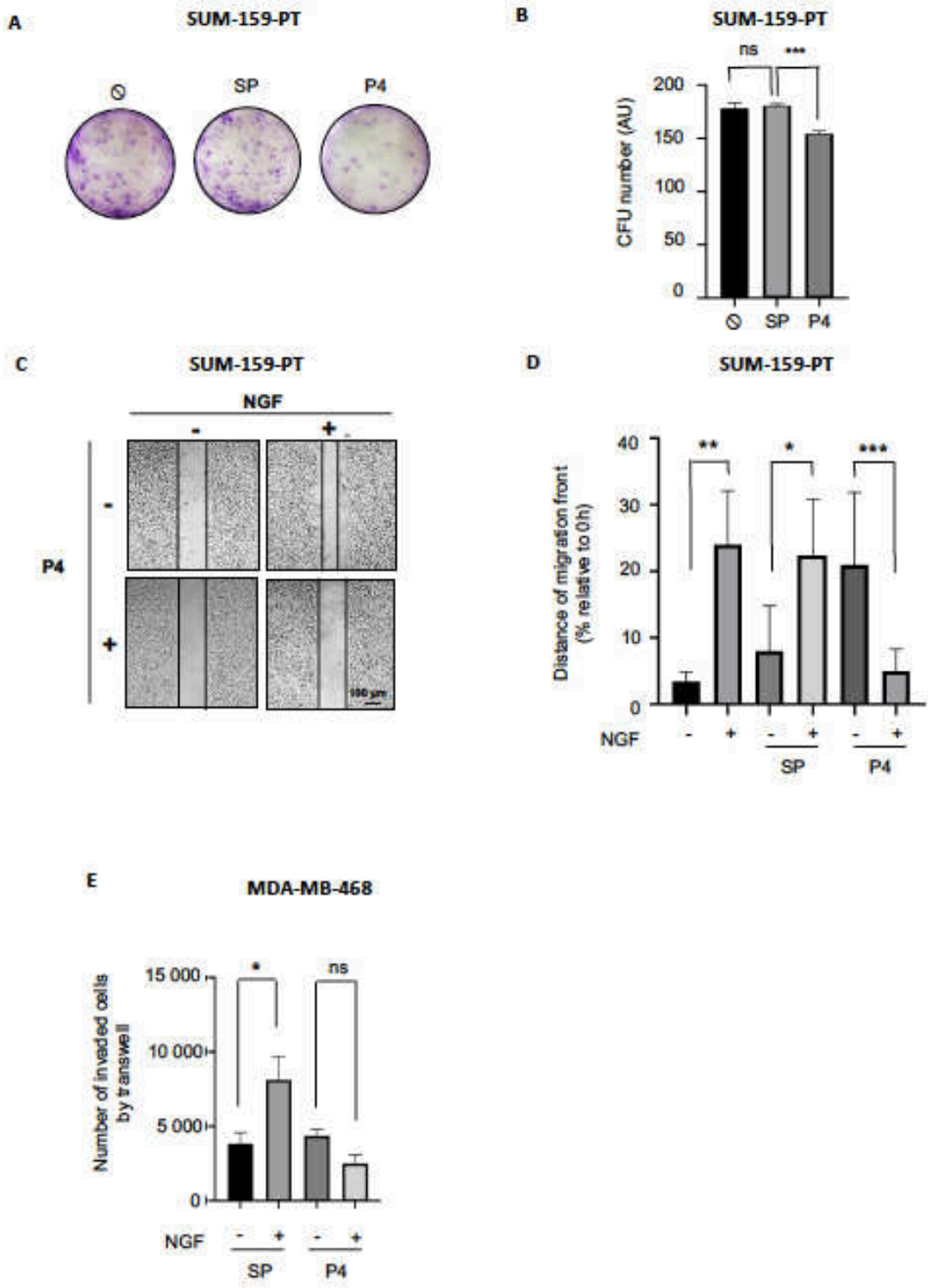


Supplementary Figure 7: Plasma membrane TrkA/CD44v3 complex formation is transient. TrkA/CD44v3 complex association was detected using the proximity ligation assay (PLA) in MDA-MB-231 breast cancer cells. Quantification of the PLA results was performed using ImageJ software (30 randomly chosen fields per condition of three different experiments). Statistical analyses were performed using one-way ANOVA followed by Bonferroni's posttest. The error bars represent the standard error of the mean (S.E.M.); *** $p<0.0001$; ns, not significant.



Supplementary Figure 8: Effects of H112A mutation on the TrkA/CD44v3 complex. TrkA/CD44v3 complex association was quantified by the proximity ligation assay (PLA) in wild-type TrkA- or TrkA_H112A- MDA-MB-231 cells. Proximity ligation assays were performed after 0, 5 and 30 min of NGF treatment (100 ng/ml) **(A)**. Migration assays were performed using Ibidi devices 24 h after treatment **(B, C)**. Invasion through collagen 1 was measured using the Transwell assay 16 h after treatment (**D, E**). Statistical analyses were performed using one-way ANOVA followed by Bonferroni's

posttest. The error bars represent the standard error of the mean (S.E.M.); * $p < 0.05$, **** p<0.0001; ns, not significant.



Supplementary Figure 9: Effects of CD44v3 mimetic peptide 4 on triple-negative breast cancer cell growth and migration/invasion. Clonogenic

SUM-159-PT cell growth was measured after 10 days in the presence of a scramble peptide (SP) or CD44v3 mimetic peptide (P4) **(A, B)**. Migration assays were performed using Ibidi devices 24 h after treatment (**C, D**). Invasion through collagen 1 of MDA-MB-468 cells was measured using the Transwell assay 16 h after treatment (**E**). Statistical analyses were performed using one-way ANOVA followed by Bonferroni's posttest. The error bars represent the standard error of the mean (S.E.M.); * $p < 0.05$, ** $p < 0.01$, *** $p<0.001$; ns, not significant.

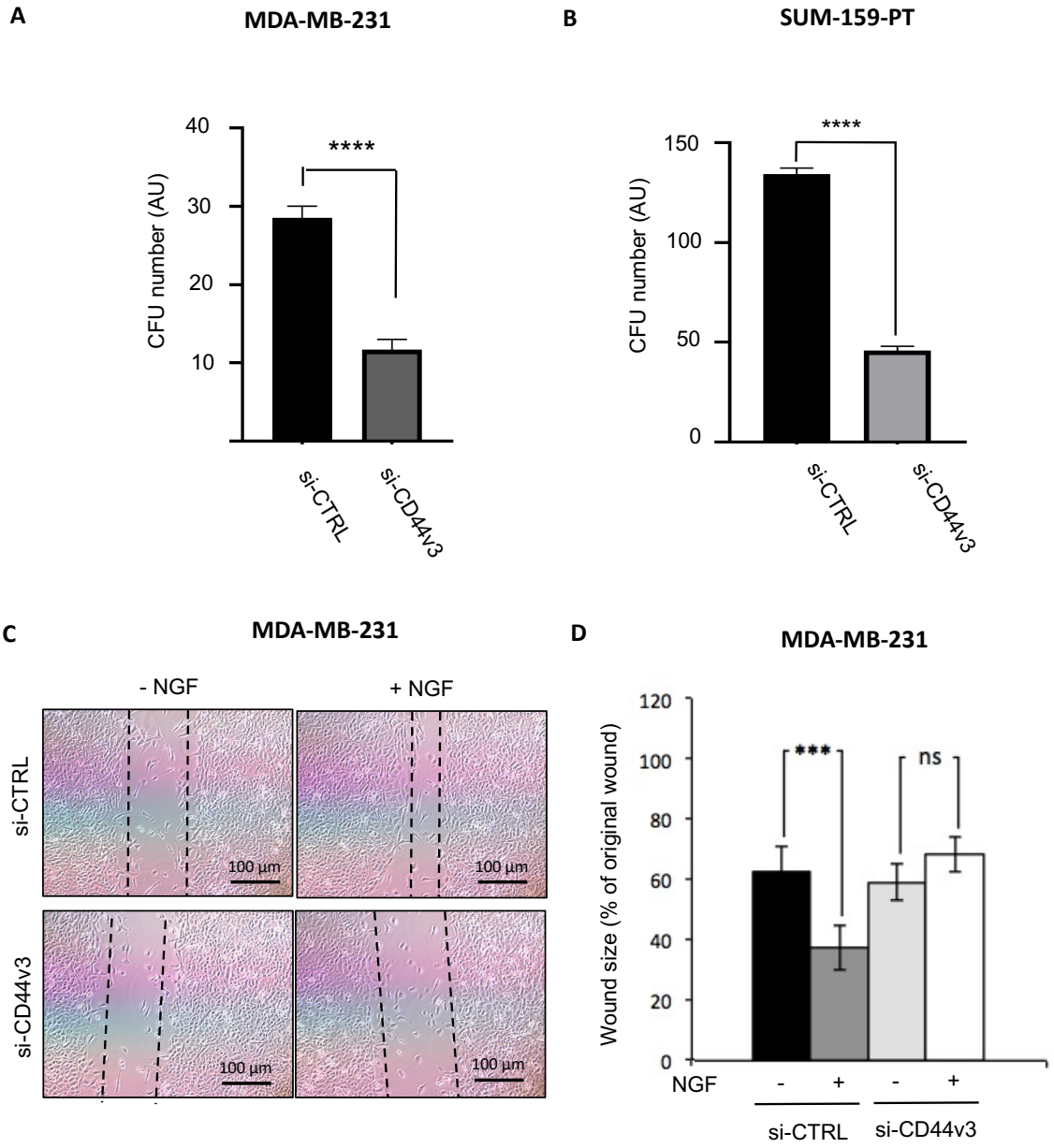
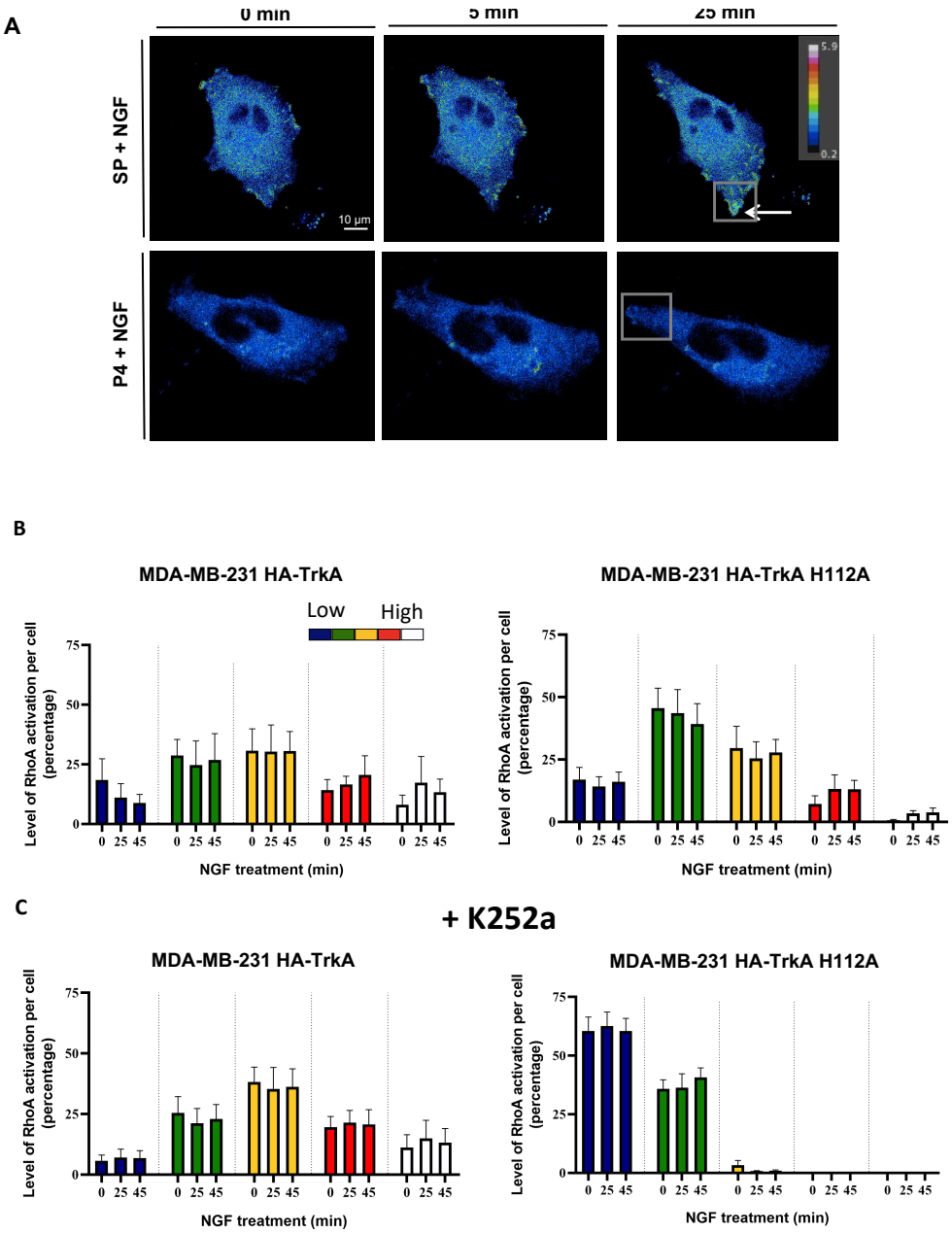


Figure Supp 10, Trouvilliez *et al.*

Supplementary Figure 10: siCD44v3 inhibits Triple negative breast cancer cell growth and migration/invasion. MDA-MB-231 cells transfected (24 h) with short interfering RNA against CD44v3 (siCD44v3) or a control (siCTL) were used to perform clonogenic cell growth, migration and invasion assays. Clonogenic cell growth (MDA-MB-231)**(A)** and SUM-159-PT **(B)** was measured 10 days after siRNA transfection. Migration assays were performed using Ibidi devices 24 h after treatment **(C, D)**. The extent of cell invasion through collagen 1 was measured using the Transwell assay 16 h after treatment **(E)**. Statistical analyses were performed using one-way ANOVA followed by Bonferroni's posttest. The error bars represent the standard error of the mean (S.E.M.); * $p < 0.05$, *** p<0.001, **** p<0.0001; ns, not significant.



Supplementary Figure 11: CD44v3 mimic peptide 4 (P4) impedes local RhoA activation independent of TrkA phosphorylation. A) Measurement of RhoA activation using the RhoA biosensor by Förster resonance energy transfer (FRET) in the presence of a scramble peptide (SP) (supplementary video 1) or CD44v3 mimetic peptide 4 (P4) (supplementary video 2) after NGF treatment of MDA-MB-231 cells expressing kinase-dead TrkA. **(B, C)** Measurement of RhoA activation using the RhoA biosensor by FRET 25 and 45 min after NGF treatment in cells expressing either HA-TrkA or HA-

TrkAH112A in the absence **(B)** or presence **(C)** of k252A (TrkA kinase inhibitor). Based on the FRET signal intensity from low to high, the cells were divided into five groups.

Supplementary video 1: Measurement of RhoA activation using the RhoA biosensor by Förster resonance energy transfer (FRET) in the presence of a scramble peptide (SP) after NGF treatment of MDA-MB-231 cells expressing kinase-dead TrkA.

Supplementary video 2: Measurement of RhoA activation using the RhoA biosensor by Förster resonance energy transfer (FRET) in the presence of CD44v3 mimetic peptide 4 (P4) after NGF treatment of MDA-MB-231 cells expressing kinase-dead TrkA.

Article 2:

Trouvilliez Sarah[1], Cicero Julien[1], Palma Martine[1], Lagadec Chann[1], Bourette Roland[1], Adriaenssens Eric[1], Van Outryve Alexandre[1], Magnez Romain[1], Thuru Xavier[1], Mysiorek Caroline[2], Gosselet Fabien[2], Tarhan Mehmet Cagatay[3], Dominique Collard Dominique[4,5], Orian-Rousseau Véronique[6], Le Bourhis Xuefen[1] & Toillon Robert-Alain[1].

A mimetic peptide of CD44v3 modulates TrkA signaling to rescues a Larotrectinib response in Triple Negative Breast Cancer.

Démarche expérimentale

En clinique, les inhibiteurs de la phosphorylation de TrkA (Larotrectinib et Entrectinib ; TKI) sont inefficaces chez les patients qui présentent une surexpression de TrkA. Or, le laboratoire a montré d'une part que TrkA est surexprimé dans les cancers du sein triple négatives (Lagadec *et al*., 2009) et d'autre part qu'il s'associe à CD44v3 pour augmenter son activité pro-oncogénique (Trouvilliez *et al*., 2022). L'objectif de cet article a été d'étudier le rôle de CD44v3 dans la résistance aux TKI. Pour se faire, nous avons tout d'abord étudié l'expression du *NGF, NTRK1 et CD44v3* dans les cancers du sein à l'aide de bases de données. Puis, nous avons comparé l'effet de TKI sur des cellules MDA-MB-231 surexprimant ou non TrkA. Pour expliquer l'inefficacité des TKI nous avons par Thermophorèse à Micro-échelle étudié l'effet de CD44v3 et d'un peptide mimétique de CD44v3 sur l'affinité de TrkA pour le NGF. Puis, par western blot, ligation de proximité et biosenseur FRET (RhoA) nous avons étudié l'effet de ce peptide mimétique de CD44v3 sur les voies canoniques (phospho-dépendante) et phospho-indépendantes de TrkA. Enfin, nous avons testé l'effet de ce peptide mimétique de CD44 sur la réponse aux TKI *in vitro* et *in vivo*.

Dans cet article nous montrons pour la première fois que l'axe NGF/TrkA/CD44v3 est impliqué dans la résistance aux inhibiteurs de la phosphorylation de TrkA (Larotrectinib et Entrectinib) dans les cellules cancéreuses mammaires qui surexpriment TrkA. De plus, nous avons pu mettre en évidence qu'en plus de la mise en place d'une signalisation non dépendante de la phosphorylation de TrkA, CD44v3 augmente l'affinité de TrkA pour le NGF. Enfin, nos travaux montrent qu'un peptide mimétique de CD44v3 qui module les signalisations de TrkA phospho-dépendantes et phospho-indépendantes restaure une réponse *in vitro* et *in vivo* au Larotrectinib.

Cet article sera soumis dans la revue : "Signal Transduction and Target Therapy"

A mimetic peptide of CD44v3 modulates TrkA signaling to rescues a Larotrectinib response in Triple Negative Breast Cancer.

Trouvilliez Sarah[1], Cicero Julien[1], Palma Martine[1], Lagadec Chann[1], Bourette Roland[1], Adriaenssens Eric[1], Van Outryve Alexandre[1], Magnez Romain[1], Thuru Xavier[1], Mysiorek Caroline[2], Gosselet Fabien[2], Tarhan Mehmet Cagatay[3], Dominique Collard Dominique[4,5], Orian-Rousseau Véronique[6], Le Bourhis Xuefen[1] & Toillon Robert-Alain[1].

[1] Univ. Lille, CNRS, Inserm, CHU Lille, UMR9020-U1277 - CANTHER - Cancer Heterogeneity Plasticity and Resistance to Therapies, F-59000 Lille, France

[2] Univ. Artois, UR 2465, Laboratoire de la Barrière Hémato-Encéphalique (LBHE), F-62300 Lens, France

[3] Univ. Lille, CNRS, Centrale Lille, Junia, Univ. Polytechnique Hauts-de-France, UMR 8520 -IEMN -Institut d'Electronique de Microélectronique et de Nanotechnologie, F-59000 Lille, France

[4] LIMMS/CNRS-IIS IRL2820, The University of Tokyo, Tokyo, Japan

[5] CNRS, IIS, COL, Univ. Lille SMMiL-E project, Lille, France

[6] Institute of Biological and Chemical Systems - Functional Molecular Systems (IBCS-FMS), Karlsruhe Institute of Technology (KIT), Hermann-von-Helmholtz-Platz 1, 76344, Eggenstein-Leopoldshafen, Germany.

Corresponding author: Prof. Robert-Alain Toillon, UMR9020-U1277 - CANTHER - Cancer Heterogeneity Plasticity and Resistance to Therapies, Bâtiment SN3, 3ème étage, Cité scientifique, Université de Lille, 59655 Villeneuve d'Ascq, France. Phone: +33 (0)3 20 43 65 59

E-mail : robert-alain.toillon@univ-lille.fr

Keywords: CD44v3, NGF, TrkA, interaction, resistance

ABSTRACT

Larotrectinib and Entrectinib have been approved by the FDA and other national agencies for cancer with fusions of *NTRK* that incode Trk proteins. NTRK-fusions are rare in cancers by contrast with TrkA overexpression. Unfortunately, in TrkA overexpressing patients these 2 inhibitors are not efficient. In this context, we studied the effects of Larotrectinib & Entrectinib on native and overexpressing TrkA breast cancer cells. We confirmed that TrkA overexpression induces a loss of sensitivity to Tki. As we had shown that the TrkA/CD44v3 complex could mediate TrkA phosphorylation-independent signaling, we tested the role of this complex in Tki resistance. We characterized the effects of the TrkA/CD44v3 complex blocking peptide and Tki. We observed that TrkA/CD44v3 peptide restores Larotrectinib and Entrectinib effect both *in vitro* and *in vivo*.

Introduction

TrkA is a prototypical member of the receptor tyrosine kinase family. The binding of NGF (Nerve Growth Factor) to TrkA induces a conformational change that allows its self-activation. The receptor is then phosphorylated on the tyrosine residues of the domain kinase and outside in its intracytoplasmic part. Tyrosine phosphorylation allows the recruitment of adapters which are in turn phosphorylated by TrkA and are the starting point of the underlying signaling pathways[1]. The effects produced by NGF in cells are pleiotropic and lead to cell growth, survival, differentiation and/or migration/invasion depending on the cellular context. In cancers, TrkA is an oncogene, its deregulation contributes to tumor transformation and progression. These pro-tumor effects have been studied and reported in many types of cancers such as breast, prostatic, pancreatic, oral squamous cell carcinoma, lung and ovarian carcinoma [2–5]. It has therefore been suggested that TrkA inhibition could be a gold standard therapy for cancers. More particularly, as the pro-tumoral effects of TrkA would be carried by its enzymatic activity, tyrosine kinase inhibitors have been developed. First compounds are derivatives of staurosporine (K252a; CEP-701 = Lestaurtinib). While they demonstrate efficacy *in vitro* and *in vivo* in pre-clinical models, they fail to demonstrate clinical efficacy. Several reasons have been suggested, such as the low bioavailability of Lestaurtinib, which prevents the effective therapeutic concentration from being reached[6], or the activation of intracellular survival pathways such as the NF-kB pathway[7]. A new generation of TrkA inhibitors has thus been developed for the treatment of tumors with TrkA fusion

transcripts. Interestingly, the efficiency of these new generation of TKIs (such as Larotrectinib), while very strong on tumors with these oncogenic fusions, is comparable to Lestaurtinib on tumors overexpressing TrkA[8]. Only a recent study by Kyker Snowman tends to show activity of Larotrectinib on MCF-10A cells transformed and rendered cancerous by overexpression of TrkA[9]. Thus, it appears that the oncogenic potential of TrkA kinase differs between models and influences the response to TrkA-targeted Tkis. In this context, we have shown that pro-tumoral effects of TrkA are not only dependent on its kinase activity. We have demonstrated that the association of TrkA and CD44 promotes pro-oncogenic signaling via RhoA independently of TrkA phosphorylation[10]. CD44 represents a heterogeneous family of proteins through the expression of numerous isoforms called variants. Thus, among the 20 exons of CD44, 12 are hyper-variable and can potentially produce more than 700 isoforms but not all combinations are expressed and only about twenty isoforms of CD44 have been observed[11]. The most abundant isoform is the CD44 standard transcript, but several variants of CD44 have been shown to be involved in cancer development and metastasis [12]. Recently, we have demonstrated that only CD44v3 binds on TrkA[13]. Moreover, we showed that a mimetic peptide of CD44v3 that impedes TrkA/CD44v3 association decreases RhoA activation, tumor growth and metastasis. We therefore hypothesized that the formation of the TrkA/CD44v3 complex could be partly responsible for intrinsic resistance to tyrosine kinase inhibitors targeting TrkA. In this article, we demonstrate that the TrkA/CD44v3 complex is indeed involved in Tki resistance. We demonstrate that the mimetic petide of the extracellular part of CD44v3 blocks a phospho-

independent pathway of TrkA implying CD44v3 and RhoA. Moreover, unexpectively we highlight that the mimetic petide of the extracellular part of CD44v3 favors TrkA-canonical signaling. Via these 2 mechanisms the mimetic petide of CD44v3 restores the oncogenic dependence on TrkA kinase and a Tki response.

Results

NGF, TrkA, CD44v3 are correlated to breast cancer aggressiveness and therapeutic failure.

In our previous studies, we have shown that TrkA/CD44v3 is specific to breast cancer tissues[13]. Breast cancer is an heterogeneous disease with different molecular profiles that conditioned the treatment response [14]. Using TGCA analysis, we investigated *NTRK1* expression and alterations in breast cancers. First, we compared its expression in patients with and without chemotherapy response, that is the base of breast cancer treatment strategy. We found that *NTRK1* is overexpressed in non-responder patients for any chemotherapy (complete response, Figure 1A; and relapse free, Figure Supp 1). *NTRK1* is also more expressed in Metastatic tissues than in Normal and Tumor (Figure 1B). Moreover, in the most aggressive and metastatic basal-like subtype, *NTRK1* is amplified and may result in more TrkA expression (Figure 1C). The basal-like subtype comprised around 70 % of triple negative breast cancer. In this subtype, *NTRK1* is overexpressed in non-responder patients (PFS). Moreover, both *NGF* and an isoform containing the variant 3 are more expressed in TNBC than in Normal tissues (Figure 1D & E). NGF/TrkA/CD44v3 signaling is associated with the triple negative breast cancer subtype. Targeting NGF/TrkA/CD44v3 may represent a new therapeutic strategy for TNBC.

As TCGA analyses show, and as we have previously reported, TrkA expression in cancer cells is lower than expression in tumors[15]. To analyze the behavior of TrkA inhibitors, it is thus preferable to compare the effects between native cells and cells overexpressing TrkA. To do so, we stably

established MDA-MB-231 cells overexpressing a HA-TrkA fusion protein. The effects of Larotrectinb and Entrectinib were compared on the clonogenicity of native MDA-MB-231 cells (Figure supp 2 A-B) and HA-TrkA overexpressing cells (Figure supp 2 C-F). Thus, we observed that Larotrectinib and Entrectinib decrease the growth of native MDA-MB-231 cells as early as 10 nM. However, no effect of the 2 TrkA inhibitors was observed on cells overexpressing HA-TrkA even for the highest doses (500 nM). Larotrectinib and Entrectinib inhibit TrkA phosphorylation in overexpressing cells for doses of around 250 nM (Figure 2 G-H) so this loss of efficacy was not due to a lack of effect on TrkA phosphorylation. Then, because TrkA/CD44v3 is associated to the activation of RhoA independentlywe have hypothesis that TrkA/CD44v3 may be involved in Tki failure.

Combinations of CD44v3 mimetic peptide 4 and TrkA Tkis abolished TrkA/CD44v3 association and RhoA activation.

Previously, we have demonstrated the existence of an interaction TrkA/CD44v3 and that a CD44v3 mimetic peptide (called P4) prevents the formation of the TrkA/CD44v3 complex. So, we have tested the effects of Larotrectinb and Entrectinib on the ability of CD44v3 mimetic peptide 4 to dissociate the complex by proximity ligation assays (Figure 2). PLA results showed that neither Larotrectinib nor Entrectinib inhibited NGF-mediated TrkA/CD44v3 complex formation. However, they confirmed that CD44v3 mimetic peptide 4 inhibits the formation of this complex. Furthermore, they demonstrated that treatment with Larotrectinib or Entrectinib did not decrease

the capacity of CD44v3 mimetic peptide 4 to inhibit the TrkA/CD44v3 complex.

We reported that biological effects Peptide 4 does not only rely on the inhibition of TrkA/CD44 association but also inhibit RhoA activation. So, activation of RhoA was measured by AB-FRET in MDA-MB-231 HA-TrkA (Figure 2 A-C). As observed NGF increased RhoA activation is inhibited by peptide 4. The mean donor peak intensity decreased from 1.42 (NGF) to 1.16 (NGF + peptide 4). Interestingly, both Larotrectinib and Entrectinib treatments inhibits RhoA activation by NGF (mean donor intensity are 1.15 and 1.21 respectively) indicating that NGF-induced RhoA activation is also partly dependent of TrkA phosphorylation. As a consequence, only a combination of both peptide 4 and TrkA Tki (Larotrectinib or Entrectinib) totally abolished RhoA activation.

Mimetic peptide of C-ter region of CD44v3 promotes NGF binding to TrkA extracellular domain, conformational change and it phosphorylation.

We previously demonstrated that under NGF treatment, the C-ter region of CD44v3 (called zone 4) interacts with TrkA via it LRR (Figure 3 A) [13]. Interestingly, in addition to IgC2, LRR has been shown to bind NGF when TrkA is not glycosylated (Figure 3 A). Using microscale thermophoresis, we investigated the effect of mimetic peptides of CD44v3 (P3 and P4; last 20 amino acid residues of the C-terminal part of exon v3) that bind on TrkA-ECD (Extracellular domain) on NGF affinity to TrkA (Figure 3 B). We obtain a Kd of 9.5 nM for NGF binding to TrkA-ECD (Figure 3 B). This value is in accordance

with values previously reported in the literature. In the presence of the peptide 3 the Kd is not significantly affected but in presence of de peptide 4 the Kd is about 0.640 nM (Figure 3 B). These results indicated that the mimetic peptide of the C-ter region of CD44v3, called P4, specificatly increase the affinity of NGF for TrkA. Hence, NGF binding to TrkA-ECD promotes it conformational change. So, by NanoDifferencial Scanning Fluorescence, we evaluated the effect of NGF binding on TrkA-ECD in presence of the mimetic peptide or no (Figure 3 C-E). In presence of the NGF, a second higher Ti is obtained (74.0), wich reflect the existence of a second conformation more stable in presence of the NGF than the TrkA-ECD alone (57.8; Figure 3 E). Then, we tested the effect of the mimetic peptide P4 on the conformational change of the extracellular part of TrkA. In presence of the P4, a second Ti is obtained higher than for TrkA/NGF (81.4 vs 74.0, Figure 3 E), indicating a more stable conformation of TrkA/NGF/P4 than TrkA/NGF. Then, we verified the functional consequences of this increase in affinity on TrkA in terms of receptor phosphorylation. Thus, we observed the effects of the mimetic peptide of CD44v3 P4 by western blot on the phosphorylation of TrkA on Tyrosine 674/675 residues of its kinase domain for low concentrations of NGF in PC-12 cells (Figure 3 F). PC-12 cells, that natively express high level of TrkA, we observe that the mimetic peptide of CD44v3 demonstrated a phosphorylation for a concentration of 0.05 nM whereas in the control conditions (control peptide) 0.5 nM NGF are required to induce TrkA phosphorylation (Figure Supp 4 A & B). So, the increase of affinity is correlated with an increase in TrkA phosphorylation. All together these data demonstrate that the mimetic peptide P4 blocks the TrkA/CD44 phospho-independent signaling and

promote TrkA canonical activation. Then, because TrkA is overexpressed in breast cancer in comparison to the cell lines, the same experiment was performed in 2 triple negative breast cancer cell lines overexpressing TrkA (Figure Supp 4 A & B). We can observe in presence of the mimetic peptide of CD44v3 a stronger phosphorylation for a concentration of 0.5 and 1 nM than in the control conditions (control peptide) in both MDA-MB-231 and BT-549 cells overexpressing TrkA (Figure Supp 4 A & B). In addition, a mimetic peptide of CD44 that binds on TrkA (called P3) but does not impede TrkA/CD44v3, has no effect on TrkA phosphorylation (Figure Supp 4 C). This observation demonstrated the specificity of the mechanism of action of the P4.

Combinaison of the mimetic peptide of the C-ter region of CD44v3 blocks TrkA/CD44v3 formation NGF-induced and TrkA phosphorylation.

Although we had demonstrated above (Figure sup 1) that the non-response to Larotrectinib and Entrectinib is not related to TrkA phosphorylation, we also verified that the inhibitors are effective in the presence of CD44v3 mimetic peptide 4 (Figure 4). We observed that NGF-induced phosphorylation in the presence or absence of CD44v3 mimetic peptide 4 is inhibited by the 2 TrkA Tkis. This indicated that although CD44v3 mimetic peptide 4 increases the affinity of NGF to TrkA and enhances TrkA phosphorylation, TrkA phosphorylation is still inhibited by Tki in presence of the mimetic peptide of CD44v3.

CD44v3 mimetic peptide rescues Larotrectinib effects on MDA-MB-231 TrkA overexpressing cells.

Effects of peptide 4, Larotrectinib and Entrectinib on tumor cell growth were assessed both *in vitro* by clonogenic assays (Figure 5 A-D) and *in vivo* using SCID mice xenograft model (Figure 5 E-H). As observed by clonogenic assay, we confirmed that Larotrectinib and Entrectinib alone do not inhibit MDA-MB-231 HA-TrkA overexpressing cells. Peptide 4 slightly decreased growth. Using CD44v3 mimetic peptide 4 with Larotrectinib or Entrectinib, we could observe that the co-treatment of CD44v3 mimetic peptide 4 and Larotrectinb significantly inhibits clonogenic growth compared to the two treatments used alone. However, the combination of CD44v3 mimetic peptide 4 and Entrectinib has no advantage over CD44v3 mimetic peptide 4 or Entrectinib alone. After demonstrating the effects *in vitro*, we decided to confirm that the combination of CD44v3 mimetic peptide 4 plus Larotrectinib is more effective in vivo on a tumor overexpressing TrkA. For this purpose, MDA-MB-231 cells overexpressing HA-TrkA were injected into the flanks of SCID mice and the survival was assessed as a function of time and treatments (Figure 5 E-H). Thus, the probability of survival was estimated by performing Kaplan-Meyer analysis. In a first experiment, we wanted to confirm that the combination of peptide 4 treatment plus Larotrectinib is more effective than the treatments alone (Figure 5 E-G). In this experiment, the median survival is estimated to be 39 days in control condition (PBS), 41 and 42 days respectively for CD44v3 mimetic peptide 4 and Larotrectinib treatment alone and 51 days for the treatment combination. These differences are significantly different. Then, because TrkA overexpression promote brain metastasis, we have tested the

effect in vitro and in vivo of another TrkA inhibitor that cross the blood brain barrier, the Entrectinib (Figure 6 A-E). The combinaison Entrectinib+P4 reduce the number of clonogenicity in vitro (Figure 6 A & B). Moreover, by PCR of the human microglobuline we study the presence of micrometastasis in the lung and the brain of mice. For the lung, nor the P4 or the Entrectinib alone or in combinaison demonstrate an effect. By contrast, both P4 and Entrectinib slightly decrease (50 % vs 66 % in the control group) the number of mice harboring a brain metastasis. Moreover, the combinaison P4+Entrectinib permits a reduction of 50 % of the brain metastasis (Figure 6 E).

Discussion

Growth factors and their receptors are important oncogenes in cancer. The management of patients has been revolutionized by the development of targeted therapies that target their activation[16]. Our TCGA analysis confirmed previous observation that TrkA are overexpressed in breast cancer[15] and we show here more precisely in triple negative breast cancer. Moreover, TCGA analyses also correlated TrkA expression with a potent oncogene in triple negative breast cancer increasing metastasis and therapy resistance which are two markers of poor prognosis. It would therefore be interesting to target TrkA and NGF in triple negative breast cancer. Then the use of TrkA tyrosine kinase inhibitors would be an option for TBNC therapies. Nevertheless, it has been shown that TrkA Tki inhibitors are only effective on tumors with an oncogenic fusion of TrkA kinase[17]. In this study, we confirm that TrkA inhibitors are effective on TrkA phosphorylation but also, we demonstrate

even more strikingly that the oncogenic activity of TrkA is not summarized as in the fusion proteins to its kinase activity. Interestingly, these kinase-independent effects of RTK are also reported for strong oncogene like EGFR and would also explain the anti-EGFR therapies Failures in tumors [18]. These results also correlate with the way that Larotrectinib is efficient only for fusion kinase expression and not to TrkA overexpression[17,19]. Thus, in the experiments conducted by loxo-oncology, they use a consecutively active TrkA mutant known to induce cell proliferation. This mutant is deleted at the IgC2 region. However, as Arevalo et al[20] point out, this mutant does not recapitulate all the biological effects of TrkA. Thus, the deletion of the extracellular domain of TrkA has a differential phenotype which implies that the other domains of TrkA have an influence in the phenotype. More specifically, we previously demonstrated that the LRR region is involved in CD44v3 binding to TrkA and induced a phospho-independent TrkA signaling[13]. Here, we show that the binding of CD44v3 to TrkA does not only act independently of its phosphorylation but also increases its phosphorylation. The demonstration of the effect of CD44v3 on TrkA in terms of affinity is a mechanism of action of CD44v3 unknown to date. Indeed, to the best of our knowledge, the pro-tumorigenic effects of CD44v3 have been reported to be dependent on the binding of its ligands (Hyaluronic acid, osteopontin) or of extracellular matrix molecules affinities for heparin (laminin, fibronectin)[21,22]. CD44v3 can also interact to form aggregates in the metastasis by homophilic interaction between two cancer cells[23]. Concerning its action on growth factors and their receptors, it has been shown that it binds heparin binding growth factors to present them to their receptors [24].

Interestingly, for NGF, ligand-presentation model does not fit perfectly. Actually, heparin-binding domain does not bind NGF by contrast with others growth factors and we previously reported no binding of NGF on CD44v3[13,25]. It suggests that CD44v3 may increase NGF affinity to TrkA following its interaction with TrkA.

We have also described that Larotrectinib and Entrectinib, induce stabilization of the TrkA/CD44v3 complex at the plasma membrane at 30 minutes. These results are in agreement with observations we also made using a TrkA kinase dead and/or Lestaurtinib[10,13] and with the work of Berg et al. showing that K252a inhibits 60 % of NGF-induced TrkA endocytosis[26]. The stabilization of the TrkA receptor at the membrane and the alteration of its intracellular traffic is not trivial. As observed for other RTKs, mutations on residues altering their traffic reinforce their oncogenic potential and may contribute to target therapy failure[27,28]. It is not excluded that a stabilization of TrkA by the Tki will do the same. Especially since this is accompanied, as we have observed, by the maintenance of the activation of a signaling independent of the phosphorylation of TrkA which is mediated by the RhoA pathway. RhoA signaling has been shown to promote tumor growth and development in triple negative breast cancer cells[29]. It is also possible that the stabilization of the TrkA/CD44v3 complex reinforces CD44v3-specific signaling that may be involved in therapy resistance. Indeed, CD44v3 has been shown to be involved in cisplatin resistance in head and neck cancers, for example[30].

Interestingly, our study also shows that the effects of Larotrectinib and Entrectinib on breast cancer cells are different. It is possible that the effects of Entrectinib may be dependent on its action on other kinases because it is less

specific than Larotrectinib and also inhibits ROS or ALK for instance[31]. However, we observe here a lack of efficacy of Entrectinib but not Larotrectinib in cells overexpressing TrkA. So, it suggests that Entrectinib inefficiency is related to the TrkA receptor. Interestingly, in cancers that have a TrkA fusion protein, and are therefore dependent on TrkA kinase activity, Entrectinib also shows lower efficacy[32]. To explain the different actions of Larotrectinib and Entrectinib, it is possible that the two inhibitors, although they block TrkA kinase activity, but because they have slightly different binding to TrkA[33], induce in addition to the kinase inhibition a different conformational change resulting in a differential recruitment of signaling proteins to the kinase domain and/or to adjacent intracellular regions. Such discrete changes in phenotype have been observed for point mutations in this region[34]. Only the exhaustive description of the conformational changes between Larotrectinib and Entrectinib as well as the identification of the differentially regulated interactants will provide answers to this question.

Taken together, our results show that targeting TrkA in triple-negative breast cancer is an interesting option but further molecular description of this receptor is needed. It is also important for these future developments to measure both the oncogenic effects of TrkA linked to its kinase and those that are independent of it. As we show with the combination of a CD44v3 mimetic peptide and Larotrectinib treatment, this consideration could lead to more effective therapeutic solutions in TrkA overexpressing cancers.

Conclusion

Our results demonstrate an original non-genetic mechanism of Tki resistance *via* a co-receptor. CD44v3 binding on TrkA promotes 1) a phospho-independent signaling though RhoA 2) NGF affinity to TrkA and it phosphodependent signaling. In breast cancer cells overexpressing TrkA, a peptide that impedes phospho-independent pathway and increases TrkA phosphorylation rescues a response to Larotrectinib. Therefore, unravel CD44v3 regulation of TrkA signaling paves the way on new therapeutic strategies against TrkA.

Abbreviations

BCA: Betweenness Centrality Analysis

BSA: Bovine Serum Albumin

CFP: Cyan Fluorescent Protein

CD44v: CD44 variant

DMEM: Dulbecco Minimum Essential Medium

EGFR: Epidermal Growth factor

EMEM: Earle's salt Minimum Essential Medium

FBS: Fetal Bovine Serum

FRET: Fluorescence Resonance Energy Transfer

IgC2 : Immunoglobulin-like C2-type

LRR: leucin Rich Region

MST: MicroScale Thermophoresis

NGF: Nerve Growth Factor

RTK : Receptor Tyrosine Kinase

TCGA : The Cancer Genome Atlas

Tki : Tyrosine kinase inhibitor

TNBC : Triple Negative Breast Cancer

Consent for publication

All the participants of this study consented to the publication of this work.

Availability of data and material

The data and materials generated in this study are available upon reasonable request from the corresponding author:

Prof. Robert-Alain Toillon, Université de Lille, Faculté des Sciences et Technologies, UMR CNRS 9020- INSERM U1277 - CANTHER - Cancer Heterogeneity Plasticity and Resistance to Therapies, Bâtiment SN3, 3ème étage, Cité scientifique, 59655 Villeneuve d'Ascq, France. Phone: +33 (0)3 20 43 65 59. E-mail: robert-alain.toillon(at)univ-lille.fr

Competing interests

The authors declare that they have no competing interests.

Fundings

This work was supported by “La ligue contre le cancer” (« comité du Nord, du Pas de Calais et de l’Aisne »), cancéropole Nord-Ouest, I-site “Université Lille Nord-Europe” and Contrat de Plan Etat-Région CPER Cancer 2015-2020. ST was funded by “conseil régional Hauts de France”, Lille University and La ligue contre le cancer.

Conflict of interest

The authors declare that they have no competing interests.

Author Contribution

ST, JC, PM, LC, BR, EC, AVO, RM, XT & R-AT conceived experiments, performed experiments and collected data. ST, JC, EA, RB, and R-AT

designed and performed *in vivo* experiments. FG, CM, XT, CL, XLB, V-OR and R-A T provided funding acquisition, resources and supervised research project. ST and R-AT wrote the manuscript in consultation with XT, VO-R.

References

1. Reichardt L. F. Neurotrophin-regulated signalling pathways. *Philos. Trans. R. Soc. B Biol. Sci.* **361**, 1545–1564 (2006).

2. Descamps S. *et al.* Nerve Growth Factor Stimulates Proliferation and Survival of Human Breast Cancer Cells through Two Distinct Signaling Pathways *. **276**, 17864–17870 (2001).

3. Licitra F. *et al.* New Insights and Emerging Therapeutic Approaches in Prostate Cancer. *Front. Endocrinol. (Lausanne).* **13**, 1–11 (2022).

4. Blondy S. *et al.* Neurotrophins and their involvement in digestive cancers. *Cell Death Dis.* **10**, (2019).

5. Rolfo C. & Raez L. New targets bring hope in squamous cell lung cancer: Neurotrophic tyrosine kinase gene fusions. *Lab. Investig.* **97**, 1268–1270 (2017).

6. Marshall J. L. *et al.* Phase I trial of orally administered CEP-701 , a novel neurotrophin receptor-linked tyrosine kinase inhibitor. 31–37 (2005).

7. Holz M. S. *et al.* Induction of Endoplasmic Reticulum Stress by Sorafenib and Activation of NF- B by Lestaurtinib as a Novel Resistance Mechanism in Hodgkin Lymphoma Cell Lines. *Mol. Cancer Ther.* **12**,

173–183 (2013).

8. Dolgin E. Loxo TRK inhibitor data wows oncologists. *Nat. Biotechnol.* **35**, 694–695 (2017).

9. Kyker-Snowman K. *et al.* TrkA overexpression in non-tumorigenic human breast cell lines confers oncogenic and metastatic properties. *Breast Cancer Res. Treat.* **179**, 631–642 (2020).

10. Aubert L. *et al.* NGF-induced TrkA / CD44 association is involved in tumor aggressiveness and resistance to lestaurtinib. **6** (2015).

11. Ponta H., Wainwright D. & Herrlich P. Molecules in focus The CD44 protein family. *Int. J. Biochem. Cell Biol.* **30**, 299–305 (1998).

12. Primeaux M., Gowrikumar S. & Dhawan P. Role of CD44 isoforms in epithelial-mesenchymal plasticity and metastasis. *Clin. Exp. Metastasis* (2022). doi:10.1007/s10585-022-10146-x

13. Trouvilliez S. *et al.* Direct interaction of TrkA / CD44v3 is essential for NGF-promoted aggressiveness of breast cancer cells. *J. Exp. Clin. Cancer Res.* 1–21 (2022). doi:10.1186/s13046-022-02314-4

14. Lehmann B. D. *et al.* Identification of human triple-negative breast cancer subtypes and preclinical models for selection of targeted therapies Find the latest version : Identification of human triple-negative breast cancer subtypes and preclinical models for selection of targ. **121**, 2750–2767 (2011).

15. Lagadec C. *et al.* TrkA overexpression enhances growth and metastasis of breast cancer cells. *Oncogene* **28**, 1960–1970 (2009).

16. Saraon P. *et al.* Receptor tyrosine kinases and cancer: oncogenic mechanisms and therapeutic approaches. *Oncogene* **40**, 4079–4093 (2021).

17. FDA Report, LOXO-oncology.

18. Thomas R. & Weihua Z. Rethink of EGFR in cancer with its kinase independent function on board. *Front. Oncol.* **9**, 1–16 (2019).

19. Hempel D. *et al.* Antitumor Activity of Larotrectinib in Esophageal Carcinoma with NTRK Gene Amplification . *Oncologist* **25**, 881–886 (2020).

20. Arevalo J. C. *et al.* TrkA Immunoglobulin-Like Ligand Binding Domains Inhibit Spontaneous Activation of the Receptor. *Mol. Cell. Biol.* **20**, 5908–5916 (2000).

21. Bourguignon L. Y. W., Singleton P. A., Zhu H. & Diedrich F. Hyaluronan-mediated CD44 Interaction with RhoGEF and Rho Kinase Promotes Grb2-associated Binder-1 Phosphorylation and Phosphatidylinositol 3-Kinase Signaling Leading to Cytokine (Macrophage-Colony Stimulating Factor) Production and Breast Tumor Progress. **278**, 29420–29434 (2003).

22. Bourguignon L. Y. W. *et al.* Hyaluronan Promotes CD44v3-Vav2 Interaction with Grb2-p185HER2 and Induces Rac1 and Ras Signaling during Ovarian Tumor Cell Migration and Growth. *J. Biol. Chem.* **276**, 48679–48692 (2001).

23. Liu X. *et al.* HHS Public Access. **9**, 96–113 (2020).

24. Szatanek R. & Baj-Krzyworzeka M. Cd44 and tumor-derived extracellular vesicles (Tevs). possible gateway to cancer metastasis. *Int. J. Mol. Sci.* **22**, 1–17 (2021).

25. Martino M. M., Briquez P. S., Ranga A., Lutolf M. P. & Hubbell J. A. Heparin-binding domain of fibrin(ogen) binds growth factors and promotes tissue repair when incorporated within a synthetic matrix. *Proc. Natl. Acad. Sci. U. S. A.* **110**, 4563–4568 (2013).

26. Berg M. M., Sternberg D. W., Parada L. F. & Chao M. V. K-252a inhibits nerve growth factor-induced trk proto-oncogene tyrosine phosphorylation and kinase activity. *J. Biol. Chem.* **267**, 13–16 (1992).

27. Kon S., Kobayashi N. & Satake M. Altered trafficking of mutated growth factor receptors and their associated molecules. *Cell. Logist.* **4**, e28461 (2014).

28. Schmidt-Arras D. & Böhmer F. D. Mislocalisation of Activated Receptor Tyrosine Kinases – Challenges for Cancer Therapy. *Trends Mol. Med.* **26**, 833–847 (2020).

29. Pillé J. Y. *et al.* Anti-RhoA and Anti-RhoC siRNAs inhibit the proliferation and invasiveness of MDA-MB-231 breast cancer cells in vitro and in vivo. *Mol. Ther.* **11**, 267–274 (2005).

30. Torre C., Wang S. J., Xia W. & Bourguignon L. Y. W. Reduction of hyaluronan-CD44-mediated growth, migration, and cisplatin resistance in head and neck cancer due to inhibition of Rho kinase and PI-3 kinase signaling. *Arch. Otolaryngol. - Head Neck Surg.* **136**, 493–501 (2010).

31. Liu D., Offin M., Harnicar S., Li B. T. & Drilon A. Entrectinib: An orally available, selective tyrosine kinase inhibitor for the treatment of NTRK, ROS1, and ALK fusion-positive solid tumors. *Ther. Clin. Risk Manag.* **14**, 1247–1252 (2018).

32. Carlson J. J. *et al.* Comparative Effectiveness of Larotrectinib and Entrectinib for TRK Fusion Cancer. *Am. J. Manag. Care* **28**, S26–S32 (2022).

33. Jiang T. *et al.* Development of small-molecule tropomyosin receptor kinase (TRK) inhibitors for NTRK fusion cancers. *Acta Pharm. Sin. B* **11**, 355–372 (2021).

34. Amodeo R. *et al.* Molecular insight on the altered membrane trafficking of TrkA kinase dead mutants. *Biochim. Biophys. Acta - Mol. Cell Res.* **1867**, 118614 (2020).

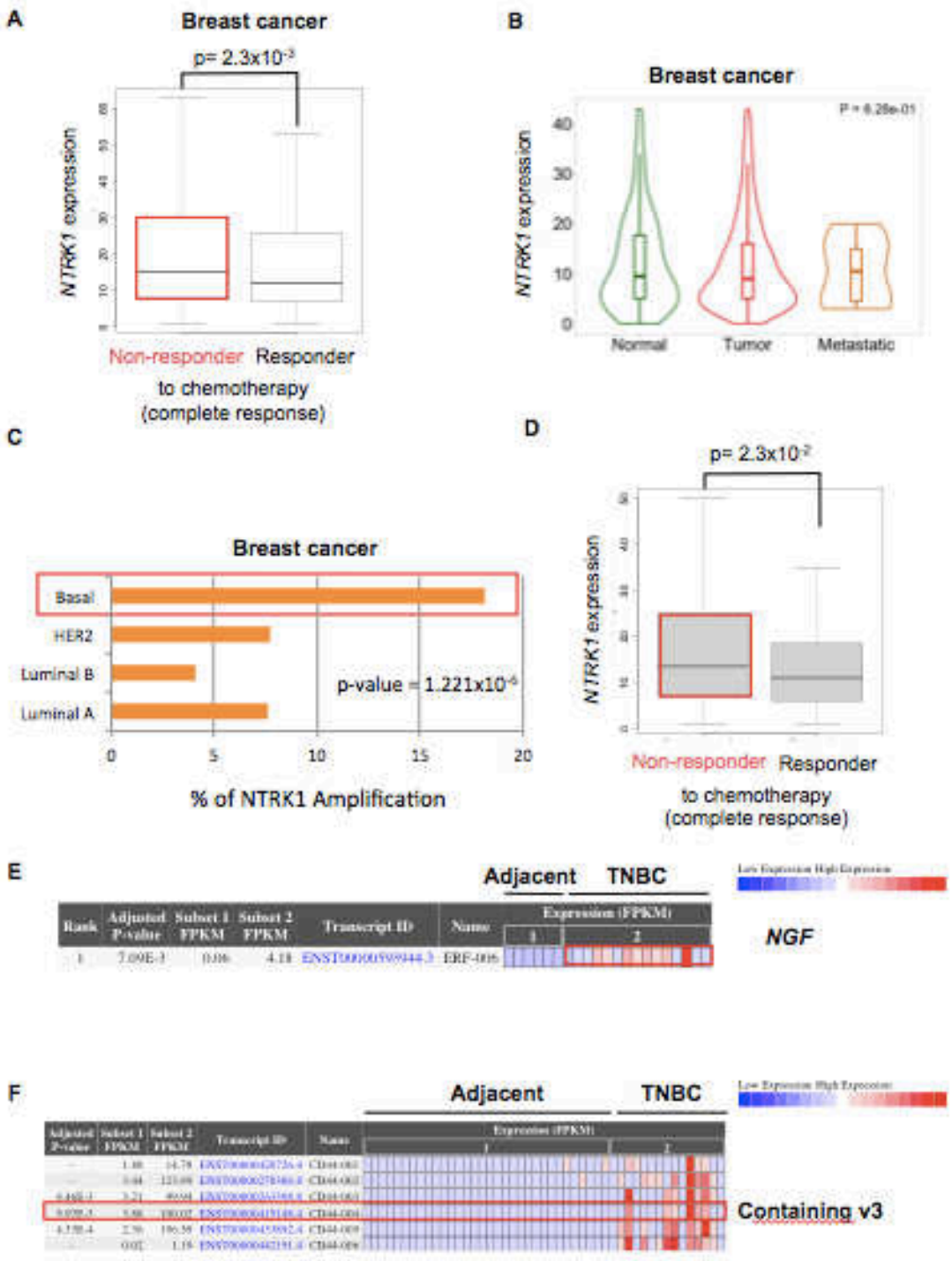


Figure 1: Correlation of TrkA, NGF and CD44v3 expression in breast cancers. TCGA analyses of NTRK1 expression revealed correlation between NTRK1 with resistance of chemotherapy **(A)**, metastasis **(B)** and Basal like subtype **(C)**. NGF **(D)** and CD44v3 **(E)** were correlated with Triple Negative breast cancer subtype.

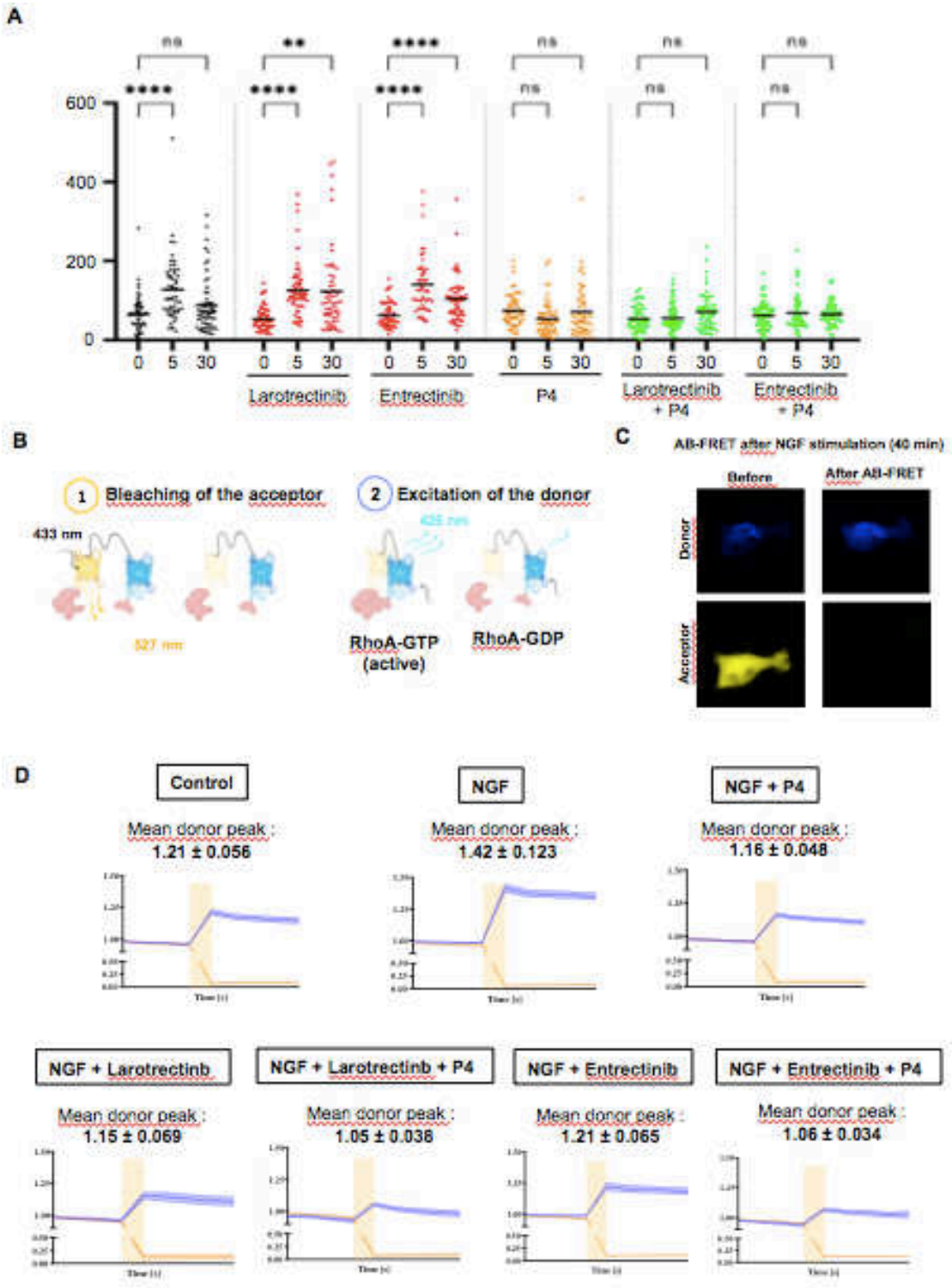
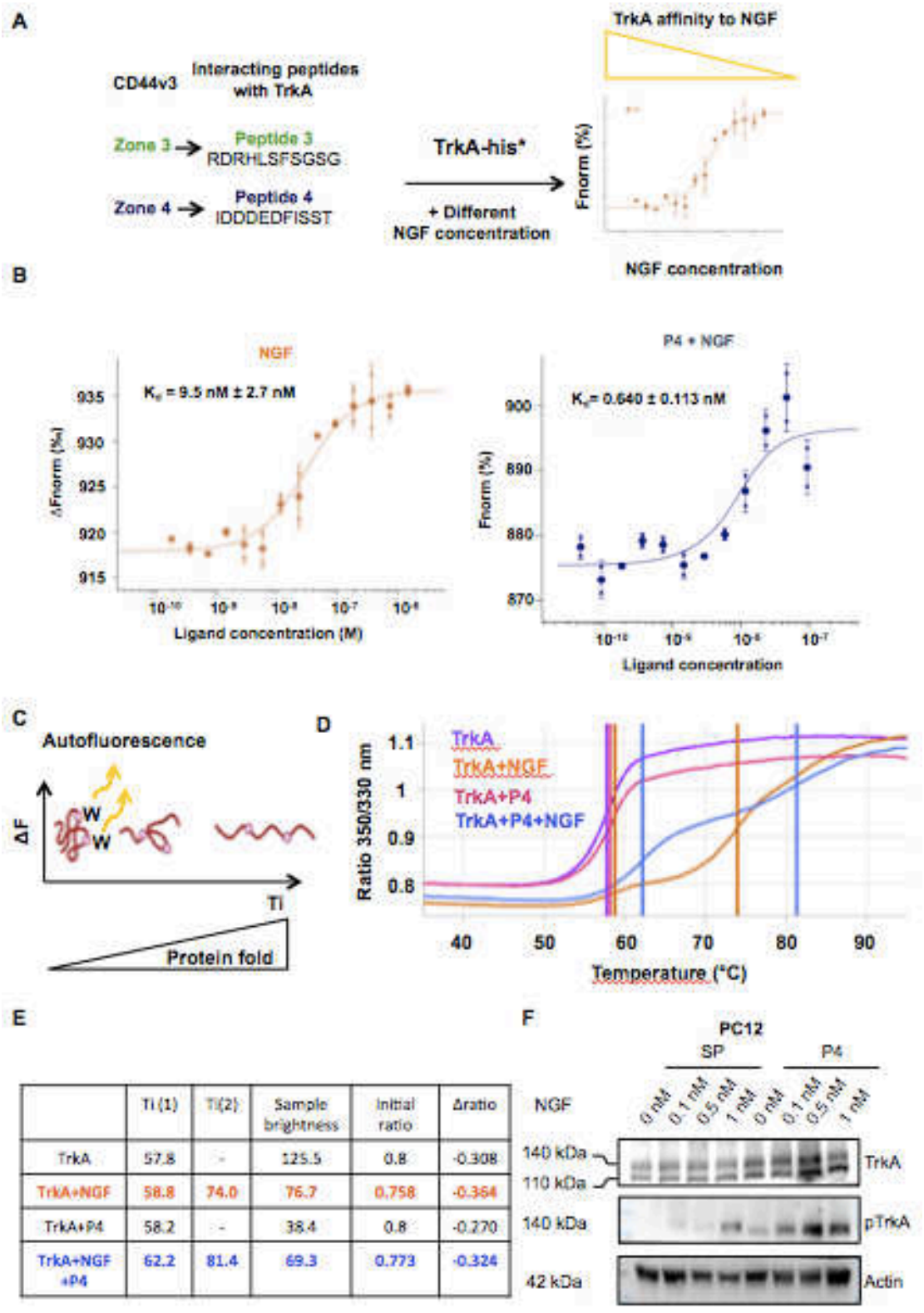


Figure 2: Cter region of CD44v3 impedes TrkA/CD44v3 and RhoA activation during TKI treatment. Effects of CD44v3 mimetic peptide 4 (IDDEDFISST) on TrkA/CD44v3 complexes formation visualized by PLA in presence of Larotrectinib or Entrectinib **(A).** Proximity ligation assay were

performed after 1 hour of LOXO-101 treatment (250 nM) and/or 30 minutes of CD44v3 mimetic peptide (P4) treatment (50 nM) following by 0, 5 and 30 minutes of NGF treatment (16 nM). Pictures were representative of PLA signal detected. Quantification of red spots was done by Image J software (30 fields per condition of three different experiments, random acquisition). Schematic representation of biosensor photobleaching **(B)**; Representative pictures of fluorescence channel before and after AB-FRET in MDA-MB-231 cells overexpressing TrkA **(D)**; Mean donor peak levels after AB-FRET in MDA-MB-231 TrkA overexpressing cells. Statistical analyses were performed with one-way ANOVA followed by Bonferroni's post-test. Error bars represent S.E.M. *** $p<0.001$, **, $p<0.01$, * $p < 0.05$, ns: non-significant.



	Ti (1)	Ti(2)	Sample brightness	Initial ratio	Δratio
TrkA	57.8	-	125.5	0.8	-0.308
TrkA+NGF	58.8	74.0	76.7	0.758	-0.364
TrkA+P4	58.2	-	38.4	0.8	-0.270
TrkA+NGF +P4	62.2	81.4	69.3	0.773	-0.324

Figure 3: Cter region of CD44v3 increases NGF affinity for TrkA. Affinities were measured in microscale thermophoresis. **(A)** Schematic representation of the principle of the experiment **(B)** Schematic representation of the

experiments of microscale thermophoresis. The experiments were performed with the ECD of TrkA tagued his and a mimetic CD44v3 peptide **(blue)** or only NGF **(orange)**. **(C)** Schematic representation of the principle of the NanDSF assay. (**D-E)** NanoDSF was performed with the ECD of TrkA and a mimetic CD44v3 peptide or only NGF. **(F)** Western blot of pTrkA in PC12 cells.

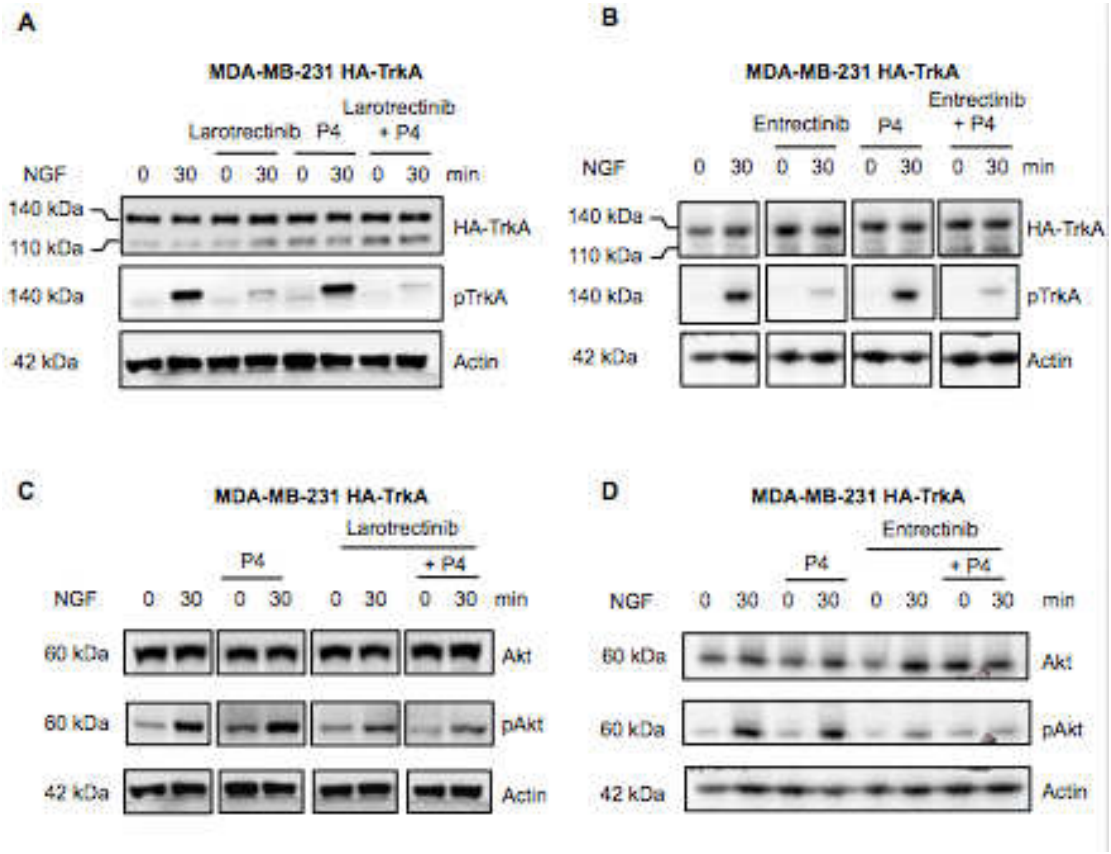
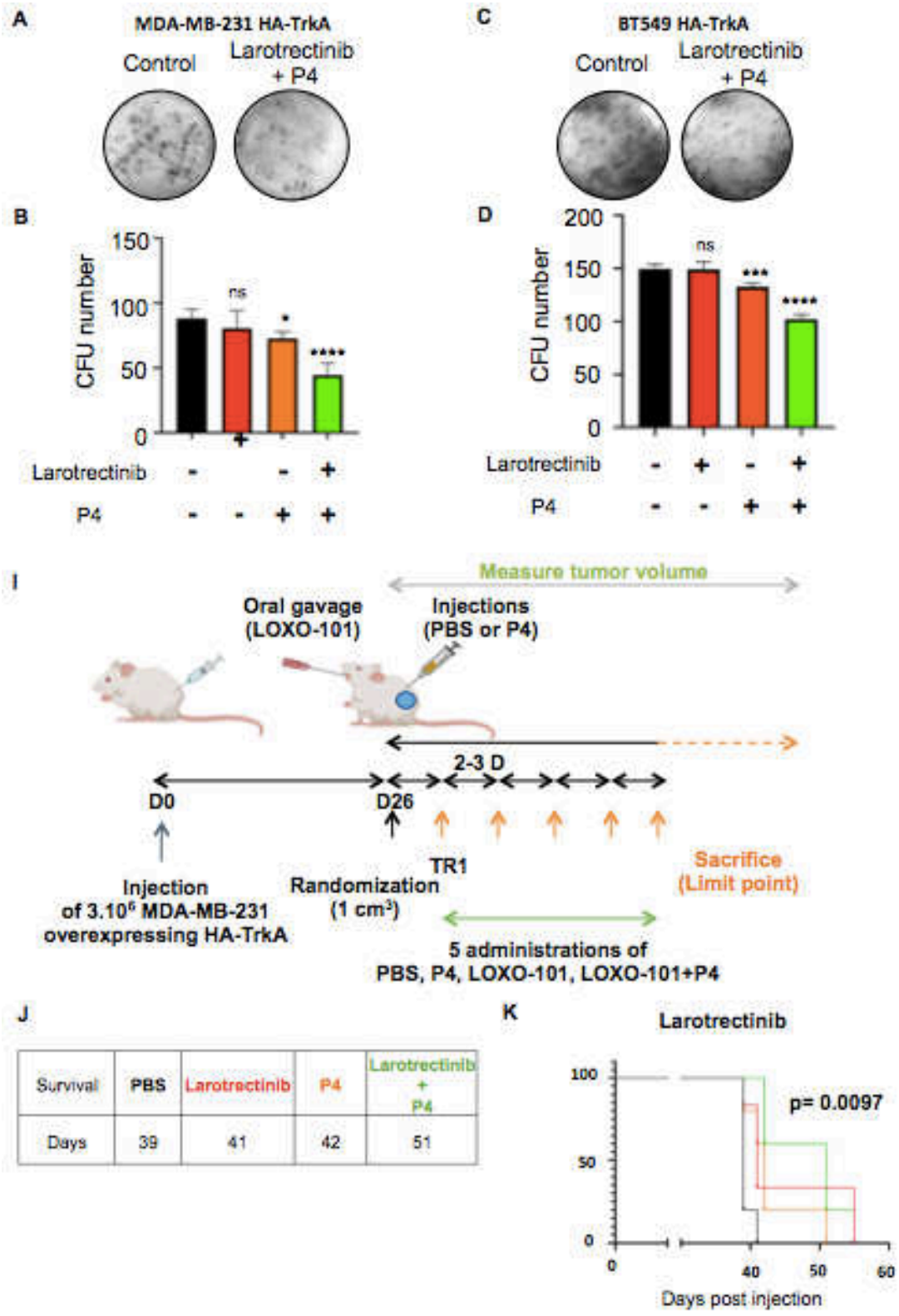


Figure 4: The mimetic peptide of CD44v3 does not modified response to larotrectinb or entrectinib. Effects of mimicking CD44v3 peptide 4 on TrkA phosphorylation were showed by western blotting in different HA-TrkA overexpressing cells **(A-D)**. Western blot results were representative of 3 independent experiments.



Survival	PBS	Larotrectinib	P4	Larotrectinib + P4
Days	39	41	42	51

Figure 5: CD44v3 mimetic peptide 4 restores sensitivity to larotrectinib in cells overexpressing TrkA. Clonogenic growth of MDA-MB-231 HA-TrkA cells in the presence of peptide 4 and Larotrectinib (**A-D**). Effects of Peptide 4/Larotrectinb and Peptide 4/Entrectinib treatment combination on survival of

SCID mice xenografted with MDA-MB-231 HA-TrkA cells **(J-K)**. Statistical analyses were performed with one-way ANOVA followed by Bonferroni's post-test (**A-D**) or Log-rank test (**E-H**). Error bars represent S.E.M. *** p<0.001, **, p<0.01, * $p < 0.05$, ns: non-significant.

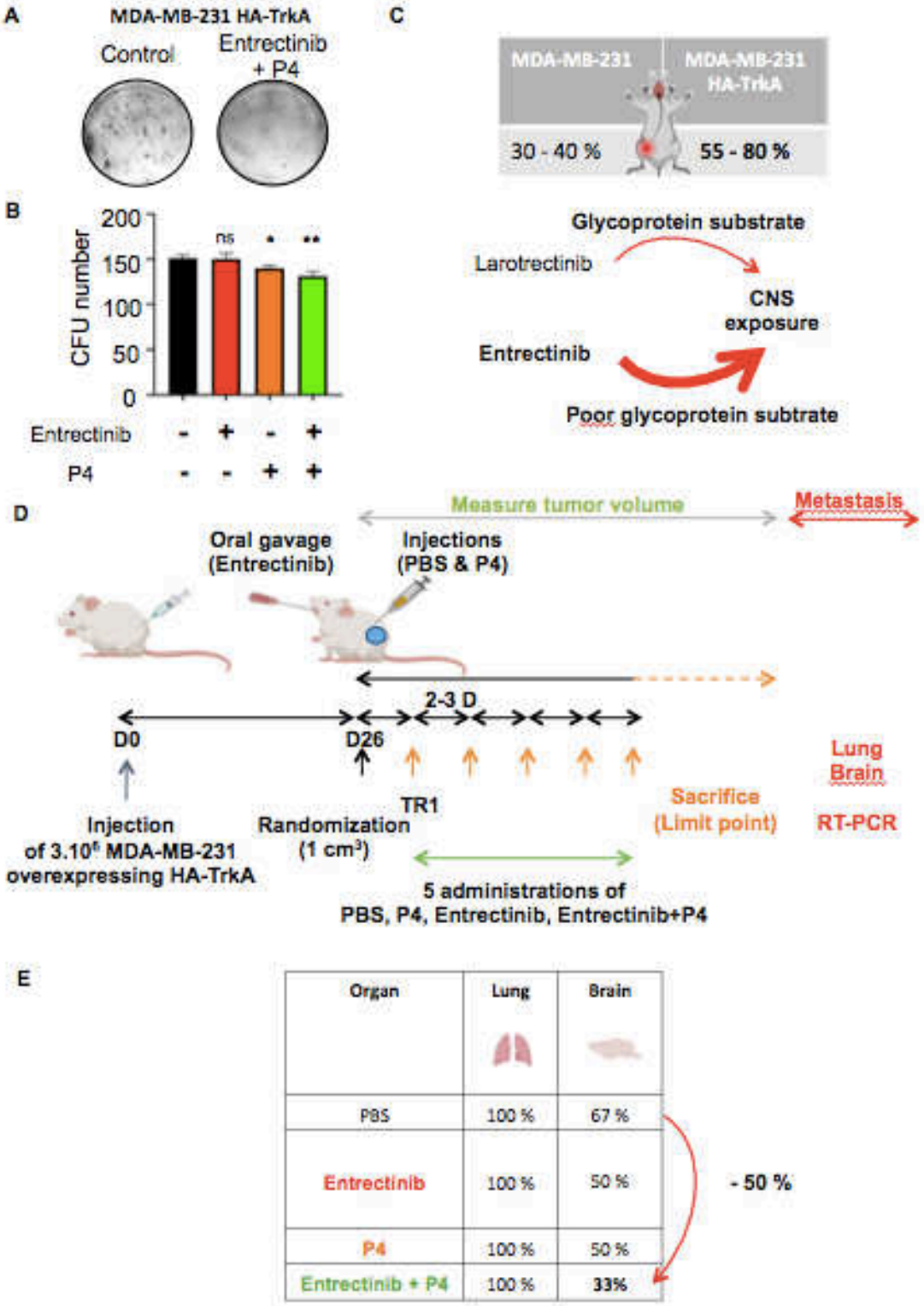


Figure 6: CD44v3 mimetic peptide 4 restores sensitivity to entrectinib in cells overexpressing TrkA. Clonogenic growth of MDA-MB-231 HA-TrkA cells in the presence of peptide 4 and Entrectinib (**A, B**). Effects of Peptide 4/Larotrectinb (**E, F**) and Peptide 4/Entrectinib (**G, H**) treatment combination

on survival of brain metastasis in SCID mice xenografted with MDA-MB-231 HA-TrkA cells. Statistical analyses were performed with one-way ANOVA followed by Bonferroni's post-test (**A-D**). Error bars represent S.E.M. *** $p<0.001$, **, $p<0.01$, * $p < 0.05$, ns: non-significant.

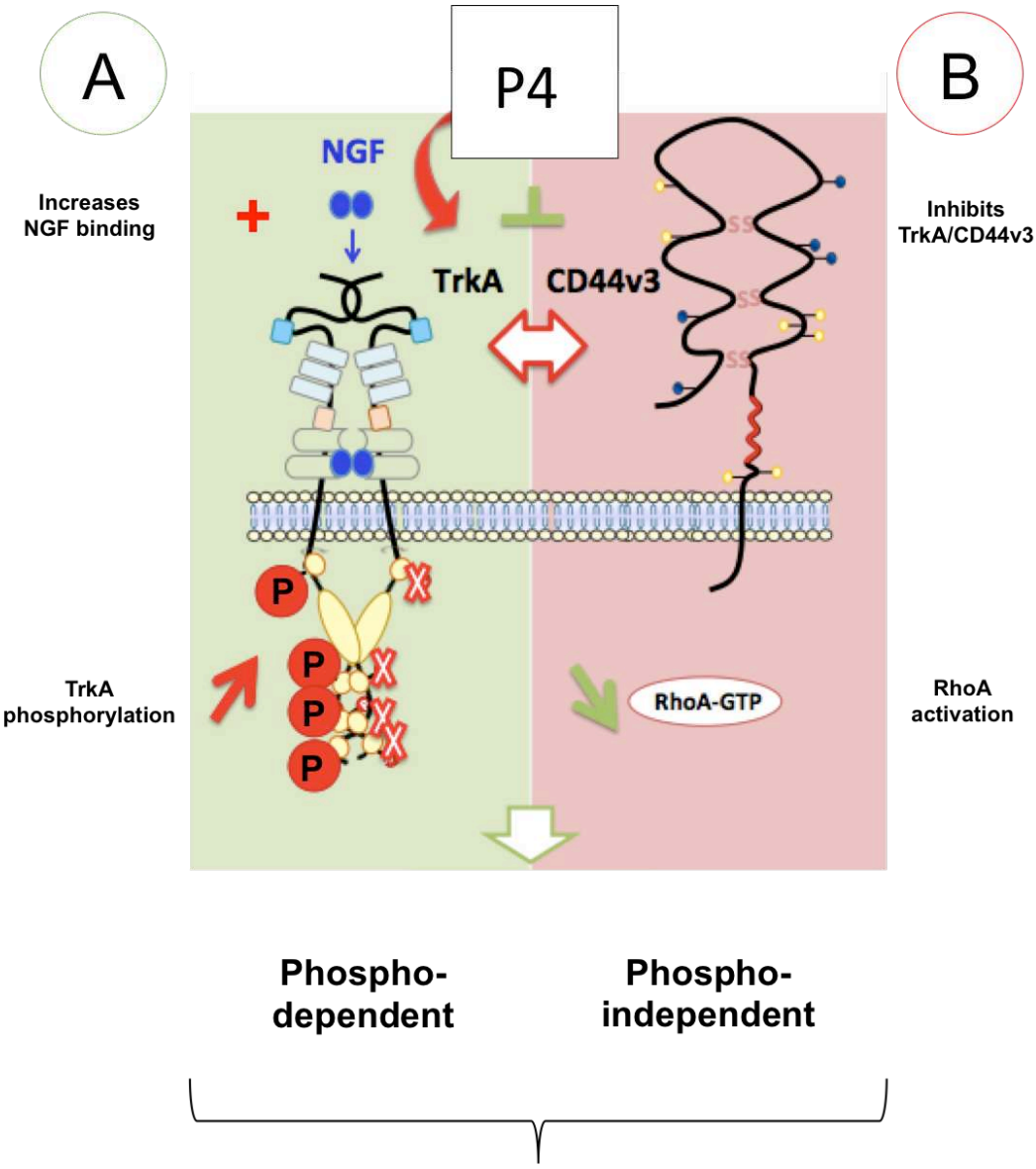


Figure 7: CD44v3 increases both TrkA phospho-dependent and phospho-independent pathways. NGF induces TrkA/CD44v3 interaction. This interaction enhances the affinity of TrkA for NGF **(A)** and also induces a TrkA phosphorylation-independent signaling pathway that passes through p115RhoGEF/RhoA/Rock **(B)**. Peptide 4 acts as CD44v3 to increase the affinity of TrkA for NGF but inhibits TrkA/CD44v3 complex formation and TrkA phosphorylation-independent signaling. By blocking TrkA phosphorylation-

independent signaling, Peptide 4 restores sensitivity to Larotrectinib.

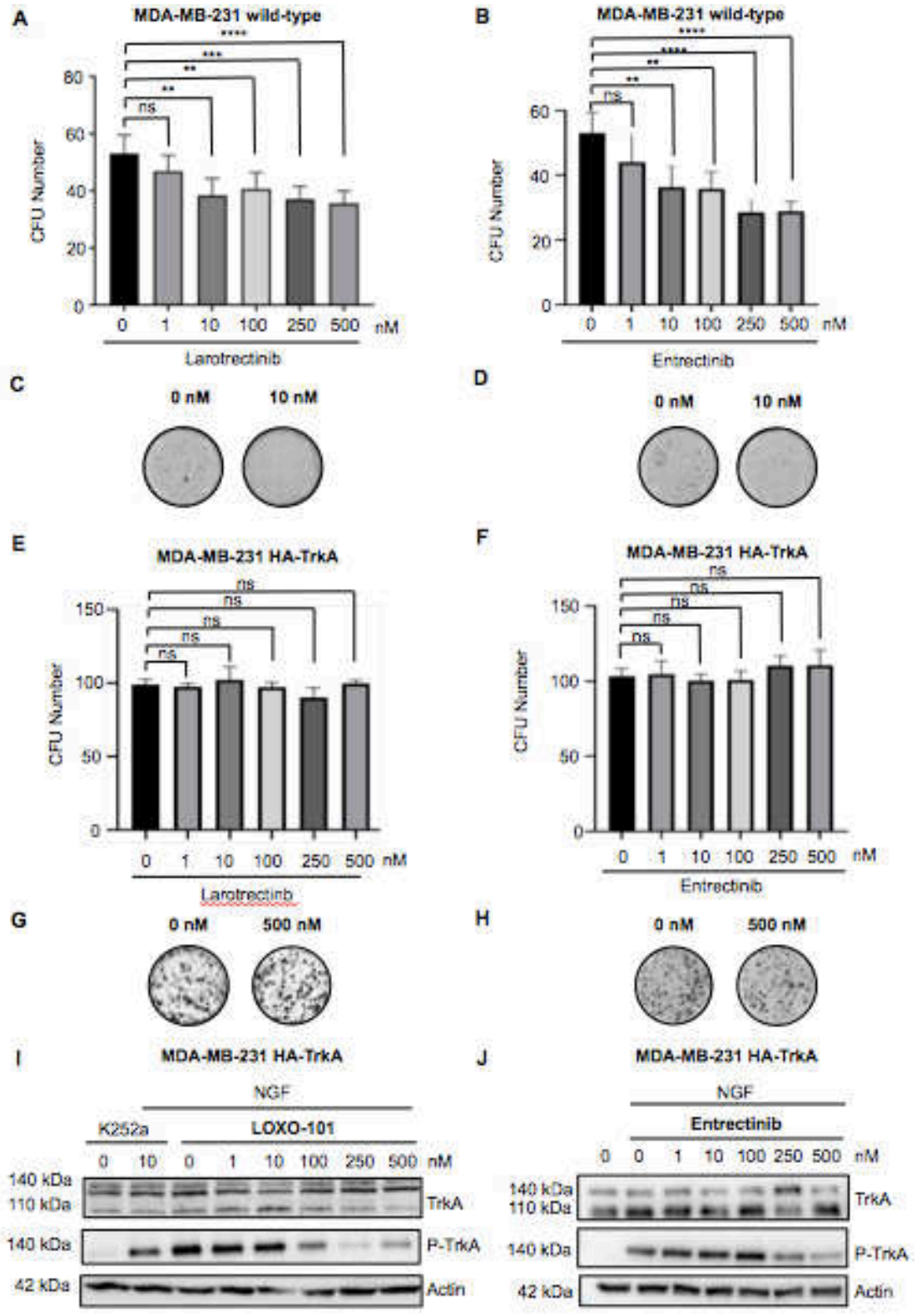


Figure sup 1: Larotrectinib and Entrectinib lose their efficiencies TrkA overexpressing MDA-MB-231 cells. Clonogenic cell growth were assessed

in native MDA-MB231 cells in presence of increasing doses (0 to 500 nM) of Larotrectinib **(A)** or entrectinib **(B)** and in TrkA overexpressing cells **(C, D)**. representative pictures of colony forming unit **(E, F)**. Western blot analyses of TrkA and pTrkA (Y674, Y675) **(G, H)**. Statistical analyses were performed with one-way ANOVA followed by Bonferroni's post-test. Error bars represent S.E.M. *** p<0.001, **, p<0.01, * $p < 0.05$, ns: non-significant.

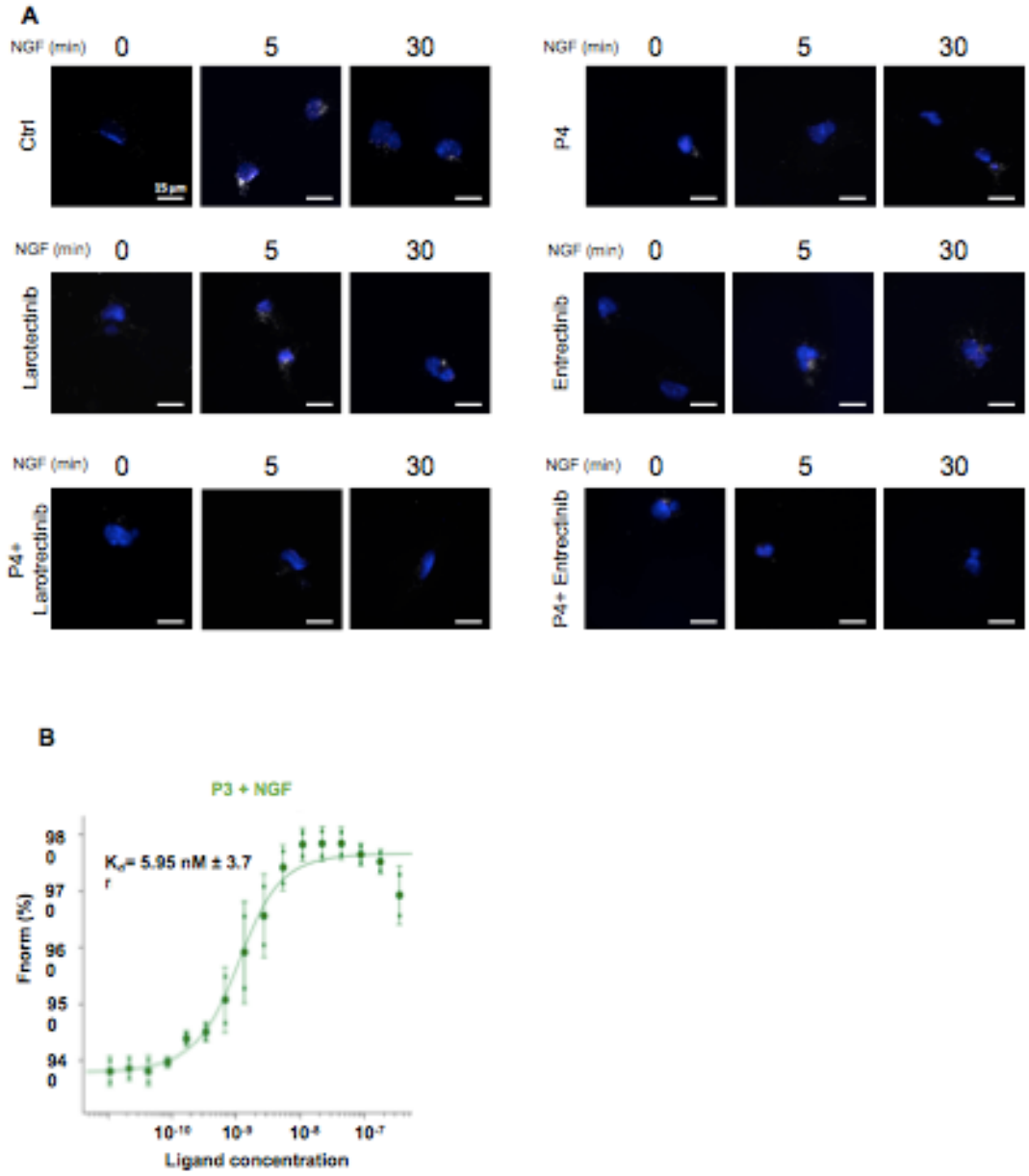


Figure sup 3: The mimetic peptide of the Cter region blocks TrkA/CD44v3 and promote TrkA phosphorylation specificatly. (A) Representative images of TrkA/CD44v3 PLA. **(B)** MST of the ECD of TrkA with the mimetic peptide of CD44v3 P3.

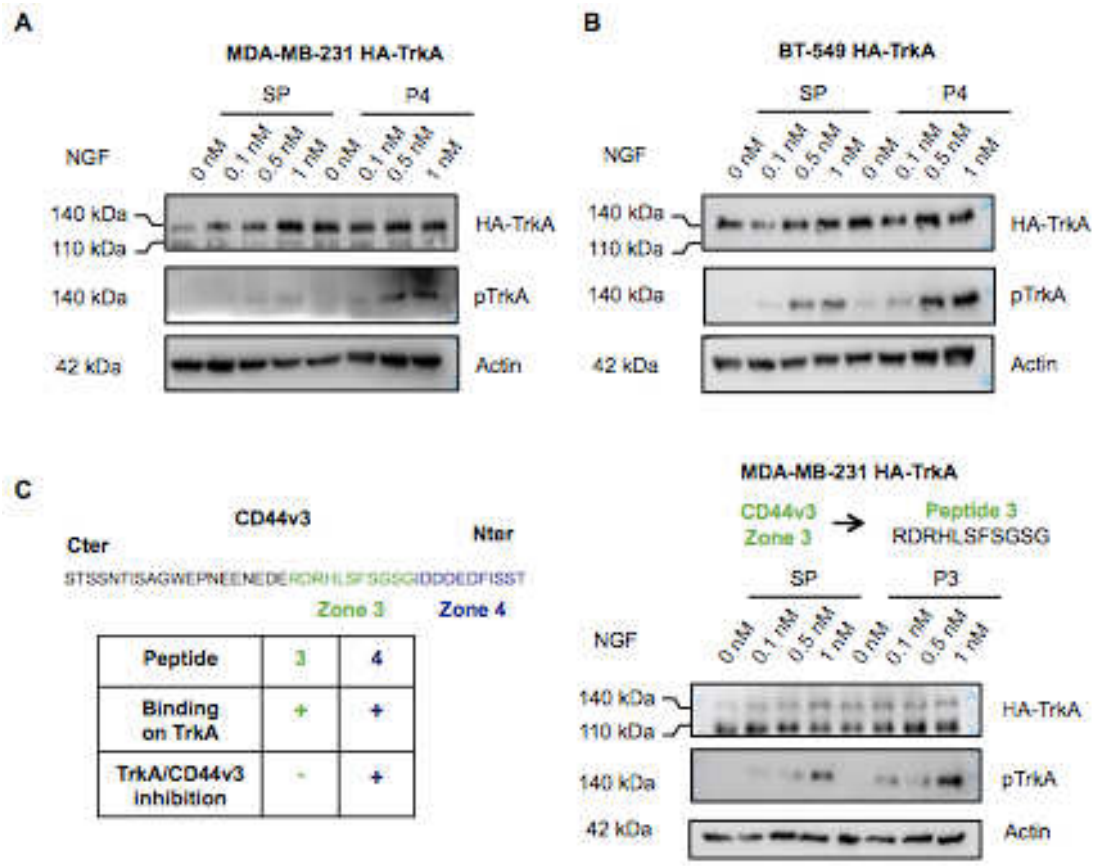


Figure sup 4: The mimetic peptide of the Cter region of CD44v3 specifically promote TrkA phosphorylation. Effects of mimicking CD44v3 peptide 4 on TrkA phosphorylation were showed by western blotting in different HA-TrkA overexpressing cells **(A-B)**. By contrast, the mimicking CD44v3 peptide 3 (zone containing the HS) does not modify TrkA phosphorylation as showed by western blot **(C)**. Western blot results were representative of 3 independent experiments

METHODS

Cell culture

PC12 and MDA-MB-231 breast cancer cell line were purchased from the American Type Culture Collection (ATCC, Manassas, VA, USA). COS-7 cell line (African green monkey kidney) was obtained from Pr. V. Orian-Rousseau (Karlsruhe Institute of Technology [KIT], Karlsruhe, Germany). MDA-MB-231, COS-7 cells overexpressing HA-TrkA were obtained after transfection (JetOptimus) of a p-Display HA-TrkA and selection with Geneticin. MDA-MB-231 cells were cultured in Eagle's Minimal Essential Medium (EMEM) supplemented with 10% inactivated Fetal Bovine Serum (FBS) (Hyclone, Belgium), 1% non-essential amino acids, 40 UI/ml Penicillin/Streptomycin and 40 µg/mL Gentamycin. The cells were incubated at 37°C in 5% CO_2-humidified atmosphere. COS-7 cells were cultured with Dulbecco's minimal essential medium (DMEM) supplemented with 10% inactivated fetal bovine serum (FBS) (HyClone, Belgium), 1% nonessential amino acids, 40 UI/ml of penicillin/streptomycin and 40 µg/mL of gentamycin. PC12 cells were cultured with Dulbecco's minimal essential medium (DMEM) supplemented with 10% inactivated fetal bovine serum (FBS) (HyClone, Belgium), 5% inactivated horse serum, 100 UI/ml of penicillin/streptomycin and 2 mM L-Glutamine. Before treatment, cells were rinsed twice with trypsin/EDTA, left for 24 h in culture medium supplemented with 10% FBS, then starved in medium supplemented with 0.1% FBS 4 h and treated with recombinant human β-NGF (16 nM) (Alomone Labs, Israel), at the indicated times.

Protein extraction

Subconfluent cells were washed twice with ice-cold PBS, and lysed (40 mM HEPES pH 7.5, 120 mM NaCl, 1 mM EDTA, 1% Triton X-100, 0.1% SDS, 10% glycerol, 10 mM sodium pyrophosphate, 50 mM sodium fluoride, 1.5 mM sodium orthovanadate, and 1 mM PMSF, supplemented with a protease inhibitor cocktail) (Sigma-Aldrich, France). Cell lysates were then clarified by centrifugation (6000 x g, 10 min, 4°C) and stored at -80°C until analysis. The supernatants were collected and protein concentration was determined using the BCA assay (Sigma-Aldrich).

Western blotting

Cell lysates proteins were separated by SDS-PAGE and transferred onto PVDF membranes (GE Whatmann, United Kingdom). The membranes were blocked with 5% bovine serum albumin (BSA) in Tris-buffered saline-0.1% Tween 20 (TBS-T) (w/v) (1h, RT) and immunoblotted (overnight, 4°C). The membranes were washed Tris-buffered saline-0.1% Tween 20 (TBS-T) (w/v) 5 times (5 min) then probed with horseradish peroxidase-conjugated secondary antibody (Jackson Immunoresearch, Beckman Coulter, France). SuperSignal West Pico Substrate (Thermo Scientific, Belgium). Chemiluminescence was detected with Fusion FX analyzer (Vilber, France). The antibodies used in this study were: anti-actin (A2066, Sigma-Aldrich), anti-TrkA (# 30697, Cell Signaling), anti-phospho-TrkA (# 4621, Cell Signaling Technologies) and anti-HA (901501, Biolegend, Germany).

In situ proximity ligation assay (PLA)

Cells (6,000 cells per well) were grown on acid-washed eight-well glass slides (Thermo Scientific) in the appropriate medium supplemented with 10% FBS for 24 h. Cells were starved (1h) and treated with the TKI (Larotrectinib or Entrectinib; 250 nM). Thirty minutes later, the CD44v3 mimetic peptide 4 (P4) is added (50 ng/mL) and after 30 minutes NGF treatments are performed. At the end of the experiment, paraformaldehyde (PAF)-fixed cells were rinsed twice with PBS and non-specific site were saturated by incubation with bovine serum albumin (BSA, 4%, 1 h, 20°C) followed by overnight incubation with primary antibodies. PLA was performed following the manufacturer's instructions in the assay kit (Duolink PLA; Sigma–Aldrich). Thirty fields per condition were analyzed using a fluorescence microscope (Eclipse TiU; Nikon, Japan). The PLA signals (red dots) were automatically quantified using ImageJ software (with an in-house-developed plug-in). After PLA, statistical analyses were performed using GraphPad Prism software to determine the mean dot intensity in the cells.

Microscale thermophoresis (MST)

MST was conducted as previously reported (Trouvilliez et al, JECCR, 2022). NT.115 A Pico MST instrument (Nano Temper Technologies GmbH) was used. The mix was incubated at RT in the dark for 30 min. Next, as previously described his-TrkA (ECD) was labeled using a Monolith His-Tag Labeling Kit with RED-Tris-NTA (Nano Temper). The mix was incubated at RT in the dark for 30 min. Then, the his-TrkA was mixed with an extract of COS-7 expressing CD44v3-labeled protein (CD44v3-His) or no (control) at a 1:1 ratio. At least,

this mix was diluted with different concentrations of NGF (Alomone). Data analyses were done using MO Control Software (Nano Temper).

Clonogenic cell growth

MDA-MB-231 HA-TrkA cells (250 cells/mL) were seeded into 6 plate wells (2% FBS medium; 2 mL/well). When the cells attached (within 3 h), they were treated with the TKI (Larotrectinib or Entrectinib). Thirty minutes later, the CD44v3 mimetic peptide 4 (P4; 50 ng/mL) is added or no (control) and cells were incubated for 24 h. The next day, a second-round treatment was performed. Three days later, the medium was changed, and the cells were incubated for another 2-3 days. Then, the medium was removed, and the cells were washed twice (PBS 1×), fixed (4% PAF for 30 min at RT), colored (violet crystal 2%; 30 min; RT) and washed twice (distilled water). The colonies were counted and representative pictures of one well were taken.

Acceptor Photobleaching- Forster Resonance Energy Transfer (AB-FRET).

MDA-MB-231 HA-TrkA cells were seeded in a type I collagen coated coverglass (Lab-Tek®) (100 µg/mL; Corning) and transfected with pBabe-Puro-RhoA FLARE.sc biosensor. This was a gift from Klaus Hahn (Addgene plasmid # 12602; http://n2t.net/addgene:12602; RRID, Addgene_12602). Prior acquisition, cells were starved in fresh EMEM containing 0.1% FBS and no phenol red and maintained at 37°C and with 5% CO_2 in an incubation chamber installed under a microscope. Images were collected using a ZEISS LSM 880 confocal microscope. The emission of the CFP, FRET and YFP

channels was recorded and the fluorescence emission ratios were computed using ImageJ software.

Tumor xenograft growth in immunodeficient SCID mice

MDA-MB-231 HA-TrkA cells (3 x 10^6) were subcutaneously injected into the flank of seven-week-old female SCID mice. One month after the injection, mice were randomized into 4 groups (n=5 or 6), oral gavages (Entrectinib 30 mg/kg or 50 mg/kg Larotrectinib) and peritumoral injections with the CD44v3 mimetic peptide 4 (P4; 20 μg/mice) were performed five times or no (Control) at 3 days intervals. Tumor volume was determined throughout the experiment by measuring the length (l) and width (w) and calculated as p/6 x 1 x w x (1+w)/2. Animals were sacrificed at similar tumor size after isoflurane anesthesia to determine overall survival.

Statistical analysis

Statistics were performed using GraphPad Prism 5.01 software. Analyses were performed using a two-way ANOVA with Bonferroni's post-test.

Article 3

Trouvilliez S, Cicero J, Corbet C, Aubert L, Van Outryve A, Lagadec C, Giraud S, Mysiorek C, Gosselet F, Tarhan Mehmet C, Collard D, Le Bourhis X and Toillon R-A.

P115RhoGEF directly interacts with TrkA to induced breast cancer cell migration.

Démarche expérimentale:

L'équipe a précédemment montré que TrkA/CD44 active une signalisation non dépendante de la phosphorylation qui repose sur : P115RhoGEF, RhoA, ROCK1. Afin d'inhiber le recrutement de P115RhoGEF nous avons étudié les modalités de son recrutement. CD44 est connu pour recruter P115RhoGEF nous avons donc inhibé l'association TrkA/CD44 à l'aide du peptide mimétique de CD44v3 et de siARN. De façon intéressante, CD44v3 n'est pas nécessaire au recrutement de P115RhoGEF. Par mutagenèse dirigée de TrkA nous avons identifié un résidu impliqué dans le recrutement de p115RhoGEF. De plus, par immunoprécipitation de TrkA et Biolayer Interférométrie nous avons montré le caractère directe et phospho-indépendant de cette association. En retour, nous avons par mutagenèse dirigée étudié les déterminants moléculaires de p115RhoGEF impliqués dans son recrutement par TrkA. Enfin, l'implication de cette interaction dans la survie/adhérence et la migration a été étudié à l'aide d'un peptide mimétique de p115RhoGEF couplé à une séquence TAT et des cellules exprimant un TrkA muté.

Ainsi dans cet article nous montrons pour la première que, contrairement à ce qui avait été décrit dans la littérature, CD44 n'est pas responsable du recrutement de p115RhoGEF par TrkA. De plus, TrkA interagit directement avec p115RhoGEF indépendamment de la phosphorylation de TrkA. Cette interaction repose sur la Tyr-490 de TrkA et 10 acides aminés de la « hinge region » de p115RhoGEF. Cette interaction contribue à la migration induite par le NGF de cellules cancéreuses mammaires triple négative surexprimant TrkA mais pas leur survie/adhérence.

Cet article sera soumis dans la revue : "Cellular and Molecular Life Science"

P115RhoGEF directly interacts with TrkA to induced breast cancer cell migration

Trouvilliez Sarah[1], Cicero Julien[1], Corbet Cyril[1,2], Aubert Léo[1,2], Van Outryve Alexandre[1], Lagadec Chann[1], Giraud Stéphane[3], Mysiorek Caroline[4], Gosselet Fabien[4], Tarhan Mehmet Cagatay[5,6], Collard Dominique[6,7], Le Bourhis Xuefen[1] & Toillon Robert-Alain[1].

[1] Univ. Lille, CNRS, Inserm, CHU Lille, UMR9020-U1277 - CANTHER - Cancer Heterogeneity Plasticity and Resistance to Therapies, F-59000 Lille, France

[2] Pole of Pharmacology and Therapeutics (FATH), Institut de Recherche Expérimentale et Clinique (IREC), UCLouvain, B-1200 Brussels, Belgium.

[3] Center for Drug Discovery and Development. Léon Bérard Center, F-69373 Lyon, France

[4] Univ. Artois, UR 2465, Laboratoire de la Barrière Hémato-Encéphalique (LBHE), F-62300 Lens, France

[5] Univ. Lille, CNRS, Centrale Lille, Junia, Univ. Polytechnique Hauts-de-France, UMR 8520 -IEMN -Institut d'Electronique de Microélectronique et de Nanotechnologie, F-59000 Lille, France

[6] LIMMS/CNRS-IIS IRL2820, The University of Tokyo, Tokyo, Japan

[7] CNRS, IIS, COL, Univ. Lille SMMiL-E project, Lille, France

Corresponding author : Prof. Robert-Alain Toillon, INSERM U908 "Cell Plasticity & Cancer", Bâtiment SN3, 3ème étage, Cité scientifique, Université Lille 1, 59655 Villeneuve d'Ascq, France. Phone: +33 (0)3 20 43 65 59; Fax: +33 (0)3 20 43 40 38

E-mail: robert.toillon@univ-lille1.fr

Keywords: CD44, NGF, TrkA, p115RhoGEF

ABSTRACT

P115RhoGEF is a GTP/GDP exchanger for Rho proteins. RhoA conformational change and activation promotes migration and metastasis in various cancers including triple negative breast cancer. In triple negative breast cancer, TrkA/CD44 recruits P115RhoGEF. Targeting P115RhoGEF recruitment by TrkA/CD44 appears as a new putative way to inhibit migration in triple negative breast cancer. Surprisingly, we found that CD44 is not necessary for P115RhoGEF recruitment by TrkA. Moreover, we demonstrated that p115RhoGEF interacts directly with TrkA. TrkA/P115RhoGEF interaction engages Tyr-490 of TrkA and 10 amino-acid region of p115RhoGEF (GPMSLESLAP). At least we showed that TrkA/P115RhoGEF interaction is involved in NGF-induced migration of triple negative breast cancer.

Introduction

P115RhoGEF is a member of the RhoGEF (Rho Guanine Exchange Factor) family. These proteins are characterized by their ability to exchange GTP/GDP for Rho proteins [1]. This family is divided into 2 subfamilies: a small subfamily of DOCK proteins (11 members) which has no similarity with the other subfamily of Dbl-like proteins (70 members) which present a Dbl Homology (DH) domain of which p115RhoGEF (DH: amino acids 416 to 605). In addition to this DH domain, p115RhoGEF has 2 other functional domains: an RH domain (RGS Homology; amino acids 41-232) and a PH domain (Plextrin Homology; amino acids 647-760). These 3 domains work together to allow its recruitment at the plasma membrane, its activation and its interaction and activation of Rho proteins[2]. High expression of RhoA and RhoC have been described to be involved in metastasis in different cancers including breast cancer [3,4]. Moreover, in the triple negative breast cancer cell line MDA-MB-231 inhibition of RhoA or RhoC block proliferation, migration and tumor growth *in vivo*[5]. RhoA and RhoC has been described to be able to transformed primary cells, including mammary cells[6,7]. Moreover, both RhoA and RhoC are involved in metastasis but they are proposed to have not exactly the same role in this process. RhoC has been proposed to be a key regulator of tumor vascularization whereas RhoA promote migration. This difference may be the consequences of their different targets[8]. RhoA promotes migration *via* the ROCK proteins. Hence, we have previously shown that TrkA/CD44 NGF-induced promotes P115RhoGEF/Rho/ROCK signaling[9]. Moreover, we recently depicted that TrkA/CD44v3 (variant 3) interaction

activates RhoA independently of TrkA phosphorylation to promote migration and metastasis *in vivo* [10]. In addition, we previously demonstrated that P115RhoGEF is recruited by TrkA/CD44 and contribute to migration/invasion NGF-induced of triple negative breast cancer (TNBC) overexpressing TrkA [9]. Hence, TNBC relapse are often due to distant metastasis[11]. Moreover, chemotherapy that is the gold standard for the treatment of this type of breast cancer has been shown to promote metastasis[12]. In this context, targeting P115RhoGEF recruitment by TrkA/CD44v3 appears as a putative way to avoid migration of triple negative breast cells and so relapse due to metastasis. Bourguignon *et al.* reported that hyaluronic acid biding to CD44 induces binding of CD44 to p115RhoGEF[13]. In order to determine whether CD44 or CD44v3 recruits P115RhoGEF to the TrkA/CD44v3 complex in the presence of NGF, invalidations of CD44 or CD44v3 were performed. Unexpectedly, after invalidation of CD44 or its variant 3, p115RhoGEF is always found in association with TrkA. *Ex cellulo* interferometry experiments on an intracellular TrkA peptide and a recombinant p115RhoGEF protein confirmed the direct association between these two proteins. This association is independent of TrkA phosphorylation and is responsible for NGF-induced migration. It involves the juxtamembrane region of TrkA and the hinge region of the p115RhoGEF protein. Finally, the use of a blocking peptide mimetic of the p115RhoGEF binding region induces both decreased survival and migration of MDA-MB-231 cells.

RESULTS

CD44v3 is not necessary for P115RhoGEF recruitment by TrkA

As described elsewhere, P115RhoGEF is associated with CD44v3 [13] (Figure 1A). To validate that NGF also induces p115RhoGEF recruitment to CD44, TrkA/CD44v3 complex formation was inhibited using a CD44v3 mimetic peptide (peptide 4) (Trouvilliez et al, JECCR, 2022) (Figure 1B). Thus, after immunoprecipitation of TrkA, the presence of p115RhoGEF is revealed in western blot after 0, 5 and 30 minutes of NGF treatment in TrkA-overexpressing MDA-MB-231 cells. Under control conditions (without peptide 4), the results confirmed that P115RhoGEF is in a protein complex with TrkA. Interestingly, dissociation of the TrkA/CD44v3 complex did not alter the association of p115RhoGEF with TrkA indicating that CD44v3 would not be involved in binding p115RhoGEF to the TrkA/CD44v3 complex. To confirm these results, invalidations of CD44v3 (Figure 1C) and CD44 (Figure 1D) by siRNA were performed. Thus, when CD44v3 or CD44 expression was inhibited, NGF still slightly induced P115RhoGEF recruitment to TrkA. All these observations made by immunoprecipitation experiments suggested that P115RhoGEF is associated with TrkA in a basal manner and it seems that in the presence of NGF there is a slight increase in its association with TrkA. Moreover, this association was independent of the presence of CD44v3 or any other form of CD44.

TrkA directly binds P115RhoGEF independently of TrkA phosphorylation.

As we previously described, the formation of the TrkA/CD44v3 complex is independent of TrkA phosphorylation [10]. As P115RhoGEF is known be recruited and interact with signaling proteins at the plasma membrane [14], a point mutation in the juxtamembrane region of TrkA was done on the Tyrosine 490 residue (Figure 2A). By immunoprecipitation, we observed that the mutation of tyrosine 490 to phenylalanine of TrkA induces a loss of P115RhoGEF recruitment either at basal level (0 min) or induced by NGF treatment (5 min). To confirm this result, inhibitors of TrkA phosphorylation (K252a or LOXO-101) were used (Figure 2 B, C). By immunoprecipitation of HA-TrkA, it was observed that P115RhoGEF is recruited even if TrkA phosphorylation is inhibited whether in the presence of K252A (Figure 2A) or LOXO-101 (Figure 2B). These results suggested that phosphorylation of TrkA is not necessary for the interaction, but that mutation of tyrosine 490 is sufficient to lose the interaction. To test this hypothesis, we performed an interaction study on recombinant proteins by biolayer interferometry (Figure 2 D, E). For this purpose, a peptide corresponding to the juxtamembrane region of TrkA was used encompassing the tyrosine-490 residue (QGHIIENPQ**Y**FSDAC). In this peptide we replaced the tyrosine 490 by a glycine (QGHIIENPQ**G**FSDAC). For P115RhoGEF, the whole recombinant protein was used (Figure 2D). Under these conditions, it appears that P115RhoGEF binds to the wild-type TrkA peptide but this interaction is lost for the peptide mutated on tyrosine 490. Taken together, these results demonstrated that TrkA phosphorylation is not required for p115rhoGEF recruitment and P115RhoGEF bound to the juxtamembrane region of TrkA.

P115RhoGEF binds to TrkA through its hinge region.

To the best of our knowledge, a direct interaction between TrkA and P115RhoGEF has never been described to date. P115RhoGEF has many protein partners that require either the RH, DH or PH domain for binding. To elucidate the binding between P115RhoGEF and TrkA, mutagenesis experiments have been performed to remove these functional domains. First, we deleted the functional domains of P115RhoGEF (RH, PH, DH domains and intermediate regions) starting from the N-terminal (Figure 3 A, B) or from the C-terminal of the P115RhoGEF protein (Figure 3C, D).

Thus, we could observe that the Delta-5-1 mutant which possesses the D2 (Hinge region) to D6 domains is able to bind TrkA whereas the delta 5-3 mutant which possesses only domains 4 to 6 is not able to do so. This result indicated that the Hinge region (D2) or the DH domain would be involved in the recruitment of TrkA. Then, the functional domains were deleted starting from the C-terminal part. The immunoprecipitation of TrkA showed that P115RhoGEF mutants that have lost the D6, D5 (PH domain), D4 and D3 (DH domain) P115RhoGEF domains still had the ability to bind to TrkA. However, the delta 3-5 mutant, that loses the hinge region, was no longer able to bind to TrkA indicating that the RH and DH domains which are known to bind Galpha13 and/or RhoA are not responsible of TrkA binding (Figure 3E).

The hinge region of p115RhoGEF is 183 amino acids long and to further investigate the interaction domain, this region was mutated by successive replacement of 10AA by 10AA with a flexible sequence (GSAGSAAGSG) (Figure 3F, G). Interestingly, the P115RhoGEF sequence involved in TrkA

binding is not found in either PDZ or LARG (Figure 3I), which are two RhoA activating RhoGEFs[15]. It suggests the specificity of P115RhoGEF recruitment by TrkA.

All these results of deletions of the functional domains of p115RhoGEF showed that the Hinge region of p115RhoGEF is involved in its recruitment to TrkA.

P115RhoGEF is implicated in NGF-induced migration.

The expression of P115RhoGEF is tightly regulated and its overexpression or knock down induces similar phenotypes (rounded cells, loss of junctions) implying a loss of these fine regulations[16]. To overcome this pitfall, the peptide sequence corresponding to the 10AA of the hinge region of P115RHoGEF that interacts with TrkA (GPMSLESLAP) was coupled to a TAT peptide (in N-terminal part) to make it a penetrating peptide (GRKKRRQRRRPQ) (Figure 4A). The effect of this peptide named TAT-P13 was thus tested on clonogenic growth (Figure 4B & C) and migration (Figure 4 D, E) induced by NGF in MDA-MB-231. Under these conditions, we can observe that inhibition of the association between TrkA and P115RhoGEF by TAT-P13 does not induce a decrease in clonogenicity in MDA-MB-231. This result indicates that P115RhoGEF recruitment and underlying signaling is not involved in MDA-MB-231 HA-TrkA clonogenic cell growth. As NGF signaling *via* the TrkA/CD44v3 complex induces migration, the effect of TAT-P13 peptide was then studied on the migration of MDA-MB-231 cells (Figure 4D & E). We thus confirmed that NGF has a pro-migratory effect on MDA-MB-231 HA-TrkA cells with a wound closure of about 60 % in 24 hours compared to 40% in the

absence of NGF. In the presence of TAT-P13, we observed that either in the presence of NGF, the migration of cells remains at the basal level (around 40% of closure). These results indicated that TAT-P13 does inhibit NGF-induced migration.

Tyr-490F mutation does not recapitulate TAT-P13 effects.

To evaluate biological importance of the residue Tyr-490 we performed an alignement of TrkA juxtamembrane region of different species (Figure 5A). Tyr-490 is conserved across Vertebrates suggested the biological importance of this residues. The mutation Tyr-490-Phe (modeled in Figure 5B) abolishs P115RhoGEF binding to TrkA but does not affect it phosphorylation (Figure 5B & C). So, the effect of mutating the residue Tyr-490 was analyzed in terms of clonogenicity (Figure 5C & D) and cell migration in MDA-MB-231 HA-TrkA (Figure 5E & F). Thus, as for the TAT-P13 peptide, the mutation of Y490F does not affect the clonogenicity of MDA-MB-231 HA-TrkA cells (Figure 5C & D). For cell migration, the tyrosine to phenylalanine mutation by itself increased the migration of MDA-MB-231 cells and the effect of NGF is lost in these cells (Figure 5E & F). It is therefore impossible to conclude what impact this mutation has on this biological phenomenon.

Discussion/conclusion

We demonstrated herein that p115RhoGEF directly interacts with TrkA independently of CD44 and is responsible of NGF-induced migration (Figure 6). Nerve Growth Factor and its receptor TrkA are involved in the development of many cancers. In particular, we have shown that NGF

induces migration/invasion and metastasis of breast cancer cells [9,10,17]. Interestingly, we have observed that NGF stimulation can act *via* the recruitment of CD44v3 and an underlying signaling involving P115RhoGEF/RhoA/ROCK. To understand the role of CD44v3 in the recruitment of this signaling, especially as a scaffolding protein, we wanted to demonstrate that CD44v3 recruits p115RhoGEF to the complex. Indeed, Bourguignon et al.[18] had shown that under the effect of hyaluronic acid treatment, CD44v3 could be in complex with P115RhoGEF. Unexpectedly, our results revealed that P115RhoGEF is not associated with CD44 but with TrkA. P115RhoGEF has many functional domains that have been described by their ability to bind its protein partners. Thus, it has been demonstrated that the binding of Galpha12 and alpha13 proteins on the RH and DH domains ensures the activation of P115RhoGEF[14,19,21]. The DH domain also allows the binding of RhoA [22]. Finally, next to the DH domain, on the C-terminal side, there is a pleckstrin homology domain (PH domain) which would not be involved in the cytoplasmic localization of P115RhoGEF but would act by reinforcing the activity of the DH domain [23]. By mutagenesis experiments, we demonstrated here that TrkA binds to P115RhoGEF outside these known regions between the RH, DH and PH domains. This region called Hinge region (or linker) is disordered but allows positioning of RH and DH domains opposite each other to allow their interactions with G-Alpha 13 [21]. It is not excluded that the binding of TrkA to this linker allows the reordering of this region and stabilizes the binding of Galpha 12/13 to P115RhoGEF.

Once activated P115RhoGEF can activate RhoA to induce the underlying signaling. In breast cancer cells, we have shown that RhoA activation is

involved in TrkA/CD44v3 induced signaling, including cell migration [10]. These results seem to be in contradiction with Kalpana et al. work that depict anti-migratory effect of RhoA overexpression in MDA-MB-231 breast cancer cells [24]. Moreover, the work of Kher et al. [16] show that overexpression of P115RhoGEF in this cell line induces a decrease in migratory capacities and cell rounding. But, others works report a pro-migratory effect of P115RhoGEF and RhoA activation [3,9]. These differences could be explained by the fact that RhoA regulation is finely regulated in space and time to allow cell migration. Without its oscillations in activity, remodeling of the cytoskeleton could not take place at the migration front and at the rear of the cells (as reviewed by O'Connor and Chen) [25]. Thus, we showed that RhoA activation is not homogeneous in MDA-MB-231 cells and localizes at migration fronts which is consistent with cell migration [10]. Moreover, like Kher *et al*, when we tried to overexpress the wild type and the delta 13 mutant that are able to homodimerized (auto-inhibition of P115RhoGEF), we inhibit the pro-migratory effects (data not shown) which reinforces the hypothesis that these equilibriums are important. The same is probably true for the unexpected results obtained following the mutation of TrkA. It is very likely that this mutation affects the homeostasis of the TrkA receptor. First of all, as can be seen on the blot, the TrkA membrane form (at 140 kDa) but especially the immature 110 kDa form in exocytic vesicles [26,27] increase when tyrosine Y490 is mutated. This tyrosine is indeed in an NPXY motif that is known to play both a role in TrkA endocytosis [28] but also exocytosis [29]. In addition, there are compensation phenomena in the functions of the tyrosine residues of the intracellular part. Thus, mutations in tyrosine 490 can be rescued by tyrosine

785 [30]. It is not excluded that such compensations exist and induce an over activation of TrkA in the absence of exogenous NGF resulting in an increase in migration in basal condition not modulated by NGF. The addition of exogenous NGF could even be inhibitory in this case because we have previously demonstrated that the effects of NGF on cell migration/invasion have a bell effect [31]. The addition of NGF would exceed the optimal dose and have an inhibitory effect.

Conclusion

In conclusion, we have shown for the first time that CD44 is not necessary for the recruitment of P115RhoGEF by TrkA but P115RhoGEF binds directly on TrkA. Moreover, we highlight that TrkA/P115RhoGEF interaction relies on TrkA Tyr-490 and 10 AA of P115RhoGEF hinge region. In addition, we demonstrated that a mimetic peptide of 10 AA region of P115RhoGEF hinge region inhibited NGF-induced migration of triple negative breast cancer cells overexpressing TrkA. For triple negative breast cancer overexpressing TrkA, TrkA/p115RhoGEF inhibitors may represent a new opportunity to avoid relapse due to distant metastasis.

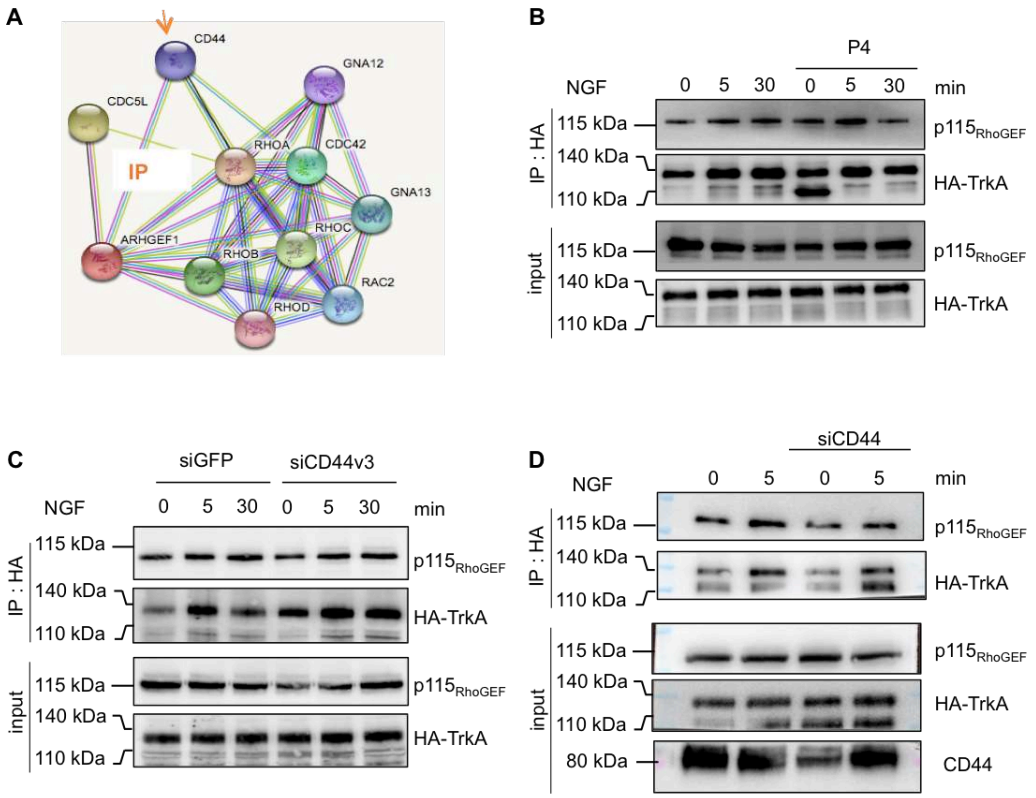


Figure 1: P115RhoGEF is not recruited by CD44v3 under NGF treatment.

(A) String protein network indicates that P115RhoGEF is found associated with CD44 in immunoprecipitation experiment. (**B)** MDA-MB-231 HA-TrkA cells were treated with NGF (5 and 30 min) or not (0 min) and CD44v3 mimetic peptide 4 (P4). Cell lysates were then subjected to immunoprecipitation using HA-Tag antibodies. P115RhoGEF was revealed by western blot. Results are representative of 3 independent experiments. (**C, D)** CD44 or CD44v3 were down regulated by siRNA in MDA-MB-231 HA-TrkA cells. Cells were treated with NGF (5 and 10 min) or not (0 min). Cell lysates were then subjected to immunoprecipitation using HA-Tag antibodies. P115RhoGEF was revealed by western blot. Results are representative of 3 independent experiments.

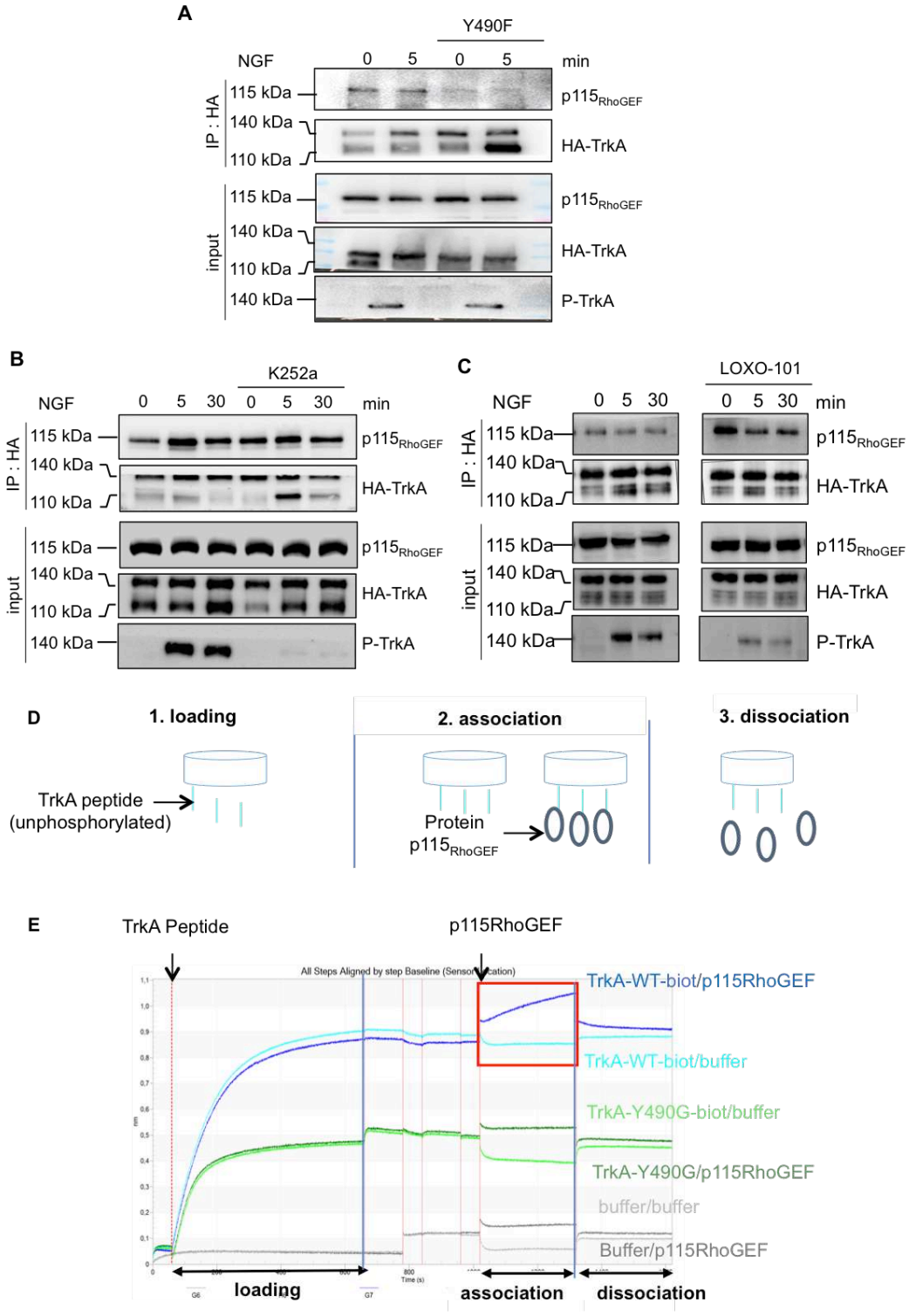


Figure 2: P115 binding to TrkA needs Tyr490 residue but not TrkA phosphorylation. (A) MDA-MB-231 HA-TrkA or Y490F HA-TrkA cells were treated with NGF (5 min) or not (0 min). Cell lysates were then subjected to

immunoprecipitation using HA-Tag antibodies. P115RhoGEF was revealed by western blot. Results are representative of 3 independent experiments. **(B, C)** MDA-MB-231 HA-TrkA cells were treated with NGF (5 and 10 min) or not (0 min) and TrkA tyrosine kinase inhibitors (K252A or LOXO-101). Cell lysates were then subjected to immunoprecipitation using HA-Tag antibodies. P115RhoGEF was revealed by western blot. Results are representative of 3 independent experiments. **(D)** Experimental setting of biolayer interferometry **(E)** Interferometry curve of P115RhoGEF and wild-TrkA peptide (QGHIIENPQ**Y**FSDAC) or Y490G mutated peptide (QGHIIENPQ**G**FSDAC).

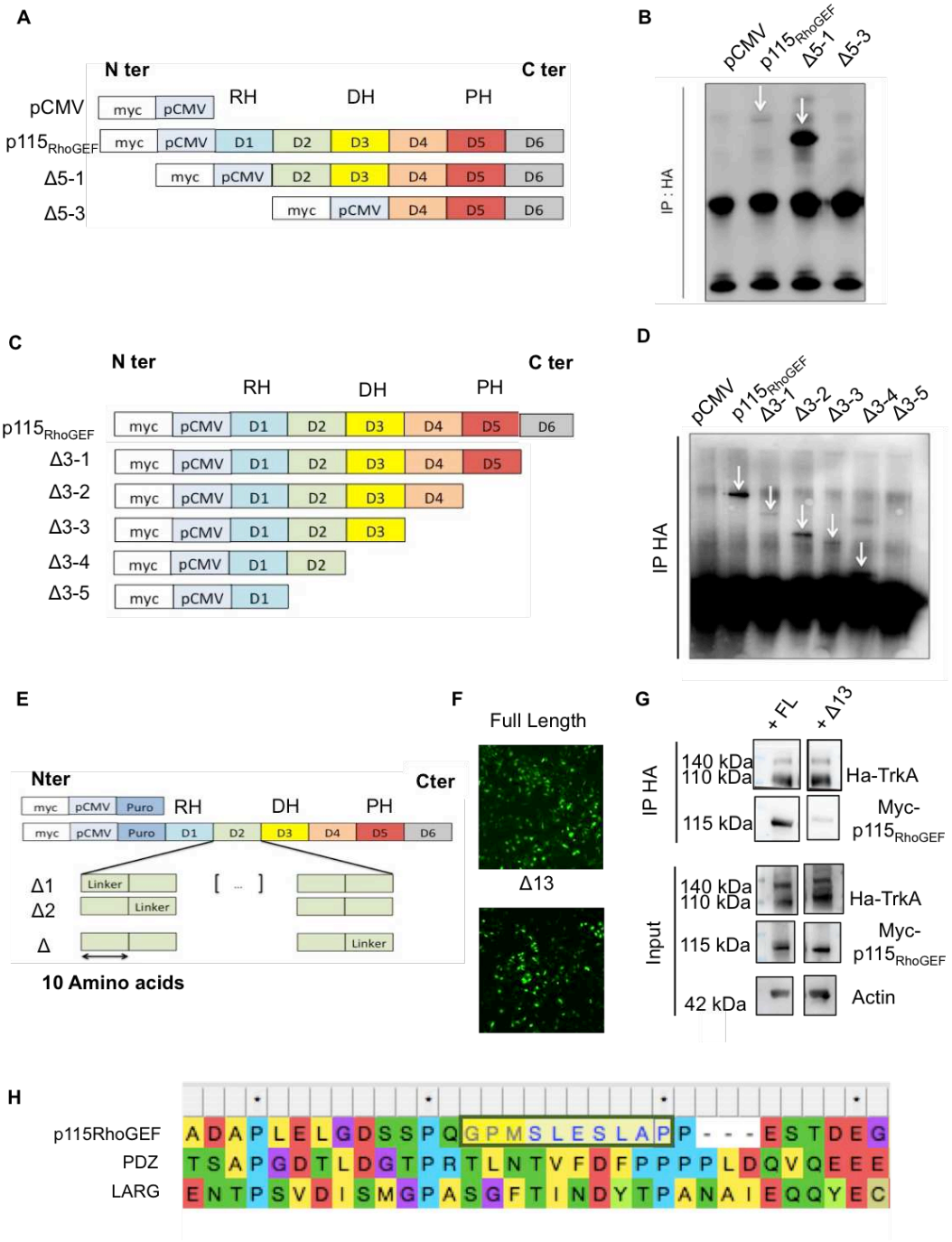


Figure 3: P115RhoGEF hinge region interacts with TrkA. (A) Schematic representation of Δ5 mutants; **(B)** MDA-MB-231 HA-TrkA cells expressing empty vector (pCMV) myc-tag p115RhoGEF or Δ5-1 or Δ5-3 mutants. Cell lysates were then subjected to immunoprecipitation using HA-Tag antibodies. P115RhoGEF was revealed by western blot; **(C)** Schematic representation of

Δ3 mutants; **(D)** MDA-MB-231 HA-TrkA cells expressing empty vector (pCMV) myc-tag p115RhoGEF or Δ3-1 to Δ3-5 mutants. Cell lysates were then subjected to immunoprecipitation using HA-Tag antibodies. P115RhoGEF was revealed by western blot; **(E)** schematic representation of Galpha13 interaction with p115RhoGEF RH, DH domains **(F)** Schematic representation of domain 2 mutants; **(G)** Representative micrograph of Full length and Δ13 mutant co-expressing GFP; **(H)** Cell lysates were then subjected to immunoprecipitation using HA-Tag antibodies. P115RhoGEF was revealed by western blot; **(I)** Sequence alignment of PDZ, P115RhoGEF and LARG hinge region.

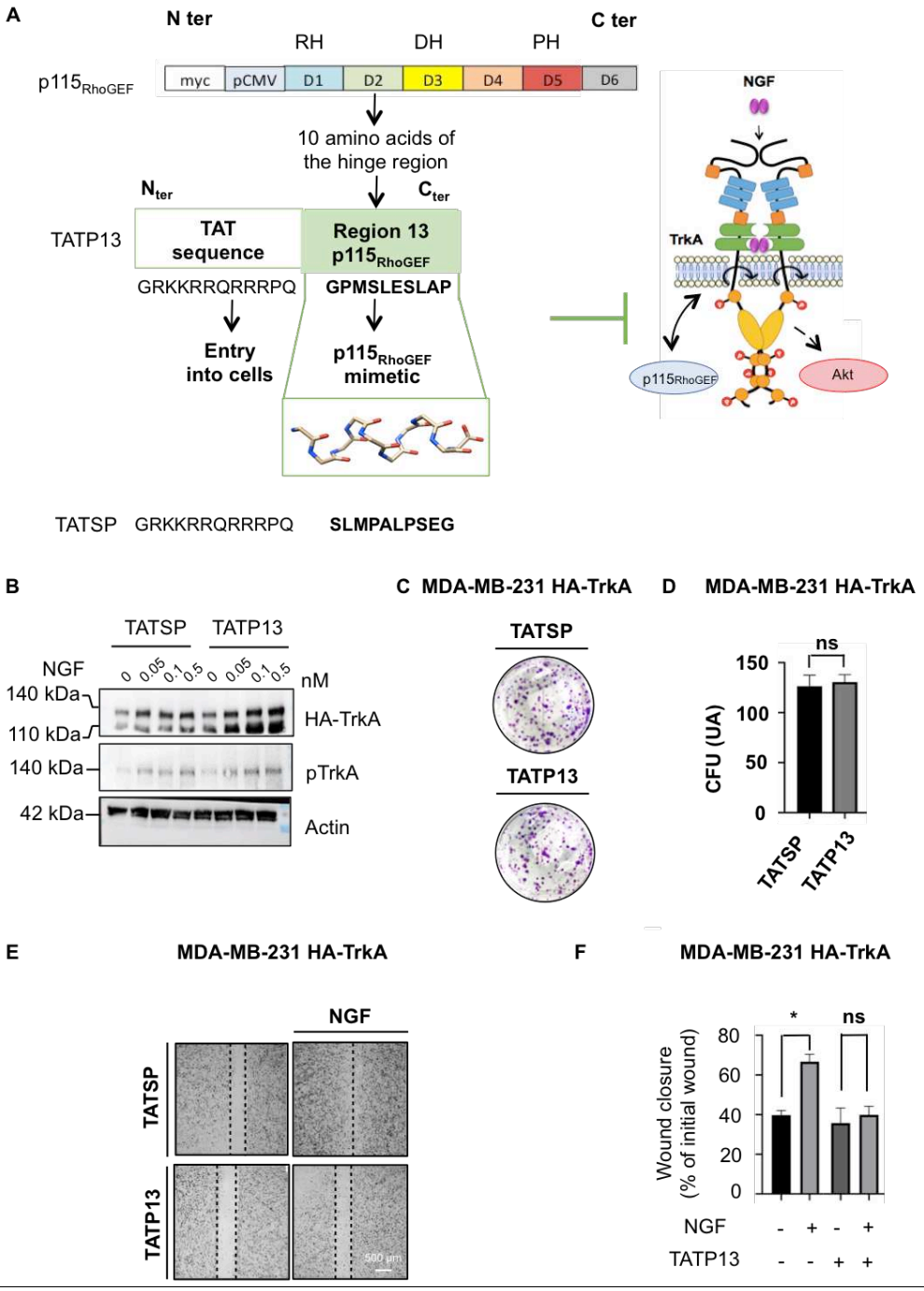
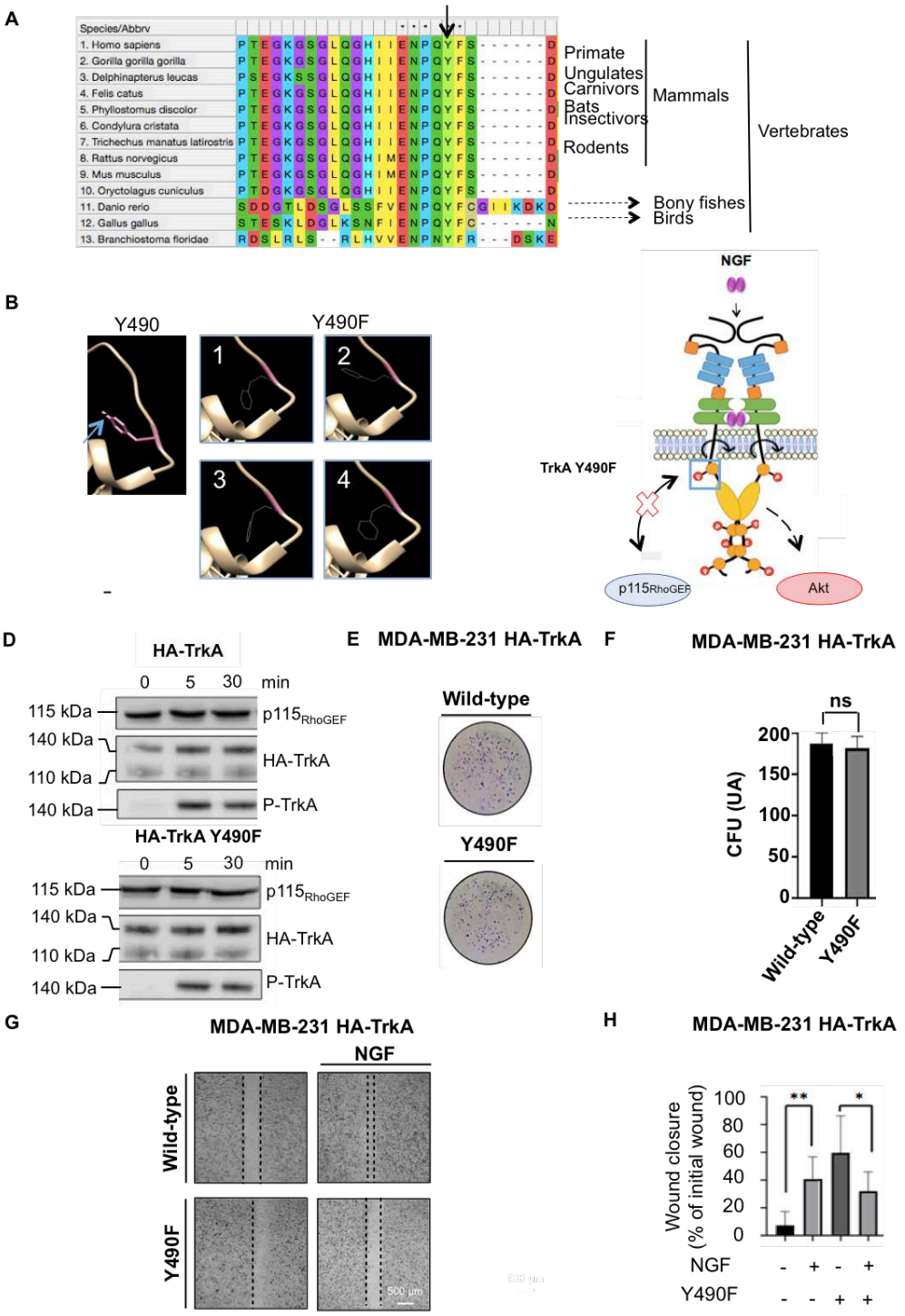


Figure 4: P115RhoGEF is involved in NGF-induced migration. (A) Schematic representation of penetrating p115RhoGEF mimetic TATP13 and its effects on TrkA signaling; **(B)** Western blot of phospho-TrkA after treatment with p115RhoGEF mimetic peptide (TATP13) or the control (TATSP) (1h) following by NGF treatment (5 min) **(C, D)** Clonogenic growth of MDA-MB-231 overexpressing TrkA was measured after 7 days in the presence of

p115RhoGEF mimetic peptide (TATP13) or the control (TATSP); **(E, F)** Migration assays were performed using Ibidi devices 20 h after treatment with p115RhoGEF mimetic peptide (TATP13) or the control (TATSP). Statistical analyses were performed using one-way ANOVA followed by Bonferroni's posttest. The error bars represent the standard error of the mean (S.E.M.); * $p < 0.05$, ns, not significant.



<u>Figure 5:</u> Tyr490F mutation does not recapitulate TAT-P13 effects.

(A) Alignment (Clustal W) of TrkA juxtamembrane region across Vertebrates was generated with MegaX **(B)** Chimera rotamer module was used to model the mutation Tyr-490-Phe **(C)** Schematic representation of mutation Tyr-490-

Phe on TrkA signaling **(D)** Western blot of phospho-TrkA after NGF treatment (5 or 30 min) **(E, F)** Clonogenic growth of MDA-MB-231 overexpressing TrkA was measured after 7 days using MDA-MB-231 HA-TrkA or Y490F HA-TrkA cells **(G, H)** Migration assays were performed using Ibidi devices 20 h after treatment using MDA-MB-231 HA-TrkA or Y490F HA-TrkA cells. Statistical analyses were performed using one-way ANOVA followed by Bonferroni's posttest. The error bars represent the standard error of the mean (S.E.M.); * $p < 0.05$, ns, not significant.

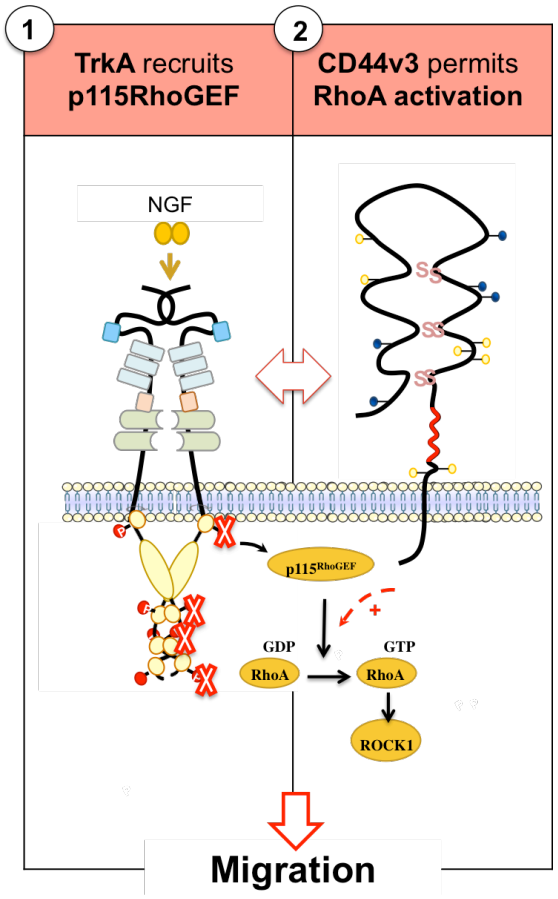


Figure 6: Schematic representation of the modalities of TrkA/CD44v3 signaling and its role. (1) TrkA permits P115RhoGEF recruitment whereas

(2) CD44v3 is necessary for RhoA activation. Inhibition of TrkA/P115RhoGEF as TrkA/CD44v3 impedes cell migration.

Methods

Cell culture

MDA-MB-231 overexpressing TrkA cells were obtained by transfection of the plasmid pDisplay HA-TrkA and geneticin selection (1 mg/mL, 2 weeks) of MDA-MB-231 breast cancer cell lines (purchased from the American Type Culture Collection, ATCC, Manassas, VA, USA). MDA-MB-231 overexpressing TrkA cells were cultured in Eagle's Minimal Essential Medium (EMEM) supplemented with 10% inactivated Fetal Bovine Serum (FBS) (Hyclone, Belgium), 1% non-essential amino acids, 40 UI/ml Penicillin/Streptomycin, 20 µg/mL Gentamycin and geneticin (0.5 mg/mL). The cells were incubated at 37°C in 5% CO_2-humidified atmosphere. Cells were cultured no more than 20 passages to avoid genetic derived. Before treatment, cells were rinsed twice with trypsin/EDTA, left for 48 h in culture medium supplemented with 10% FBS. Then, cells were rinsed with medium supplemented with 0.1% FBS for 3h30, treated with the peptide control (SP) or the P4 (50 ng/mL) during 30 minutes and the recombinant human β-NGF (5 min, at the concentration indicated) (Alomone Labs, Israel).

Plasmids

Constructions. The HA-TrkA expression vectors Wild-type and Tyr-490-Phe were generated by site-directed mutagenesis and cloning of the HA-tagged TrkA sequence (N-ter side) into the P-Display vector (Adgene). The myc-tagged (C-ter side; sequence: EQKLISEEDL) p115RhoGEF expression vectors were produced by e-Zyvec from a commercial pCMV vector containing the p115RhoGEF sequence (ORIGENE, NM_199002). For the

serie of p115RhoGEF constructs deleted of 10 AA into the hinge region, 10 AA were replace by a flexible linker to ensure protein expression [32]. Moreover, these constructs co-express GFP that permits expression validiation before cell lysis.

Vector amplification. After incubation of 1 µL of plasmids with 25 µL of bacteria (One Shot Top 10; Promega) (25 min, 4°C), a heat shock is performed (42°C, 30s; 4°C, 2 min) and 150 µL of S.O.C. medium (invitogen™) is added. The mixture is incubated (1h, 37°C, 250 RPM, Forma Orbital Shaker Thermo) and 30 µL is spread on an LB agar (100 g/ml ampicillin) dish (16 h, 37°C). One colonie was placed in 5 ml of LB medium (25g/L, sigma; 100 µg/ml ampicillin) and incubated (24 h, 37°C, 250 RPM). The plasmids were purified according to the protocol of the QIAprep® Spin Miniprep kit (Qiagen). The concentration and ratio 260/230 and 260/280 were assed by spectrophotometry (nanodrop).

Protein extraction

Sub confluent cells were washed twice with ice-cold PBS, and lysed (40 mM HEPES pH 7.5, 120 mM NaCl, 1 mM EDTA, 1% Triton X-100, 0.1% SDS, 10% glycerol, 10 mM sodium pyrophosphate, 50 mM sodium fluoride, 1.5 mM sodium orthovanadate, and 1 mM PMSF, supplemented with a protease inhibitor cocktail) (Sigma-Aldrich, France). Cell lysates were then cleared by centrifugation (6000 x g, 10 min, 4°C) and stored at -80°C until analysis. The supernatants were collected and protein concentration was determined using the BCA assay (Sigma-Aldrich).

Immunoprecipitation

Proteins (1 mg in 400 µl of lysis buffer) are incubated (1 h, 4°C, 10 RPM, on wheel) with 100 µL of G beads (Protein G Agarose, Upstate) and 10 µL of IGg2 (0.5 µg/µL). After centrifugation (5 min, 4°C, 13 800g) the supernatant was incubated (2h, 4°C, 10 RPM, on wheel) with 12.5 µL of anti-

HA CA (0.4 µg/µL; Roche 12CA5). G beads (100 µL, Protein G Agarose, Upstate) were added and then the supernatant was returned to incubate (16 h, 4°C, 10 RPM, on wheel). After 3 washes in lysis buffer by centrifugation (5 min, 4°C, 13,800 g). Protein complexes are recovered from the pellet by addition of Laemmli 2X buffer (25.2 mM Tris HCl, 4% glycerol, 0.8% SDS, 2% β-mercaptoethanol, 0.01% Bromophenol Blue, pH 6.8; 7 min; 95°C; under stirring).

Western blotting

Cell lysates proteins were separated by SDS-PAGE and transferred onto PVDF membranes (GE Whatman, United Kingdom). The membranes were blocked with 5% bovine serum albumin (BSA) in Tris-buffered saline-0.1% Tween 20 (TBS-T) (w/v) (1h, RT) and immunoblotted (overnight, 4°C). The membranes were washed Tris-buffered saline-0.1% Tween 20 (TBS-T) (w/v) 5 times (5 min) then probed with horseradish peroxidase-conjugated secondary antibody (Jackson Immunoresearch, Beckman Coulter, France) and washed again. SuperSignal West Pico Substrate (Thermo Scientific, Belgium). Chemiluminescence was detected with Fuji LAS-4000 luminescent image analyzer. The antibodies used in this study were: anti-actin (A2066, Sigma-Aldrich), anti-TrkA (Cell Signaling), anti-HA (901501, Biolegend, Germany), anti-phospho-TrkA (Cell Signaling Technologies, Netherlands).

Scratch wound migration assay

Scratch wound migration assay were performed as previously described (Trouvilliez et al. 2022). Briefly, inserts were placed onto 6-well plates before

and cells were seeded ($4x10^5$ cells/mL) and incubated overnight at 37°C to subclonfluent stage. Then inserts were removed, cells were rinsed (1 ml 0,1 % SVF medium) and starved (1h). Pictures of the initial wound were done using an invert microscope at the beginning of the starvation. One hour later, the cells are treated with the LOXO-101 (250 nM) or no. Thirty minutes later the peptide control (TATSP) or the TATP13 was added (50 ng/mL). At least, 30 minutes later, the cells were stimulated or no (Control) with NGF (100 ng/ml). After 20h, pictures of the wounds were taken at the same place than initial picture. Quantifications were performed using the Fiji software.

Clonogenicity assay

Clonogenicity assay were conducted as previously described (Trouvilliez et al., 2022). Briefly, MDA-MB-231 HA-TrkA cells (250 cells/mL) were seeded into 6 plate wells (2% FBS medium; 2 mL/well). When the cells attached, they were treated with the LOXO-101, 30 minutes later with the peptide (50 ng/mL) and cells were incubated for 24 h. The next day, a second-round treatment was performed. Three days later, the medium was changed, and the cells were incubated for another 2-3 days. Then, the medium was removed, and the cells were washed twice (PBS 1×), fixed (4% PAF for 30 min at RT), colored (violet crystal 2%; 30 min; RT) and washed twice (distilled water). Representative pictures of one well were taken, and the colonies were counted.

Modeling of the peptide structures

The structure of the peptide was produced *de novo* using the PEP-FOLD 3.5 webserver. The amino acid sequence of the peptide was used as input.

Modeling was performed using standard parameters. The representation of the best model was then visualized using Chimera software.

Statistical analyses

Statistical analyses were performed using GraphPad Prism 5.01 software. Analyses were performed using one-way analysis of variance (ANOVA) for the wound and clonogenicity assay data followed by Bonferroni's post-test.

Abbreviations

BSA: Bovine Serum Albumin

CD44v: CD44 variant

DH: Dbl Homology

EMEM: Earle's salt Minimum Essential Medium

FBS: Fetal Bovine Serum

NGF: Nerve Growth Factor

PBS-T: phosphate-buffered saline – Tween 20

PH: Plextrin Homology

RH: RGS Homology

SD: Standard Deviation

TBS: Tris-buffered saline

TN: Triple Negative

TNBC: Triple Negative Breast Cancer

TrkA: Tropomyosin kinase A

Consent for publication

All the participants of this study consented to the publication of this work.

Availability of data and material

The data and materials generated in this study are available upon reasonable request from the corresponding author:

Prof. Robert-Alain Toillon, Université de Lille, Faculté des Sciences et Technologies, UMR CNRS 9020- INSERM U1277 - CANTHER - Cancer Heterogeneity Plasticity and Resistance to Therapies, Bâtiment SN3, 3ème étage, Cité scientifique, 59655 Villeneuve d'Ascq, France. Phone: +33 (0)3 20 43 65 59. E-mail: robert-alain.toillon(at)univ-lille.fr

Competing interests

The authors declare that they have no competing interests.

Funding

This work was supported by “La ligue contre le cancer” (« comité du Nord, du Pas de Calais et de l’Aisne »), cancéropole Nord-Ouest, I-site “Université Lille Nord-Europe” and Contrat de Plan Etat-Région CPER Cancer 2015-2020. ST was funded by “conseil régional Hauts de France”, Lille University and La ligue contre le cancer.

Author contributions

ST, JC, LA, CC, AVO, GB & R-AT conceived experiments, performed experiments and collected data. FG, CM, XT, CL, XLB, V-OR and R-A T provided funding acquisition, resources. R-A T supervised research project. ST and R-AT wrote the manuscript in consultation with XLB and SG.

References

1. Joo E. & Olson M. F. Regulation and functions of the RhoA regulatory guanine nucleotide exchange factor GEF-H1. *Small GTPases* **12**, 358–371 (2021).

2. Sjöblom T. *et al.* The Consensus Coding Sequences of Human Breast and Colorectal Cancers. *Science (80-.).* **314**, 268 LP – 274 (2006).

3. Privat M. *et al.* A high expression ratio of RhoA/RhoB is associated with the migratory and invasive properties of basal-like breast tumors. *Int. J. Med. Sci.* **17**, 2799–2808 (2020).

4. Lang S. *et al.* Specific role of RhoC in tumor invasion and metastasis. *Oncotarget* **8**, 87364–87378 (2017).

5. Pillé J. Y. *et al.* Anti-RhoA and Anti-RhoC siRNAs inhibit the proliferation and invasiveness of MDA-MB-231 breast cancer cells in vitro and in vivo. *Mol. Ther.* **11**, 267–274 (2005).

6. Zhao X. *et al.* Overexpression of RhoA Induces Preneoplastic Transformation of Primary Mammary Epithelial Cells. *Cancer Res.* **69**, 483–491 (2009).

7. Van Golen K. L., Wu Z. F., Qiao X. T., Bao L. W. & Merajver S. D. RhoC GTPase overexpression modulates induction of angiogenic factors in breast cells. *Neoplasia* **2**, 418–425 (2000).

8. Vega F. M., Fruhwirth, G., Ng, T. & Ridley, A. J. RhoA and RhoC have distinct roles in migration and invasion by acting through different targets. *J. Cell Biol.* **193**, 655–665 (2011).

9. Aubert L. *et al.* NGF-induced TrkA / CD44 association is involved in tumor aggressiveness and resistance to lestaurtinib. **6** (2015)

10. Trouvilliez, S. *et al.* Direct interaction of TrkA / CD44v3 is essential for NGF-promoted aggressiveness of breast cancer cells. *J. Exp. Clin. Cancer Res.* 1–21 (2022). doi:10.1186/s13046-022-02314-4

11. Haffty B. G. *et al.* Locoregional relapse and distant metastasis in conservatively managed triple negative early-stage breast cancer. *J. Clin. Oncol.* **24**, 5652–5657 (2006).

12. Middleton J. D., Stover D. G. & Hai T. Chemotherapy-exacerbated breast cancer metastasis: A paradox explainable by dysregulated adaptive-response. *Int. J. Mol. Sci.* **19**, 1–14 (2018).

13. Bourguignon L. Y. W., Singleton P. A., Zhu H. & Diedrich F. Hyaluronan-mediated CD44 Interaction with RhoGEF and Rho Kinase Promotes Grb2-associated Binder-1 Phosphorylation and Phosphatidylinositol 3-Kinase Signaling Leading to Cytokine (Macrophage-Colony Stimulating Factor) Production and Breast Tumor Progress. **278**, 29420–29434 (2003).

14. Bhattacharyya R., Banerjee J., Khalili K. & Wedegaertner P. B. Differences in Galpha12- and Galpha13-mediated plasma membrane

recruitment of p115-RhoGEF. *Cell. Signal.* **21**, 996–1006 (2009).

15. Chikumi H. *et al.* Homo- and hetero-oligomerization of PDZ-RhoGEF, LARG and p115RhoGEF by their C-terminal region regulates their in vivo Rho GEF activity and transforming potential. *Oncogene* **23**, 233–240 (2004).

16. Kher S. S., Struckhoff A. P., Alberts A. S. & Worthylake R. A. A novel role for p115RhoGEF in regulation of epithelial plasticity. *PLoS One* **9**, (2014).

17. Lagadec C. *et al.* TrkA overexpression enhances growth and metastasis of breast cancer cells. *Oncogene* **28**, 1960–1970 (2009).

18. Lilly Y.W. Bourguignon. Hyaluronan-mediated CD44 activation of RhoGTPase signaling and cytoskeleton function promotes tumor progression. *Semin. Cancer Biol.* **18**, 251–259 (2008).

19. Grabocka E. & Wedegaertner P. B. Functional consequences of Gα13 mutations that disrupt interaction with p115RhoGEF. *Oncogene* **24**, 2155–2165 (2005).

20. Bhattacharyya, R. & Wedegaertner, P. B. Gα13 requires palmitoylation for plasma membrane localization, Rho- dependent signaling, and promotion of p115-RhoGEF membrane binding. *J. Biol. Chem.* **275**, 14992–14999 (2000).

21. Chen Z. *et al.* Activation of p115-RhoGEF Requires Direct Association of G _, 13 and the Dbl Homology Domain * □. **287**, 25490–25500 (2012).

22. Kristelly R., Gao G. & Tesmer J. J. G. Structural determinants of RhoA binding and nucleotide exchange in leukemia-associated Rho guanine-nucleotide exchange factor. *J. Biol. Chem.* **279**, 47352–47362 (2004).

23. Jaiswal M. *et al.* Mechanistic insights into specificity, activity, and regulatory elements of the regulator of G-protein signaling (RGS)-containing Rho-specific guanine nucleotide exchange factors (GEFs) p115, PDZ-RhoGEF (PRG), and leukemia-associated RhoGEF (LARG). *J. Biol. Chem.* **286**, 18202–18212 (2011).

24. Kalpana G., Figy C., Yeung M. & Yeung K. C. Reduced RhoA expression enhances breast cancer metastasis with a concomitant increase in CCR5 and CXCR4 chemokines signaling. *Sci. Rep.* **9**, 1–12 (2019).

25. O'Connor K. L. & Chen M. Dynamic functions of RhoA in tumor cell migration and invasion. *Small GTPases* **4**, 141–147 (2013).

26. Jullien J., Guili V., Reichardt L. F. & Rudkin B. B. Molecular kinetics of

nerve growth factor receptor trafficking and activation. *J. Biol. Chem.* **277**, 38700–38708 (2002).

27. Martin-Zanca D., Oskam R., Mitra G., Copeland T. & Barbacid M. Molecular and biochemical characterization of the human trk proto-oncogene. *Mol. Cell. Biol.* **9**, 24–33 (1989).

28. Goh L. K. & Sorkin, A. Endocytosis of receptor tyrosine kinases. *Cold Spring Harb. Perspect. Biol.* **5**, 1–17 (2013).

29. Fuschini G. *et al.* Syntaxin-1/TI-VAMP SNAREs interact with Trk receptors and are required for neurotrophin-dependent outgrowth. *Oncotarget* **9**, 35922–35940 (2018).

30. Biarc J., Chalkley, R. J., Burlingame, A. L. & Bradshaw, R. A. Dissecting the roles of tyrosines 490 and 785 of TrkA protein in the induction of downstream protein phosphorylation using chimeric receptors. *J. Biol. Chem.* **288**, 16606–16618 (2013).

31. Demont Y. *et al.* Pro-nerve growth factor induces autocrine stimulation of breast cancer cell invasion through tropomyosin-related kinase A (TrkA) and sortilin protein. *J. Biol. Chem.* **287**, 1923–1931 (2012).

32. Pinto, F., Thornton, E.L. & Wang, B. An expanded library of orthogonal split inteins enables modular multi-peptide assemblies. *Nat Commun* **11,** 1529 (2020). https://doi.org/10.1038/s41467-020-15272-2

5. Discussion/Perspectives

Dans notre étude, nous avons montré que **CD44v3 interagirait directement avec TrkA** *via* la région **C-ter de CD44v3** et la région **LRR de TrkA**. Différents variants de CD44 sont connus pour être des co-récepteurs pour les RTKs. CD44v3 et CD44v6 s'associent avec les récepteurs ErbB1, VEGFR, Met et Erb4 (Tremmel *et al.*, 2009; Volz *et al.*, 2015). Cependant, ces études suggèrent une association *via* le ligand et non une interaction entre les 2 récepteurs. De plus, la caractérisation moléculaire de l'interaction TrkA/CD44v3 a permis de montrer son rôle dans la survie, la migration, l'invasion, la croissance tumorale et le processus métastatique des cellules cancéreuses mammaires triples négatives. Or, la prise en charge des cancers du sein triples négatifs repose aujourd'hui sur la chimiothérapie, efficace dans moins de 50 % des cas. L'interaction TrkA/CD44v3 pourrait ainsi constituer une nouvelle cible thérapeutique pour ce type de cancers. Néanmoins, l'utilisation des thérapies ciblées conduit à des rechutes en raison de la mise en place de mécanismes de résistance d'origine génétique ou liés au microenvironnement (Fuse *et al.*, 2017; Labrie *et al.*, 2022). Afin d'allier efficacité et spécificité des thérapies, des ADC (Antibody Drug Conjugates) reconnaissant le complexe TrkA/CD44v3, spécifique des cellules cancéreuses, pourrait constituer une approche prometteuse pour les patientes présentant le complexe (Drago *et al.*, 2021).

De plus, nous avons montré qu'en plus de la mise en place d'une signalisation phospho-indépendante, **CD44v3 augmente l'affinité de TrkA pour le NGF** ce qui favorise les signalisations canoniques de TrkA. $P75^{NTR}$, le récepteur de basse affinité du NGF est également connu pour augmenter l'affinité de TrkA pour le NGF. Néanmoins, les mécanismes mis en jeu dans le cas de $P75^{NTR}$ et CD44v3 présentent des différences. En effet, $P75^{NTR}$ ne semble pas suffisant pour induire une augmentation d'affinité contrairement à la partie C-ter de CD44v3 (Jing *et al.*, 1992; Klein *et al.*, 1991). De plus, l'augmentation d'affinité associée à $P75^{NTR}$ varie de 10 à 100 selon les modèles cellulaires utilisés tandis que nos expériences montrent une augmentation de 10 fois avec des extraits exprimant CD44v3 et un peptide

mimétique de CD44v3 (système *ex vitro*). Enfin, la littérature suggère que $P75^{NTR}$ augmenterait l'affinité de TrkA pour le NGF *via* une présentation du NGF à TrkA et non une interaction TrkA/ $P75^{NTR}$ comme pour TrkA et CD44v3. Il est ainsi possible que CD44v3 et $P75^{NTR}$ agissent *via* 2 mécanismes distincts ou complémentaires pour augmenter l'affinité de TrkA pour le NGF. Cette seconde hypothèse est étayé par une étude qui soulève la nécessité d'un changement de conformation de la partie extracellulaire de TrkA pour permettre l'association NGF/TrkA/$P75^{NTR}$ (Wehrman *et al.*, 2007). CD44v3 pourrait ainsi en interagissant avec TrkA induire un changement de conformation qui permettrait la présentation du NGF par $P75^{NTR}$ et ainsi la pleine activation de TrkA par le NGF.

Nos travaux montrent également que l'association TrkA/CD44v3 permet **l'activation d'une signalisation indépendante de la phosphorylation** de TrkA. Cette signalisation contribue à l'inefficacité des Tki comme le suggéraient de précédents travaux du laboratoire (Aubert *et al.*, 2015). En particulier, nous avons montré qu'un **peptide mimétique de la partie C-terminale de CD44v3 restaure une réponse au Larotrectinib** *in vitro* et *in vivo* en bloquant l'activation de la signalisation phospho-indépendante de TrkA et augmentant la phosphorylation de TrkA. Néanmoins, ce peptide ne restaure pas de réponse à l'Entrectinib, un autre inhibiteur de TrkA. Or, bien que le Larotrectinib et l'Entrectinib se fixent tous 2 au niveau de la poche ATPasique de TrkA, leur liaison à TrkA ne met pas en jeu les mêmes résidus (Jiang *et al.*, 2021). Il se pourrait ainsi que le Larotrectinib bloque le recrutement de certaines molécules mais pas l'Entrectinib. Ces résultats suggèrent le potentiel d'un ciblage simultané de la phosphorylation de TrkA et de la signalisation TrkA/CD44v3. Néanmoins, le peptide mimétique de CD44v3 augmente le potentiel oncogénique de TrkA. L'utilisation de la combinaison Larotrectinib+P4 en clinique semble ainsi une stratégie relativement risquée. C'est pourquoi pour pouvoir contrer les effets pro-tumoraux de la signalisation TrkA/CD44v3 phospho-indépendante sans moduler la phosphorylation de TrkA, nous avons étudié les modalités de la mise en place de la signalisation de TrkA/CD44v3.

Précédemment, notre équipe a montré que TrkA/CD44 permet la mise en place d'une signalisation qui repose sur p115RhoGEF, RhoA, ROCK1 (Aubert *et al.*, 2015). Dans cette étude, nous montrons pour le première fois, que **CD44 n'est pas nécessaire au recrutement de p115RhoGEF** par le complexe TrkA/CD44v3 contrairement à ce que suggère la littérature (Bourguignon *et al.*, 2003). De plus, p115RhoGEF peut être recruté par Shc (Wu *et al.*, 2016). Or, la protéine Shc peut-être recrutée par la Tyr-490 de TrkA phosphorylée et interagit alors avec une protéine de 115 kDa (Dikic *et al.*, 1995). Ces éléments suggèrent l'existence d'une association indirecte entre TrkA phosphorylé et p115RhoGEF. De façon intéressante, notre étude décrit l'existence d'une i**nteraction directe TrkA/p115RhoGEF indépendante de la phosphorylation** de TrkA. De plus, la « hinge region » de p115RhoGEF impliquée dans son recrutement par TrkA ne correspond pas au domaine de liaison des protéines α13, connues pour activer p115RhoGEF, mais intervient dans la régulation de l'activité de p115RhoGEF (Chen *et al.*, 2011; Chen *et al.*, 2012). Cette région joue le rôle d'inhibiteur lorsque la protéine est libre (non liée à un récepteur) et présente une structure désordonnée. Il est ainsi possible que son association à TrkA ordonne la région et lève l'auto-inhibition associée à cette région. Dans ce sens, un peptide mimétique de 10 acides aminés de cette région impliqués dans l'association TrkA/p115RhoGEF, bloque la migration NGF-induite. Or, dans la prise en charge des TNBC, les récidives sont associés à la formation de métastases et la chimiothérapie, traitement standard dans la prise en charge des TNBC peut pardoxalement favoriser la formation de métastases (Haffty *et al.*, 2006). Le développement de composés ciblant l'interaction TrkA/p115RhoGEF pourrait ainsi permettre de retarder voire d'empêcher la mise en place des métastases. Néanmoins, la synthèse de ce type de composés nécessite de parfaire notre connaissance des modalités de l'association TrkA/p115RhoGEF et d'obtenir une résolution atomique de l'interaction. Or, la structure de la « hinge region » de p115RhoGEF n'a pas été résolue expérimentalement. La modélisation de l'interaction TrkA/p115RhoGEF s'avère ainsi délicate. Néanmoins, il a été montré que l'interaction de ce type de région avec d'autres protéines peut ordonner celle-ci et permettre la caractérisation de l'interaction protéine/protéine

expérimentalement. Dans le cas de TrkA/p115RhoGEF, il pourrait ainsi être possible d'obtenir une structure du complexe par cristallographie ou CryoEM.

Les travaux décrits dans ma thèse se limitent aux cancers du sein triples négatifs, cependant, d'autres études menées dans notre équipe ces dernières années suggèrent également son implication dans les cancers des voies aérodigestives supérieures. En effet, TrkA/CD44v3 semble associé à la migration/invasion cellulaire et est corrélé avec l'invasion périneurale. De plus, l'association TrkA/CD44v3 a également été retrouvée dans des cellules prostatiques PC3 et pourrait ainsi contribuer au processus migratoire et métastatique dans les cancers de la prostate. D'autre part, les travaux du laboratoire montrent l'existence d'une association de TrkA et d'EphA2 (Ephrin type-A receptor 2) suite à une stimulation avec du ProNGF (Lévêque *et al.*, 2019). Ce complexe contribue également au processus métastatique. De plus, TrkA présente de nombreux co-récepteurs qui pourraient également contribuer à l'agressivité tumorale et l'inefficacité des inhibiteurs de la phosphorylation de TrkA *via* différents mécanismes que nous avons décrits dans une revue intitulée « TrkA co-receptors : the janus face of TrkA ? ».

TrkA co-receptors: the janus face of TrkA?

Trouvilliez Sarah[1], Toillon Robert-Alain[1*].

[1] Univ. Lille, CNRS, INSERM, CHU Lille, UMR9020-U1277 - CANTHER - Cancer Heterogeneity Plasticity and Resistance to Therapies, F-59000 Lille, France

*** Corresponding author:** Prof. Robert-Alain Toillon, UMR9020-U1277 - CANTHER - Cancer Heterogeneity Plasticity and Resistance to Therapies, Bâtiment SN3, 3ème étage, Cité scientifique, Université de Lille, 59655 Villeneuve d'Ascq, France. Phone: +33 (0)3 20 43 65 59
E-mail: robert-alain.toillon@univ-lille.fr

Keywords: TrkA - Co-receptors - Aggressiveness - Drug resistance

Abstract

Larotrectinib (Vitrakvi®) and Entrectinib are specific pan-Trk Tyrosine Kinase Inhibitors (TKI) approved by the Food and Drug Administration (FDA) for cancers harboring *NTRK*-fusion in 2018. Despite first enthusiasm for these compounds, French agency (HAS) recently reported their lack of efficiency. In addition, primary and secondary resistance to these Tki have been observed in absence of other mutation in cancers with NTRK-fusion. Furthermore, when TrkA is overexpressed, it promotes ligand-independent activation bypassing TKI. All these clinical and experimental observations show that genetics does not explain all therapeutic failures. It is thus necessary to explore new hypotheses to explain these failures. In this review, the current status of therapeutic strategies with TrkA inhibitors was summarized by focusing on the mechanisms potentially involved in these failures and more specifically on the role of TrkA.

Introduction

The tyrosine kinase receptor TrkA, the high affinity receptor of the Nerve Growth Factor (NGF), is essencial for both survival and differenciation of the nerve's cells. The receptor TrkA, encoded by the *NTRK1* gene, was discovered by Martin Zanca *et al*. as an oncogene in colon cancer[1]. Then, this oncogene was detected others cancers as in human breast tumor cells and in papillary thyroid carcinoma [2,3]. Somatic rearrangements occur between the tyrosine kinase domain of TrkA to the 5'-end fused with the gene encoded for another protein (TPM3, TP53, ATP1B,…). As a result, this genomic event produces a constitutively activated chimeric protein. In addition, punctual mutations, missense mutations and deletion of TrkA have been described in congenital insensitivity to pain and cancer. These mutations can affect the 3 parts of TrkA: extracellular, transmembrane and intracellular part. In cancers, mutations that increase TrkA activation independently of ligand binding or via ligand affinity binding modulation have been described. For example, P203A punctual mutation in the extracellular domain increases NGF binding to TrkA, the deleted ΔTrkA (75 AA of the extracellular domain) and NTRK-fusions result in its constitutive activation[4–6]. These last years, a special attention has been paid on *NTRK1*-fusion in cancers. In fact, in different cancers, cells with NTRK1 fusions, have been shown to have a response to Tyrosine Kinase Inhibitor (TKI) *in vitro* and *in vivo*. For this reason, different molecules including have been designed: belizatinib, AZ23, Cpd5n, PHA-E429, milciclib, GNF-5837, cabozantinib, sitravatinib, altiratinib, Larotrectinib or Entrectinib. Nowadays, 2 inhibitors, the Larotrectinib and the Entrectinib have been accepted by various drug agencies in the world. Larotrectinib (Vitrakvi®) is a specific pan-Trk TKi approved in November 2018 by the Food and Drug Administration (FDA) for cancers harboring *NTRK* fusion. Larotrectinib approval was based on three clinical trials: LOXO-TRK-14001 (NCT02122913), SCOUT (NCT02637687), and NAVIGATE (NCT02576431). Moreover, Entrectinib (Rozlytrek®) was approved around one year latter (August 2019) by the FDA for patients with NTRK-fusions. The emergence of this drug was a real breakthrough for cancer treatment. In fact, by contrast with the traditional cancer strategy treatment, Larotrectinib and Entrectinib are

approved based on biomarkers (NTRK fusion) independently of tumor cell-type. Quickly, other countries have provided authorizations for these drugs with variable restrictions. In France, Larotrectinib received a temporary authorization for cohort between April and November 2019 and then a conditional European visa in September 2019. Nevertheless, only one year latter (July 2020) French drug agency considers the apports of Larotrectinib as moderate for infantile fibrosarcoma and soft tissues sarcoma with NTRK-fusions and as insufficient for the other cancers. These disappointed conclusions were reinforced by several clinical trials in which patients' responses is absent or poor. To explain TKI failure, punctual mutations that abolished TKI binding have been proposed and new Trk inhibitors with distinct binding-mode have been generated to overcome resistance: XL184 MGCD516, DS-6051, TSR-011, DCC2701, LOXO-195 and TPX-0005. Nevertheless, TKI primary and secondary resistances have been observed in absence of mutation in cancers with NTRK-fusion, which calls into question these hypotheses. Moreover, when TrkA is overexpressed, it promotes ligand-independent activation but TKI are not efficient. It rises that genetic cannot explain all the implicated mechanisms and it is necessary to investigate other possibilities to explain these therapeutic failures.

In this review, the therapeutic potential of NGF/TrkA inhibitors (anti-NGF and TKI) in cancers as curative and palliative drugs are presented. Then, mechanisms involved in therapeutic failure will be analyzed and more particularly, besides the "genetic" mechanisms, we will expose the role of TrkA co-receptors.

10. State of art: Therapeutic potential of NGF/TrkA axis

Many studies have reported the importance of the NGF/TrkA axis in cancers. This has led to the development of molecules that block the NGF binding to its receptor or the phosphorylation of TrkA. Here, we discuss the therapeutic potential of these 2 types of compounds to cancer treatment in a curative or palliative way.

10.1. Anti-(Pro)NGF: next generation of anti-pain?

NGF/TrkA axis has been targeted using Tanezumab**,** an antibody against NGF. The efficiency of this molecule in pain treatment was first shown in osteoarthritis of knee and hip and chronic low back pain [7,8]. Moreover, in cancer, recent phase III study demonstrated that Tanezumab reduces pain cause by bone metastasis [9]. Nevertheless, Tanezumab has been associated with adverse effects including arthralgia and paresthesia [8]. It is probably due to the fact that NGF can also bind $P75^{NTR}$, it low affinity receptor. $P75^{NTR}$ has no kinase domain, but thank's to death domains $P75^{NTR}$ can activate the RhoA pathway. To bypass this problem, anti-NGF inhibitors that have different binding modes than Tanezumab have been generated like peptide A2 or BVNP-0197 (peptide that binds the loop II/IV of the NGF)[10,11]. Although side effects still need to be reduced, NGF inhibitors remain interesting tools to increase the quality of life of cancer patients. Especially since these anti-NGFs have shown no effect leading to tumor growth or increased metastasis.

1.2. Kinase inhibitors: next generation of target therapies?

In addition to anti-NGFs, the investigations have been focused on the development and the use of tyrosine kinase inhibitors as targeted therapy against TrkA. The kinase activation loop contains a conserved Asp-Phe-Gly sequence, call DFG motif, which regulates its enzymatic activity. This loop is ordered when TrkA is inactive which prevents ATP binding to the active site by an allosteric effect. In the DFG-out conformation, the phenylalanine of the DFG motif is located in an hydrophobic pocket whereas the DFG-in conformation is characterized by a rotation of the DFG residues out of the active site [12]. As a result, ATP can bind to the kinase and transfers its phosphate group. Pan-Trk inhibitors Lestaurtinib, Larotrectinib and Entrectinib bind the kinase pocket of TrkA to prevent ATP binding (ATP competitor) and its phosphorylation. Although they have a similar action, they are different because of their specificity and their efficiency.

Lestaurtinib (CEP-701) is an analog of K252a orallly administrated. These molecules are indozolocarbazole staurosporine derivative inhibitors. It was the first TrkA inhibitor to demonstrate an effect *in vitro* and *in vivo* (preclinical

model) in prostatic cancers [13]. Other studies suggest that K252a also has an effect on pancreatic and breast cancers [14,15]. Nevertheless, the results of clinical trials in both solid and blood cancers were disappointed (Collins et al., 2007). For instance, Lestaurtinib fails to achieve the primary goal of reducing circulating PSA (Prostate Specific Antigen) levels in the blood. Interestingly, *in vitro* CEP-701 decreased the number of cancer cells but result in more PSA production. This first observation shows the importance of the choice of the parameters for monitoring the response. Moreover, it was proposed that the bioavailability of CEP701 is not optimal and did not allow to obtain the desired therapeutic effect (Collins et al., 2007). In pancreatic cancer, a combination of gemcitabine and CEP701 was evaluated (phase I clinical trial). This trial was discontinued due to the absence of benefit and adverse effects (nausea, vomiting, fever…) (Chan et al., 2008). CEP701 Side effects have been attributed to its lack of specificity. In fact, CEP701 was a multi-kinase inhibitor that inhibits in addition to TrkA, TrkB, TrkC, FLT3, FGFR and JAK2. So, CEP-701 effects on cancer with alterations of JAK2 and FLT3 have been evaluated. Various responses have been obtained depending of the cancer type. For example, a phase II trial of Lestaurtinib in 22 patients with relapsed or refractory JAK2-mutated myelofibrosis demonstrated an overall response rate of 27 %, with a median duration of 14 months [17]. By contrast, similar clinical trial for polycythaemia vera or essential thrombocythaemia with JAK2 mutation was very disappointing: only a modest reductions in JAK2-V617F allele burden and spleen size in subsets of treated patients [18]. For both acute myeloid leukemia (AML)[19] and Acute Lymphocytic Leukemia (ALL) [20] FLT3 mutated, no benefit on overall survival was demonstrated of Lestaurtinib in addition to chemotherapy. However, for AML and ALL in a subset of patients who achieved sustained levels of FLT3 inhibitory activity, Lestaurtinib correlated with lower rates of relapse and improved overall survival[20,21]. It rises the potential for blood cancers of TKI but also the importance of patient selection [20]. In solid cancers, to explain the lack of efficiency of Lestaurtinib different hypotheses have been made as low bioavailability and/or specificity[16]. More recently, an intrinsic resistance mechanism involving NF-kappa B signaling has also been described[22]. Moreover, new Trk inhibitors have been designed in order to overcome the low bioavailability and

specificity of Lestaurtinib. Nowadays, 2 of them are approved by the FDA (Food and Drug Association) for the treatment of cancers harboring NTRK fusion: Larotrectinib (LOXO-101) and Entrectinib.

Both Larotrectinib and Entrectinib inhibit phosphorylation of the 3 members of the Trk family (TrkA, B and C). Both inhibitors have been described to have an activity in cancers harboring NTRK-fusions but Larotrectinib is more specific than Entrectinib that also inhibits ALK and ROS. NTRK1-fusion results in an intracellular protein. NTRK1-fusion is a driver mutation identified across diverse cancers. This mutation results from a chromosomal fusion of the sequence encoding the intracellular domain of TrkA and another protein sequence. The literature reports fusions of NTRK1 with various proteins: BCAN (Brevican), LMNA (Lamin A/C), NFASC (Neurofascin), TPM3 (Tropomyosin 3), MDM4, PEAR1 (Platelet Endothelial Aggregation Receptor-1), CGN (Common Gα Numbering), GATAD2B (GATA Zinc Finger Domain Containing 2B) [23]. All of these *NTRK1* alterations lead to the overexpression of a chimeric protein without the extracellular and transmembrane domain of TrkA. For instance, TPM3-NTRK1 fusion protein is composed of the N-terminal domain of TPM3 (codons 1-221) and the transmembrane/intracellular domains of TrkA (codons 419-end). Fusion proteins that have an intracellular (cytoplasmic) localisation have a ligand independent activation. As a result, TrkA signaling pathways (MAPK, Akt, PLC) are consecutively activated. This oncogene addiction explains why cancers harboring fusions have a primary response to Larotrectinib and/or Entrectinib[4]. A clinical trial on 159 adult and pediatric patients with TRK fusion-positive solid tumors demonstrated that Larotrectinib treatment shows a response of 35.2 months (median) and a progression-free survival of 28.3 months (median) [24]. Moreover, Larotrectinib may be more efficient to improve quality of life in pediatric and adult cancers [25]. Larotrectinib seems also more efficient than Entrectinib in Non-Small Cell Lung Cancer. In fact, treatment with larotrectinib and entrectinib resulted respectively in 5.4 and 1.2 median progression life-years and 7.0 and 1.8 median total life-years[26]. Even though the recent authorization of Larotrectinib and Entrectinib, these inhibitors only demonstrate efficiency in patients harboring *NTRK*-fusion and the mutation

frequency depends on the tumor type. In fact, NTRK1-fusions are frequent in spitz tumors (16 %) but rare in the most frequent cancers. For example, for the most aggressive and clinical challenging Triple Negative Breast Cancer subtype (TNBC), Wu and coll. report only 13 patients with NTRK fusion for 305 TNBC using FISH. Moreover, another pitfall is that even if a primary response was observed, others Trk alterations can occur and compromise Larotrectinib or Entrectinib effects on tumor with NTRK-fusion.

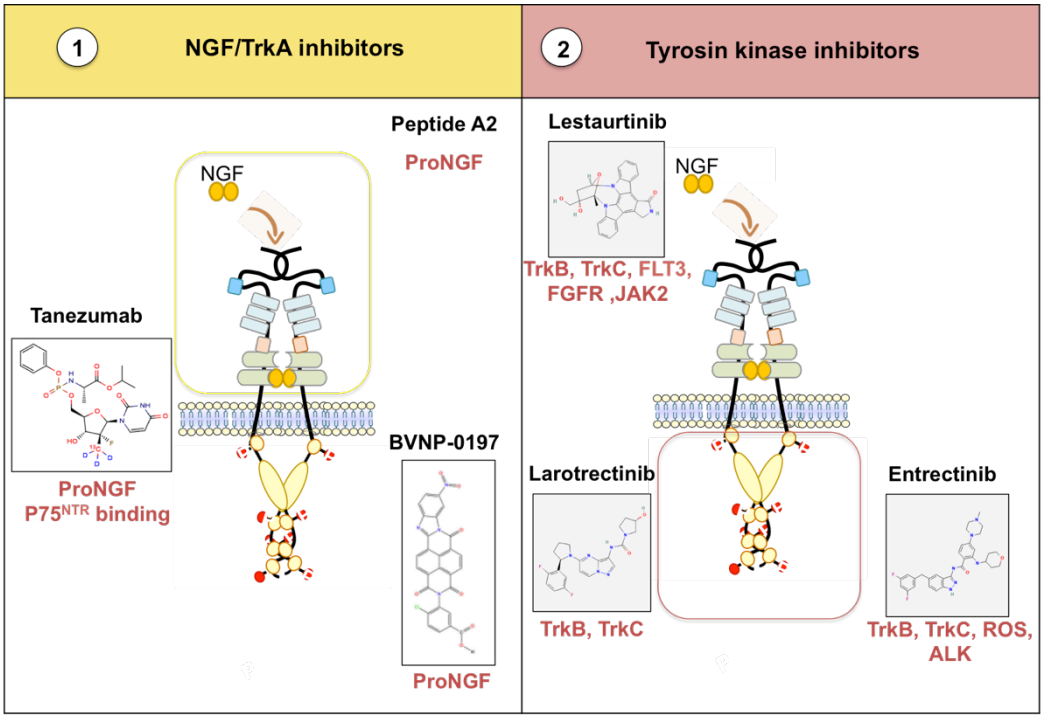


Figure 1: NGF/TrkA inhibitors. Two main types of molecules have been designed to impedes NGF/TrkA signaling (1 & 2). They have different off target (red). First, molecules that block NGF/TrkA association (1). The Tanezumab is a monoclonal antibody that bind on NGF. Peptide A2 and BVNP-0197 also bind on NGF but does not promote $P75^{NTR}$ signaling. Second compounds that inhibit TrkA phosphorylation (2). The 3 inhibitors are ATP competitor but have different specificity.

1.3. Second generation of Trk inhibitors for cancers with punctual mutation(s)

While NTRK-fusions are rare events (0.3 %), genomic (point mutations, amplification) and transcriptomic (overexpression) *NTRK* alterations occur at

higher frequencies (14 % of samples) and may contribute to TKI resistance [27,28]. Indeed, point mutations have been reported to cause secondary resistance to Entrectinib or Larotrectinib. These point mutations affect different residues near to the TrkA ATP-binding pocket: F589L G595R, G667C, G667S, V573M. As a result, it impairs TKI fixation on the ATP-ase site of TrkA. To overcome this resistance LOXO-195 that differently binds TrkA than LOXO-101 has been designed. LOXO-195 is efficient for cancers with point mutations of TrkA [29]**.** These point mutations have also be reported to be responsible of primary resistance [28]. While there are great hopes in these molecules, the contribution of Larotrectinib already appears to be moderate and even insufficient (HAS, technical control, 22/09/2021) and punctual mutations are not always found in patients with TKI resistance.

1.4. *TrkA inhibitors + other TKI for cancers with co-alterations?*

Another resistance mechanism relies on intracellular alterations is co-alterations of TrkA. Co-alterations of TrkA frequently affect TrkA signaling molecules: PI3K signaling (61 % of patient samples) and MAPK pathways (32 % of patient samples). In addition, these mutations can also alter cell-cycle machinery (58 % of patient samples) and tyrosine kinase families (58% of patient samples)[27]. Nevertheless, investigations of genomic events in tumors with primary and secondary resistance show that they cannot recapitulate all TKI resistance mechanisms.

2. *Genomic alterations cannot recapitulate all resistance mechanisms*

Interestingly, cut-off that defined NTRK-fusion positive tumor is 15 % of cells. So, a large number of cells of NTRK-fusion positive tumor do not expresse the chimeric Trk protein but expresse a full-length TrkA (containing its extracellular part). This full-length TrkA has an extracellular domain that allows NGF and ProNGF fixation. Upon ligand fixation, TrkA is phosphorylated and signaling pathways are activated. As a resut this full length TrkA promote tumor growth and metastasis. TrkA is expressed in various cancers including lung, breast, prostate and colon and it overexpression is associated with a poor prognosis[1,30–32].

2.1. Can TrkA homodimerization explain the lack of TKI efficiency?

Studies using TrkA overexpression showed that it promotes cancer development and metastatic process of non-neuronal tumors. Interestingly, in normal breast epithelial cells, TrkA is expressed and ligand fixation leads to TrkA phosphorylation but does not promote proliferation and survival as in breast cancer cell lines[33]. It is probably due to the fact that, in cancer cells, downregulation of phosphatase may lead to less negative feedback of kinase[34]. Using siRNA directed against TrkA or TrkA overexpression in cell lines, studies show that TrkA promotes cancer development and metastatic process of different non-neuronal tumors including breast, prostate and colon [31,35,36]. TrkA overexpression results in TrkA constitutive activation but at a lower level than the fused TrkA protein. Moreover, when TrkA is overexpressed TrkA phosphorylation is still ligand inducible. Nevertheless, while TrkA overexpression is more frequent among cancers than NTRK-fusion, TKI effect on cancer cells overexpressing TrkA has been less study than in cells harboring NTRK-fusion. Using immortalized breast cells MCF10A, Kyker-Snowman and coll. have tested the effect of Larotrectinib on non-mutated TrkA overexpressing cells. Interestingly, they demonstrated that Larotrectinib inhibited TrkA phosphorylation and cell survival *in vitro* [37]. Nevertheless, *in vivo* experiment was done using MCF7 breast cancer cell line overexpressing TrkA and not “normal” breast cells MCF10A. So this paper does not permit to conclude on the potential of Larotrectinib *in vivo* when TrkA is overexpressed. Moreover, to the best of our knowledge Larotrectinib and Entrectinib had not demonstrated an effect during a clinical trial in cancers overexpressing TrkA. Because principal function of TrkA extracellular and transmembrane domains are respectively binding ligand and conformational change, it was hypothesis that this resistance resulted of TrkA homodimerization and transactivation induced by NGF and/or ProNGF. But molecules blocking ligand fixation on TrkA were not able to abolish all TrkA pro-tumorigenic effects. So TrkA homodimerization could not recapitulate all the biological effects. Hence, TrkA co-receptor(s) can modulate it signaling. Indeed, numerous studies have focused on $P75^{NTR}$/TrkA interaction to explain such discrepancies. Nevertheless, it seems that TrkA interactome is much more complex and TrkA interplays not only with $P75^{NTR}$.

2.2. Can TrkA and their co-receptors elicit TKI lack of efficiency?

TrkA co-receptors may acts through 1) Modulation of TrkA-ligand affinity, 2) TrkA phosphorylation or 3) TrkA phospho-independent pathways. These associations can be induced in a ligand-dependent and independent manner. In both cases, The TrkA/co-receptor association modulates TrkA structure/function and may contribute to TKI failure.

First, TrkA hetero-complexes can favor ligand binding. The $P75^{NTR}$ receptor is a member of the tumor necrosis factor receptor superfamily. It is a type II receptor encoded by the *NGFR* (Nerve Growth Factor Receptor) gene located on the 17q21-q22. The affinity of the NGF for this receptor is weaker (10^{-9} M) than TrkA affinity (10^{-11}M) [38]. The formation of the $P75^{NTR}$/TrkA heterodimer (stoichiometry 1:2:1) induces a 100-fold increase of NGF affinity to TrkA [39,40]. As we previously described, 2 mechanisms were proposed to explain how $P75^{NTR}$ increase NGF affinity to TrkA *via* its extracellular domain[41]. The most probable model is the ligand passing model: $P75^{NTR}$ presents NGF to TrkA and so do not interact directly with TrkA. This extracellular indirect interaction of $P75^{NTR}$/TrkA promotes TrkA activation, signaling and so pro-tumoral effects of TrkA. In addition, we recently demonstrated that a mimetic peptid of the C-ter region of CD44v3 (called P4), promote NGF binding on TrkA by microscale thermophoresis (Trouvilliez *et al*., submitted). The glycoprotein CD44 (Cluster of Differenciation 44), encoded by *CD44* gene (20 exons) located on locus 11p13. The transcription of *CD44* allows the production of a standard form consisting of exons 1 to 5 and exons 6 to 10. The alternative splicing of the 10 central exons of *CD44* permits the production of more than 20 isoforms[42]. Two of these isoforms, CD44v3 and CD44v6, have been described to promote ligand binding on RTK [43–45]. Especially, EGF binding on the heparan sulfate chain of CD44v3 promote its binding on the EGFR and it activation. Interestingly, beacause a mimetic peptide of CD44v3 promote NGF binding to TrkA, TrkA extracellular domain conformational change and TrkA phosphorylation[46]. Moreover, we previously demonstrated that TrkA/CD44v3 involved C-ter region of CD44v3, interaction promote NGF binding to TrkA. Alltogether these results suggest

that the mechanism by wich CD44v3 promoted NGF binding on TrkA and EGF binding on EGFR are different[47].

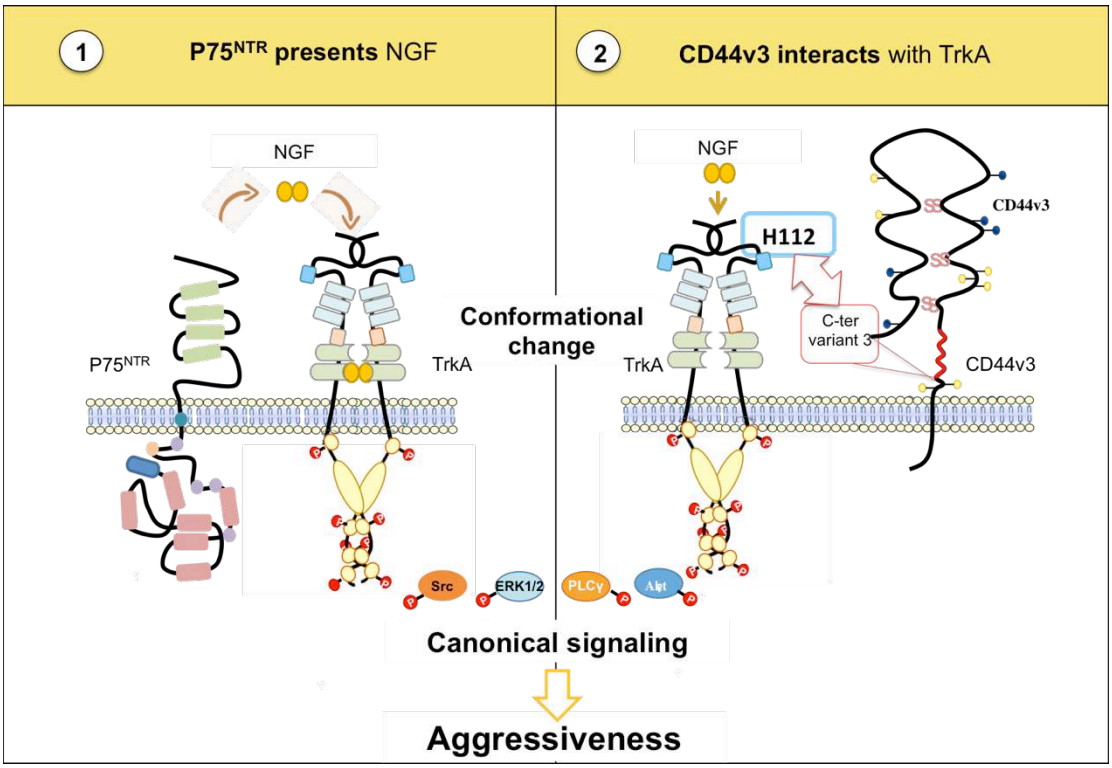


Figure 2: Comparison of P75^{NTR} and CD44v3 role on NGF binding to TrkA. P75^{NTR} presents NGF to TrkA (1) whereas CD44v3 interacts with TrkA (2) to increase NGF affinity to TrkA.

Second, the co-receptors can regulate TrkA activation *via* their intracellular part. The association TrkA/P75^{NTR} not only involves extracellular part of these 2 receptors. In fact, the formation of the complex TrkA/P75 ^{NTR} was proposed to rely on intracellular interactions with the receptor Kidins220 [48]. The intracellular parts of the receptors are also crucial in the pro-tumoral effect of this complex. First, P75 ^{NTR} delays TrkA ubiquitination *via* TRAF6 and so TrkA internalization [49,50]. Second, NGF stimulation of TrkA promotes P75^{NTR} cleavage and the intracellular fragment of P75^{NTR}, called P75^{NTR}-ICD, induces a conformational change of TrkA extracellular domain that promotes it signaling [51]. In turn, TrkA activation increases P75^{NTR} cleavage by ADAM17 that produces the fragment P75^{NTR}-CTF. This fragment is relocalized in endosomes where it is cleaved by gamma-secretase to produce the fragment P75^{NTR}-ICD [52]. In addition, GPCR (G-Protein Coupled Receptors)

transactivate TrkA. GPCR is a family of receptors encoded by more than 800 genes. GPCR are seven-transmembrane receptors that bound heterodimeric G proteins inactive (GDP). When ligand-fixation on GPCR occurs, the GPCR changes of conformation that activates (GTP) and dissociates from the G protein. This free protein G can activate various signaling partners thanks to GTP hydrolysis. Different GPCR have been reported to transactivate TrkA especially in neuronal PC12 cells. In PC12 cells, derived of rat adrenal medullary tumor, the A2a receptor following its activation by adenyl cyclase activates TrkA that promote Akt, ERK1/2 and SAPK/JNK but not p38 MAPK. Interestingly this mechanism is calcium dependent [53,54,53,54]. In addition, others ligand of GPCR have been reported to support TrkA transactivation in PC-12 including PACAP (pituitary adenylate cyclase-activating protein) or LPA1 (lysophosphatidate 1). In NG108 cells, a hybrid between neuroblastoma and glioma, (AT2 Angiotensin 2) receptor activation by Ang II induces the phosphorylation of TrkA. TrkA activation results in a sustained MAPK (p42/p44) activation that promotes neurite outgrowth [55]. Interestingly, MAPK activation mechanism does not relies on PKA (Protein Kinase A) activation but on Fyn, a member of the Src Family Kinases[56]. Moreover, GPCR activation can be ligand-induced but also ligand-independent. For instance, NOX-2 (NADPH oxidase 2), the major ROS (Reactive Oxygen Species), can via $p47^{phox}$ phosphorylation activates the GPCR FPR1 and so TrkA transactivation[57]. The TrkA transactivation by GPCR induces MAPK activation much delayed compared with that induced by NGF activation or following other RTKs activation including EGFR. Members of the Epidermal growth factor family have also been shown to be involved in the control of TrkA activation. A crosstalk between TrkA and EGFR signaling has been demonstrated in monocytes. In fact, inhibition of TrkA phosphorylation results in EGFR inhibition and the specific EGFR inhibitor, Tyrphostin AG1478, abolished TrkA phosphorylation. Moreover, knock-out of EGFR by siRNA abolished NGF-induced TrkA phosphorylation (Tyrosin 490) and reciprocally siTrkA abolished EGFR phosphorylation EGF-induced[58]. More recently, in cancers, the combination of TrkA inhibitor GNF5837 (ATP competitor) and the EGFR specific inhibitor Erlotinib demonstrates it efficiency *in vitro* and *in vivo* [59]. Moreover, the receptor HER2 ($p185^{HER2}$), is overexpressed in breast

cancer (30 %) and is associated with a lower free survival and brain metastasis[60]. Interestingly, by coimmunoprecipitation Tagliabue et coll. have demonstrated that NGF stimulation promotes TrkA/HER2 complex formation, fellowed by the phosphorylation of HER2 that activates MAPK signaling and so promotes cell proliferation [61].

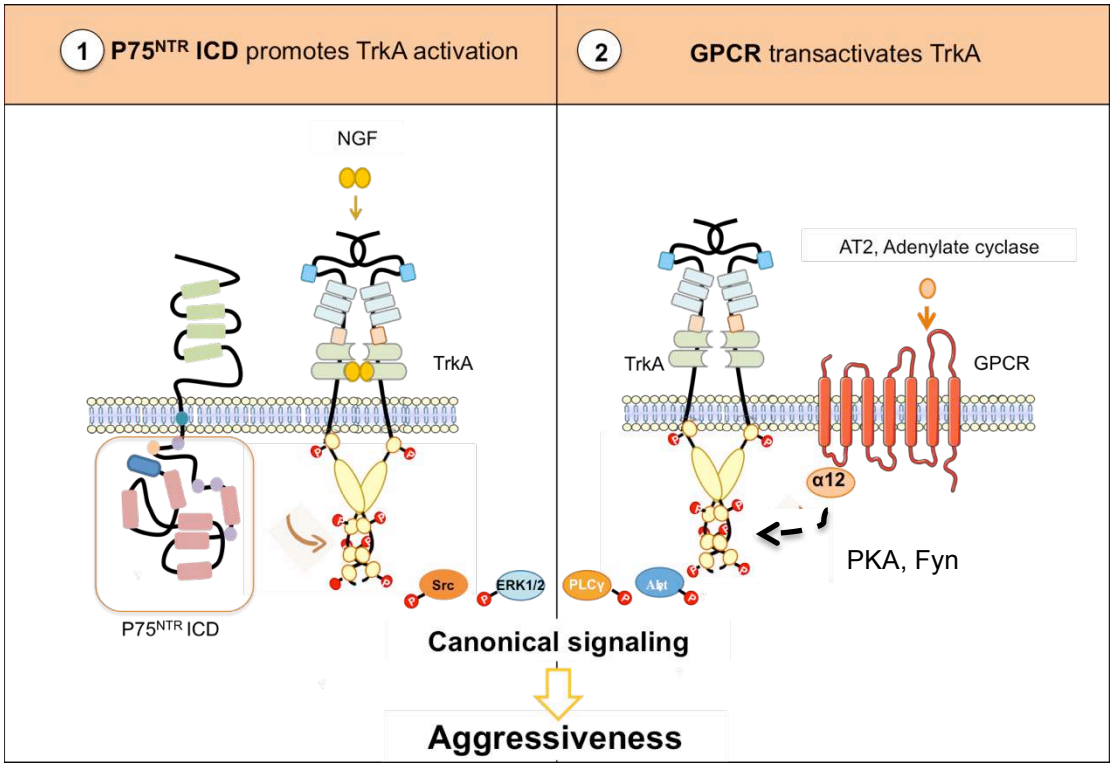


Figure 3: P75^{NTR} and GPCR promote activation of TrkA via their intracellular part. Following NGF stimulation, intracellular part of P75^{NTR} is cleaved and promote TrkA phosphorylation. In addition, GPCR transactivate TrkA via different proteins (PKA, Fyn…) in a ligand-independent-manner.

Third, co-receptors can activate TrkA phospho-independent pathway. CD44v3 interaction with TrkA is associated with an phospho-independent signaling pathway implying: p115RhoGEF/RhoA/RhoC/ROCK1 (Aubert et al., 2015). Interestingly, this signaling is not affect by K252a, LOXO-101 or Entrectinib treatment that inhibit pTrkA (Trouvilliez et al., submitted). So, TrkA/CD44 and their signaling partners may represent a promising target to overcome LOXO-101 resistance in TrkA overexpressing cancers. Interestingly, P75^{NTR} can also activate GTPases including RhoA and NGF results in its inactivation [63–65]. Hence, dynamic RhoA activation permits

dynamic activation of actin and so migration (cancer cells) or differentiation neurons). Additional investigations are needed to understand the role of TrkA/P75^{NTR} and NGF/TrkA/CD44v3 in dynamic RhoA activation. In addition, TrkA phosphorylation can also be induce by ProNGF that promotes other(s) resistance mechanism(s). Recently, our team has shown the role of EphA2 (Ephrin type-A receptor 2) in breast cancer aggressiveness and TKI resistance (Lévêque et al., 2009). EphA2 is a tyrosine kinase receptor of 135 kDa. This receptor is a member of the A-family of Eph kinases. EphA2 has 8 different ligands (ephrin A) anchored to cell membrane [66]. Its overexpression has been reported in different cancers including breast and is associated with higher tumor aggressiveness. In breast cancer, EphA2 overexpression is associated with the most aggressive triple negative breast cancer subtype [67]. The overexpression of the receptor EphA2 in MCF10A cells leads to their malignant-transformation. The overexpression causes defects in cell-cell contacts[68]. Moreover low molecular weight tyrosine phosphatase has been reported to inhibit EphA2 phosphorylation[69]. However, EphA2 can be phosphorylated by a ligand-independent mechanism. The phosphorylation of the serine 897 of EphA2 by Akt promotes EphA2 relocalization at the front edge and so promotes migration induced by different growth factors [70]. On the contrary, ligand fixation on EphA2 inhibits EphA2 relocalization and chemotaxis. Moreover, our team has highlighted another mechanism in which EphA2 promotes metastasis *via* ProNGF. In fact, in breast cancer, ProNGF stimulation (0.5 nM) causes the formation of the complex TrkA/EphA2/Sortilin that induces the phosphorylation of Src with a pTrkA independent mechanism. Interestingly, by siRNA we highlight that this signaling is dependent of EphA2[71]. So, targeting TrkA/CD44v3 and TrkA/EphA2 and their downstream signaling pathways may be interesting for tumors with respectively high NGF and ProNGF staining.

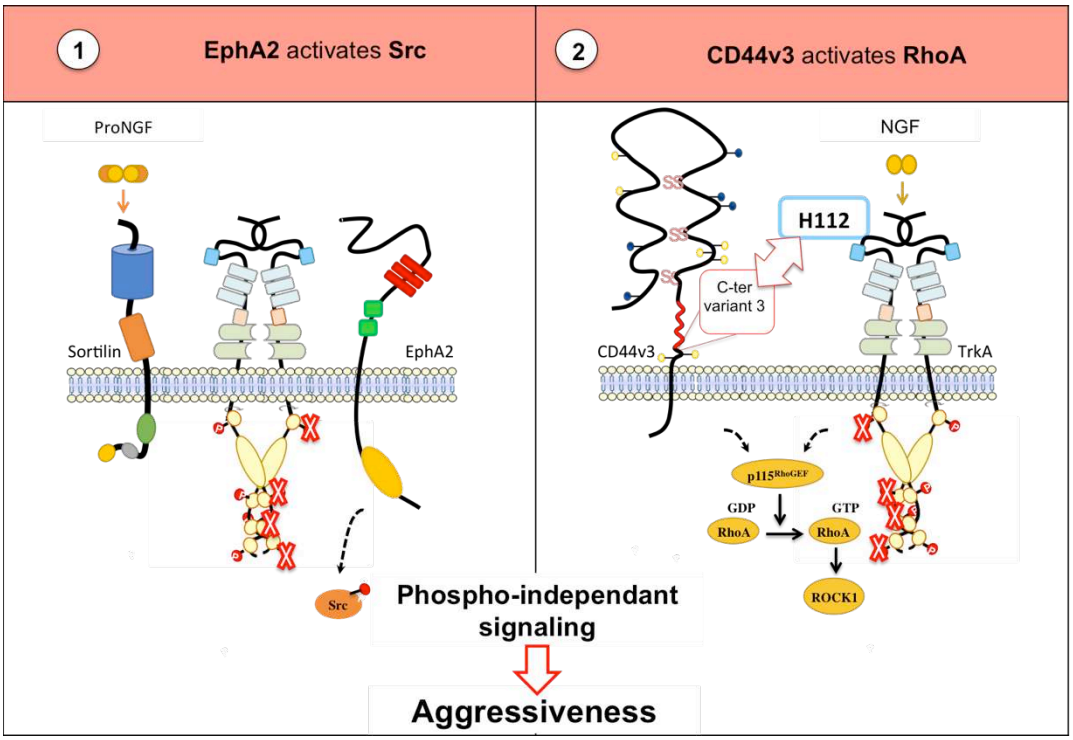


Figure 4: CD44v3 and EphA2 promote activation of TrkA phospho-independent pathway. Following NGF stimulation, TrkA interacts with CD44v3. CD44v3 permits RhoA activation independently of TrkA phosphorylation. Following ProNGF stimulation, TrkA/EphA2 association occurs and permits Src phosphorylation independently of TrkA phosphorylation. As a result, TrkA/CD44v3 and TrkA/EphA2 contribute to breast cancer aggressiveness and TKI failure.

Perspectives

In this review, we exposed the place of NGF/TrkA inhibitors in cancer therapeutic strategy. First, anti-NGF compounds may be useful in a palliative way. Second, TKI (Larotrectinib and Entrectinib) seems globally disappointing even for cancers. Even thought for cancers harboring *NTRK*-fusion a primary response can be achieved it not always the case. Actually, it is probably due to the fact that not all tumor cells harbored NTRK-fusion. Cells without NTRK-fusion may contribute to the emergence of acquired resistance (TrkA punctual mutations and co-alterations). These resistance mechanisms may be bypassed using respectively allosteric Trk inhibitors and combination of Trk inhibitors with another TKI. But, TrkA mutation and co-alterations cannot explained all resistance mechanisms. In addition to these 2 genetic

mechanisms, we depicted how TrkA co-receptors contribute to TKI therapeutic failure. We described 3 mechanisms of action of TrkA co-receptors: ligand affinity enhances, TrkA transactivation, activation of phospho-independent pathway. To bypass this type of resistance mechanisms, different approaches should be promising. First, TKI may be used in combination with Protein-Protein inhibitors (PPI). PPI choice may be done according to TrkA/co-receptor complexe(s) harbored by the tumor. Nevertheless, this approach needs to investigate optimal concentrations of the 2 compounds. Moreover, as TKI, PPI inhibitors may not only bind to TrkA but also TrkB/C and result in side effects. To avoid this problem, TrkA allosteric inhibitors (type III) that specifically bind to TrkA juxtamembrane region have been designed [72–74]. Interestingly, this region is critical for TrkA/CD44v3 signaling and its role in triple negative breast cancer cell migration[75]. Design of a new allosteric TrkA inhibitor that impedes TrkA/CD44v3 signaling may be a new therapeutic opportunity to avoid metastasis in triple negative breast. Nevertheless, this approach may result in secondary resistance due to the interaction of TrkA with other co-receptors. Hence, a TrkA inhibitor that act as molecular glue to stabilize TrkA dimers have been designed (VMD-928). These inhibitors are selective to TrkA and binds ATP-binding site [76]. The efficiency of the VMD-928 is currently evaluated in patients with different cancers overexpressing TrkA (adenoid cystic carcinoma, cholangiocarcinoma, lung cancer, pancreatic cancer, parotid, and squamous cell carcinoma of head and neck; phase I clinical study) [77]**.** Even though these new TrkA inhibitor could increase survival of patients with a cancer overexpressing TrkA, others Receptors Tyrosin Kinase are overexpressed in cancers and could compromise the long-lasting efficiency of TrkA inhibitors. However, knowledge of TrkA/co-receptors may be not only useful for development of new palliative cancer treatment.

To avoid side effects and ensure efficiency, ADC (Antibody Drug Conjugated) have been developed these last years. To do so, ADC are composed of a humanized antibody that recognizes membrane proteins that are specific to cancer cells, a linker and a play load that are highly cytotoxic (tubulin inhibitors DNA-damaging agents)[78]. Major challenge in ADC development is the identification of cancer-specific membrane proteins. Hence, recently, we

showed that TrkA/CD44v3 is specific to breast cancer cells. So, this complex may be used specific delivery of a drug to breast cancer cells. It should be interesting to investigate the formation of this complex in others cancers types. Moreover, others TrkA/co-receptors may be also specific to cancer tissues. Further investigations are needed to explore TrkA/co-receptors specificity across cancers but advantage of such strategy is its adaptability. In fact, proximity ligation assay can be quickly and easily performed on cancer tissues along cancer treatment to identify TrkA/co-receptor associations. As a result, even if TrkA/co-receptor evolved, ADC that recognizes another complex may be used. At least, here, we focused on TrkA co-receptors, but similar mechanisms should exist with others RTK. So, these considerations may be useful not only for the design of new TrkA inhibitors but more generally to target therapy against RTK. At least, understanding of mechanisms that regulate Trk activation could have an impact not only for cancer treatment but also for the treatment of others diseases including chronical pain, inflammatory diseases or neuropathology. For example, in Alzheimer disease a deficit in NGF/TrkA signaling and an increase of ProNGF/P75^{NTR} signaling has been demonstrated [79]. But mechanisms involved in this shift between NGF/TrkA and ProNGF/P75^{NTR} signaling is still unclear and TrkA co-receptors could play a role in this unbalance.

TrkA/Co-receptors are :	1 Involved alternative pathway		2 Cancer cells specific
Therapeutic strategy	Combinaison Trk inhibitor + others inhibitor	Allosteric inhibitors Competition glue	ADC
Theorical long lasting Therapeutic effect	Relapse due to other TrkA alternative pathway	Relapse due to other RTK pathway	Relapse due to other(s) TrkA/co-receptor
			Quick treatment adaptation

Table 1: Used of TrkA/co-receptors in cancer treatment.

References

1. Martin-Zanca D., Hughes S. H. & Barbacid M. A human oncogene formed by the fusion of truncated tropomyosin and protein tyrosine kinase sequences. *Nature* **319**, 743–748 (1986).

2. Butti M. G. *et al.* A Sequence Analysis of the Genomic Regions Involved in the Rearrangements between TPM3 and NTRK1 Genes Producing TRK Oncogenes in Papillary Thyroid Carcinomas. *Genomics* **28**, 15–24 (1995).

3. Greco A. *et al.* The DNA rearrangement that generates the TRK-T3 oncogene involves a novel gene on chromosome 3 whose product has a potential coiled-coil domain. *Mol. Cell. Biol.* **15**, 6118–6127 (1995).

4. Drilon A. TRK inhibitors in TRK fusion-positive cancers. *Ann. Oncol.* **30**, VIII23–VIII30 (2019).

5. Arevalo J. C. *et al.* A novel mutation within the extracellular domain of TrkA causes constitutive receptor activation. *Oncogene* **20**, 1229–1234 (2001).

6. Reuther G. W., Lambert Q. T., Caligiuri M. A. & Der C. J. Identification and Characterization of an Activating TrkA Deletion Mutation in Acute Myeloid Leukemia. *Mol. Cell. Biol.* **20**, 8655–8666 (2000).

7. Tive L. *et al.* Pooled analysis of tanezumab efficacy and safety with subgroup analyses of phase iii clinical trials in patients with osteoarthritis pain of the knee or hip. *J. Pain Res.* **12**, 975–995 (2019).

8. Kivitz A. J. *et al.* Efficacy and safety of tanezumab versus naproxen in the treatment of chronic low back pain. *Pain* **154**, (2013).

9. Nalley C. Study Explores Efficacy & Safety of Tanezumab for Cancer Pain. *Oncol. Times* **43**, 24–24 (2021).

10. Poole A. J. *et al.* A C-terminal cysteine residue is required for peptide-based inhibition of the NGF/TrkA interaction at nM concentrations: implications for peptide-based analgesics. *Sci. Rep.* **9**, 1–11 (2019).

11. Kennedy A. E. *et al.* Nerve growth factor inhibitor with novel-binding domain demonstrates nanomolar efficacy in both cell-based and cell-free assay systems. **5**, (2017).

12. Somwar R. *et al.* NTRK kinase domain mutations in cancer variably impact sensitivity to type I and type II inhibitors. *Commun. Biol.* **3**, 1–13 (2020).

13. George D. J. *et al.* Sustained in Vivo Regression of Dunning H Rat Prostate Cancers Treated with Combinations of Androgen Ablation and Trk Tyrosine Kinase Inhibitors, CEP-751 (KT-6587) or CEP-701 (KT-5555)1. *Cancer Res.* **59**, 2395–2401 (1999).

14. Miknyoczki S. J., Chang, H., Klein-Szanto, A., Dionne, C. A. & Ruggeri, B. A. The Trk tyrosine kinase inhibitor CEP-701 (KT-5555) exhibits significant antitumor efficacy in preclinical xenograft models of human pancreatic ductal adenocarcinoma. *Clin. Cancer Res.* **5**, 2205–2212 (1999).

15. Dollé L., El Yazidi-Belkoura I., Adriaenssens E., Nurcombe V. & Hondermarck H. Nerve growth factor overexpression and autocrine loop in breast cancer cells. *Oncogene* **22**, 5592–5601 (2003).

16. Collins C., Carducci, M.A. Eisenberger M.A., Partin J.T., Partin A.W., Pili R., Sinibaldi V., Walczak J.S., Denmeade S.R. Preclinical and Clinical Studies with the Multi-Kinase Inhibitor CEP-701 as Treatment for Prostate Cancer Demonstrate the Inadequacy of PSA Response as a Primary Endpoint. *Cancer Biol. Ther.* **23**, 1–7 (2007).

17. Mascarenhas J., Baer M.R., Kessler C., Hexner E., Tremblay D., Price L., L Sandy, Weinberg R., Pahl R., Silverman L.R., Goldberg J.D., Kosiorek H., Dueck A. Phase II trial of Lestaurtinib, a JAK2 inhibitor, in patients with myelofibrosis. *Leuk. Lymphoma* **176**, 139–148 (2019).

18. Hexner E. *et al.* Open-label study of oral CEP-701 (lestaurtinib) in patients with polycythaemia vera or essential thrombocythaemia with JAK2-V617F mutation. *Br. J. Haematol.* **164**, 83–93 (2014).

19. Levis M. *et al.* Results from a randomized trial of salvage chemotherapy followed by lestaurtinib for patients with FLT3 mutant AML in first relapse. *Blood* **117**, 3294–3301 (2011).

20. Brown P. A. *et al.* FLT3 inhibitor lestaurtinib plus chemotherapy for newly diagnosed KMT2A-rearranged infant acute lymphoblastic leukemia: Children's Oncology Group trial AALL0631. *Leukemia* **35**, 1279–1290 (2021).

21. Knapper S. *et al.* A randomized assessment of adding the kinase inhibitor lestaurtinib to first-line chemotherapy for FLT3-mutated AML. *Blood* **129**, 1143–1154 (2017).

22. Holz M. S. *et al.* Induction of Endoplasmic Reticulum Stress by Sorafenib and Activation of NF- B by Lestaurtinib as a Novel Resistance Mechanism in Hodgkin Lymphoma Cell Lines. *Mol. Cancer Ther.* **12**, 173–183 (2013).

23. Wilson T., Sokol E. S., Ross J. S. & Maund S. L. 131P NTRK1/2/3 fusions in secretory versus non-secretory breast cancers. *Ann. Oncol.* **31**, S292 (2020).

24. Hong D. S. *et al.* Larotrectinib in patients with TRK fusion-positive solid tumours: a pooled analysis of three phase 1/2 clinical trials. *Lancet Oncol.* **21**, 531–540 (2020).

25. Kummar S. *et al.* Quality of Life in Adult and Pediatric Patients with Tropomyosin Receptor Kinase Fusion Cancer Receiving Larotrectinib. *Curr. Probl. Cancer* **45**, 100734 (2021).

26. Roth J.A., Carlson J.J., Fang Xia P., Williamson T., Sullivan S.D. The potential long-term comparative effectiveness of larotrectinib and entrectinib for second-line treatment of trk fusionpositive metastatic lung cancer. *J. Manag. Care Spec. Pharm.* **26**, 1616–1617 (2020).

27. Okamura R. *et al.* Malignancies : Implications for NTRK-Targeted Therapeutics. (2019). doi:10.1200/PO.18.00183.Analysis

28. Fuse M. J., Okada K., Oh-hara T., Ogura H. & Fujita N. Mechanisms of resistance to NTRK inhibitors and therapeutic strategies in NTRK1-rearranged cancers. 3–8 (2017). doi:10.1158/1535-7163.MCT-16-0909

29. Drilon A. *et al.* A next-generation TRK kinase inhibitor overcomes acquired resistance to prior trk kinase inhibition in patients with TRK fusion-positive solid tumors. *Cancer Discov.* **7**, 963–972 (2017).

30. Gao F. *et al.* The neurotrophic tyrosine kinase receptor TrkA and its ligand NGF are increased in squamous cell carcinomas of the lung. *Sci. Rep.* **8**, 1–11 (2018).

31. Lagadec C. *et al.* TrkA overexpression enhances growth and metastasis of breast cancer cells. *Oncogene* **28**, 1960–1970 (2009).

32. MacGrogan D., Saint-André J.-P. & Dicou E. Expression of Nerve Growth Factor and Nerve Growth Factor Receptor Genes in Human Tissues and in Prostatic Adenocarcinoma Cell Lines. *J. Neurochem.* **59**, 1381–1391 (1992).

33. Descamps S. *et al.* Nerve Growth Factor Stimulates Proliferation and Survival of Human Breast Cancer Cells through Two Distinct Signaling Pathways *. **276**, 17864–17870 (2001).

34. Qi X. M., Wang F., Mortensen M., Wertz R. & Chen G. Targeting an oncogenic kinase/phosphatase signaling network for cancer therapy. *Acta Pharm. Sin. B* **8**, 511–517 (2018).

35. di Donato M., Cernera G., Migliaccio A. & Castoria G. Nerve growth factor induces proliferation and aggressiveness in prostate cancer cells. *Cancers (Basel).* **11**, 1–24 (2019).

36. Bapat A. A., Munoz R. M., Von Hoff D. D. & Han H. Blocking nerve growth factor signaling reduces the neural invasion potential of pancreatic cancer cells. *PLoS One* **11**, 1–15 (2016).

37. Kyker-Snowman K. *et al.* TrkA overexpression in non-tumorigenic human breast cell lines confers oncogenic and metastatic properties.

Breast Cancer Res. Treat. **179**, 631–642 (2020).

38. Vale R. D. & Shooter E. M. Assaying binding of nerve growth factor to cell surface receptors. in *Hormone Action Part I: Peptide Hormones* **109**, 21–40 (Academic Press, 1985).

39. Barker P. A. & Shooter E. M. Disruption of NGF binding to the low affinity neurotrophin receptor $p75^{LNTR}$ reduces NGF binding to TrkA on PC12 cells. *Neuron* **13**, 203–215 (1994).

40. Wehrman T. *et al.* Structural and Mechanistic Insights into Nerve Growth Factor Interactions with the TrkA and p75 Receptors. *Neuron* **53**, 25–38 (2007).

41. Trouvilliez S. & Toillon R.A.T. TrkA, behind the RTK transactivation model. Submited (2022)

42. Ponta H., Wainwright D. & Herrlich P. Molecules in focus The CD44 protein family. *Int. J. Biochem. Cell Biol.* **30**, 299–305 (1998).

43. Tremmel M. *et al.* A CD44v6 peptide reveals a role of CD44 in VEGFR-2 signaling and angiogenesis. *Blood* **114**, 5236–5244 (2009).

44. Matzke-Ogi A. *et al.* Inhibition of Tumor Growth and Metastasis in Pancreatic Cancer Models by Interference with CD44v6 Signaling. *Gastroenterology* **150**, 513-525.e10 (2016).

45. Morath I. *et al.* Differential recruitment of CD44 isoforms by ERBB ligands reveals an involvement of CD44 in breast cancer. *Oncogene* **37**, 1472–1484 (2018).

46. Trouvilliez S. *et al.* A mimetic peptide of CD44v3 rescues a Larotrectinib response in TrkA overexpressing cells. submited (2022).

47. Trouvilliez, S. *et al.* Direct interaction of TrkA / CD44v3 is essential for NGF-promoted aggressiveness of breast cancer cells. *J. Exp. Clin. Cancer Res.* 1–21 (2022). doi:10.1186/s13046-022-02314-4

48. Chang M. S., Arevalo J. C. & Chao M. V. Ternary complex with Trk,

p75, and an ankyrin-rich membrane spanning protein. *J. Neurosci. Res.* **78**, 186–192 (2004).

49. Geetha T., Jiang J. & Wooten M. W. Lysine 63 polyubiquitination of the nerve growth factor receptor TrkA directs internalization and signaling. *Mol. Cell* **20**, 301–312 (2005).

50. Makkerh J. P. S. *et al.* p75 neurotrophin receptor reduces ligand-induced Trk receptor ubiquitination and delays Trk receptor internalization and degradation. *EMBO Rep.* **6**, 936–941 (2005).

51. Matusica D. *et al.* An intracellular domain fragment of the p75 neurotrophin receptor (p75 NTR) enhances tropomyosin receptor kinase A(TrkA) receptor function. *J. Biol. Chem.* **288**, 11144–11154 (2013).

52. Urra S. *et al.* TrkA receptor activation by nerve growth factor induces shedding of the p75 neurotrophin receptor followed by endosomal γ-secretase-mediated release of the p75 intracellular domain. *J. Biol. Chem.* **282**, 7606–7615 (2007).

53. Lee F. S. & Chao M. V. Activation of Trk neurotrophin receptors in the absence of neurotrophins. *Proc. Natl. Acad. Sci. U. S. A.* **98**, 3555–3560 (2001).

54. Malek R. L., Nie Z., Ramkumar V. & Lee N. H. Adenosine A(2A) receptor mRNA regulation by nerve growth factor is TrkA- , Src-, and Ras-dependent via extracellular regulated kinase and stress- activated protein kinase/c-Jun NH2-terminal kinase. *J. Biol. Chem.* **274**, 35499–35504 (1999).

55. Plouffe B., Guimond M. O., Beaudry H. & Gallo-Payet N. Role of tyrosine kinase receptors in angiotensin II AT2 receptor signaling: Involvement in neurite outgrowth and in p42/p44mapk activation in NG108-15 cells. *Endocrinology* **147**, 4646–4654 (2006).

56. Guimond M.-O., Roberge C. & Gallo-Payet N. Fyn is involved in

angiotensin II type 2 receptor-induced neurite outgrowth, but not in p42/p44mapk in NG108-15 cells. *Mol. Cell. Neurosci.* **45**, 201–212 (2010).

57. Castaldo M., Zollo C., Esposito G., Ammendola R. & Cattaneo F. NOX2-Dependent Reactive Oxygen Species Regulate Formyl-Peptide Receptor 1-Mediated TrkA Transactivation in SH-SY5Y Cells. *Oxid. Med. Cell. Longev.* **2019**, (2019).

58. El Zein N., D'Hondt S. & Sariban E. Crosstalks between the receptors tyrosine kinase EGFR and TrkA and the GPCR, FPR, in human monocytes are essential for receptors-mediated cell activation. *Cell. Signal.* **22**, 1437–1447 (2010).

59. Lin C. *et al.* Nerve growth factor (NGF)-TrkA axis in head and neck squamous cell carcinoma triggers EMT and confers resistance to the EGFR inhibitor erlotinib. *Cancer Lett.* **472**, 81–96 (2020).

60. Palmieri D. *et al.* Her-2 overexpression increases the metastatic outgrowth of breast cancer cells in the brain. *Cancer Res.* **67**, 4190–4198 (2007).

61. Tagliabue E. *et al.* Nerve growth factor cooperates with p185(HER2) in activating growth of human breast carcinoma cells. *J. Biol. Chem.* **275**, 5388–5394 (2000).

62. Aubert L. *et al.* NGF-induced TrkA / CD44 association is involved in tumor aggressiveness and resistance to lestaurtinib. **6** (2015)

63. Blöchl A., Blumenstein L. & Ahmadian M. R. Inactivation and activation of Ras by the neurotrophin receptor p75. *Eur. J. Neurosci.* **20**, 2321–2335 (2004).

64. Deponti D. *et al.* The Low-Affinity Receptor for Neurotrophins p75NTR Plays a Key Role for Satellite Cell Function in Muscle Repair Acting via RhoA. *Mol. Biol. Cell* **20**, 3620–3627 (2009).

65. Yamashita T., Tucker K. L. & Barde Y. A. Neurotrophin binding to the

p75 receptor modulates Rho activity and axonal outgrowth. *Neuron* **24**, 585–593 (1999).

66. Davis S. *et al.* Ligands for EPH-related receptor tyrosine kinases that require membrane attachment or clustering for activity. *Science (80-.).* **266**, 816 LP – 819 (1994).

67. Eckhardt B. L. *et al.* Abstract P3-07-04: EphA2: An emerging target in triple-negative breast cancer. *Cancer Res.* **78**, P3-07-04 LP-P3-07–04 (2018).

68. Zelinski D. P., Zantek N. D., Stewart J. C., Irizarry A. R. & Kinch M. S. EphA2 overexpression causes tumorigenesis of mammary epithelial cells. *Cancer Res.* **61**, 2301–2306 (2001).

69. Kikawa K. D., Vidale D. R., Van Etten R. L. & Kinch M. S. Regulation of the EphA2 kinase by the low molecular weight tyrosine phosphatase induces transformation. *J. Biol. Chem.* **277**, 39274–39279 (2002).

70. Miao H. *et al.* EphA2 Mediates Ligand-Dependent Inhibition and Ligand-Independent Promotion of Cell Migration and Invasion via a Reciprocal Regulatory Loop with Akt. *Cancer Cell* **16**, 9–20 (2009).

71. Lévêque R. *et al.* ProNGF increases breast tumor aggressiveness through functional association of TrkA with EphA2. *Cancer Lett.* **449**, 196–206 (2019).

72. Su H. P. *et al.* Structural characterization of nonactive site, TrkA-selective kinase inhibitors. *Proc. Natl. Acad. Sci. U. S. A.* **114**, E297–E306 (2017).

73. Furuya N., Momose T., Katsuno K., Fushimi N. & Muranaka H. Bioorganic & Medicinal Chemistry Letters The juxtamembrane region of TrkA kinase is critical for inhibitor selectivity. **27**, 1233–1236 (2017).

74. Bagal S. K. *et al.* Discovery of Allosteric, Potent, Subtype Selective, and Peripherally Restricted TrkA Kinase Inhibitors. *J. Med. Chem.* **62**, 247–265 (2019).

75. Trouvilliez *et al.*, p115RhoGEF interacts directly with TrkA to promote migration, to be submited (2022).

76. Furuya N. *et al.* An isoform-selective inhibitor of tropomyosin receptor kinase A behaves as molecular glue. *Bioorg. Med. Chem. Lett.* **30**, 126775 (2020).

77. Chung V. *et al.* First-time in-human study of VMD-928, an oral allosteric TrkA selective inhibitor targeting TrkA protein overexpression, in patients with solid tumors or lymphoma. *J. Clin. Oncol.* **39**, 3081 (2021).

78. Criscitiello C., Morganti S. & Curigliano G. Antibody–drug conjugates in solid tumors: a look into novel targets. *J. Hematol. Oncol.* **14**, 1–18 (2021).

79. Canu N. *et al.* The intersection of NGF/TrkA signaling and amyloid precursor protein processing in Alzheimer's disease neuropathology. *Int. J. Mol. Sci.* **18**, 1–17 (2017).

La connaissance de ces mécanismes non génétiques d'échappement aux thérapies pourrait permettre d'améliorer la sélection des patients pour une thérapie ciblée donnée mais aussi permettre un ciblage plus spécifique des cellules cancéreuses en fonction des complexes exprimés. De plus, l'axe NGF/TrkA pourrait contribuer à l'émergence et à l'évolution d'autres maladies dont les maladies inflammatoires, les douleurs chroniques (hausse) et les maladies neurodégénératives (diminution) (Canu *et al.*, 2017).

L'axe NGF/TrkA est impliqué dans le syndrome d'insensibilité à la douleur (CIPA), une maladie neurodégénérative qui résulte de mutations ponctuelles ou de délétions qui peuvent toucher les 3 domaines du récepteur. Ces différents événements conduisent à des altérations de production, d'exocytose ou d'activation de TrkA (Franco *et al.*, 2016; Shaikh *et al.*, 2017). Dans tous les cas il en résulte un moindre taux d'activation des voies de signalisations sous-jacentes à TrkA dans les cellules nerveuses qui conduit à une altération de la perception de la douleur et des déficits mentaux plus ou moins importants. Ces altérations de TrkA altèrent également le fonctionnement des systèmes immunitaire et osseux. En effet, d'une part, les patients présentent une immunodéficience innée. L'altération de TrkA dans les monocytes et les macrophages les rend par exemple plus sensibles aux infections à *Staphylococcus aureus* (Hepburn *et al.*, 2014). D'autre part, les fractures sont plus fréquentes, non seulement parce que les patients ne ressentent pas la douleur (ce qui favorise les blessures) mais aussi en raison d'une capacité de consolidation osseuse moindre (Vugar *et al.*, 2018). En effet, après une fracture, les fibres nerveuses stimulée par le NGF produisent des facteurs qui stimulent la réparation osseuse par les ostéoblastes (activation de la voie Wnt/β-catenin) (Li et al., 2019). Ces observations montrent l'importance de l'axe NGF/TrkA dans de nombreux systèmes de l'organisme et sa nécessité pour le maintien de l'organisme en bonne santé.

Dans les maladies neurodégénératives, l'axe NGF/TrkA qui promeut normalement la survie des cellules nerveuses, est inhibé au profit de la signalisation du ProNGF/P75^{NTR} qui induit la mort cellulaire. Afin de rétablir l'équilibre entre ces 2 signalisations, l'administration d'agonistes de TrkA a montré un effet neuroprotecteur. Néanmoins, ce type d'approche nécessite de développer des composés spécifiques de TrkA afin de ne pas affecter les

signalisations des autres récepteurs Trk et de $P75^{NTR}$ (Cattaneo and Capsoni, 2019; Kargbo, 2019). De plus, TrkA contribue également aux douleurs chroniques et aigues.

Avec le vieillissement de la population mondiale, garantir la qualité de vie tout au long de celle-ci est devenu un nouvel enjeu de société majeur. Or, avec le vieillissement et l'évolution des modes de vie, a fait avancer le nombre de personnes souffrant de douleurs chroniques. Lors de la prise en charge des douleurs chroniques, le schéma thérapeutique pour assurer la qualité de vie du patient inclus plusieurs techniques médicamenteuses ou non. Néanmoins l'efficacité des traitements est souvent partielle et limitée dans le temps. Ceci conduit à la prise chronique d'anti-douleurs de plus en plus puissants et à des doses de plus en plus élevées. La prise prolongée de certains de ces médicaments (opioïdes ou morphiniques) conduit à l'addiction qui peut mener à des insuffisances hépatiques voire même des overdoses (Borsook and Becerra, 2006). Or, les molécules inhibant l'association NGF/TrkA n'entrainent pas de dépendance et pourraient ainsi constituer une nouvelle thérapie pour ces patients. Cette nouvelle catégorie d'antidouleurs pourrait également servir dans le cadre des soins palliatifs. En effet, les composés à la disposition des soignants pour gérer les douleurs intenses/aigues présentent des limites en terme d'efficacité, de dose tolérée et d'incompatibilité avec d'autres molécules (Platt, 2010).

Bibliographie

Abdulkarim B.S., Cuartero J., Hanson J., Deschênes J., Lesniak D., Sabri S. (2011). Increased risk of locoregional recurrence for women with T1-2N0 triple-negative breast cancer treated with modified radical mastectomy without adjuvant radiation therapy compared with breast-conserving therapy. J. Clin. Oncol. *29*, 2852–2858.

Adriaenssens E., Vanhecke E., Saule P., Mougel A., Page A., Romon R., Nurcombe V., Le Bourhis X., Hondermarck H. (2008). Nerve Growth Factor Is a Potential Therapeutic Target in Breast Cancer. 346–351.

Alblas J., Ulfman L., Hordijk P., Koenderman L. (2001). Screening Review. *12*, 2137–2145.

Aubert L., Guilbert M., Corbet C., Génot E., Adriaenssens E., Chassat T., Bertucci F., Daubon T. (2015). NGF-induced TrkA / CD44 association is involved in tumor aggressiveness and resistance to lestaurtinib. Oncotarget. *6*.

Azevedo R., Gaiteiro C., Peixoto A., Relvas-Santos M., Lima L., Santos L.L., Ferreira J.A. (2018). CD44 glycoprotein in cancer: A molecular conundrum hampering clinical applications. Clin. Proteomics *15*, 1–5.

Hsieh CC, Walker AM, Trapido EJ, Crosson AW, MacMahon B. Age at first birth and breast atypia. *Int J Cancer*. 1984;33(3):309-312. doi:10.1002/ijc.2910330306

Al Bazaz M., Lerch S., Hannen R., Lauber K., Dikomey E., Engenhart-Cabillic R., Schötz U. (2020). PH-0236: CD44v3-10 affects G2-arrest and radiosensitivity of S-phase cells via homologous recombination. Radiother. Oncol. *152*, S121.

Bellanger M., Zeinomar N., Tehranifar P., Terry M.B. (2018). Are Global Breast Cancer Incidence and Mortality Patterns Related to Country-Specific Economic Development and Prevention Strategies? J. Glob. Oncol. 1–16.

Bhattacharyya R., Banerjee J., Khalili K., Wedegaertner P.B. (2009). Differences in Galpha12- and Galpha13-mediated plasma membrane recruitment of p115-RhoGEF. Cell. Signal. *21*, 996–1006.

Bidard FC., Conforti R., Boulet T., Michiels S., Delaloge S., André F. (2007). Does triple-negative phenotype accurately identify basal-like tumour? An immunohistochemical analysis based on 143 “triple-negative” breast cancers [5]. Ann. Oncol. *18*, 1285–1286.

Borsook D. and Becerra LR. (2006). Breaking down the barriers: fMRI applications in pain, analgesia and analgesics. Mol. Pain *2*.

Bouafia A., Lofek S., Bruneau J., Chentout L., Lamrini H., Trinquand A., Deau M.C., Heurtier L., Meignin V., Picard C. (2019). Loss of ARHGEF1 causes a human primary antibody deficiency. J. Clin. Invest. *129*, 1047–1060.

Boureux A., Vignal E., Faure S., Fort P. (2007). Evolution of the Rho family of ras-like GTPases in eukaryotes. Mol. Biol. Evol. *24*, 203–216.

Bourguignon LYW., Singleton PA., Zhu H., Diedrich F. (2003). Hyaluronan-mediated CD44 Interaction with RhoGEF and Rho Kinase Promotes Grb2-associated Binder-1 Phosphorylation and Phosphatidylinositol 3-Kinase Signaling Leading to Cytokine (Macrophage-Colony Stimulating Factor) Production and Breast Tumor Progress. *278*, 29420–29434.

Brenton JD., Carey LA., Ahmed AA., Caldas C. (2005). Molecular Classification and Molecular Forecasting of Breast Cancer : Ready for Clinical Application ? *23*.

Canu N., Amadoro G., Triaca V., Latina V., Sposato V., Corsetti V., Severini C., Ciotti M.T., Calissano P. (2017). The intersection of NGF/TrkA signaling and amyloid precursor protein processing in Alzheimer's disease neuropathology. Int. J. Mol. Sci. *18*, 1–17.

Cattaneo A. and Capsoni S. (2019). Painless Nerve Growth Factor: A TrkA biased agonist mediating a broad neuroprotection via its actions on microglia cells. Pharmacol. Res. *139*, 17–25.

Chen Z., Guo L., Sprang SR., Sternweis PC. (2011). Modulation of a GEF switch: Autoinhibition of the intrinsic guanine nucleotide exchange activity of p115-RhoGEF. Protein Sci. *20*, 107–117.

Chen Z., Guo L., Hadas J., Gutowski S., Sprang SR., Sternweis, PC. (2012). Activation of p115-RhoGEF Requires Direct Association of G ⎯ 13 and the Dbl Homology Domain . *287*, 25490–25500.

Chikumi H., Barac A., Behbahani B., Gao Y., Teramoto H., Zheng Y., Gutkind JS. (2004). Homo- and hetero-oligomerization of PDZ-RhoGEF, LARG and p115RhoGEF by their C-terminal region regulates their in vivo Rho GEF activity and transforming potential. Oncogene *23*, 233–240.

Chow CR., Suzuki N., Kawamura T., Hamakubo T., Kozasa T. (2013). Modification of p115RhoGEF Ser(330) regulates its RhoGEF activity. Cell. Signal. *25*, 2085—2092.

Dalchau R., Kirkley J., Fabre JW. (1980). Monoclonal antibody to a human brain-granulocyte-T lymphocyte antigen probably homologous to the W 3/13 antigen of the rat. Eur. J. Immunol. *10*, 745–749.

Davies AM., Minichiello L., Klein R. (1995). Developmental changes in NT3 signalling via TrkA and TrkB in embryonic neurons. *The EMBO journal*, *14*(18), 4482–4489.

Demaria S. and Formenti SC. (2012). Radiation as an immunological adjuvant: current evidence on dose and fractionation. Front. Oncol. *2*, 1–7.

Descamps S., Toillon R., Adriaenssens E., Cool SM., Nurcombe V., Le Bourhis X., Peyrat J., Hondermarck H., Davis P. (2001). Nerve Growth Factor Stimulates Proliferation and Survival of Human Breast Cancer Cells through Two Distinct Signaling Pathways *. *276*, 17864–17870.

Dikic I, Batzer AG, Blaikie P, et al. Shc binding to nerve growth factor receptor is mediated by the phosphotyrosine interaction domain. *J Biol Chem*. 1995;270(25):15125-15129. doi:10.1074/jbc.270.25.15125

Drago JZ., Modi S., Chandarlapaty S. (2021). Unlocking the potential of antibody–drug conjugates for cancer therapy. Nat. Rev. Clin. Oncol. *18*, 327–344.

Dubash AD., Wennerberg K., García-Mata R., Menold MM., Arthur WT., Burridge K. (2007). A novel role for Lsc/p115 RhoGEF and LARG in regulating RhoA activity downstream of adhesion to fibronectin. J. Cell Sci. *120*, 3989–3998.

Kalish ED, Iida N, Moffat FL, Bourguignon LY. A new CD44V3-containing isoform is involved in tumor cell growth and migration during human breast carcinoma progression. *Front Biosci*. 1999;4:A1-A8. Published 1999 Jan 1. doi:10.2741/kalish

Emdal KB., Pedersen AK., Bekker-Jensen DB., Tsafou KP., Horn H., Lindner S., Schulte JH., Eggert A., Jensen LJ., Francavilla C. (2015). Temporal proteomics of NGF-TrkA signaling identifies an inhibitory role for the E3 ligase Cbl-b in neuroblastoma cell differentiation. Sci. Signal. *8*, ra40 LP-ra40.

Erika R., Franzmann E., Goodwin W. (2007). Role of CD44v3 and CD44s in head and neck cancer. Cancer Res. *67*, 3371.

Fasano O., Birnbaum D., Edlund L., Fogh J., Wigler M. (1984). New human transforming genes detected by a tumorigenicity assay. Mol. Cell. Biol. *4*, 1695–1705.

Fayaz S., Demian G.A., El-Sherify M., Eissa H., Aziz M., Abuzallouf, S. (2019). Triple Negative Breast Cancer: 10-Year Survival Update of The Applied Treatment Strategy in Kuwait. Gulf J. Oncolog. *1*, 53–59.

Festuccia C., Gravina GL., Muzi P., Millimaggi D., Dolo V., Vicentini C., Ficorella C., Ricevuto E., Bologna M. (2009). Her2 crosstalks with TrkA in a subset of prostate cancer cells: Rationale for a guided dual treatment. Prostate *69*, 337–345.

Franco ML., Melero C., Sarasola E., Acebo P., Luque A., Calatayud-Baselga I., García-Barcina M., Vilar M. (2016). Mutations in TrkA causing congenital insensitivity to pain with anhidrosis (CIPA) induce misfolding, aggregation, and mutation-dependent neurodegeneration by dysfunction of the autophagic flux. J. Biol. Chem. *291*, 21363–21374.

Fu WF, Chen QX, Wang XX, Zhang J, Song CG. The Survival Outcomes of T1aN0M0 Triple-Negative Breast Cancer With Adjuvant Chemotherapy. *Front Oncol*. 2020;10:1753. Published 2020 Sep 30. doi:10.3389/fonc.2020.01753

Fuse MJ., Okada K., Oh-hara T., Ogura H., Fujita N. (2017). Mechanisms of resistance to NTRK inhibitors and therapeutic strategies in NTRK1-rearranged cancers. 3–8.

Freedman GM, Li T, Anderson PR, Nicolaou N, Konski A. Health states of women after conservative surgery and radiation for breast cancer. *Breast Cancer Res Treat*. 2010;121(2):519-526. doi:10.1007/s10549-009-0552-5

Guilluy C., Brégeon J., Toumaniantz G., Rolli-Derkinderen M., Retailleau K., Loufrani L., Henrion D., Scalbert E., Bril A., Torres RM., (2010). The Rho exchange factor Arhgef1 mediates the effects of angiotensin II on vascular tone and blood pressure. Nat. Med. *16*, 183–190.

Haffty B.G., Yang Q., Reiss M., Kearney T., Higgins, SA., Weidhaas J., Harris L., Hait W., Toppmeyer D. (2006). Locoregional relapse and distant metastasis in conservatively managed triple negative early-stage breast cancer. J. Clin. Oncol. *24*, 5652–5657.

Hakem A., Sanchez-Sweatman O., You-Ten A., Duncan G., Wakeham A., Khokha R., Mak TW. (2005). RhoC is dispensable for embryogenesis and tumor initiation but essential for metastasis. Genes Dev. *19*, 1974–1979.
Hall, A. (1998). Rho GTPases and the Actin Cytoskeleton. Science (80-.). *279*, 509 LP – 514.

Harrison GM, Davies G, Martin TA, Mason MD, Jiang WG. The influence of CD44v3-v10 on adhesion, invasion and MMP-14 expression in prostate cancer cells. *Oncol Rep*. 2006;15(1):199-206.

Hart MJ., Eva A., Evans T., Aaronson SA., Cerione RA. (1991). Catalysis of guanine nucleotide exchange on the CDC42Hs protein by the dbloncogene product. Nature *354*, 311–314.

Hart MJ., Sharma S., Elmasry N., Qiu RG., McCabe P., Polakis P., Bollag G. (1996). Identification of a novel guanine nucleotide exchange factor for the Rho GTPase. J. Biol. Chem. *271*, 25452–25458.

Hartmann M., Parra LM., Ruschel A., Bohme S., Li Y., Morrison H., Herrlich A., Herrlich P. (2015). Tumor suppressor NF2 blocks cellular migration by

inhibiting ectodomain cleavage of CD44. Mol. Cancer Res. *13*, 879–890.

Hepburn L., Prajsnar TK., Klapholz C., Moreno P., Loynes CA., Ogryzko, N. V., Brown, K., Schiebler, M., Hegyi, K., Antrobus, R., et al. (2014). A Spaetzle-like role for nerve growth factor β in vertebrate immunity to Staphylococcus aureus. Science (80-.). *346*, 641–646.

Huttlin EL., Bruckner RJ., Paulo JA., Cannon JR., Ting L., Colby G., Gebreab, F., Gygi MP., Parzen H., Szpyt J. (2017). Communities and Disease Networks. Nature *545*, 505–509.

Javed A. and Lteif A. (2013). Development of the human breast. Semin. Plast. Surg. *27*, 5–12.

Jiang T., Wang G., Liu Y., Feng L., Wang M., Liu J., Chen Y., Ouyang L. (2021). Development of small-molecule tropomyosin receptor kinase (TRK) inhibitors for NTRK fusion cancers. Acta Pharm. Sin. B *11*, 355–372.

Jing S., Tapley P., Barbacid M. (1992). Nerve growth factor mediates signal transduction through trk homodimer receptors. Neuron *9*, 1067–1079.

Karagiannis GS., Goswami S., Jones JG., Oktay MH., Condeelis JS. (2016). Signatures of breast cancer metastasis at a glance. J. Cell Sci. *129*, 1751–1758.

Kargbo RB. (2019). Modulation of Tropomyosin Receptor Kinase for the Treatment of Neurotrophin Diseases: Alzheimer's, Huntington's and Parkinson's. ACS Med. Chem. Lett. *10*, 1590–1591.

Kassam F., Enright K., Dent R., Dranitsaris G., Myers J., Flynn C., Fralick M., Kumar R., Clemons M. (2009). Survival outcomes for patients with metastatic triple-negative breast cancer: Implications for clinical practice and trial design. Clin. Breast Cancer *9*, 29–33.

Kennedy AE., Laamanen CA., Ross MS., Vohra R., Boreham DR., Scott JA., Ross GM. (2017). Nerve growth factor inhibitor with novel-binding domain demonstrates nanomolar efficacy in both cell-based and cell-free assay systems. *5*.

Kim JE., Ahn HJ., Ahn JH., Yoon DH., Kim SB., Jung KH., Gong GY., Kim MJ., Son BH., Ahn SH. (2012). Impact of triple-negative breast cancer phenotype on prognosis in patients with stage i breast cancer. J. Breast Cancer *15*, 197–202.

Klein R., Jing S., Nanduri V., O'Rourke E., Barbacid M. (1991). The trk proto-oncogene encodes a receptor for nerve growth factor. Cell *65*, 189–197.

Kolečková M., Kolář Z., Ehrmann J., Kořínková G., Trojanec R. (2017). Age-associated prognostic and predictive biomarkers in patients with breast cancer. Oncol. Lett. *13*, 4201–4207.

Labrie M., Brugge JS., Mills GB., Zervantonakis IK. (2022). Therapy resistance: opportunities created by adaptive responses to targeted therapies in cancer. Nat. Rev. Cancer.

Lagadec C., Meignan S., Adriaenssens E., Foveau B., Vanhecke E., Romon R., Toillon RA., Oxombre B., Hondermarck H. and Le Bourhis, X. (2009). TrkA overexpression enhances growth and metastasis of breast cancer cells. Oncogene *28*, 1960–1970.

Lee JH., Katakai T., Hara T., Gonda H., Sugai M., and Shimizu A. (2004). Roles of p-ERM and Rho-ROCK signalling in lymphocyte polarity and uropod formation. J. Cell Biol. *167*, 327–337.

Lefeuvre D., Catajar N., Le Bihan Benjamin C., Ifrah N., De Bels F., Viguier J., and Bousquet PJ. (2019). Breast cancer screening: Impact on care pathways. Cancer Med. *8*, 4070–4078.

Legg JW., and Isacke CM. (1998). Identification and functional analysis of the ezrin-binding site in the hyaluronan receptor, CD44. Curr. Biol. *8*, 705–708.

Lehmann BDB., Bauer JaJ., Chen X., Sanders ME., Chakravarthy B., Shyr Y., and Pietenpol J. (2011). Identification of human triple-negative breast cancer subtypes and preclinical models for selection of targeted therapies. J. Clin. Invest. *121*, 2750–2767.

Li J., Yu K., Pang D., Wang C., Jiang J., Yang S., Liu Y., Fu P., Sheng Y., Zhang G. (2020). Adjuvant capecitabine with docetaxel and cyclophosphamide plus epirubicin for triple-negative breast cancer (CBCSG010): An open-label, randomized, multicenter, phase III Trial. J. Clin. Oncol. *38*, 1774–1784.

Li S., Sun Y., and Gao D. (2013). Role of the nervous system in cancer metastasis (Review). Oncol. Lett. *5*, 1101–1111.

Li S., Ma D., Shi HH., Yu K. Da and Zhang Q. (2018). The effect of delayed adjuvant chemotherapy on relapse of triplenegative breast cancer. J. Thorac. Dis. *10*, 2837–2841.

Li Z., Meyers CA., Chang L., Lee S., Li Z., Tomlinson R., Hoke A., Clemens TL. and James AW. (2019). Fracture repair requires TrkA signaling by skeletal sensory nerves. J. Clin. Invest. *129*, 5137–5150.

Liao WS., Ho Y., Lin YW., Naveen Raj E., Liu KK., Chen C., Zhou XZ., Lu KP. and Chao JI. (2019). Targeting EGFR of triple-negative breast cancer enhances the therapeutic efficacy of paclitaxel- and cetuximab-conjugated nanodiamond nanocomposite. Acta Biomater. *86*, 395–405.

Liedtke C., Mazouni C., Hess KR., André F., Tordai A., Mejia JA., Symmans WF., Gonzalez-Angulo AM., Hennessy B., Green M. (2008). Response to

neoadjuvant therapy and long-term survival in patients with triple-negative breast cancer. J. Clin. Oncol. *26*, 1275–1281.

Lin C., Ren Z., Yang X., Yang R., Chen Y., Liu Z., Dai Z., Zhang Y., He Y., Zhang C. (2020). Nerve growth factor (NGF)-TrkA axis in head and neck squamous cell carcinoma triggers EMT and confers resistance to the EGFR inhibitor erlotinib. Cancer Lett. *472*, 81–96.

Lin NU., Vanderplas A., Hughes ME., Theriault RL., Edge SB., Wong YN., Blayney DW., Niland JC., Winer EP., and Weeks JC. (2012). Clinicopathologic features, patterns of recurrence, and survival among women with triple-negative breast cancer in the National Comprehensive Cancer Network. Cancer *118*, 5463–5472.

Lokeshwar V.B., Fregien N., and Bourguignon LYW. (1994). Ankyrin-binding domain of CD44(GP85) is required for the expression of hyaluronic acid-mediated adhesion function. J. Cell Biol. *126*, 1099–1109.

Louderbough JMV., Brown JA., Nagle RB., and Schroeder JA. (2011). CD44 Promotes Epithelial Mammary Gland Development and Exhibits Altered Localization during Cancer Progression. Genes and Cancer *2*, 771–781.

Lv Y., Ma X., Du Y., and Feng J. (2021). Understanding patterns of brain metastasis in triple-negative breast cancer and exploring potential therapeutic targets. Onco. Targets. Ther. *14*, 589–607.

Daly MB, Pal T, Berry MP, et al. Genetic/Familial High-Risk Assessment: Breast, Ovarian, and Pancreatic, Version 2.2021, NCCN Clinical Practice Guidelines in Oncology. *J Natl Compr Canc Netw*. 2021;19(1):77-102. Published 2021 Jan 6. doi:10.6004/jnccn.2021.0001

Macias H. and Hinck L. (2012). Mammary gland development. Wiley Interdiscip. Rev. Dev. Biol. *1*, 533–557.

Madaule P. and Axel R. (1985). A novel ras-related gene family. Cell *41*, 31–40.

Masuda H., Baggerly KA., Wang Y., Zhang Y., Gonzalez-Angulo AM., Meric-Bernstam F., Valero V., Lehmann BD., Pietenpol JA., Hortobagyi GN. (2013). Differential response to neoadjuvant chemotherapy among 7 triple-negative breast cancer molecular subtypes. Clin. Cancer Res. *19*, 5533–5540.

McBryan J., Howlin J., Napoletano S. and Martin F. (2008). Amphiregulin: Role in Mammary Gland Development and Breast Cancer. J. Mammary Gland Biol. Neoplasia *13*, 159–169.

Miles FL., Pruitt FL., van Golen KL. and Cooper CR. (2008). Stepping out of the flow: capillary extravasation in cancer metastasis. Clin. Exp. Metastasis *25*, 305–324.

Mori T., Kitano K., Terawaki SI., Maesaki R., Fukami Y. and Hakoshima T. (2008). Structural basis for CD44 recognition by ERM proteins. J. Biol. Chem. *283*, 29602–29612.

Noguchi T., Galland F., Batoz M., Mattei MG. and Birnbaum D. (1988). Activation of a mcf.2 oncogene by deletion of amino-terminal coding sequences. Oncogene *3*, 709—715.

Okada M., Wang Y., Jang SW., Tang X., Neri LM., and Ye K. (2009). Akt phosphorylation of merlin enhances its binding to phosphatidylinositols and inhibits the tumor-suppressive activities of merlin. Cancer Res. *69*, 4043–4051.

Orian-Rousseau V., Chen L., Sleeman JP., Herrlich P. and Ponta H. (2002). CD44 is required for two consecutive steps in HGF/c-Met signaling. Genes Dev. *16*, 3074–3086.

Pandy JGP., Balolong-Garcia JC., Cruz-Ordinario MVB. and Que FVF. (2018). Triple negative breast cancer and platinum-based systemic treatment: Meta-analysis and systematic review. Ann. Oncol. *29*, ix2.

Park YH., Lee SJ., Cho EY., La Choi Y., Lee JE., Nam SJ., Yang JH., Shin JH., Ko EY., Han BK. (2011). Clinical relevance of TNM staging system according to breast cancer subtypes. Ann. Oncol. *22*, 1554–1560.

Peng J., He F., Zhang C., Deng X. and Yin F. (2011). Protein kinase C-α signals P115RhoGEF phosphorylation and RhoA activation in TNF-α-induced mouse brain microvascular endothelial cell barrier dysfunction. J. Neuroinflammation *8*, 28.

Perou CM., Sùrlie T., Eisen MB., Van De Rijn M., Jeffrey SS., Rees CA., Pollack, J.R., Ross, D.T., Johnsen, H., Akslen, L.A., et al. (2000). Molecular portraits of human breast tumours. *533*, 747–752.

Phillips HS., & Armanini MP. (1996). Expression of the trk Family of Neurotrophin Receptors in Developing and Adult Dorsal Root Ganglion Neurons. *Philosophical Transactions: Biological Sciences*, *351*(1338), 413–416.

Plasilova ML., Hayse B., Killelea BK., Horowitz NR., Chagpar AB. and Lannin DR. (2016). Features of triple-negative breast cancer Analysis of 38,813 cases from the national cancer database. Med. (United States) *95*.

Platt M. (2010). Pain Challenges at the End of Life—Pain and Palliative Care Collaboration. Rev. Pain *4*, 18–23.

Poole AJ., Frigotto L., Smith ME., Baar C., Ivanova-Berndt G., Jaulent A., Stace C., Ullman CG. and Hine AV. (2019). A C-terminal cysteine residue is required for peptide-based inhibition of the NGF/TrkA interaction at nM concentrations: implications for peptide-based analgesics. Sci. Rep. *9*, 1–11.

Quigley MR., Fukui O., Chew B., Bhatia S. and Karlovits S. (2013). The shifting landscape of metastatic breast cancer to the CNS. Neurosurg. Rev. *36*, 377–382.

Rahman M. and Mohammed S. (2015). Breast cancer metastasis and the lymphatic system (Review). Oncol. Lett. *10*, 1233–1239.

Reddy SM., Barcenas CH., Sinha AK., Hsu L., Moulder SL., Tripathy D., Hortobagyi GN. and Valero V. (2018). Long-term survival outcomes of triple-receptor negative breast cancer survivors who are disease free at 5 years and relationship with low hormone receptor positivity. Br. J. Cancer *118*, 17–23.

Ridley, A. J., & Hall, A. (1992). The small GTP-binding protein rho regulates the assembly of focal adhesions and actin stress fibers in response to growth factors. *Cell*, *70*(3), 389–399.

Sabatier R., Lopez M., Guille A., Billon E., Carbuccia N., Garnier S., Adelaide J., Extra JM., Cappiello MA., Charafe-Jauffret E. (2019). High Response to Cetuximab in a Patient With EGFR -Amplified Heavily Pretreated Metastatic Triple-Negative Breast Cancer . JCO Precis. Oncol. 1–8.

Sanguinetti A., Polistena A., Lucchini R., Monacelli M., Galasse S., Avenia S., Triola R., Bugiantella W., Cirocchi R., Rondelli F. (2016). Male breast cancer, clinical presentation, diagnosis and treatment: Twenty years of experience in our Breast Unit. Int. J. Surg. Case Rep. *20*, 8–11.

Schmid P., Adams S., Rugo HS., Schneeweiss A., Barrios CH., Iwata H., Dieras V., Hegg R., Im SA., Shaw Wright G. (2018). Atezolizumab and nab-paclitaxel in advanced triple-negative breast cancer. N. Engl. J. Med. *379*, 2108–2121.

Scott D.W., Tolbert C.E., and Burridge K. (2016). Tension on JAM-A activates RhoA via GEF-H1 and p115 RhoGEF. Mol. Biol. Cell *27*, 1420–1430.

Shaikh S.S., Chen Y.C., Halsall S.A., Nahorski M.S., Omoto K., Young G.T., Phelan A., and Woods C.G. (2017). A Comprehensive Functional Analysis of NTRK1 Missense Mutations Causing Hereditary Sensory and Autonomic Neuropathy Type IV (HSAN IV). Hum. Mutat. *38*, 55–63.

Shield K.D., Marant Micallef C., Hill C., Touvier M., Arwidson P., Bonaldi C., Ferrari P., Bray F., and Soerjomataram I. (2018). New cancer cases in France in 2015 attributable to different levels of alcohol consumption. Addiction *113*, 247–256.

Singh N.K., Janjanam J., and Rao G.N. (2017). p115 RhoGEF activates the Rac1 GTPase signaling cascade in MCP1 chemokine – induced vascular smooth muscle cell. *292*, 14080–14091.

Sjöblom T., Jones S., Wood L.D., Parsons D.W., Lin J., Barber, T.D.

Mandelker D., Leary R.J., Ptak J., Silliman N., et al. (2006). The Consensus Coding Sequences of Human Breast and Colorectal Cancers. Science (80-.). *314*, 268 LP – 274.

Sternlicht M.D. (2006). Key stages in mammary gland development The cues that regulate ductal branching morphogenesis. *11*.

Tolg C., Yuan H., Flynn S.M., Basu K., Ma J., Tse K.C.K., Kowalska, B., Vulkanesku, D., Cowman, M.K., McCarthy, J.B., et al. (2017). Hyaluronan modulates growth factor induced mammary gland branching in a size dependent manner. Matrix Biol. *63*, 117–132.

Tremmel M., Matzke A., Albrecht I., Laib A.M., Olaku V., Ballmer-Hofer K., Christofori G., Héroult M., Augustin H.G., Ponta H., et al. (2009). A CD44v6 peptide reveals a role of CD44 in VEGFR-2 signaling and angiogenesis. Blood *114*, 5236–5244.

Tsuzuki S., Park S.H., Eber M.R., Peters C.M., and Shiozawa Y. (2016). Skeletal complications in cancer patients with bone metastases. Int. J. Urol. *23*, 825–832.

Urru S.A.M., Gallus S., Bosetti C., Moi T., Medda R., Sollai E., Murgia A., Sanges F., Pira G., Manca A. et al. (2018). Clinical and pathological factors influencing survival in a large cohort of triple-negative breast cancer patients. BMC Cancer *18*, 1–11.

Vargo-Gogola T. and Rosen J.M. (2007). Modelling breast cancer: One size does not fit all. Nat. Rev. Cancer *7*, 659–672.

Volz Y., Koschut D., Matzke-Ogi A., Dietz M.S., Karathanasis C., Richert L., Wagner M.G., Mély Y., Heilemann M., Niemann H.H. et al. (2015). Direct binding of hepatocyte growth factor and vascular endothelial growth factor to CD44v6. Biosci. Rep. *35*, 1–16.

Nabyev V.N., Seneran H., Aksoy3M.C. (2018). Congenital Insensitivity to Pain Syndrome with Anhidrosis. Review of Literature. J. Pediatr. Pediatr. Med. *2*, 14–20.

Wang S.J., Wreesmann V.B., and Bourguignon L.Y.W. (2007). Association of CD44 V3-containing isoforms with tumor cell growth, migration, matrix metalloproteinase expression, and lymph node metastasis in head and neck cancer. Head Neck *29*, 550–558.

Wehrman T., He X., Raab B., Dukipatti A., Blau H., and Garcia K.C. (2007). Structural and Mechanistic Insights into Nerve Growth Factor Interactions with the TrkA and p75 Receptors. Neuron *53*, 25–38.

Wells C.D., Gutowski S., Bollag G., and Sternweis P.C. (2001). Identification of Potential Mechanisms for Regulation of p115 RhoGEF through Analysis of Endogenous and Mutant Forms of the Exchange Factor. J. Biol. Chem. *276*,

28897–28905.

Wolff A.C., Hammond M.E.H., Hicks D.G., Dowsett M., McShane L.M., Allison K.H., Allred D.C., Bartlett J.M.S., Bilous M., Fitzgibbons P. et al. (2013). Recommendations for human epidermal growth factor receptor 2 testing in breast. J. Clin. Oncol. *31*, 3997–4013.

Wu Q., Li J., Zhu S., Wu J., Chen C., Liu Q., Wei W., Zhang Y., and Sun S. (2017). Breast cancer subtypes predict the preferential site of distant metastases: A SEER based study. Oncotarget *8*, 27990–27996.

Wu R.F., Liao C., Fu G., Hayenga H.N., Yang K., Ma Z., Liu Z., and Terada L.S. (2016). p66 Shc Couples Mechanical Signals to RhoA through Focal Adhesion Kinase-Dependent Recruitment of p115-RhoGEF and GEF-H1 . Mol. Cell. Biol. *36*, 2824–2837.

Xiaolu D., Jing P., Fang H., Lifen Y., Liwen W., Ciliu Z., and Fei Y. (2011). Role of p115RhoGEF in lipopolysaccharide-induced mouse brain microvascular endothelial barrier dysfunction. Brain Res. *1387*, 1–7.

Xu Y., Zhang Y., Yang Y., Liu Y., Tian Q., Liu P., Ding Z., Cheng H., Zhang X., and Ke Y. (2020). Tyrosine phosphatase Shp2 regulates p115RhoGEF/Rho-dependent dendritic cell migration. Cell. Mol. Immunol.

Yan B., Mu Y., Cui M., and Liu L. (2020). Clinicopathological significance and prognostic implication of CD44 and its splice variants (v3 and v6) in colorectal cancer. Transl. Cancer Res. *9*, 1215–1224.

Yao Y., Chu Y., Xu B., Hu Q. and Song Q. (2019). Radiotherapy after surgery has significant survival benefits for patients with triple-negative breast cancer. Cancer Med. *8*, 554–563.

Yu X.F., Feng W.L., Miao L.L., Chen B., and Yang H.J. (2013). The prognostic significance of molecular subtype for male breast cancer: A10-year retrospective study. Breast *22*, 824–827.

Zbuk K., and Anand S.S. (2012). Declining incidence of breast cancer after decreased use of hormone-replacement therapy: magnitude and time lags in different countries. J. Epidemiol. Community Health *66*, 1 LP – 7.

Zhang Y., Wang S., Yang B., Lu S., Du Y. and Liu H. (2019). Adjuvant treatment for triple-negative breast cancer: a retrospective study of immunotherapy with autologous cytokine-induced killer cells in 294 patients. Cancer Biol. Med. *16*, 350–360.